

1930-1940

1930-1940

Development of the Field Ion Microscope

1935: Erwin Müller

1935

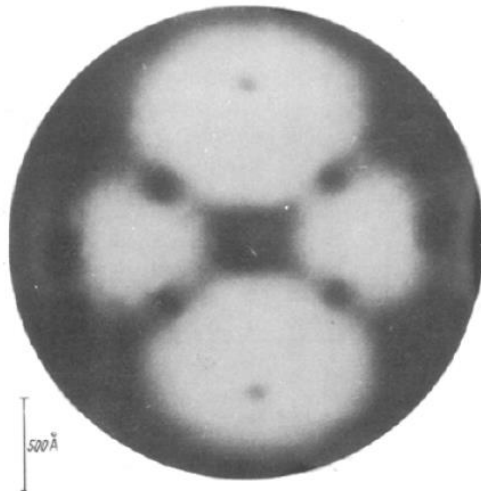
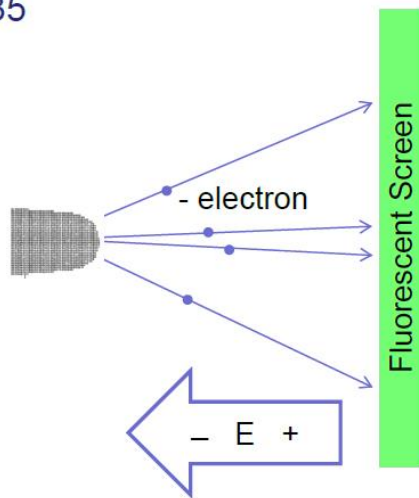
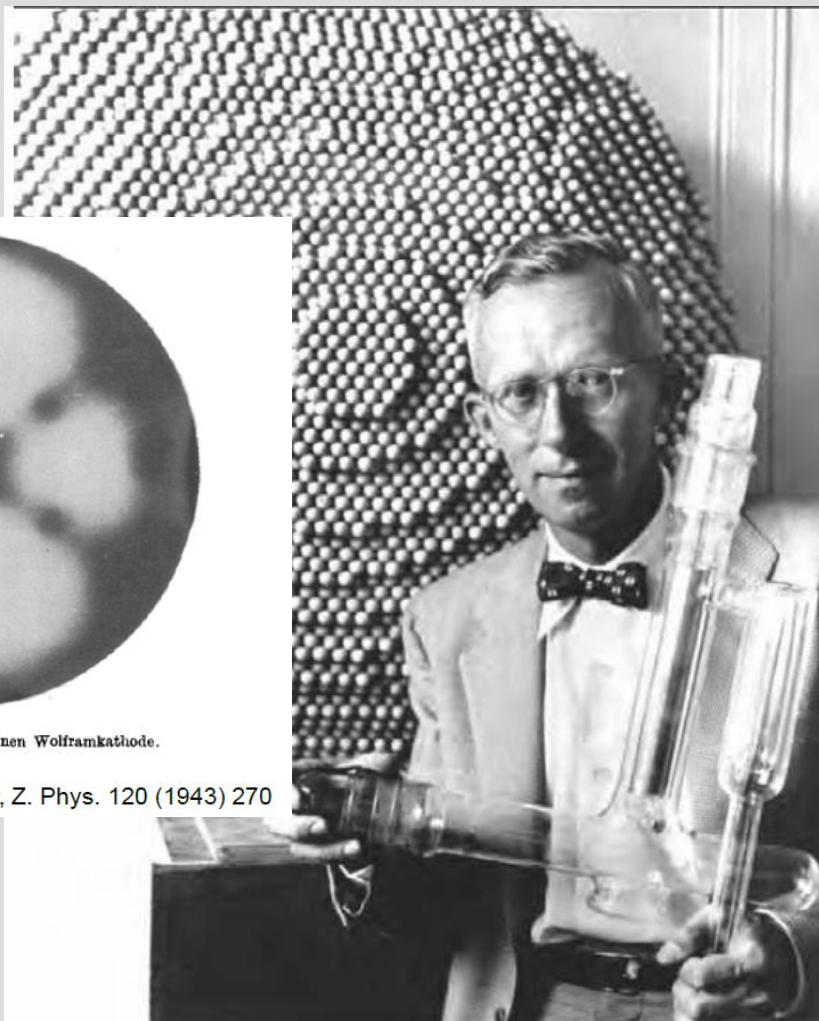


Fig. 5. Elektronenbild einer reinen Wolframkathode.

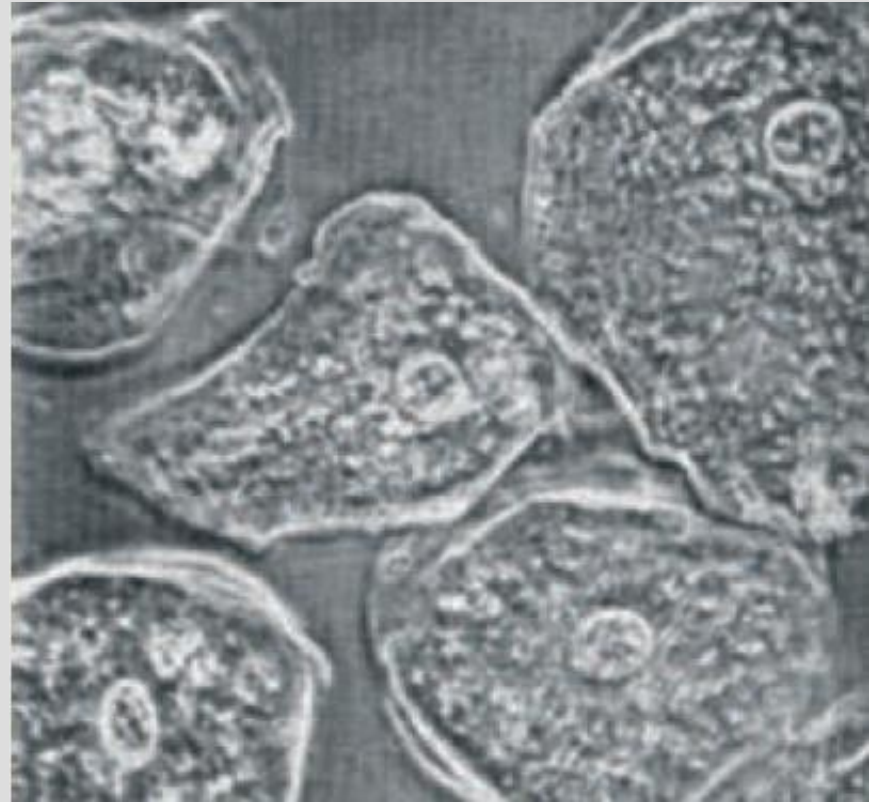
E. W. Müller, Z. Phys. 120 (1943) 270



1930-1940

Development Phase-contrast Light Microscopy

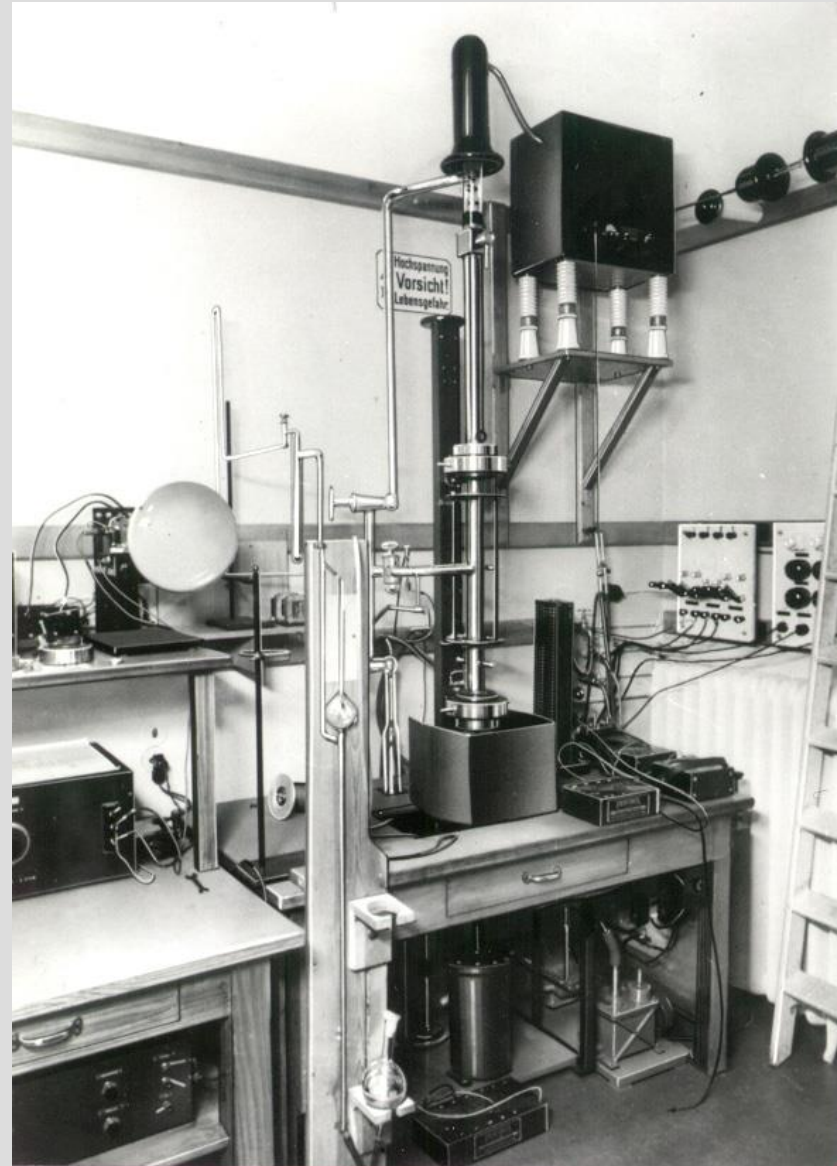
1935: Frits Zernike



1930-1940

First Implementation of the SEM

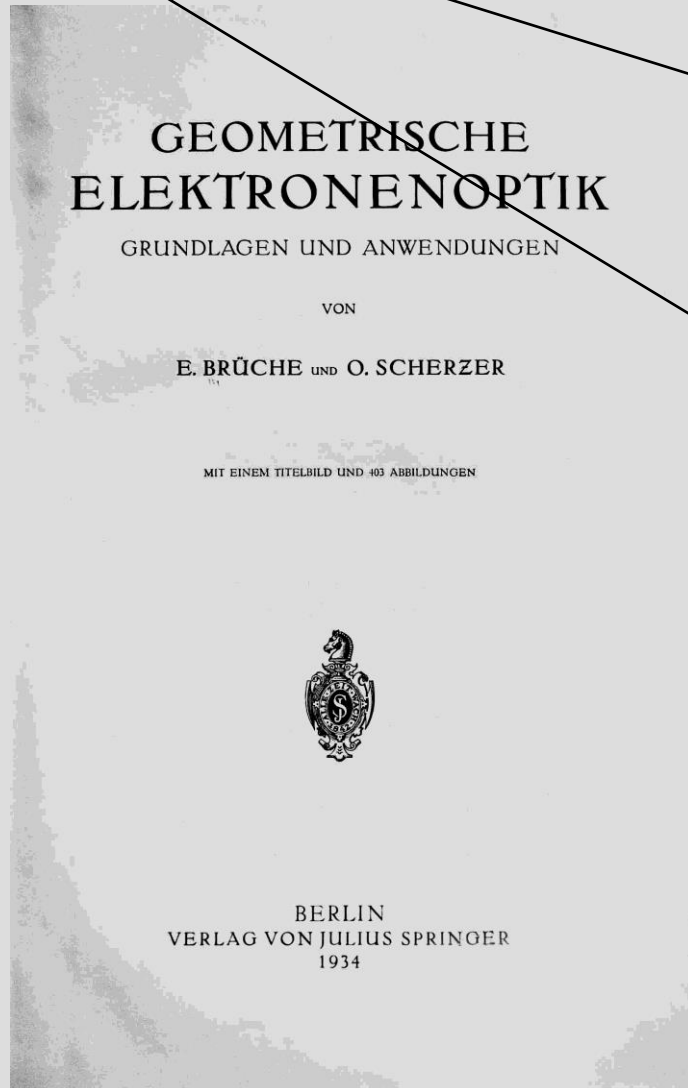
1943: Manfred von Ardenne



1930-1940

First Text on Electron Optics

1934: Brüche and Scherzer



1930-1940

Theory of Aberration Correction

1936, 1945: Otto Scherzer



Über einige Fehler von Elektronenlinsen.

Von O. Scherzer in Darmstadt.

Mit 3 Abbildungen. (Eingegangen am 4. Juni 1936.)

Unmöglichkeit des Achromaten. Die Bildfehler dritter Ordnung. Unvermeidbarkeit der sphärischen Aberration.

1. Unmöglichkeit des Achromaten.

Die wichtigste Forderung, die ein chromatisch korrigiertes Linsensystem erfüllen muß, ist die, daß zwei Strahlen benachbarter Farbe, die von der Objektmitte unter kleinem Winkel gegen die optische Achse ausgehen, sich in der Bildmitte treffen; bei Elektronenlinsen tritt an die Stelle der „Farbe“ die Elektronengeschwindigkeit. Wir werden zeigen, daß sich diese Forderung bei raumladungsfreien Elektronenlinsen niemals in Strenge erfüllen läßt.

Die Bewegung der achsennahen Elektronen (Gaußscher Strahlengang) genügt bekanntlich der Gleichung

$$\Phi r'' + \frac{1}{2} \Phi' r' = -\frac{r}{4} \Phi'' - \frac{er}{8m} \mathcal{E}^2. \quad (1)$$

Sphärische und chromatische Korrektur von Elektronen-Linsen.

Von O. Scherzer, z. Zt. USA.

(Aus den Süddeutschen Laboratorien in Mosbach.)

(Mit 7 Textabbildungen.)

Die Brauchbarkeit des Elektronenmikroskops bei hohen Vergrößerungen wird durch den Öffnungsfehler und die chromatische Aberration beeinträchtigt. Beide Fehler sind unvermeidlich, solange die abbildenden Felder rotations-symmetrisch, ladungsfrei und zeitlich konstant sind. Die vorliegende Untersuchung soll zeigen, daß die Aufhebung irgendeiner dieser drei Einschränkungen genügt, um den Weg zur sphärischen und chromatischen Korrektur und damit zu einer erheblichen Steigerung des Auflösungsvermögens freizugeben.

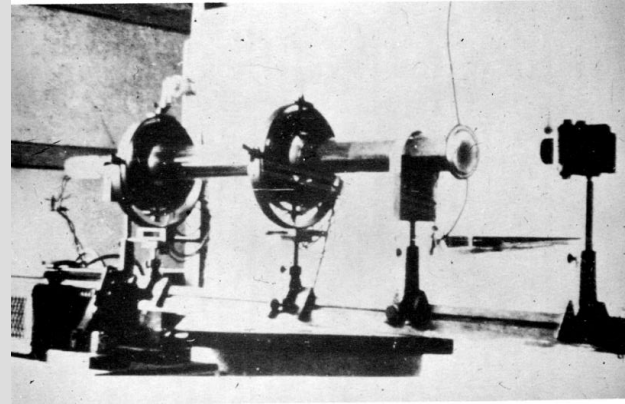
Solange nicht klar zu sehen ist, welche Art Linsen das beste Mikroskop ergibt, müssen alle sich bietenden Wege verfolgt werden. Es scheint daher angebracht, etwas ausführlicher auf die verschiedenen Arten korrigierter Linsen einzugehen.

1930-1940 Nobel Prize #1

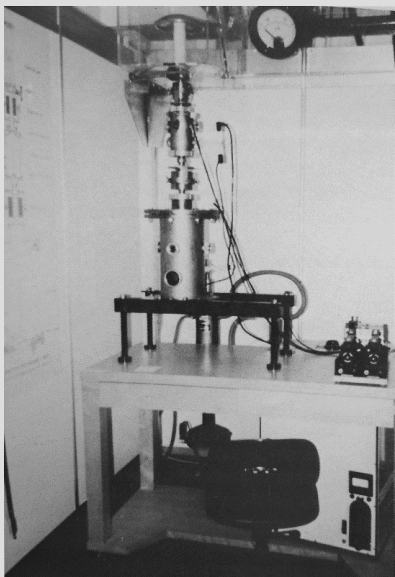
Development of the TEM

Ernst Ruska

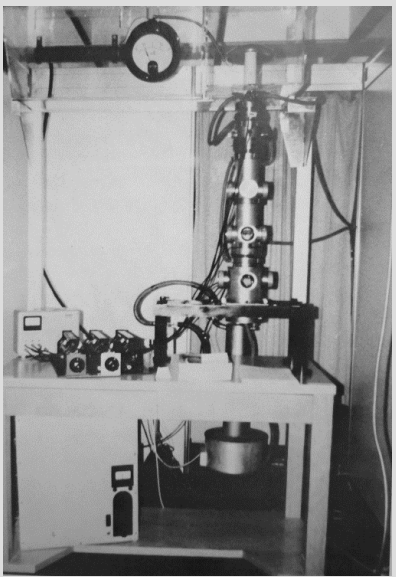
Second instrument, 1931, with Max Knoll



First instrument, 1931



2nd, 1931



3rd, 1933, higher mag than LM



In 1939



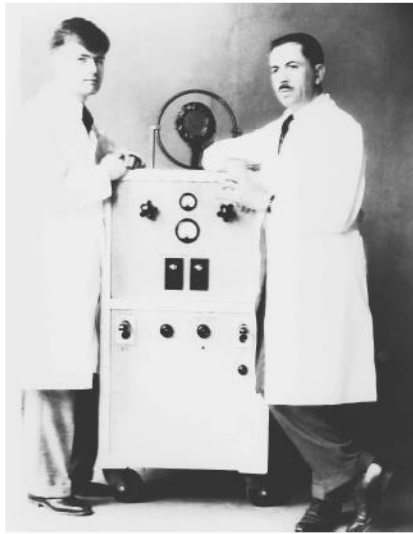
With Nobel Prize, 1986

1930-1940

Development of the EM

1935: Emission Microscopy – “biological microanalysis”

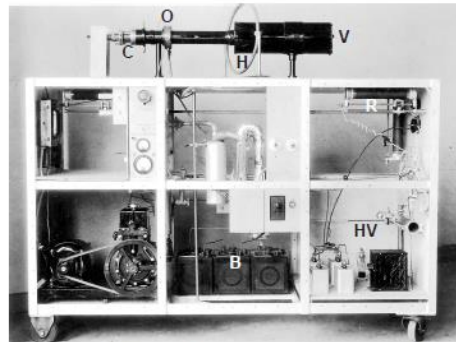
Washington University, St. Louis



McMillen (l) and Scott with the second Washington University emission microscope. Viewing screen at (V).



Donald Packer



Side view of the second emission microscope. Cathode (C), objective lens (O), Helmholtz coil (H), diffusion pump (D), Batteries (B), High-voltage supply (HV), rheostat for cathode heater (R), viewing screen (V).

First application of EM microanalysis

Scott was interested in the function and location of soluble salts in tissue. In order to retain the original distribution of the salts, he improved rapid freezing techniques and low-temperature light microscopy. He also improved optical spectroscopy and microincineration techniques. McMillen reasoned that since tissue structure is still visible in microincinerated samples, an emission electron microscope might reveal the location of trace elements such as magnesium, calcium and iron in tissue.

The cathode of the emission microscope consisted of a nickel thimble coated with barium and strontium carbonates. Tissue was freeze-dried and vacuum-embedded in paraffin. A thin section was placed on the cathode. As the temperature was raised, the organic materials burned off, the carbonates were converted to oxides, and the salts were deposited on the cathode. At emission temperature, there was a local increase in emission by about three orders of magnitude at points where the specimen had magnesium, calcium, or iron. Although it was not possible to distinguish between elements if more than one were present, this was the first example of elemental mapping by electron microscopy, many years ahead of its time.

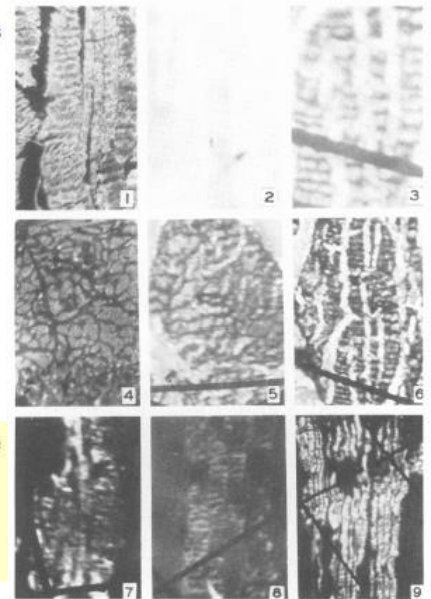
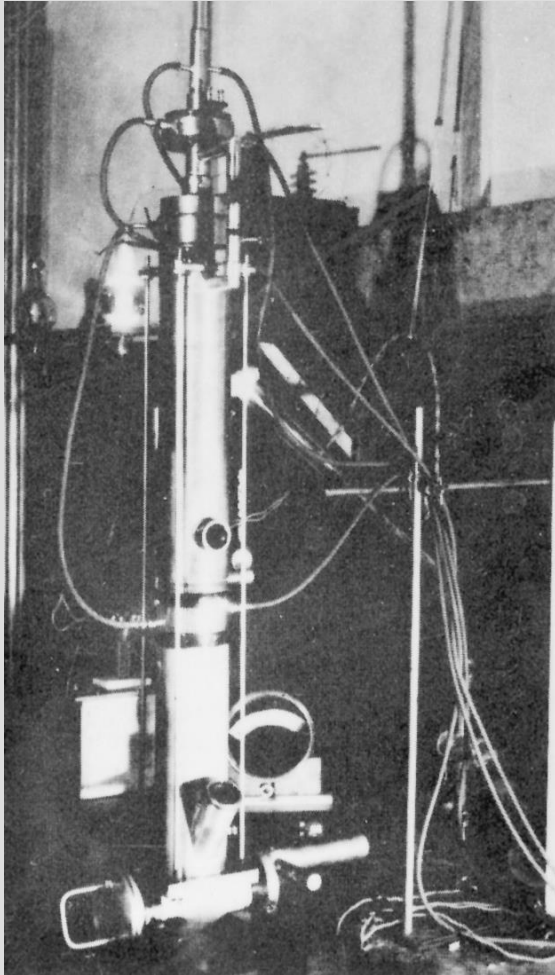


Figure 10. 1-9—Representative electron emission images from the microscope. Copied from the Anatomical record, Scott and Packer (1939). 1. Microincinerated section of skeletal muscle of cat. Note differentiation in amount of ash deposit in the most central muscle fiber, X 150; 2. Photograph of area of cathode surface used to obtain electron microscope picture shown in 3 and 6. There is no detectable optical differentiation on the cathode surface, X 150; 3. Electron microscope picture showing calcium and magnesium in the contraction nodes of skeletal muscle. Compare with 1 in which the total ash is shown, X 150; 4. Electron microscope picture of cross section of frog sartorius muscle showing magnesium and calcium only in the muscle fibers. The “tissue spaces” show little if any of these elements, X 25; 5. Electron microscope picture of cross section of cat skeletal muscle. Compare with 4, X 66; 6. Electron microscope picture of the same area as that in 3 at lower magnification, X 67; 7 and 8. Electron microscope pictures of skeletal muscle fibers showing localization of magnesium and calcium. The light areas represent these elements in the muscle fibers, X 86 and X72; 9. Low power electron microscope pictures of skeletal muscle fibers. Note lack of magnesium and calcium in the “tissue spaces,” the deposits being confined almost entirely to the muscle cells, X 32.

1930-1940

Development of the TEM

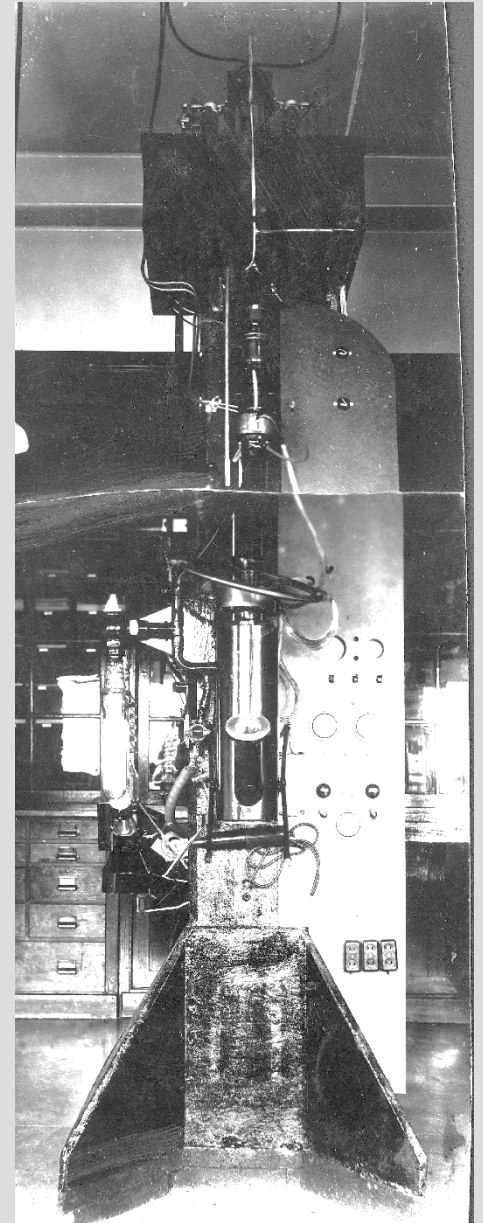
The first US TEMs



Fitzsimmons-Anderson (1937)
Washington State University



Newberry-Packer (1938)
Washington University, St. Louis



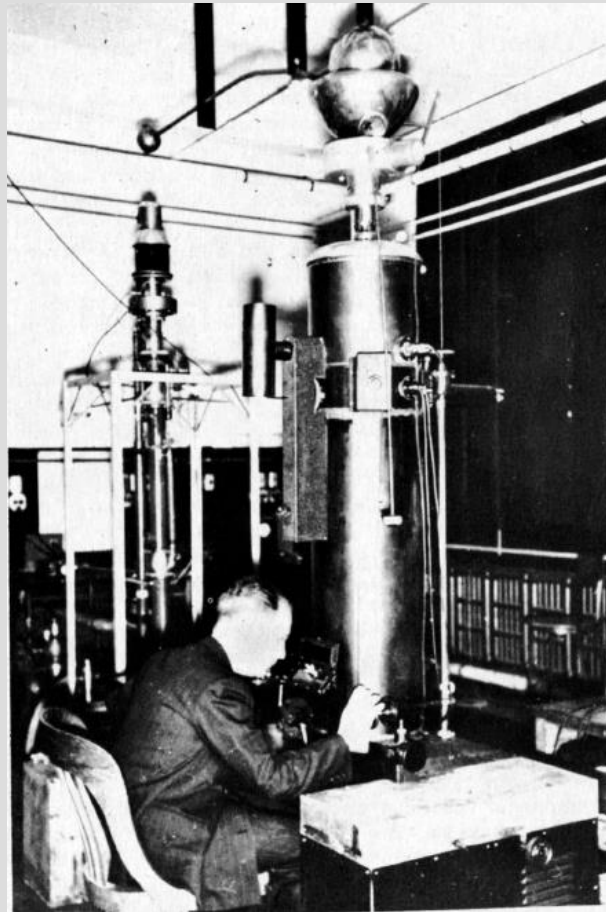
1930-1940

Development of the TEM

The first biological electron micrograph

Ladislau Marton
Hungarian / Swiss

Started in Belgium, then RCA, Stanford, NBS



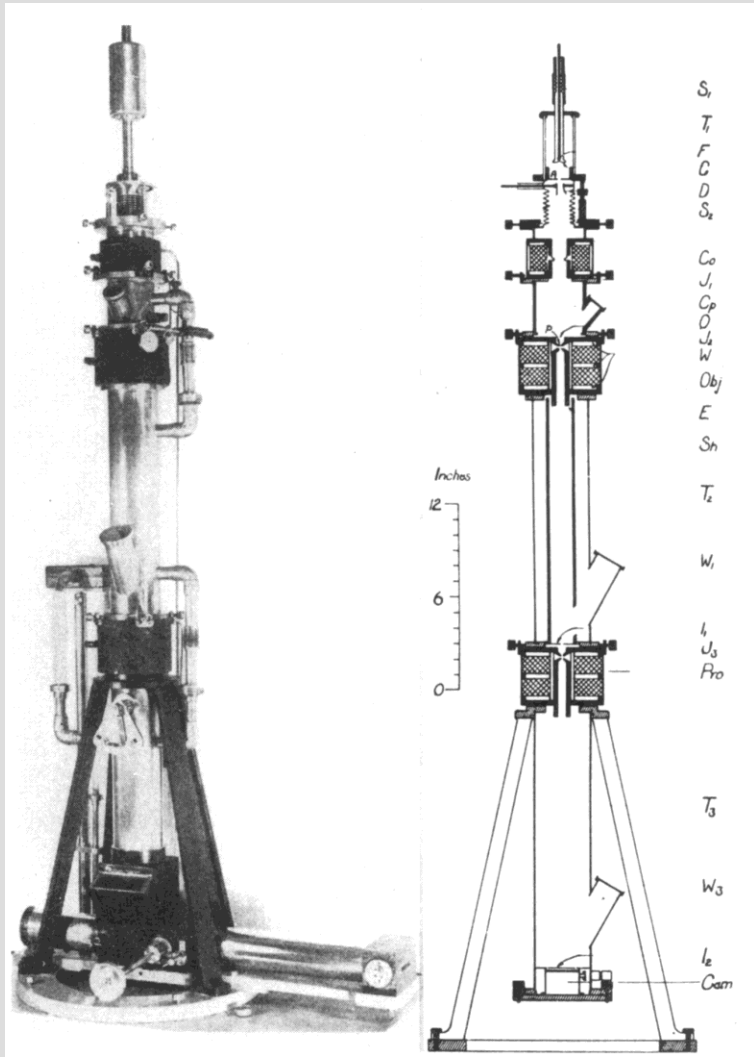
First-ever biological object (slice of leaf)
Brussels, 1934 (450x)

- First to use thin slices (15 μ m thick!)
- First to use osmium fixation/staining
- First to use copper grids for support

1930-1940

Development of the TEM

The first high-resolution electron microscopes in North America



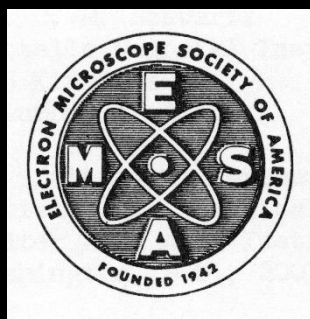
E F Burton,
Toronto:
Hillier and
Prebus,
1938



1930-1940

**Group of
E.F. Burton
in Toronto**



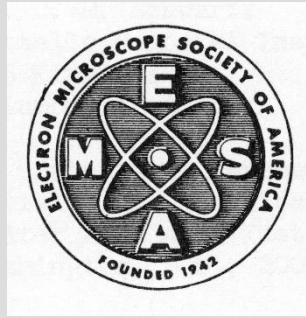


1940-1950

1940-1950

Founding of EMSA

1942



1940-1950

Development of the TEM

Otto Scherzer 1949: Scherzer Focus; Will atoms be visible in the TEM?

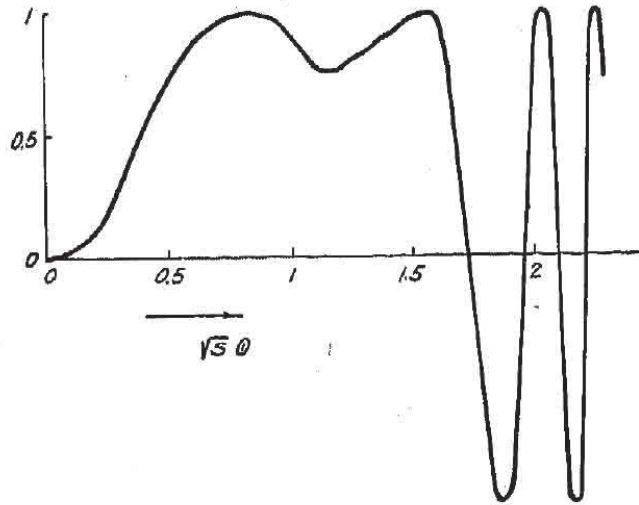


FIG. 4. The function $\sin(3s^3 - s^4)$, describing the phase shift in case of optimum contrast.

VOLUME 20, JANUARY, 1949

PHYSIKALISCHE BLÄTTER

1949 Heft 10.11 Seite 460 -- 463

Prof. O. Scherzer

Können Atome im Elektronen-Mikroskop sichtbar werden?

... des Auflösungsvermögens für möglich. Es ist also anzunehmen, daß die weitere Entwicklung des Elektronen-Mikroskops eines Tages nicht nur die schweren Jod-Atome des Moleküls, das wir unseren Betrachtungen zu Grunde gelegt haben, sichtbar machen wird, sondern auch die leichten Kohlenstoffatome und damit die Struktur von Molekülen, die weniger übersichtlich gebaut sind.

1940-1950

Development of the TEM

Ernst Ruska and
Siemens manufacture

ÜM-100
First series
production,
1939



ÜM-100
Prototype



Ernst Ruska at
Elmiskop I,
(Introduction, 1954)

ÜM-100 at
NMHM, Silver
Spring, MD
(40 produced)

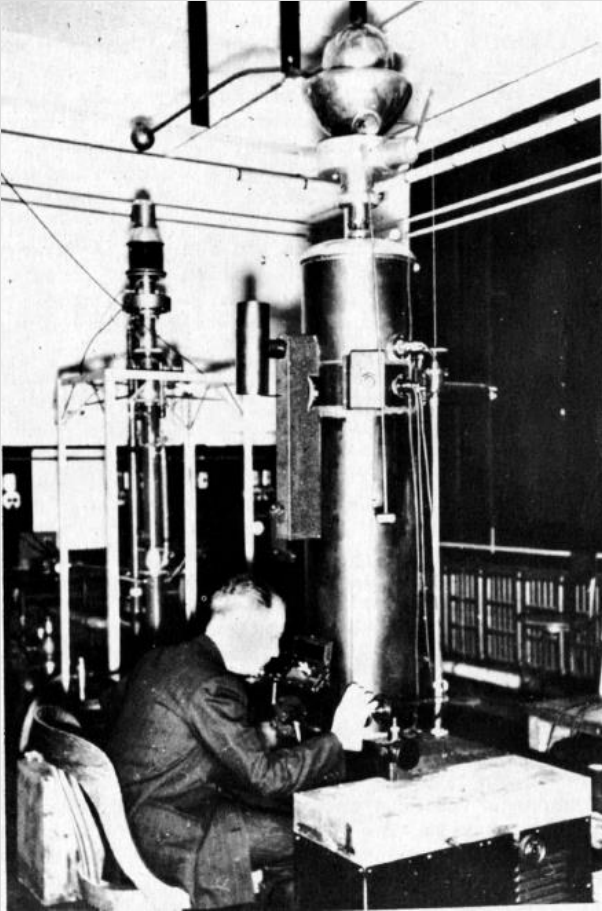


Helmut Ruska and
George Edwards
at Elmiskop I,
Albany, 1957

1940-1950

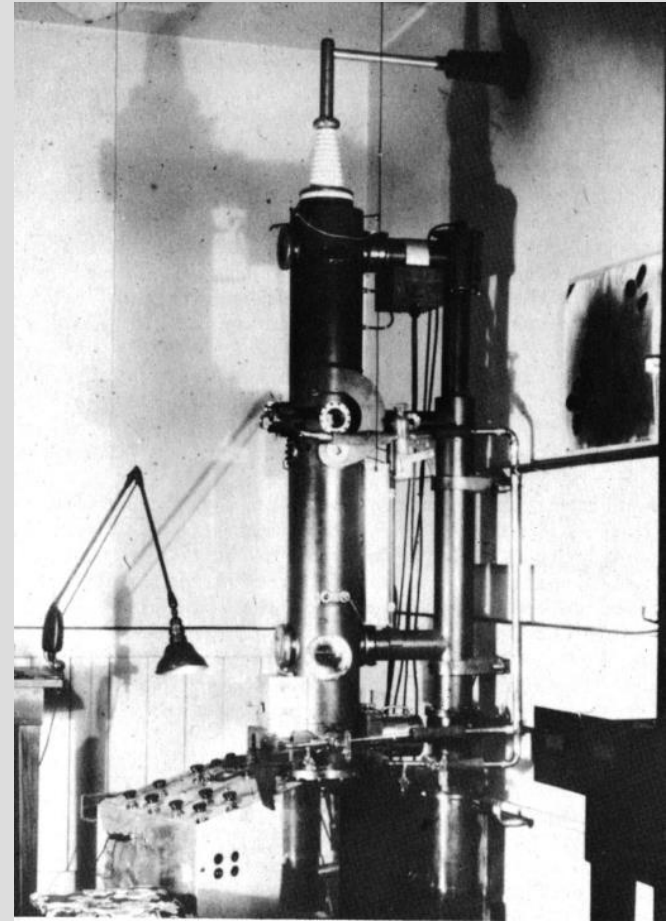
Development of the TEM

TEM development by Marton



1939 RCA Model A (4th TEM),

- Entire EM inside shielded vacuum chamber
- 3rd TEM (1938, from Brussels) is in the back



Stanford TEM, 1943

- Adjustable polepieces
- Double condenser
- Hydraulic specimen stage

1940-1950

Development of the TEM

Hillier and Zworykin at RCA



James Hillier and Alexander Zworykin with first production RCA EM: EMB, 1941 (60 manufactured)

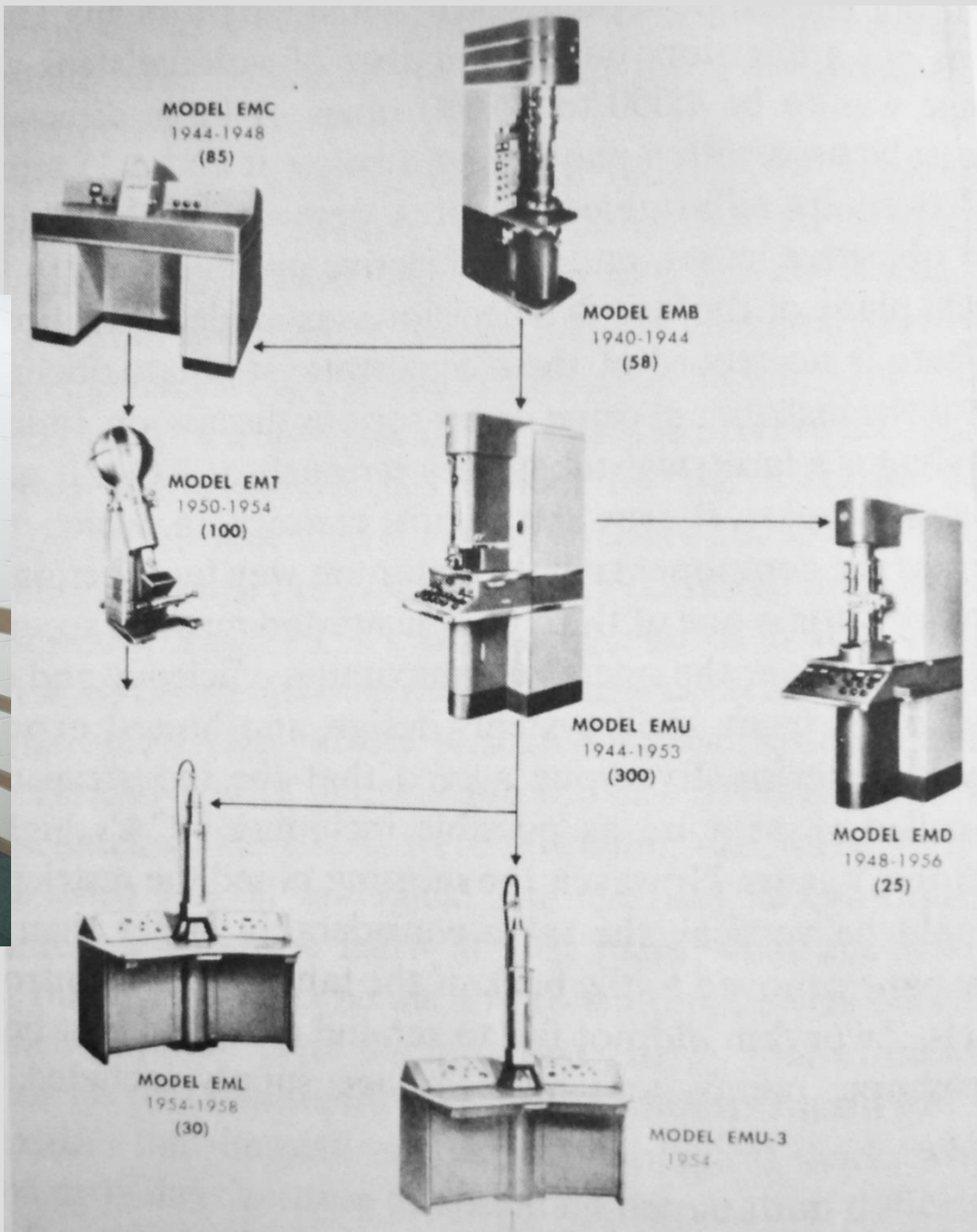


RCA EMU, 1944 (with Delbert Philpott) (First EMU sold in 1945)

1940-1950

Development of the TEM

RCA history



MSA President
John Reisner at
RCA tabletop
TEM

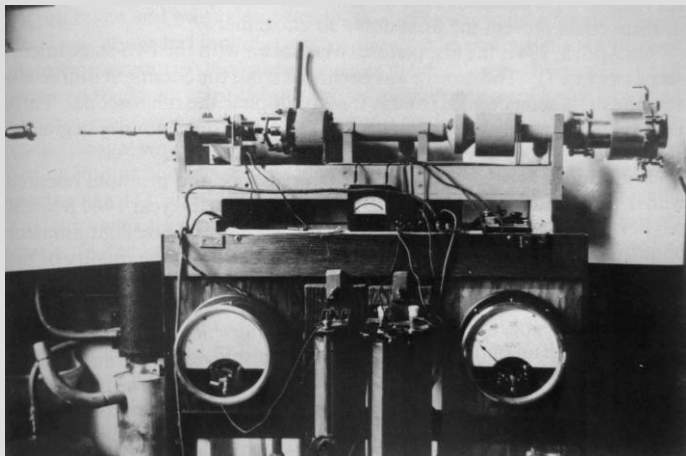


EMB
First production
model

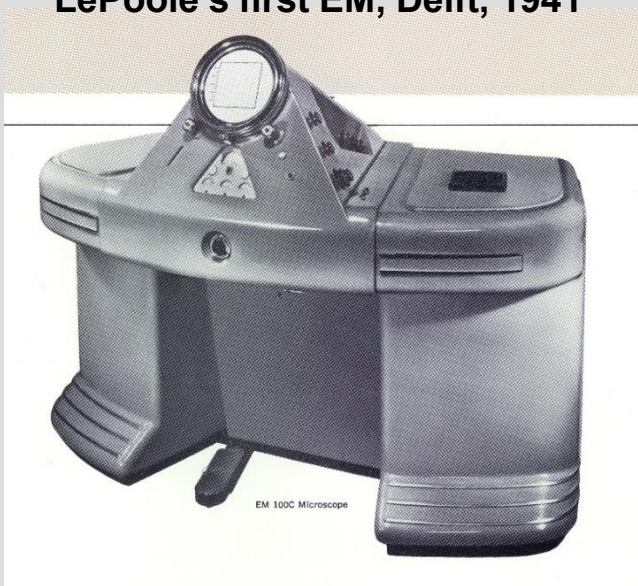
1940-1950

Development of the TEM

Netherlands (Philips)



LePoole's first EM, Delft, 1941



Philips EM100 (LePoole and van Dorsten)

Most-produced TEM of any single model (1850)



Philips EM300, 1966: First transistorized TEM

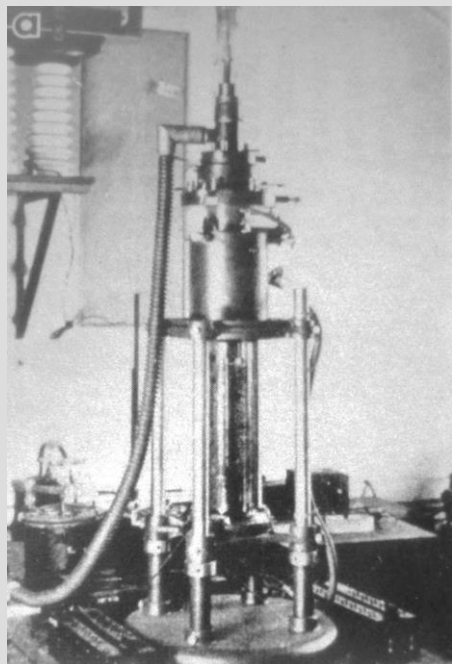


Introduction of Philips EM100, 1949: Image wobbler

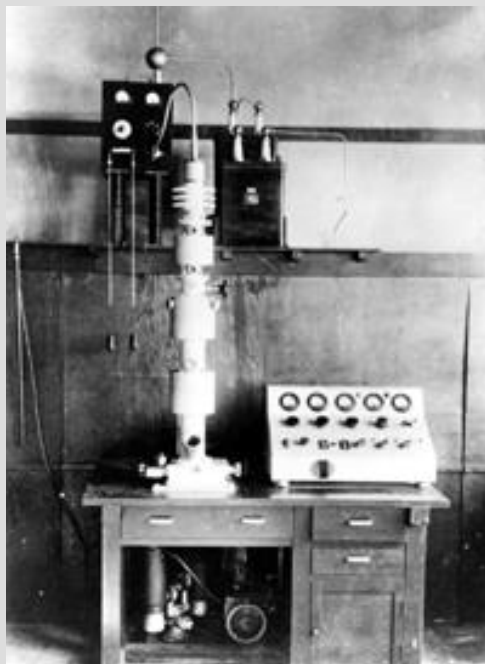
1940-1950

Development of the TEM

Japan



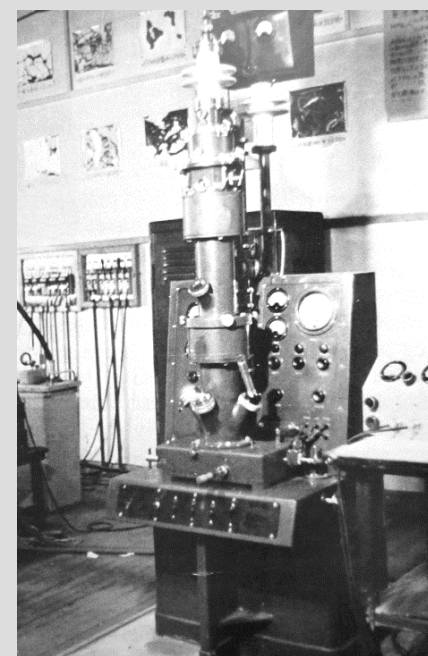
Osaka, 1939
(higher-res
than a light
microscope)



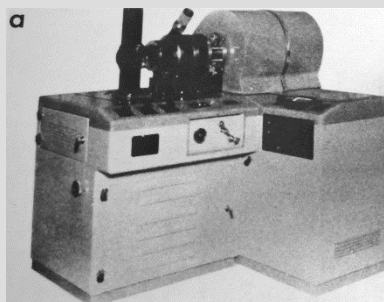
JEOL DA-1, 1947



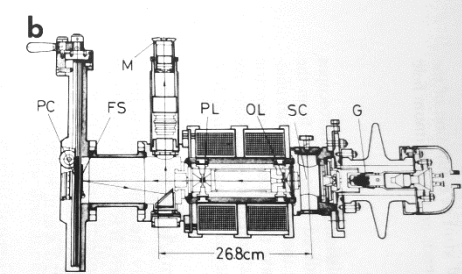
Hitachi Prototype, 1947



Hitachi HU-6, 1948



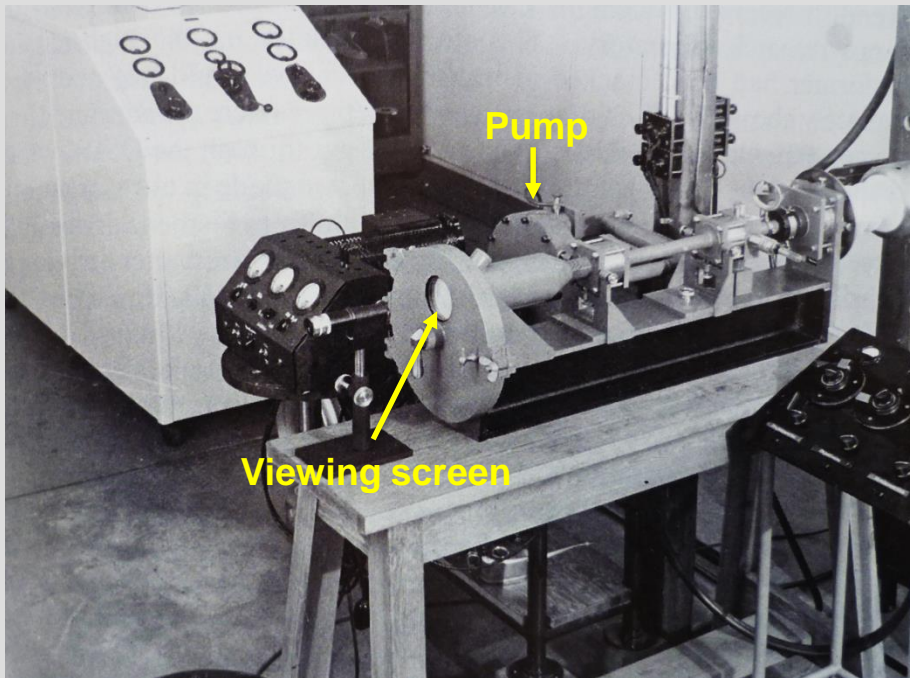
Shimadzu, 1950



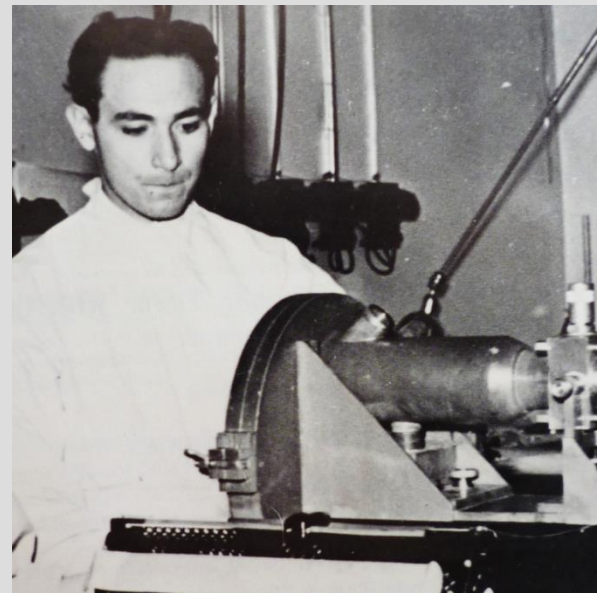
1940-1950

Development of the TEM

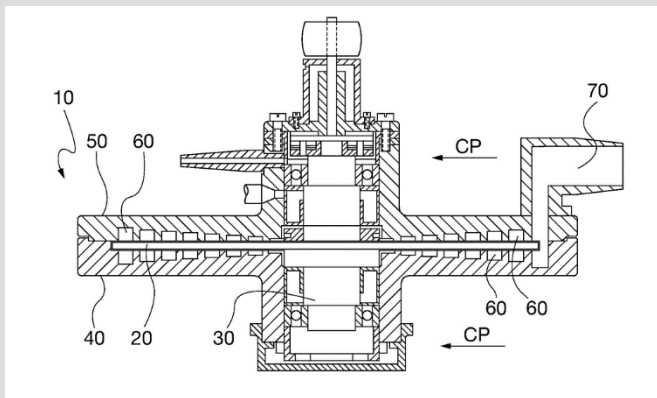
Sweden



Siegbahn TEM, 1942



Fernandez-Moran at Siegbahn TEM:
2 nm resolution in 1940s because of
oil-free vacuum system.



Siegbahn oil-free
vacuum pump

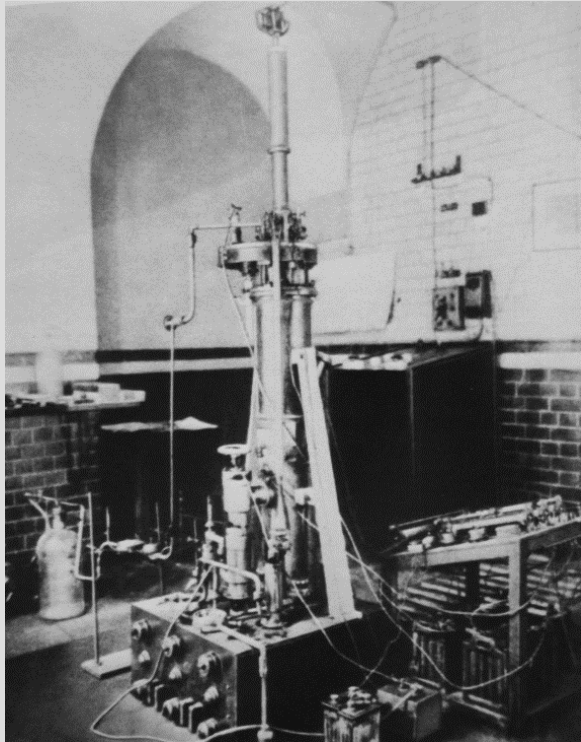


Manne
Siegbahn

1940-1950

Development of the TEM

UK



Metropolitan-Vickers EM1, 1936
First commercial EM (but not series-produced)

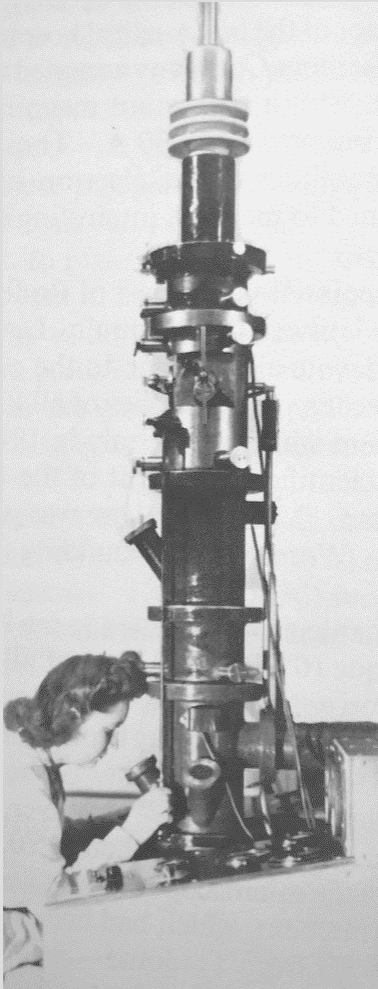


Metropolitan-Vickers EM2, 1946
(series-produced)

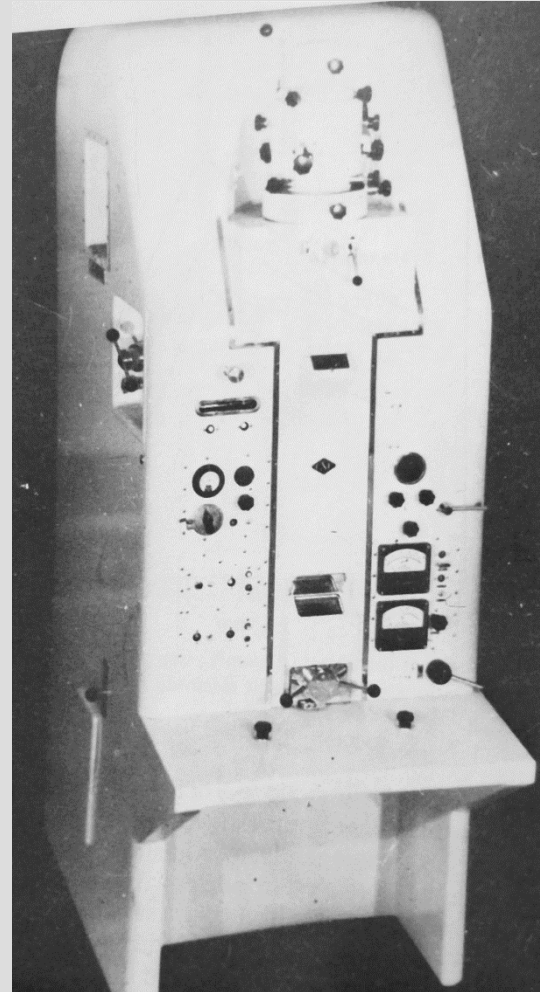
1940-1950

Development of the TEM

France



1940s Toulouse TEM –
magnetic lenses



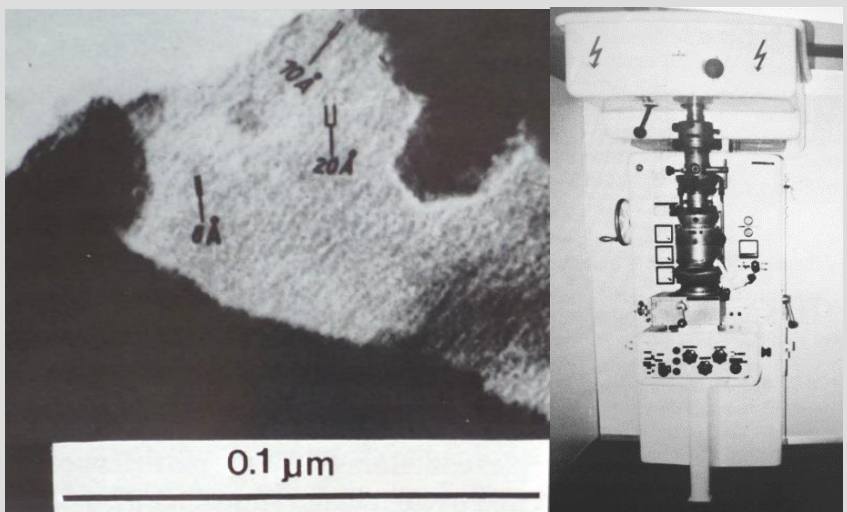
CSF type M III, 1943 (Production from 1945) –
electrostatic lenses

1940-1950

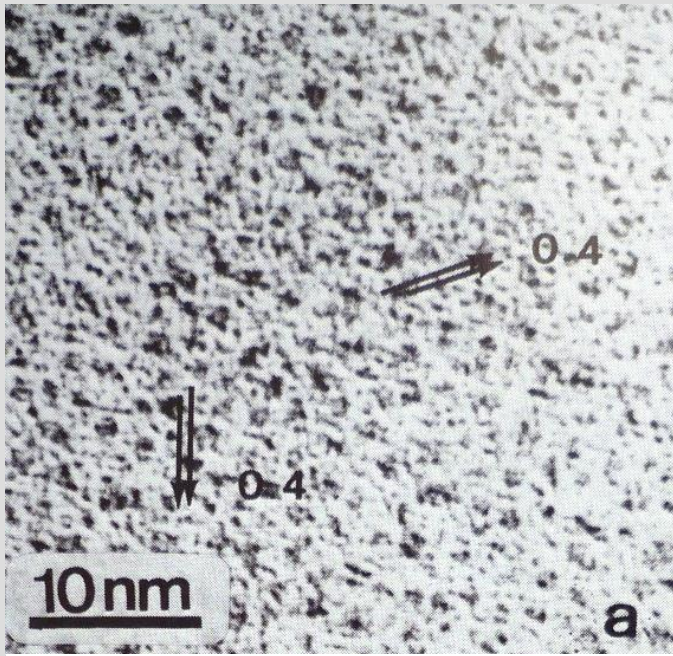
Development of the TEM

Siemens manufacturing

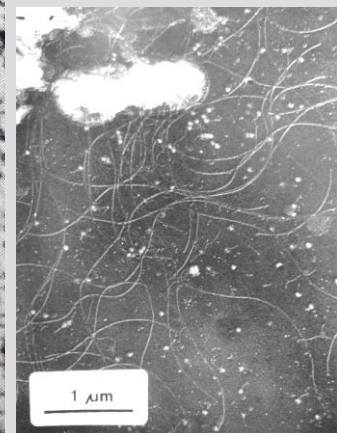
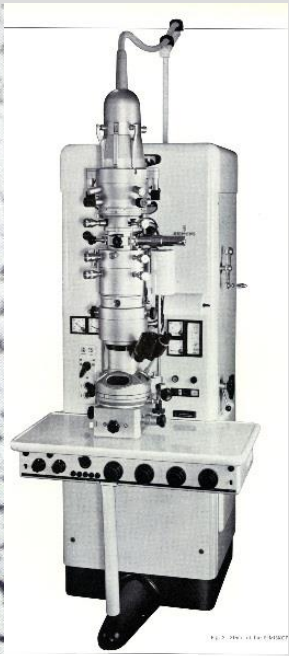
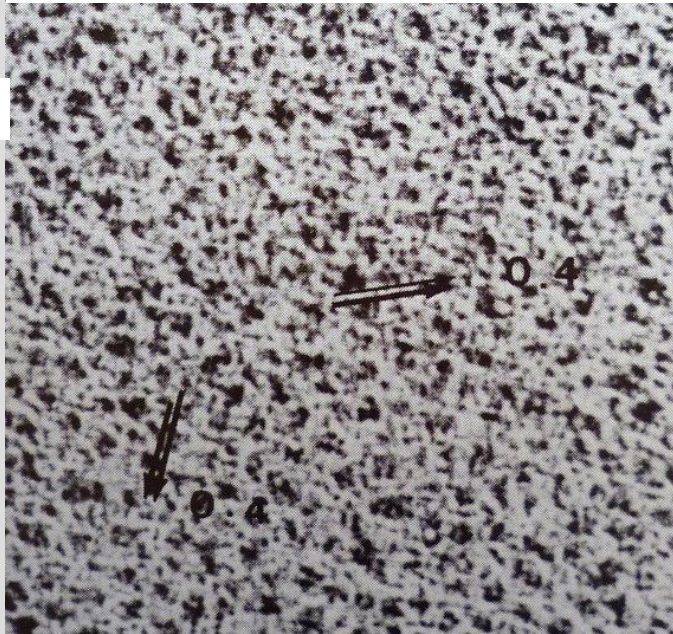
Difficulties in finding resolution-test specimen!



1940 UM100: (Be-coated peat), 4 nm (labels wrong!)



1964 Elmiskop Ia: (evaporated Pt / Ir alloy), 4 Å

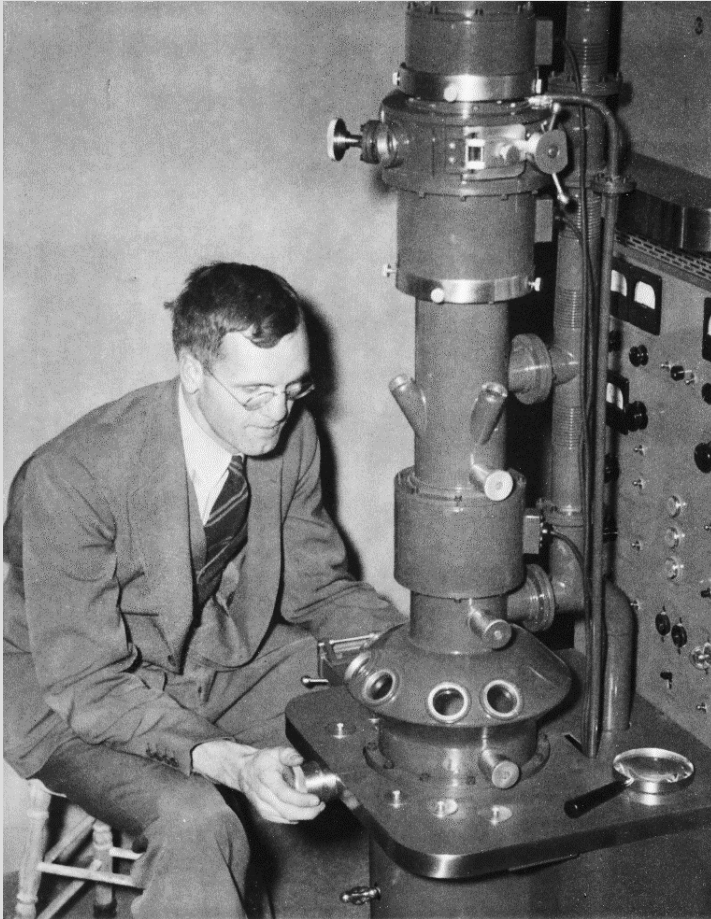


Siemens applications lab, 1930s,40s

1940-1950

Early development of specimen preparation

First whole-cell imaging



Ernest F. Fullam with RCA EMB, 1944



Keith Porter

- One of the founders of Cell Biology*
- First whole-cell EM micrograph
- Ultramicrotome development
- Founded Boulder HVEM lab

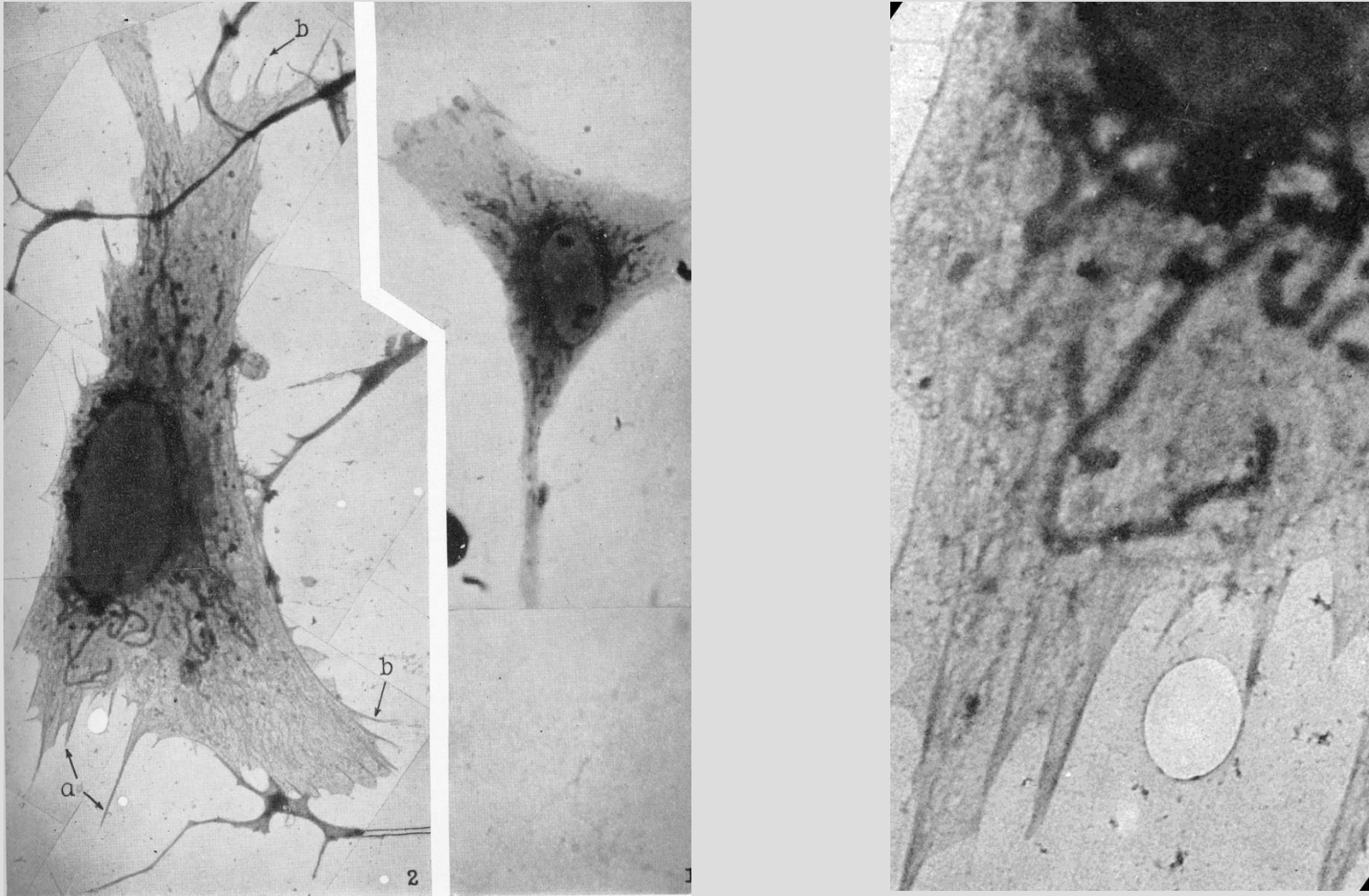
*

- 1955 started *Journal of Biophysical and Biochemical Cytology*
- 1956 “Conference on Tissue Fine Structure” at NIH: Start of “Cell Biology”
- 1962 JBBC renamed *Journal of Cell Biology*

1940-1950

Early development of specimen preparation

First whole-cell imaging



Chicken heart cell (osmium fixed, dried), prepared by Keith Porter, photographed by Ernest F. Fullam (1944)

1940-1950

Early development of specimen preparation

Early images of bacteria and viruses – air-dried

THE INTERNAL STRUCTURE OF CERTAIN BACTERIA AS REVEALED BY THE ELECTRON MICROSCOPE—A CONTRIBUTION TO THE STUDY OF THE BACTERIAL NUCLEUS

GEORGES KNAYSI AND STUART MUDD

The Laboratory of Bacteriology, New York State College of Agriculture, Cornell University, Ithaca; the Department of Bacteriology, The School of Medicine, University of Pennsylvania, Philadelphia; and the Research Laboratories, RCA Manufacturing Company, Camden, N. J.

Received for publication September 8, 1942



PATHOGENIC BACTERIA, RICKETTSIAS AND VIRUSES AS SHOWN BY THE ELECTRON MICROSCOPE

THEIR RELATIONSHIPS TO IMMUNITY AND CHEMOTHERAPY

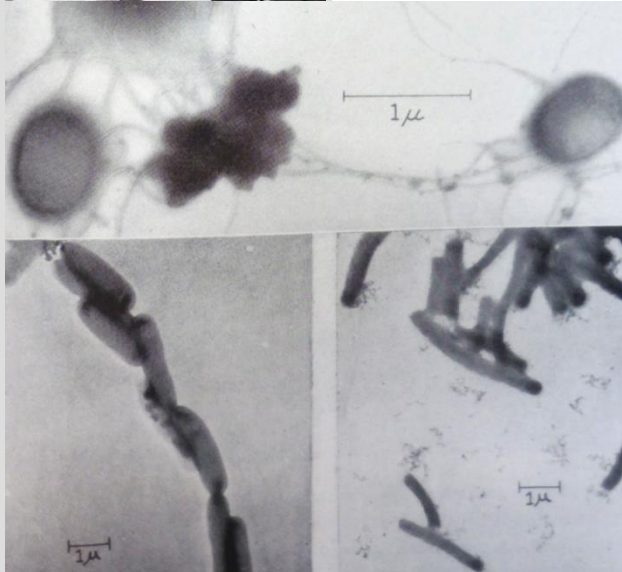
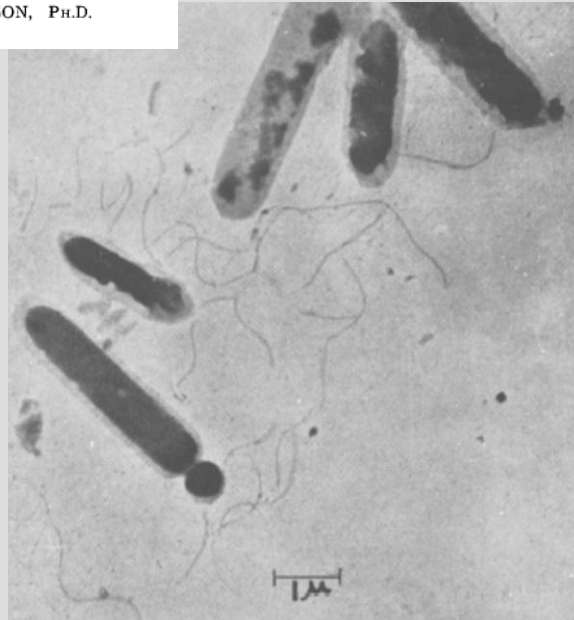
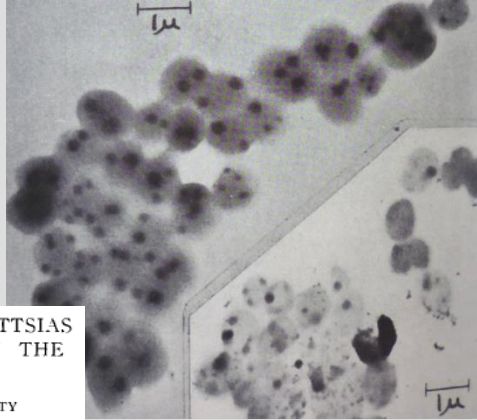
I. MORPHOLOGY

STUART MUDD, M.D.

AND

THOMAS F. ANDERSON, Ph.D.

PHILADELPHIA



BACTERIAL MORPHOLOGY AS SHOWN BY THE ELECTRON MICROSCOPE

I. STRUCTURAL DIFFERENTIATION WITHIN THE STREPTOCOCCAL CELL¹

STUART MUDD AND DAVID B. LACKMAN

Department of Bacteriology, School of Medicine, University of Pennsylvania

Received for publication August 1, 1940

BACTERIAL MORPHOLOGY AND ELECTRON MICROSCOPE 417

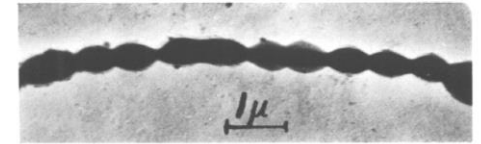


FIG. 2. C203 MUCOID; PREPARED FROM AN 18-HOUR BLOOD AGAR PLATE CULTURE; MAGNIFICATION 11,000 DIAMETERS

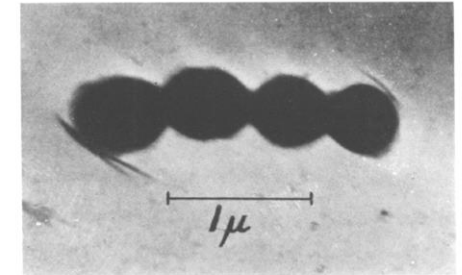


FIG. 3. C203 SMOOTH; PREPARED FROM AN 18-HOUR BLOOD AGAR PLATE CULTURE; ELECTRONIC MAGNIFICATION 12,000 DIAMETERS; TOTAL MAGNIFICATION 26,500 DIAMETERS

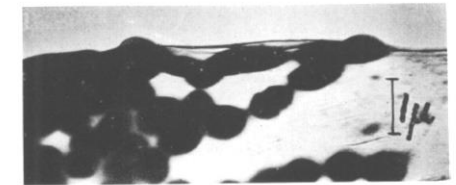


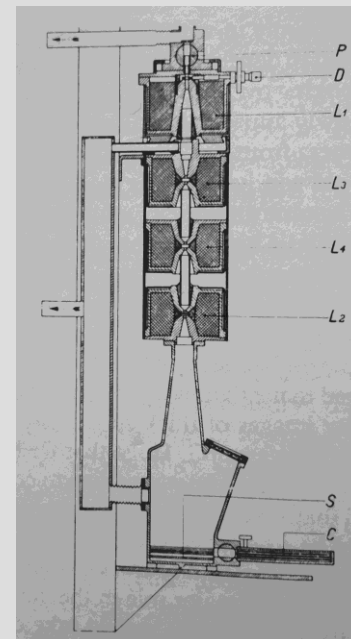
FIG. 4. C203 MUCOID; PREPARED FROM AN 18-HOUR BLOOD AGAR PLATE CULTURE; MAGNIFICATION 11,000 DIAMETERS; FILM BROKEN, SHOWING STREPTOCOCCI IN PROFILE

1940-1950

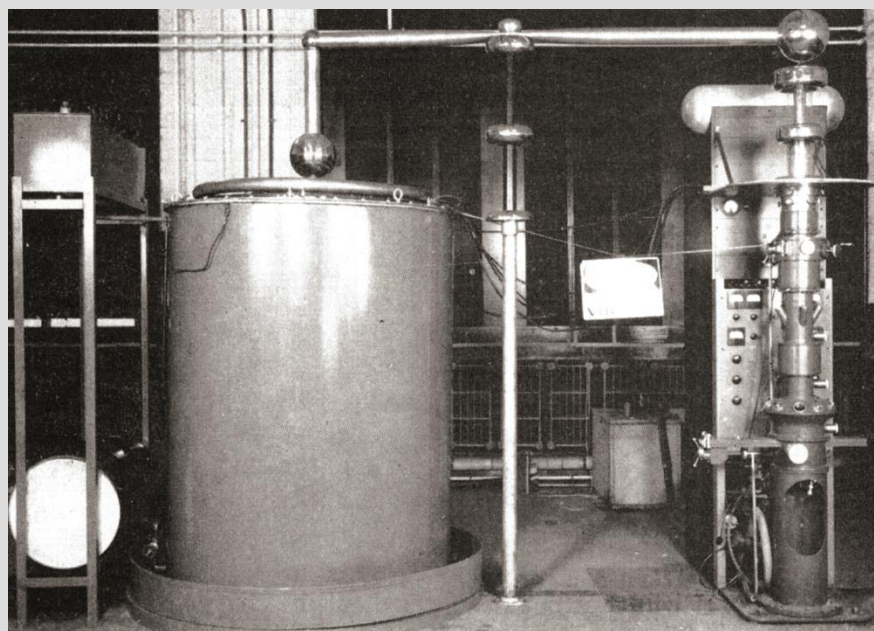
Early development of specimen preparation

400 keV to deal with specimen thickness

First 400 keV TEM:
LePoole, ~1941



RCA 400 keV TEM, ~1942



50 keV



200 keV



400 keV

1940-1950

Early development of specimen preparation

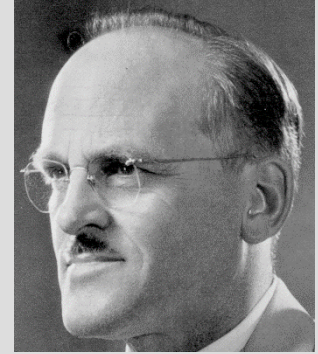
Early images of muscle fibers – PTA-stained

The Structure of Certain Muscle Fibrils as Revealed by the Use of Electron Stains*

C. E. HALL, M. A. JAKUS, AND F. O. SCHMITT

Department of Biology and Biological Engineering, Massachusetts Institute of Technology, Cambridge, Massachusetts

(Received April 4, 1945)



AN INVESTIGATION OF CROSS STRIATIONS AND MYOSIN FILAMENTS IN MUSCLE *

C. E. HALL, M. A. JAKUS, AND F. O. SCHMITT

Department of Biology, Massachusetts Institute of Technology, Cambridge, Massachusetts

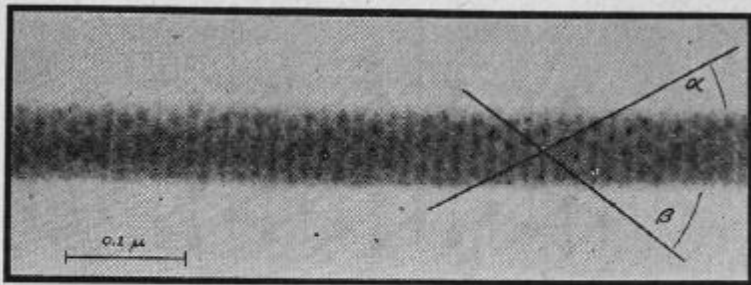
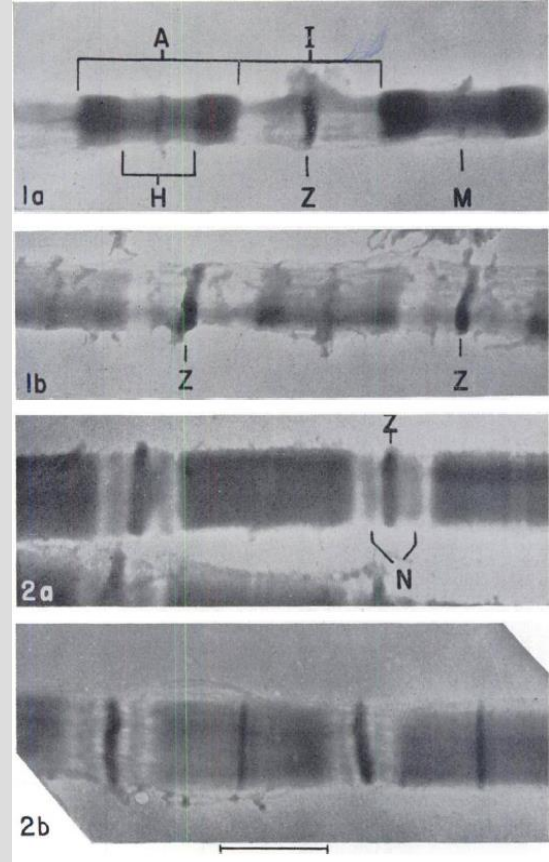


FIG. 4. Portion of muscle fibril showing geometrical disposition of stained regions ($\times 113,000$).



1940-1950

Early development of specimen preparation

Metal shadowing for higher resolution



Robley Williams

Formvar replicas used in material sciences; yielded high-resolution surface structure without thinning the sample.

TECHNICAL PAPERS

Electron Micrographic Observations of Tobacco Mosaic Virus in Crude, Undiluted Plant Juice¹

Robley C. Williams and Russell L. Steere
University of Michigan, Ann Arbor

Several reports have been published (2, 3, 4, 5, 6) of electron microscopic studies of the tobacco mosaic virus in various degrees of impurity. In no study, however, has the infected juice been used in its crude, undiluted form. There has always been some degree of treatment, if only with distilled water, prior to observation in the electron microscope. The published micrographs of the impure material are qualitatively similar to those obtained from freshly purified material.

We have recently obtained electron micrographs of a wild strain of tobacco mosaic¹ grown in White Burley

up in a micropipette, and a bubble was blown over the surface of the specimen screen. The bubble was quickly wiped across the screen, and a very thin film of material was left behind. This film dried almost instantly, and the dried specimen was then shadowed with uranium. The total elapsed time between expressing the juice and drying the film was about 15 sec.

A typical micrograph from a 14-day-old infection is shown in Fig. 1. As can be readily seen, the virus particles appear in the form of large bundles, or sheaves, whose length is roughly 1 to 3 μ , and whose diameter, or width, varies greatly but might average 150 m μ . The background appears quite coarse, since it consists of all of the nonvolatile plant material. Uninfected plants are found to exhibit none of these bundle-like forms. The size and frequency of the typical forms shown in Fig. 1 increase with the age of the infection, being barely visible at 36 hrs after inoculation.

Fig. 2 illustrates the probable reason why previous work with "crude" juice has not exhibited the sheaves

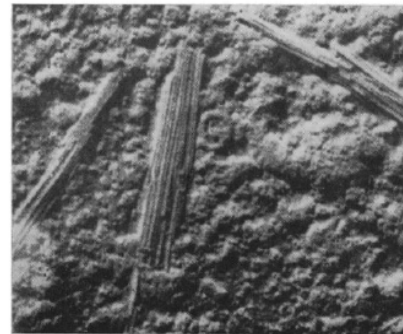


FIG. 1. Electron micrograph of expressed, crude juice of White Burley tobacco leaf infected with a wild strain of tobacco mosaic virus. Note the bundle-like forms in which the virus is seen. Magnification is 30,000 \times .

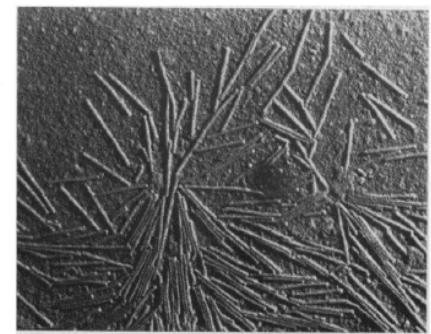
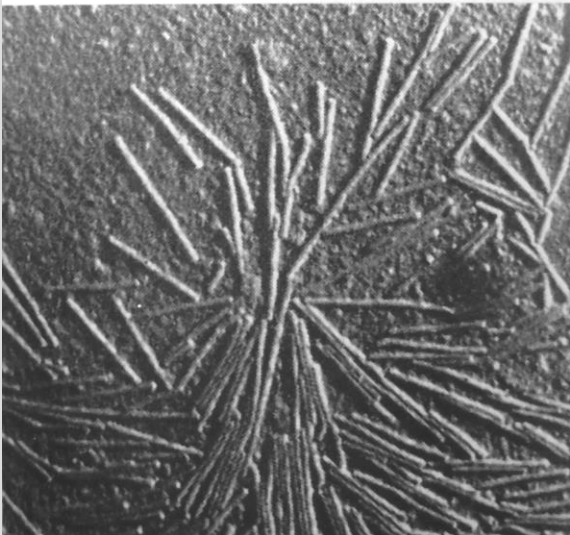
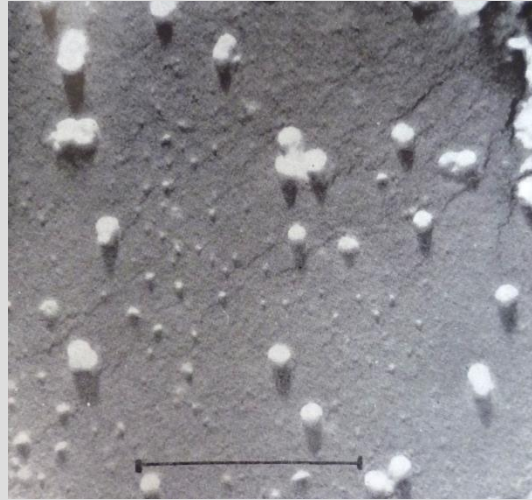
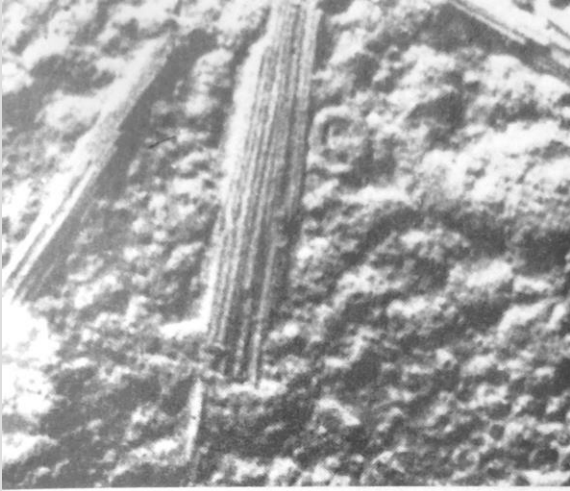


FIG. 2. Electron micrograph of the same infected material as is shown in Fig. 1, except that the dried preparation was washed briefly with distilled water. Note that the virus particles are now partially dispersed in individual rods. Magnification is 30,000 \times .

1940-1950

Early development of specimen preparation

Metal shadowing for higher resolution



T4

TMV

1940-1950

Early development of specimen preparation

Microtomy

Sectioning Techniques for Electron Microscopy Using a Conventional Microtome.

DANIEL C. PEASE AND RICHARD F. BAKER.

From the Departments of Anatomy and Experimental Medicine, School of Medicine, The University of Southern California, Los Angeles, Calif.

Reduced smallest advance from $1\ \mu\text{m}$ to $0.1\ \mu\text{m}$, but embedment too soft.

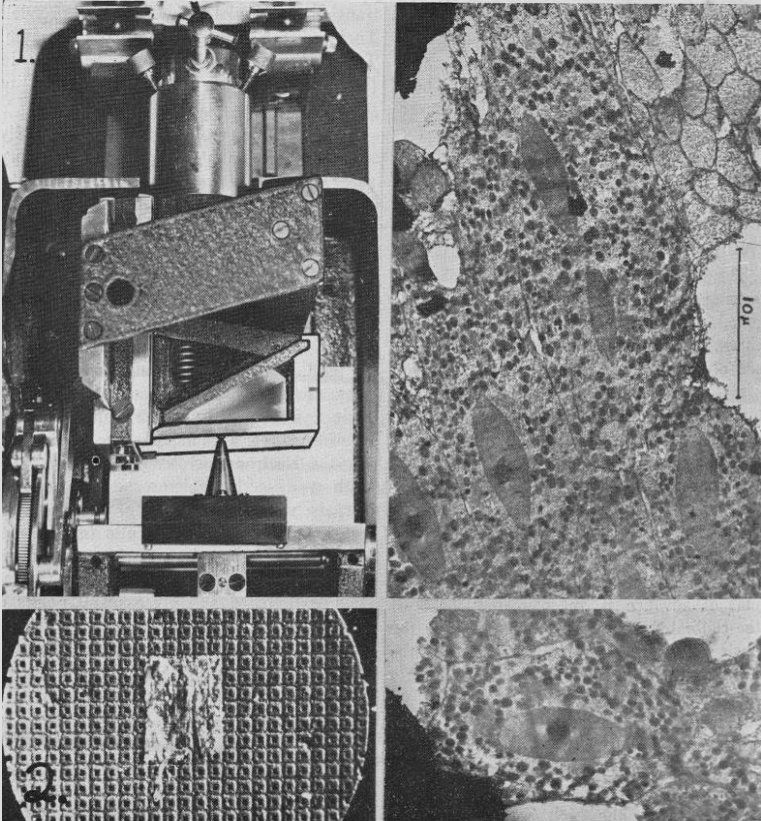


FIG. 1.
Vertical view of Spencer microtome modified by the outlined attachment to cut 0.1 micron.

1940-1950

Early development of specimen preparation

Microtomy

Reprinted from THE AMERICAN JOURNAL OF ANATOMY
Vol. 78, No. 2, March, 1946

SECTIONING FOR THE ELECTRON MICROSCOPE ACCOMPLISHED BY THE HIGH SPEED MICROTOME

ALBERT E. GESSLER AND ERNEST F. FULLAM
Research Laboratories of Interchemical Corporation, New York¹

ELEVEN PLATES (TWELVE FIGURES)

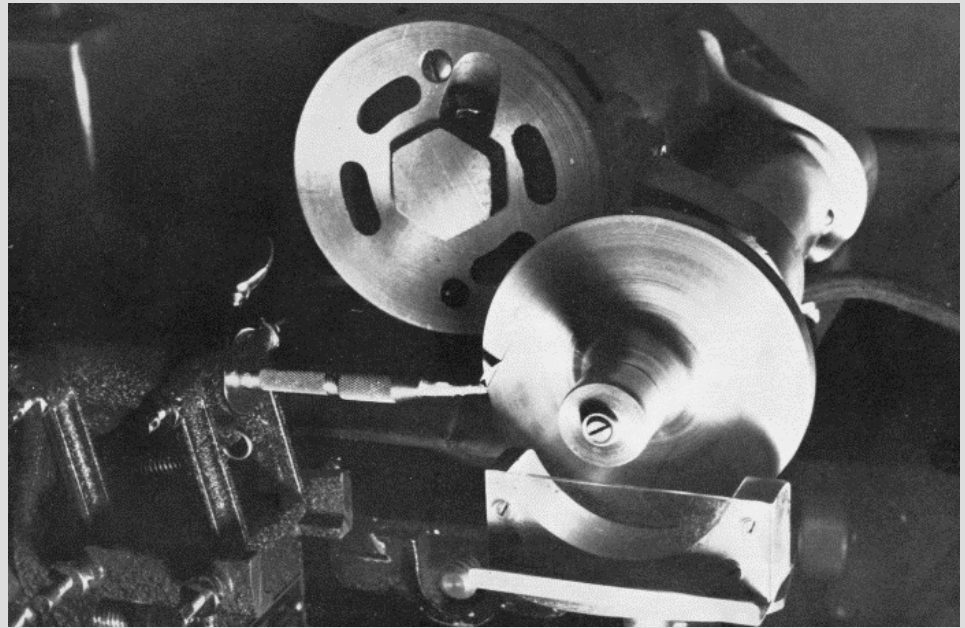
During the few years since the electron microscope has become available as a scientific instrument, its great advantages as well as its disadvantages in comparison to the light microscope have unfolded to many observers. The amount of useful magnification which a microscope is capable of producing is limited by its power of resolution which is the instrument's ability to register fine detail. A light microscope is quite capable of a high degree of magnification, but the instrument's limit of resolution is reached around 1200-1500 magnification.² Further magnification above that limit by optical or photographic means will further enlarge the object or its picture, but will bring out no further detail. It is the fundamental endowment and outstanding advantage of the electron microscope to possess excellent power of resolution and sharp definition up to 20,000 diameters (Zworykin and Hillier, '44). Micrographs of such magnification, by virtue of their sharp definition, can very advantageously be further enlarged photographically up to 100,000 diameters.

Another great advantage of the electron microscope is its much greater depth of field. It presents the invaluable possibility of stereoscopic micrographs possessing such good con-

¹The authors wish to express their full appreciation for the support of this work by a specific grant from the Lillia Babbitt Hyde Foundation.

²Using ultra violet illumination, resolution is increased to about 2,000 diameters of useful magnification.

Fullam: Existed up until 2005 – up to 49,000 RPM!



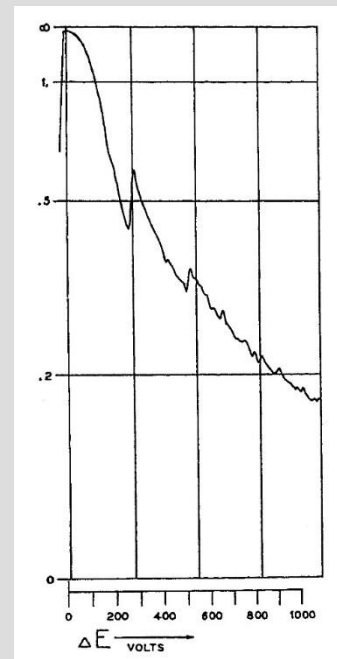
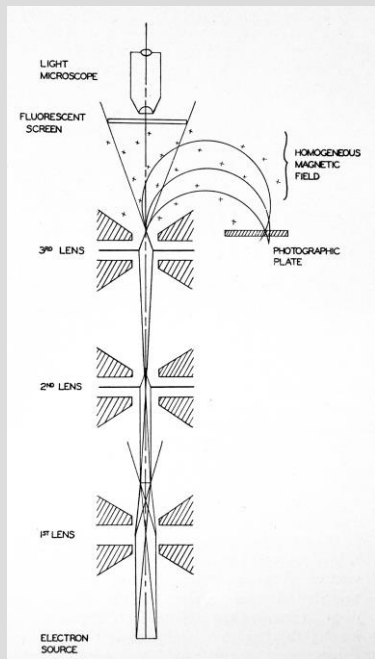
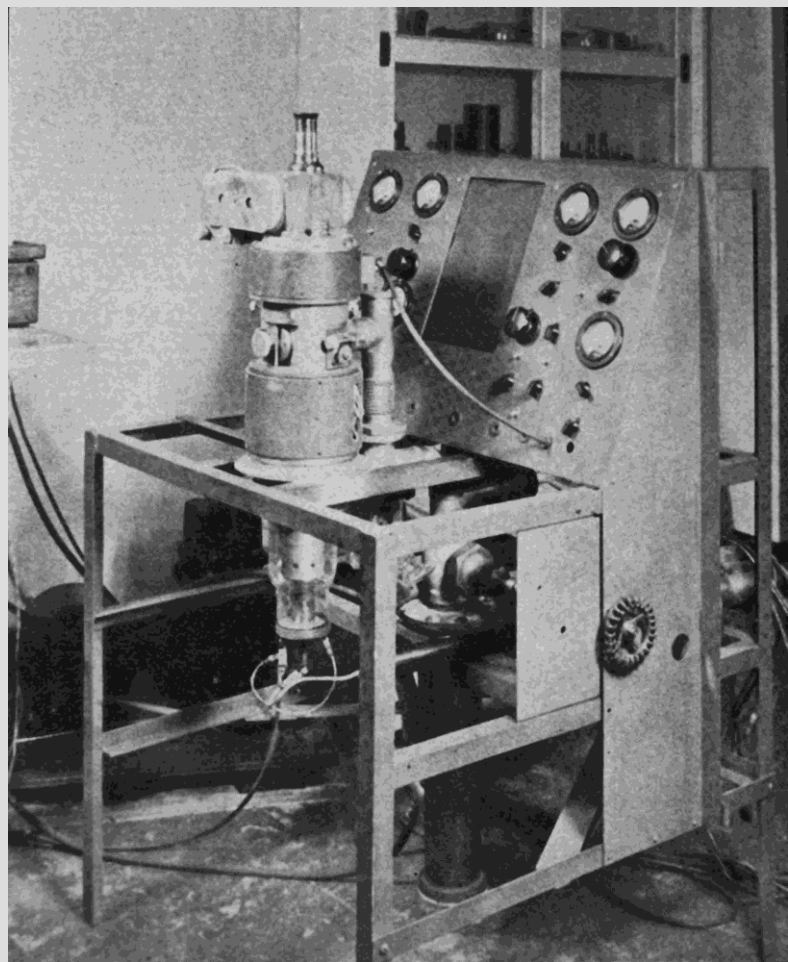
Theory: High speed produces a section before the material can compress.

But soft embedding media needed, which must be removed before imaging because no staining was done.

1940-1950

Very early electron probe microanalysis

James Hillier, "EELS" in 1945!



1940-1950

Early developments in physical sciences

1946: Electron Diffraction – John Cowley



NATURE No. 4016 October 19, 1946

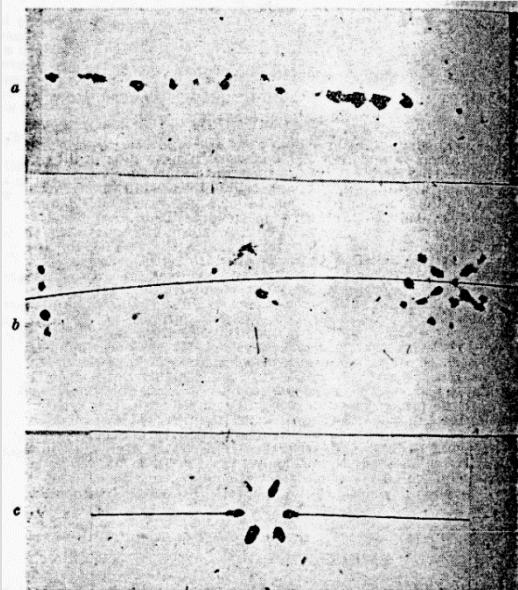


Fig. 1. EXAMPLES OF GROUPS OF REFLEXIONS RESULTING FROM REFRACTION BY CUBES OF MAGNESIUM OXIDE FOR (a) (200), (b) (220) and (c) (422) PLANES. UNDISPLACED RING POSITIONS ARE INDICATED BY THE CONTINUOUS LINE IN (b) AND (c). ENLARGEMENT FROM ORIGINAL PATTERN, 56 DIAMETERS



Fig. 2. PORTION OF ELECTRON DIFFRACTION PATTERN FROM CADMIUM OXIDE PARTICLES, SHOWING DIFFERENT LINE BREADTHS FOR 222, 400, 420 AND 422 REFLEXIONS. ENLARGEMENT 16 DIAMETERS

ELECTRON DIFFRACTION AND RECTIFICATION FROM SILICON AND PYRITE SURFACES

By J. M. COWLEY AND J. L. SYMONDS.

Received 3rd October, 1946.

Summary.

Electron diffraction and rectification investigations have been conducted on surfaces of pyrite and silicon for different surface conditions. There is evidence that, for the best rectification, the crystal lattice should be almost perfect and free from fracture or mosaic structure. A general picture of the polish layer on pyrite is built up from electron diffraction evidence.

Physics Department,
University of Adelaide,
South Australia.

ELECTRON DIFFRACTION BY FATTY ACID LAYERS ON METAL SURFACES.

By J. M. COWLEY.*

Received 3rd October, 1946.

Summary.

The structure and effect of heating of layers of palmitic acid on various metals have been investigated. The temperature at which the orientation of the molecules is lost, is below the bulk melting point for crystalline layers, and is 105°C . for monolayers, being independent of the metal used as base.

A new orientation in layers formed from fatty acids on metals is described, corresponding to an orthorhombic structure and giving a characteristic pattern. Such layers are not soluble in the usual solvents, do not lose their orientation until heated to over 400°C ., and remain on the surface in crystalline form to about 800°C . It is suggested that these properties arise from a change taking place under the influence of the electron beam.

Physics Department,
University of Adelaide,
South Australia.

1940-1950

Early developments in physical sciences

1946: Electron Diffraction – John Cowley

Acta Cryst. (1953). **6**, 522

Structure Analysis of Single Crystals by Electron Diffraction. II. Disordered Boric Acid Structure

BY J. M. COWLEY

Chemical Physics Section, Division of Industrial Chemistry, Commonwealth Scientific and Industrial Research Organization, Melbourne, Australia

(Received 11 December 1952)

The techniques of structure analysis using single-crystal electron-diffraction patterns have been applied to the study of very small boric acid crystals in which there is almost complete disorder in the stacking of the two-dimensional layers of atoms. The structure of the layers and the nature of the order present are derived by a method involving a 'distribution function' which defines the distribution in space of equivalent points in the layers. The hydrogen ions in the hydrogen bonds are shown to have their most probable positions approximately 1 Å from an oxygen atom. An apparent interaction between parallel hydrogen bonds is observed. Suggestions are made for the further application of the distribution-function method.

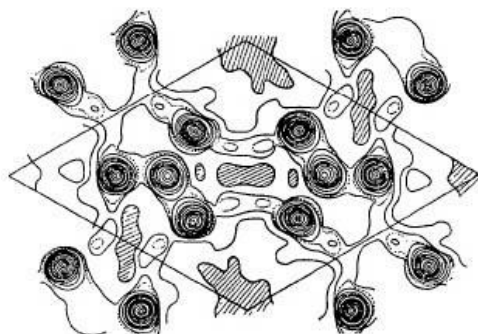


Fig. 6. Fourier projection of a boric acid layer, corrected for the effects of ordering by the distribution-function method.

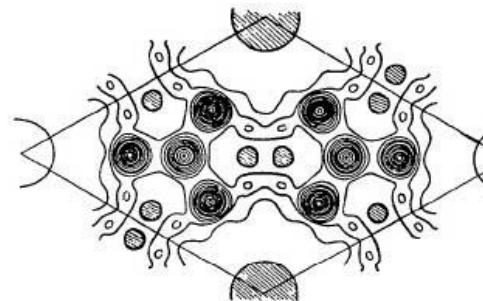


Fig. 8. Fourier projection of a boric acid layer obtained by using the corrected structure factors and assuming hexagonal symmetry.

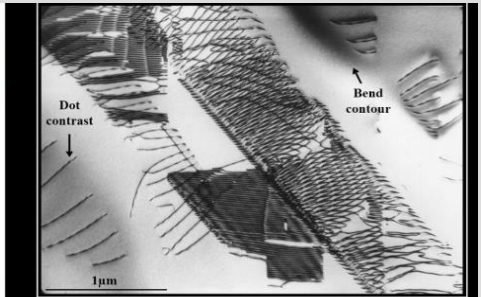
1940-1950

Early developments in physical sciences

1956: Hirsch et al.
First imaging of dislocations in metals



Electron Microscope used by Hirsch, Whelan, and Horne in 1956 when they made the first recorded observations of dislocations in the interior of a metal.



Dislocations in a Cu 8%Al alloy (1956)



1940-1950

Beginnings of TEM aberration correction

Otto Scherzer, 1945

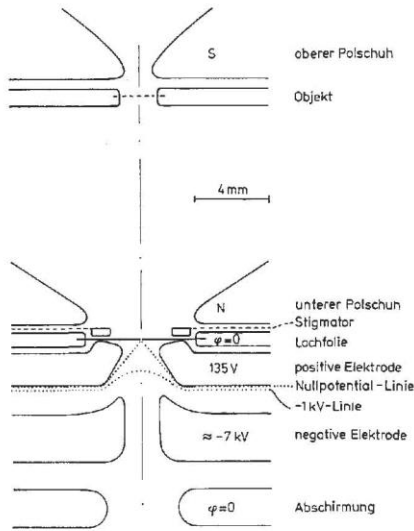


Abb. 3. Schnitt durch eine korrigierte Linse für $U = 60 \text{ kV}$, $A = 0$ (schematisch).

Sphärische und chromatische Korrektur von Elektronen-Linsen.

Von O. Scherzer, z. Zt. USA.

(Aus den Süddeutschen Laboratorien in Mosbach.)

(Mit 7 Textabbildungen.)

Die Brauchbarkeit des Elektronenmikroskops bei hohen Vergrößerungen wird durch den Öffnungsfehler und die chromatische Aberration beeinträchtigt. Beide Fehler sind unvermeidlich, solange die abbildenden Felder rotations-symmetrisch, ladungsfrei und zeitlich konstant sind. Die vorliegende Untersuchung soll zeigen, daß die Aufhebung irgendeiner dieser drei Einschränkungen genügt, um den Weg zur sphärischen und chromatischen Korrektur und damit zu einer erheblichen Steigerung des Auflösungsvermögens freizugeben.

Solange nicht klar zu sehen ist, welche Art Linsen das beste Mikroskop ergibt, müssen alle sich bietenden Wege verfolgt werden. Es scheint daher angebracht, etwas ausführlicher auf die verschiedenen Arten korrigierter Linsen einzugehen.

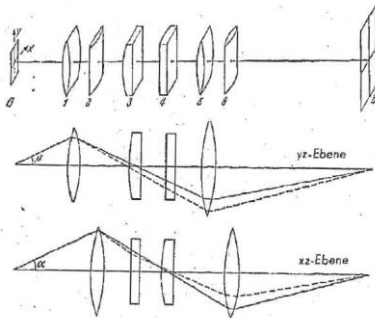
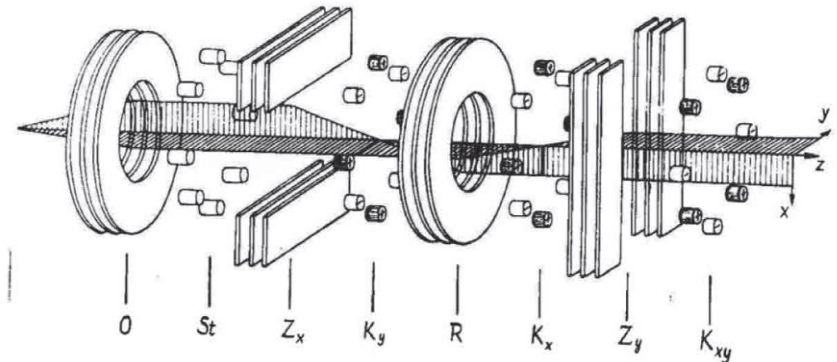
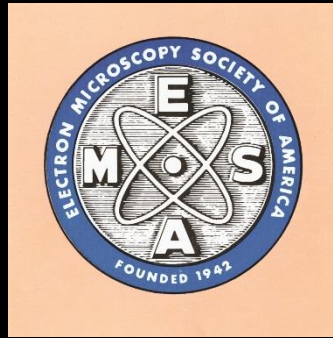


Abb. 2. Achromatische Abbildung durch Zylinderlinsen und Korrekturstücke.
— mittelschnelle Elektronen, - - - langsamere Elektronen.

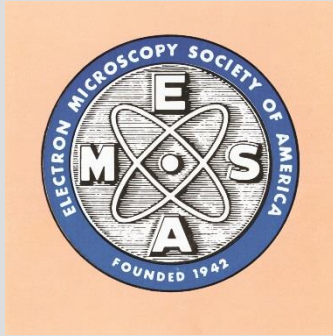




1950-1960



1950-1960



**New logo:
EMSA name changes from
Electron Microscope...
to Electron Microscopy...**

1952 Council (plus others)

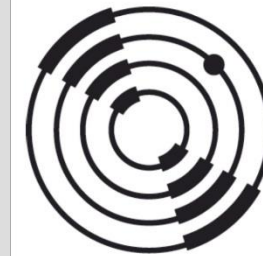
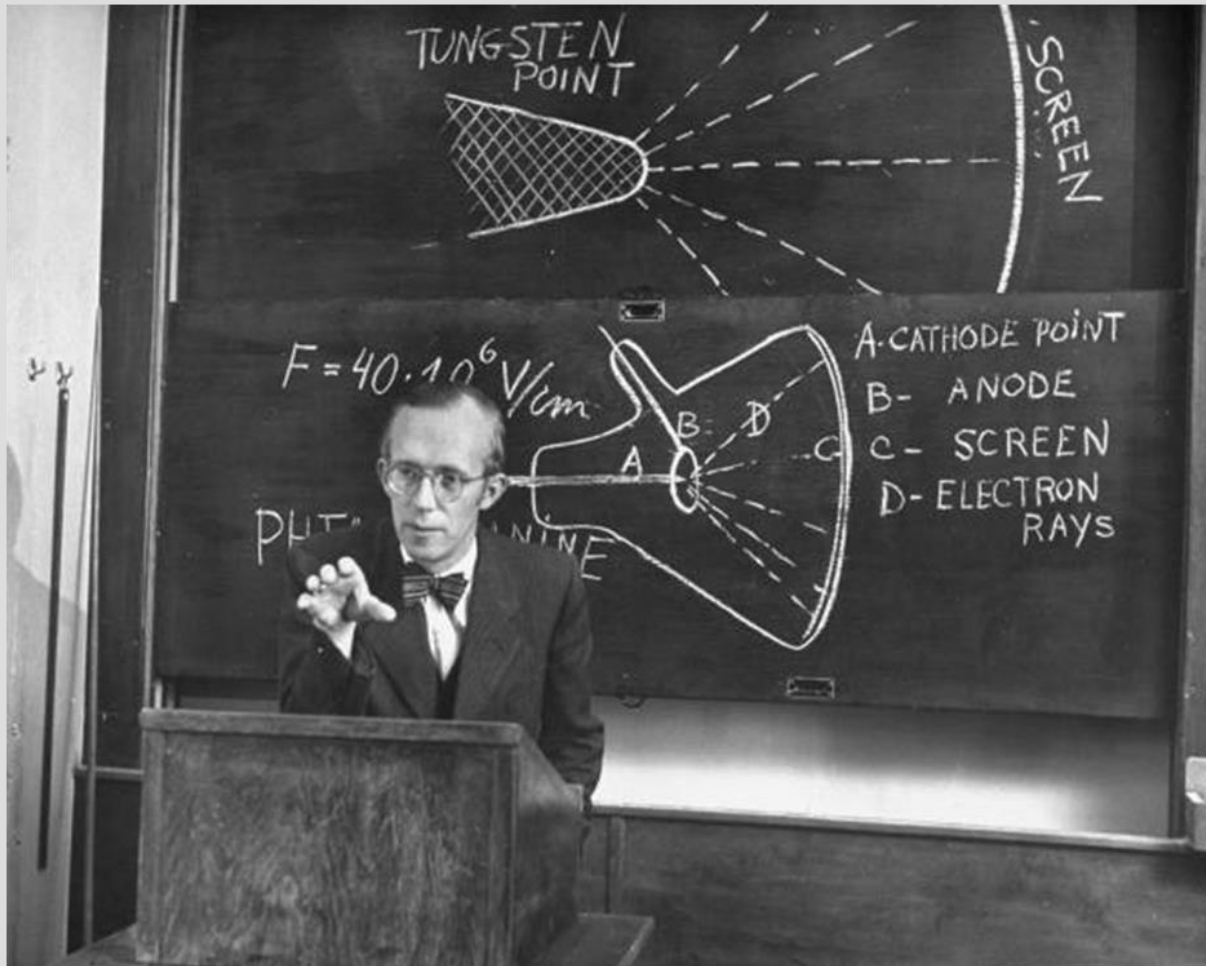


Left to right: Helmut Ruska, unidentified, R. C. Williams (Past President), Cecil Hall (President-Elect), George L. Clark, R. D. Heidenreich (President), W. L. Grube (Treasurer), T. L. Rochow (Secretary), James Hillier, Fritiof Sjostrand.

1950-1960

Founding of IFES (1952)

Led by Erwin Müller's work

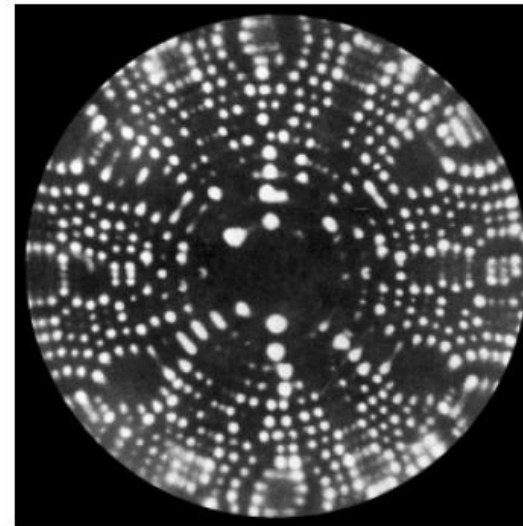
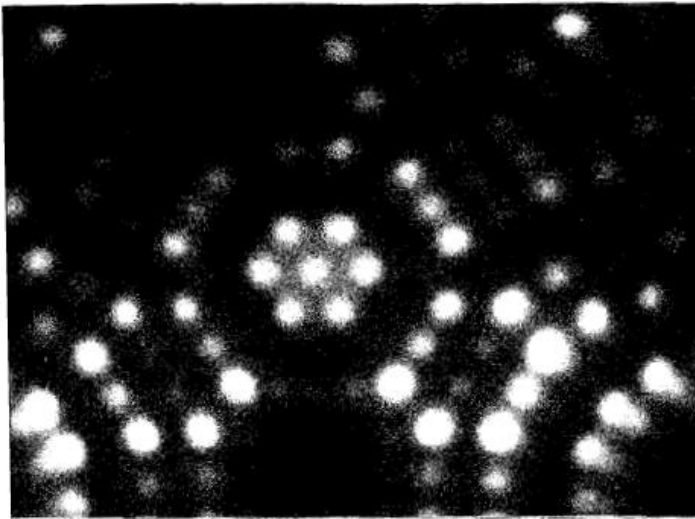


International
Field
Emission
Society

1950-1960

Early field-ion microscopy

First images of atoms, 1951,55



First images ever of atoms (on ledges of tip surface): Summer 1951, Müller
First atomically resolved lattice on surface: October 11, 1955, Bahadur and Müller

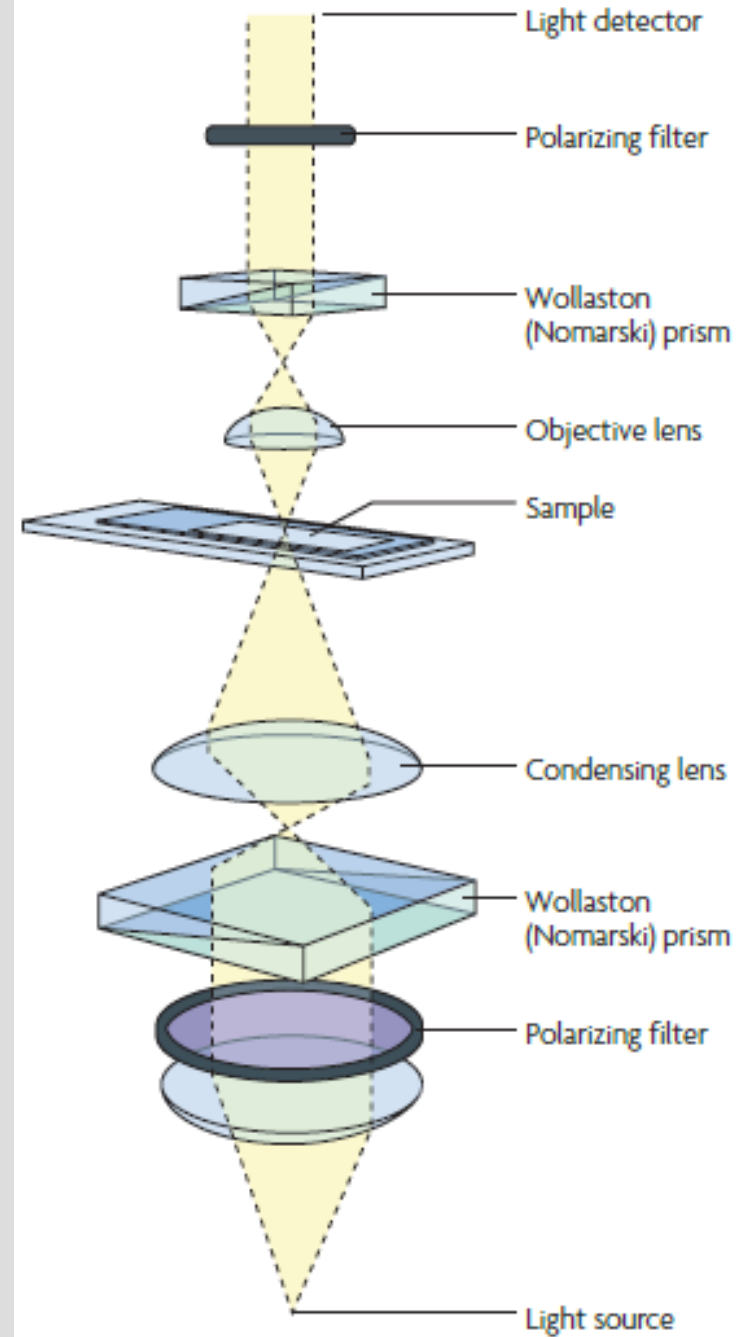
1950-1960

Differential-interference-contrast (DIC) light microscopy

Nomarski, Smith, 1955



1970s: Video-enhanced DIC
Shinya Inoué, Allen, etc.

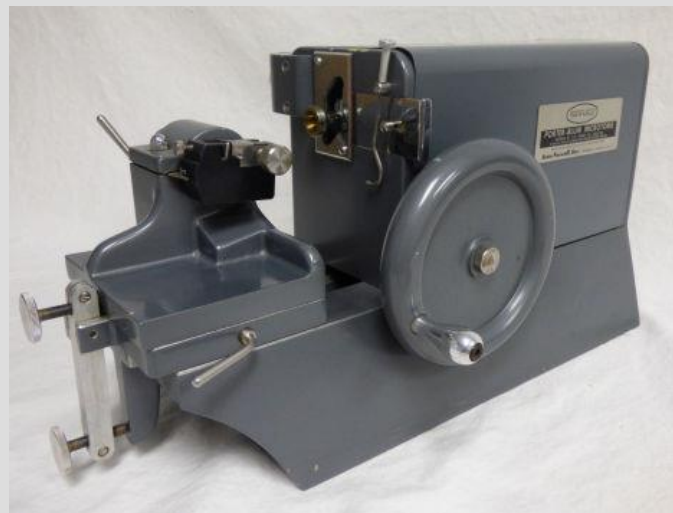
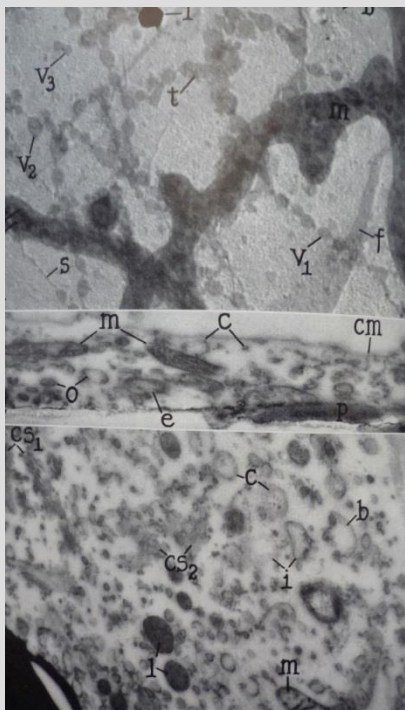
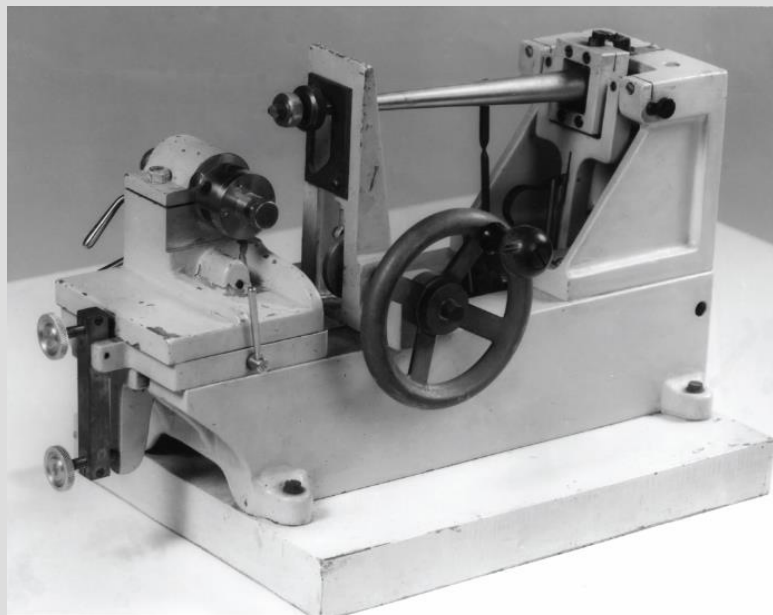


1950-1960

Perfection of ultramicrotomy

MT-1

- Built by Joe Blum for Keith Porter and Albert Claude
- Sold by Sorvall
- Worked with glass knives (Latta and Hartmann, 1950)



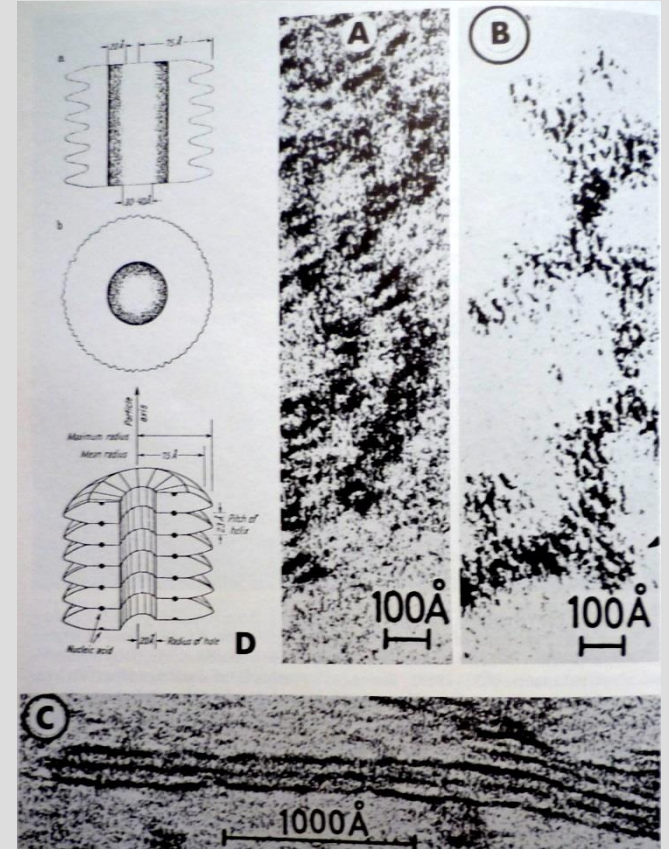
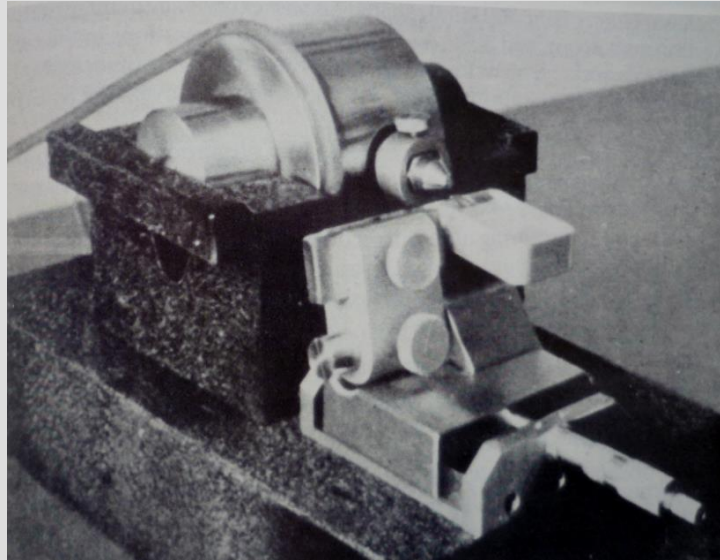
1950-1960

Perfection of ultramicrotomy

Microtomy – diamond knives -- 1953

Humberto Fernández-Morán

- Developed the first diamond microtome knives.
- Capable of producing 2-nm-thick sections.
- Also developed an ultramicrotome.



TMV and microtubules

1950-1960

Perfection of ultramicrotomy

Greatly improved ultrastructure

Fritiof Sjöstrand

Microtome for serial sections



Experimental Cell Research, 7, 393-414 (1954)

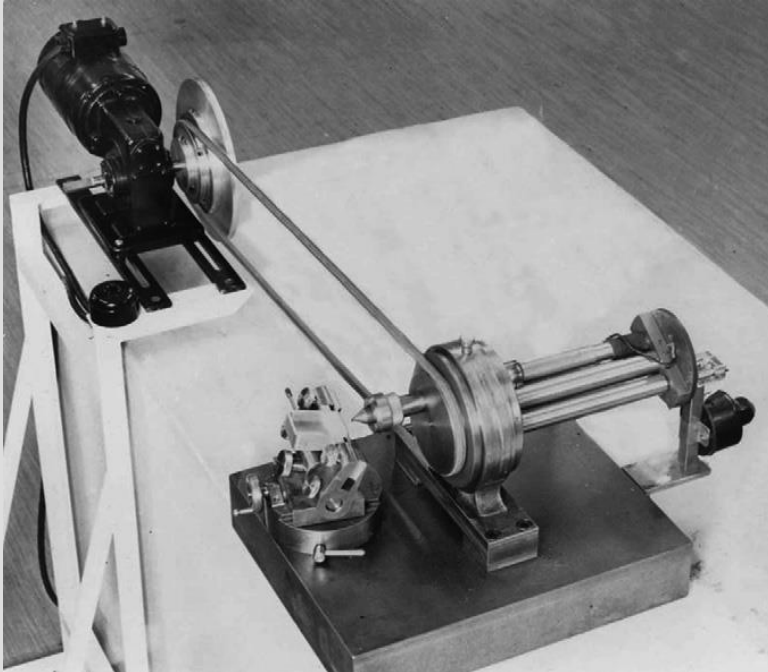
393

✓ MEMBRANE STRUCTURES OF CYTOPLASM AND MITOCHONDRIA IN EXOCRINE CELLS OF MOUSE PANCREAS AS REVEALED BY HIGH RESOLUTION ELECTRON MICROSCOPY

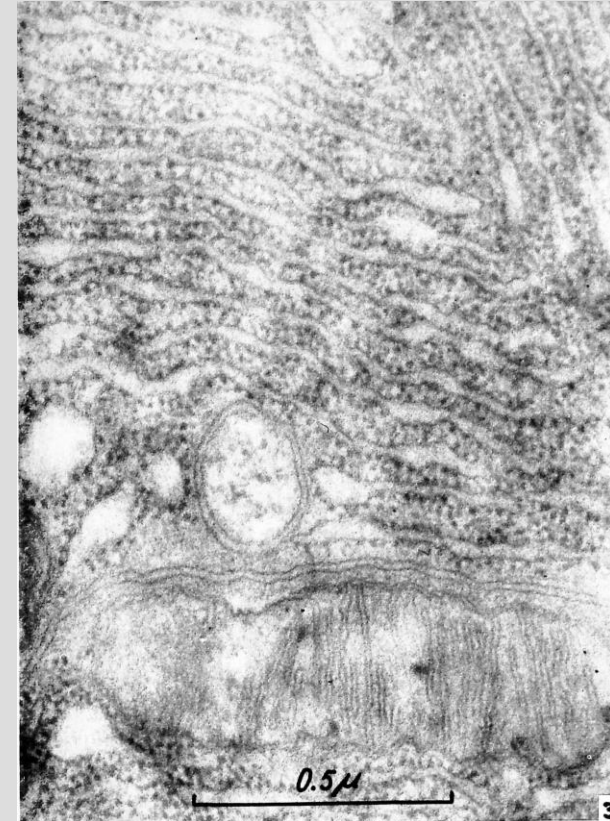
F. S. SJÖSTRAND and V. HANZON

Department of Anatomy, Karolinska Institutet, Stockholm, Sweden

Received April 1, 1954



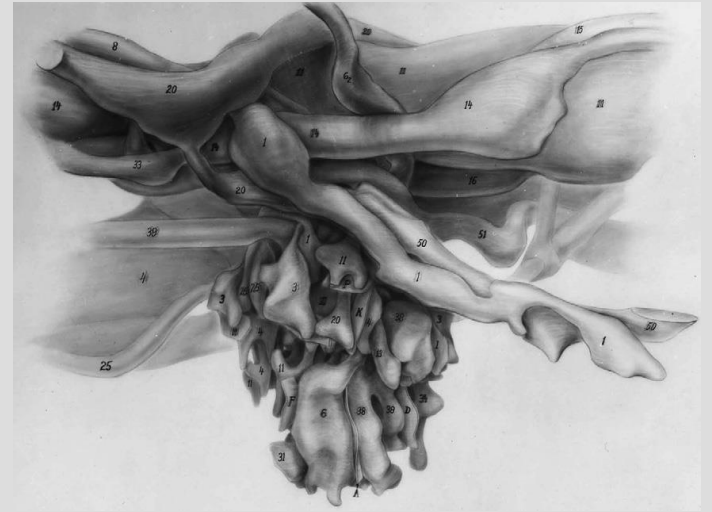
Thermal advance microtome: Further developed and sold by LKB



1950-1960

Perfection of ultramicrotomy

Microtomy – Serial-section 3-D reconstruction



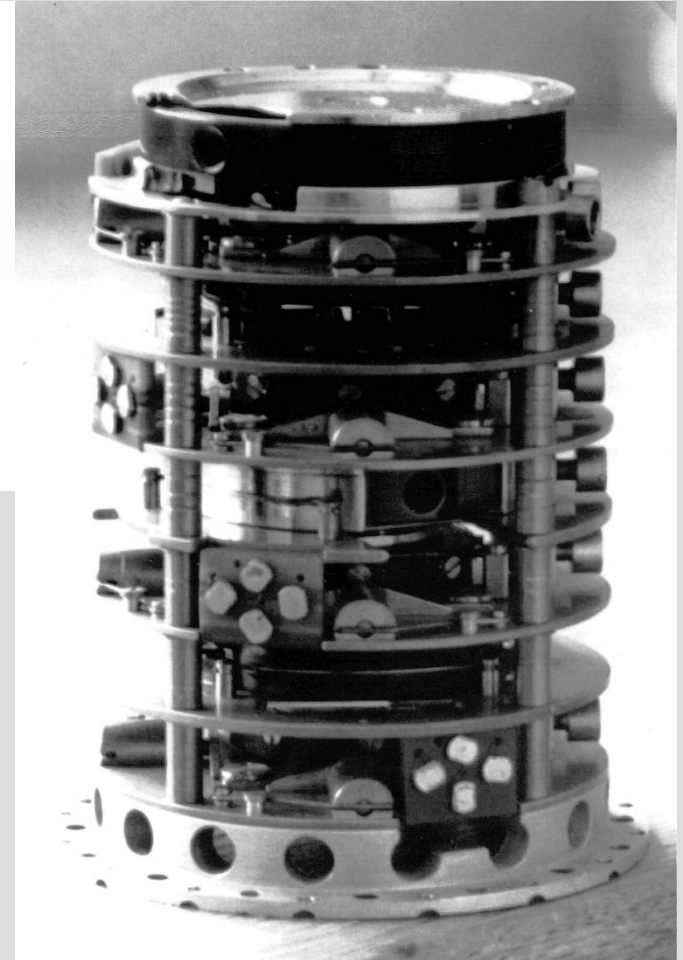
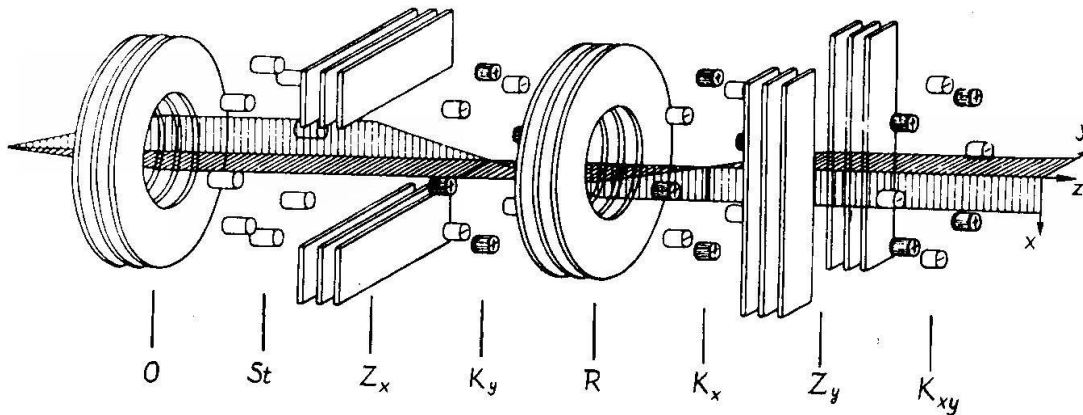
Sjöstrand: 3-D reconstruction of Mitochondria, Chloroplasts, Retina, etc.

1950-1960

Development of TEM aberration correction

Scherzer-Seeliger Corrector, 1950

First proof of spherical aberration correction



Möllenstedt tested the Seeliger corrector in Tübingen. He employed critical illumination with a large cone angle of 0.02 rad. As a result, the spherical aberration increased to such an extent that it became by far the dominant aberration, which strongly blurred the image. After compensating for the spherical aberration by means of the corrector octopoles, the **resolution improved** by a factor of about seven, accompanied by a **striking increase in contrast**.

1950-1960

Development of microprobe analysis

Raimond Castaing, 1951

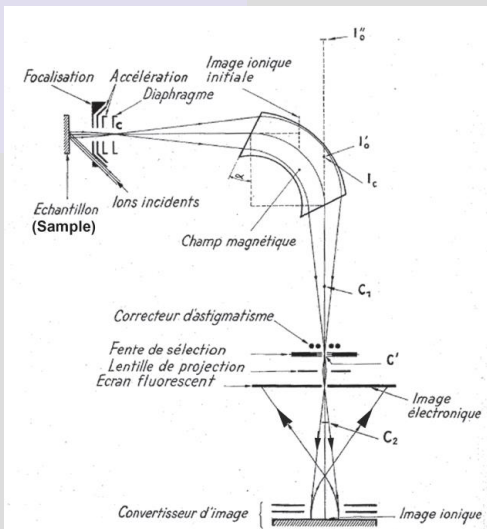
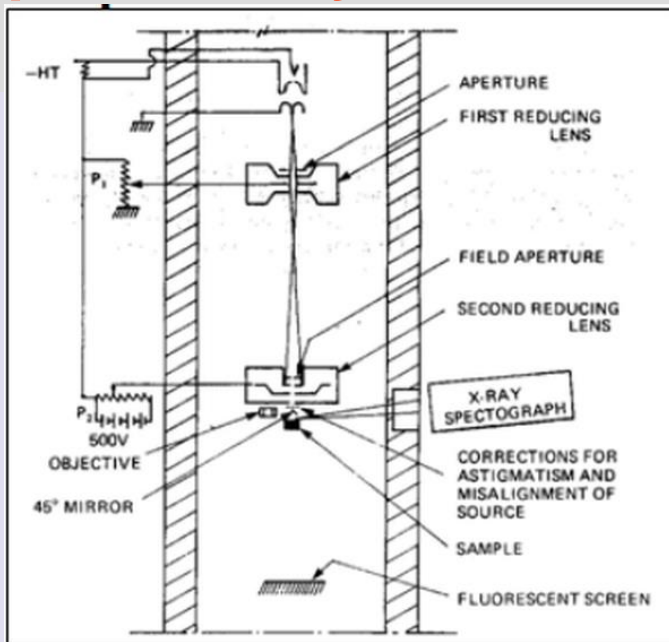
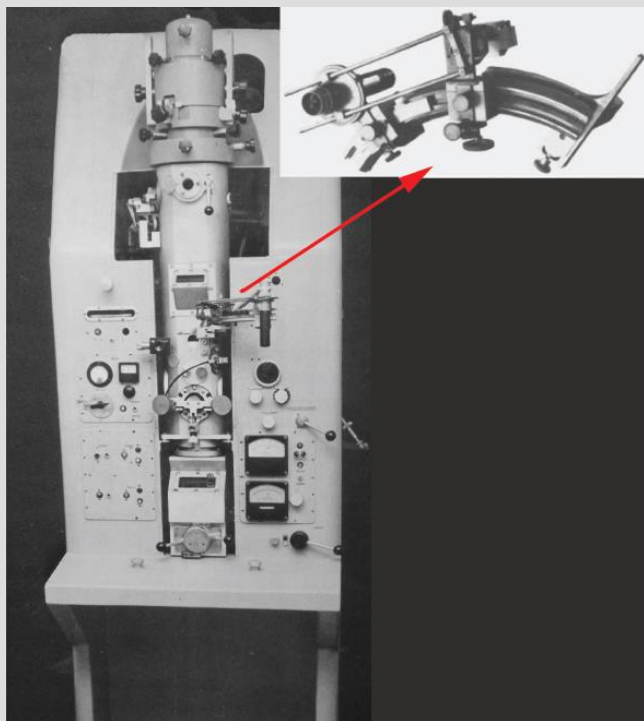


FIGURE 1. Schéma de principe.

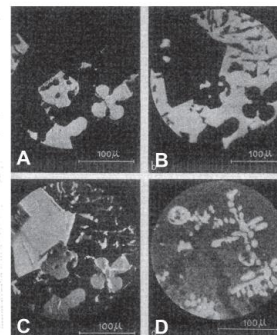
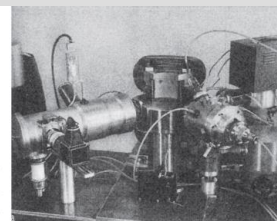
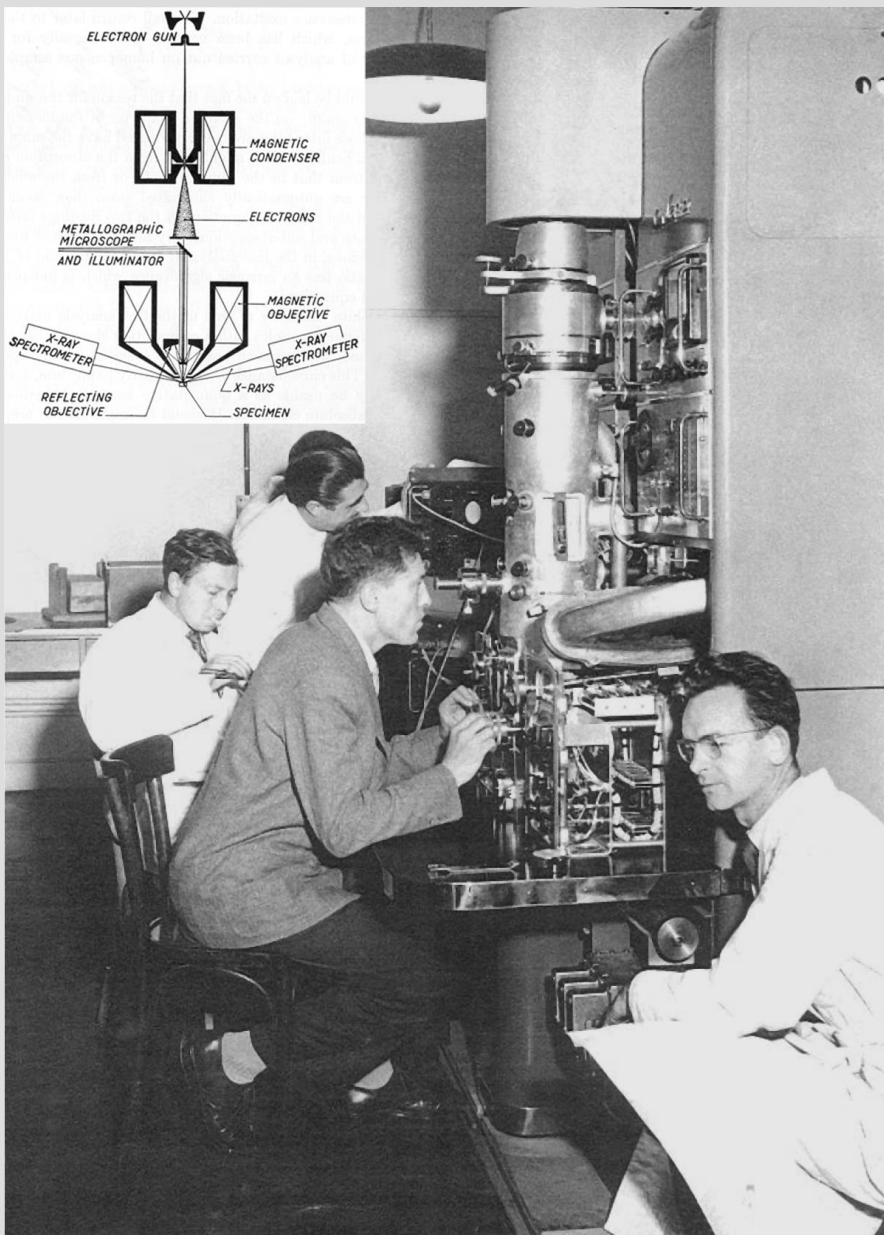
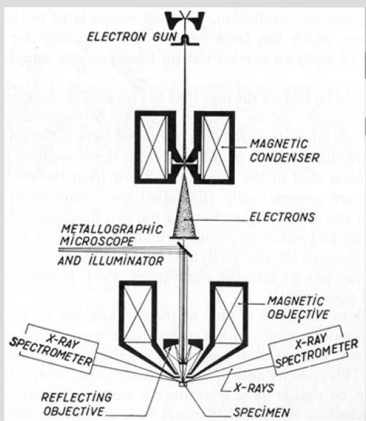
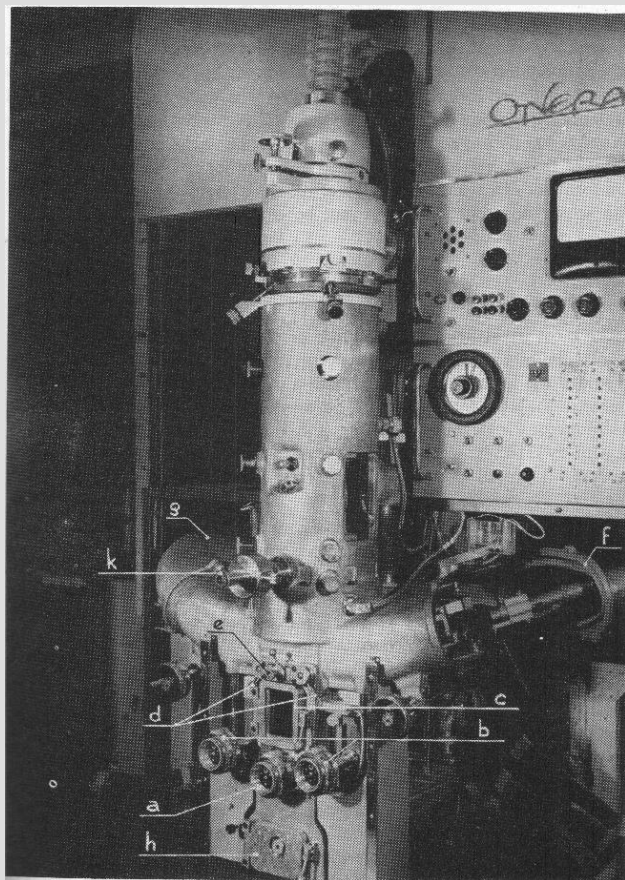


Fig. 5. Diagram and picture of the first secondary-ion microscope. Note that the ion-to-electron converter projects the image back to the fluorescent screen. Images: (A) Mg⁺ image of an Al-Mg-Si alloy, (B) Al⁺ image of the same specimen, (C) Si⁺ image of the same specimen, (D) Cu⁺ image of solid Cu with Cu₂O inclusions. (from Castaing and Slodxian, 1962).

1950-1960

Further development of microprobe analysis

Raimond Castaing, mid 50s

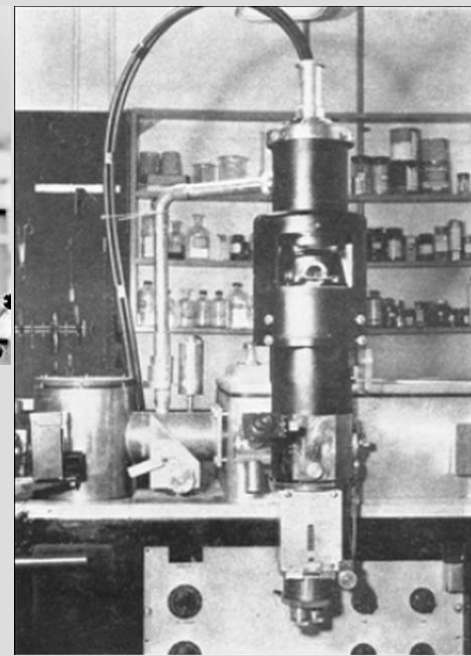


1950-1960

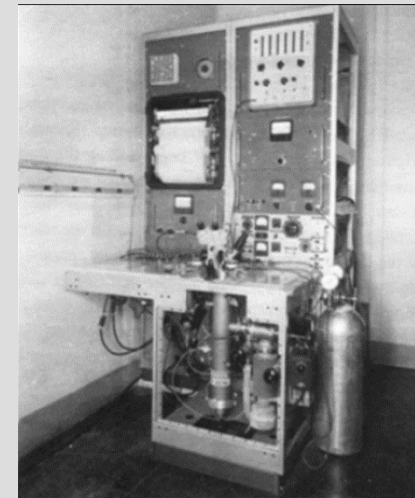
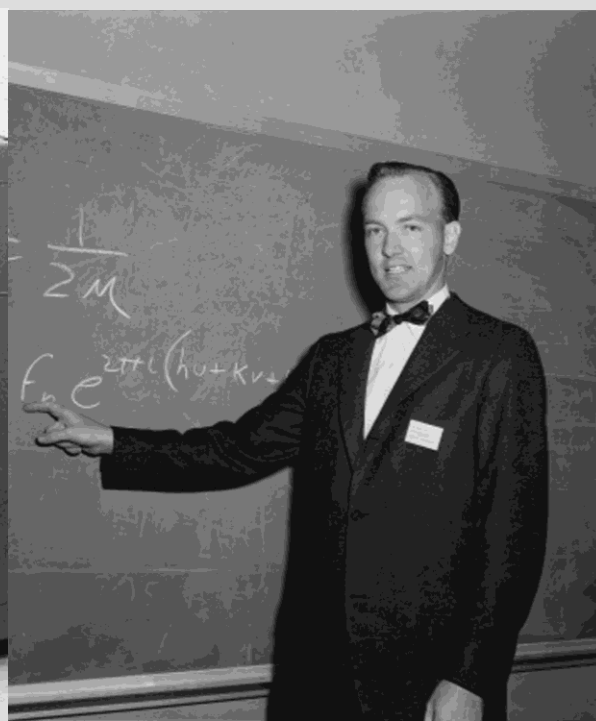
Development of microprobe analysis



Wittry, 1957



Ogilvie, MIT, mid 1950s



GE (Buschmann), 1955

1950-1960

Early SEM development

Everhart – Thornley detector

Developed in the group of V. E. Cosslett

Wide-band detector for micro-microampere low-energy electron currents

by T. E. EVERHART, Ph.D.,* and R. F. M. THORNLEY, B.A., Department of Engineering, University of Cambridge

[Paper received 25 January, 1960]



T.E. Everhart



V.E. Cosslett

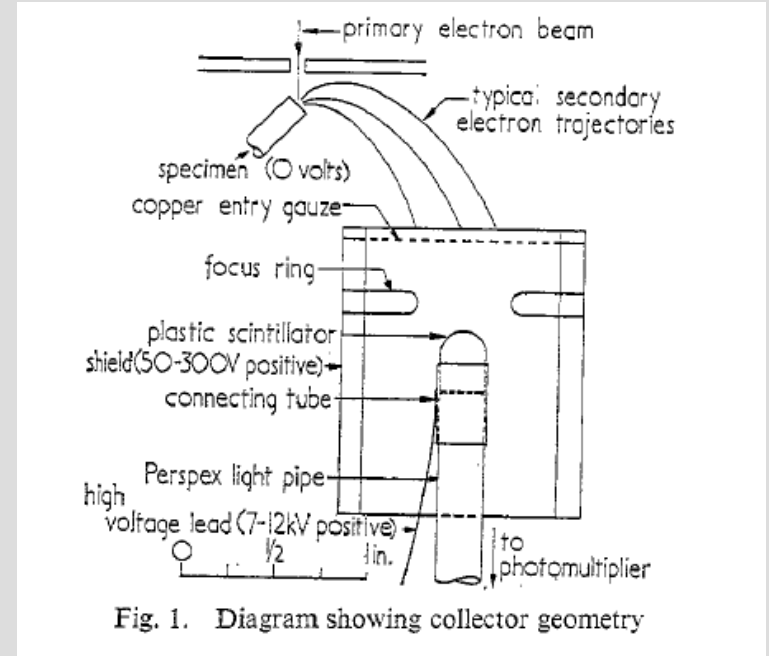


Fig. 1. Diagram showing collector geometry

1950-1960

Early SEM development

Oliver Wells and Dennis McMullan, 1957

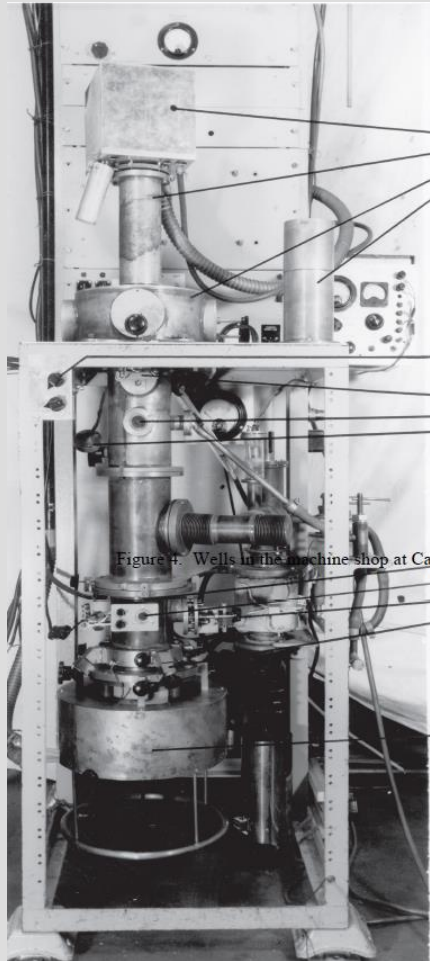


Fig. 2.2.a.
The main column.

The head amplifier.
The electron multiplier.
The specimen chamber.
Holder for electron multiplier.

Electrical shift.

Lens 2.
Observation port.
flap valve.

Figure 4. Wells in the machine shop at Cambridge (courtesy of James Wells)

Observation port.
aperture movement.
column tilt.

electron gun.

FIG 2.2 BLOCK DIAGRAM OF COMPLETE MICROSCOPE.

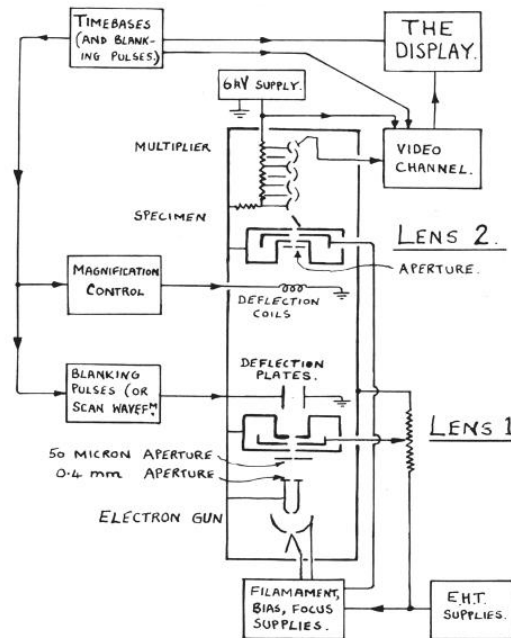
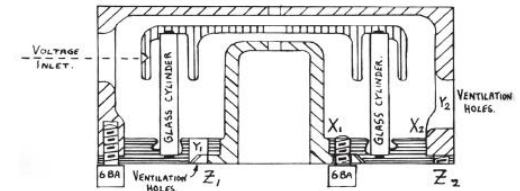


FIG 3.3.a

ELECTROSTATIC LENS:

(TWICE FULL-SIZE.)



NOTES:

THE LENS IS ASSEMBLED WITH SLIDING FITS AT X₁ AND X₂.
VENTILATION (i.e. PUMPING) IS PROVIDED BY HOLES Y₁ AND Y₂.
THE LENS COMPONENTS CAN BE SEPARATED BY MEANS OF SCREWS INSERTED AT Z₁ (HOLE NOT SHOWN) AND Z₂.
ALL INTERNAL SURFACES ARE POLISHED.

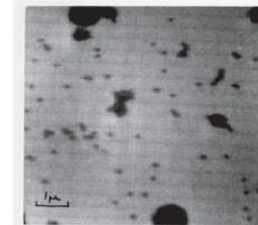
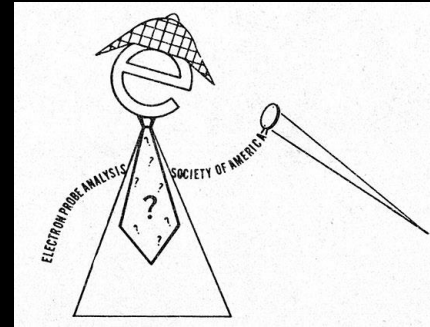
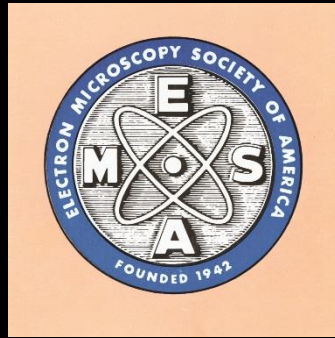


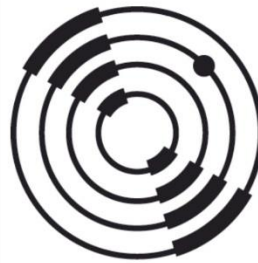
FIG. 3.10

Polystyrene latex particles in transmission.

x 10,000



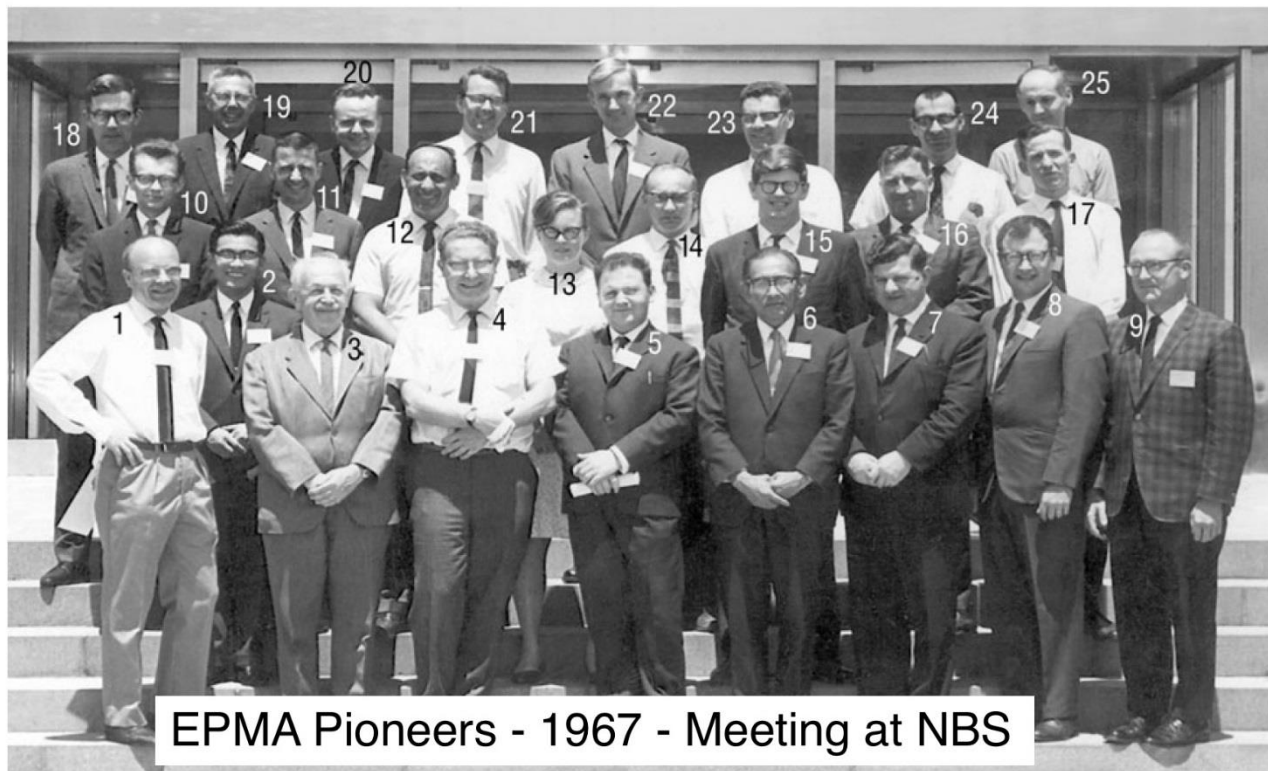
1960-1970



International
Field
Emission
Society

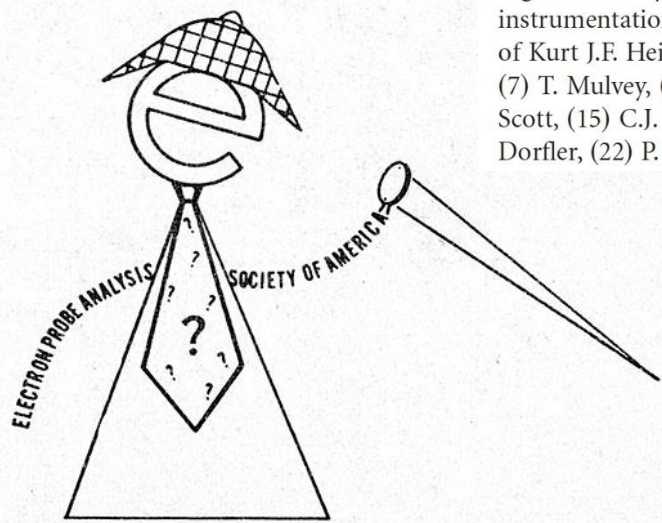
1960-1970

Founding of the Electron Probe Analysis Society of America



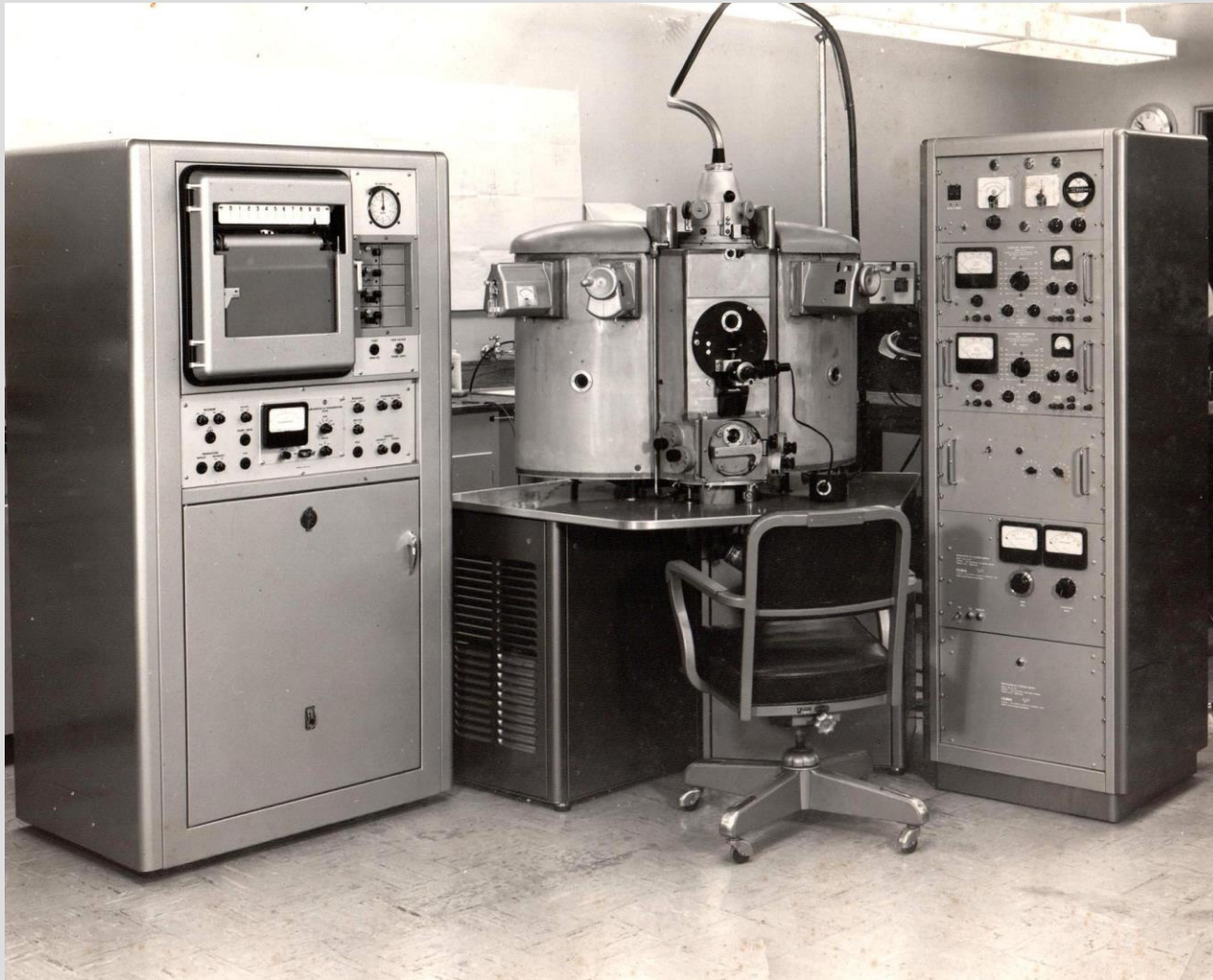
EPMA Pioneers - 1967 - Meeting at NBS

Figure 1. Early pioneers, including Peter Duncumb and LaVerne Birks, in EPMA theory, design, development, instrumentation, and application. Meeting at the National Bureau of Standards, Gaithersburg, MD, USA, 1967 (courtesy of Kurt J.F. Heinrich). (1) J. Philibert, (2) S. Sawatani, (3) L.L. Marton, (4) K.F.J. Heinrich, (5) J. Henoc, (6) G. Shinoda, (7) T. Mulvey, (8) J.I. Goldstein, (9) D. Brown, (10) J.W. Criss, (11) D.J. Nagel, (12) I. Adler, (13) M.A. Giles, (14) V.D. Scott, (15) C.J. Powell, (16) W.J. Campbell, (17) D.M. Poole, (18) S.J.B. Reed, (19) L.S. Birks, (20) N.E. Weston, (21) G. Dorfler, (22) P. Duncumb, (23) D.B. Wittry, (24) J.D. Brown, (25) T. Hall.



1960-1970

Early microprobe pioneers



Applied Research Laboratories (ARL) electron microprobe
At University of California at La Jolla in 1961

1960-1970

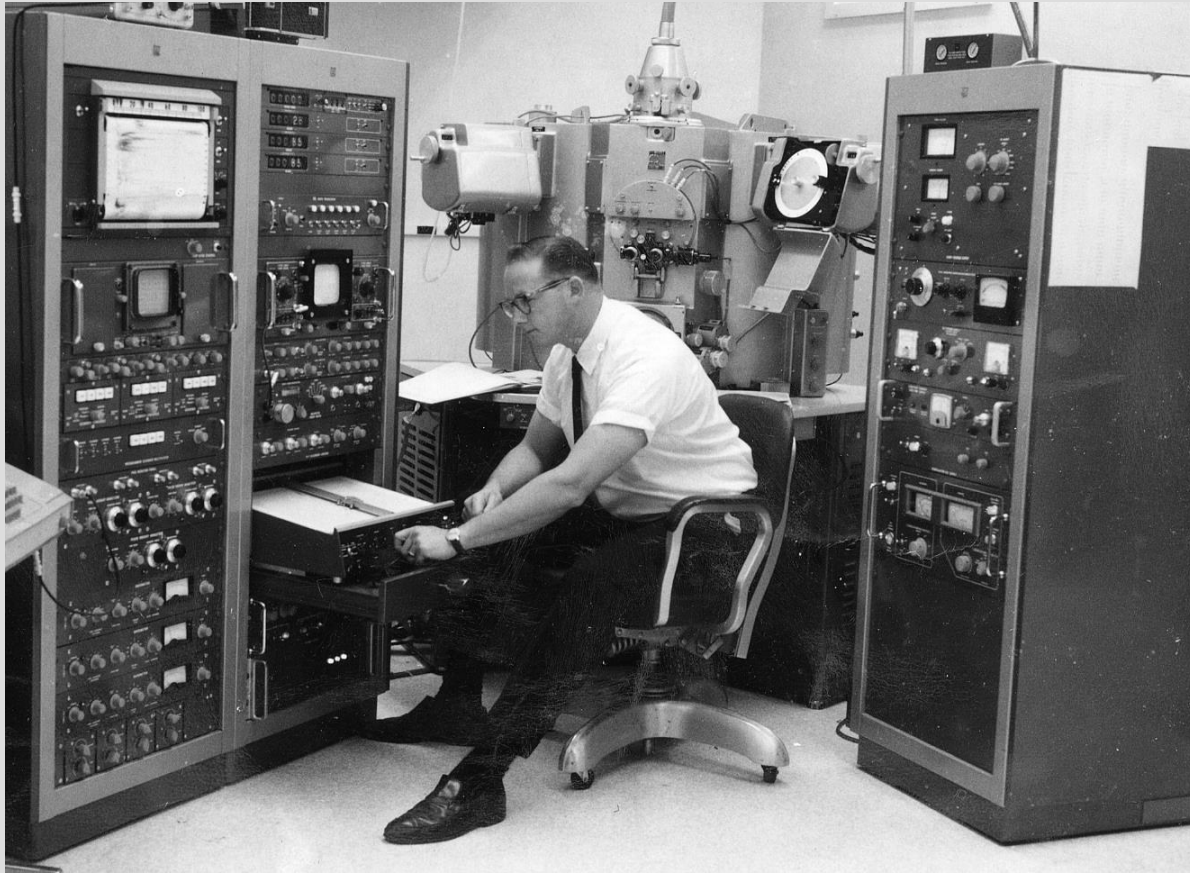
Early microprobe pioneers



Klaus Keil: in his office at NASA Ames Research Center, Moffett Field, California, while working on the development of the first EDS spectrometer for electron probe microanalysis.

1960-1970

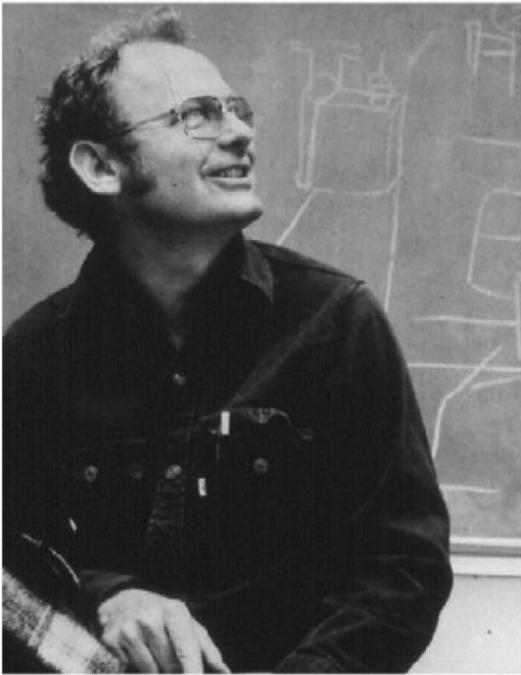
Early microprobe pioneers



Frank Drogosz in front of an EMX-SM in 1967

1960-1970

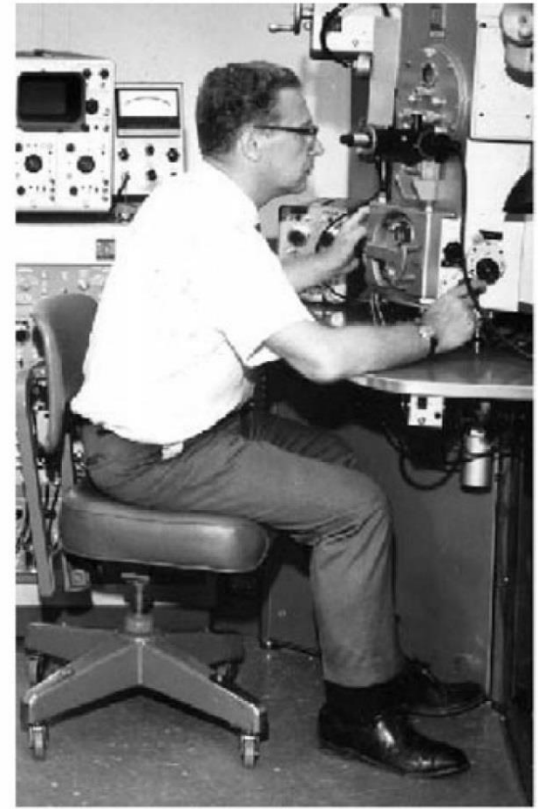
Early microprobe pioneers



(A)



(B)



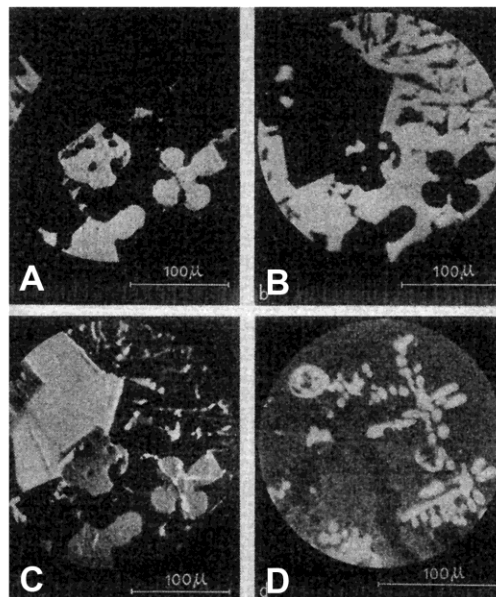
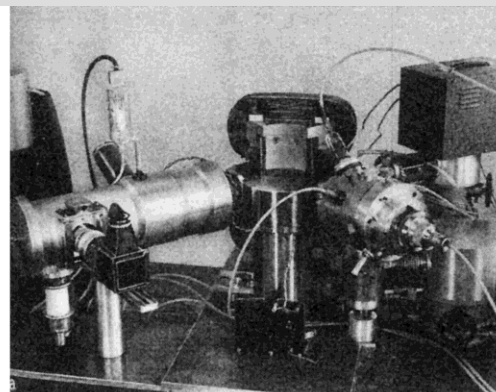
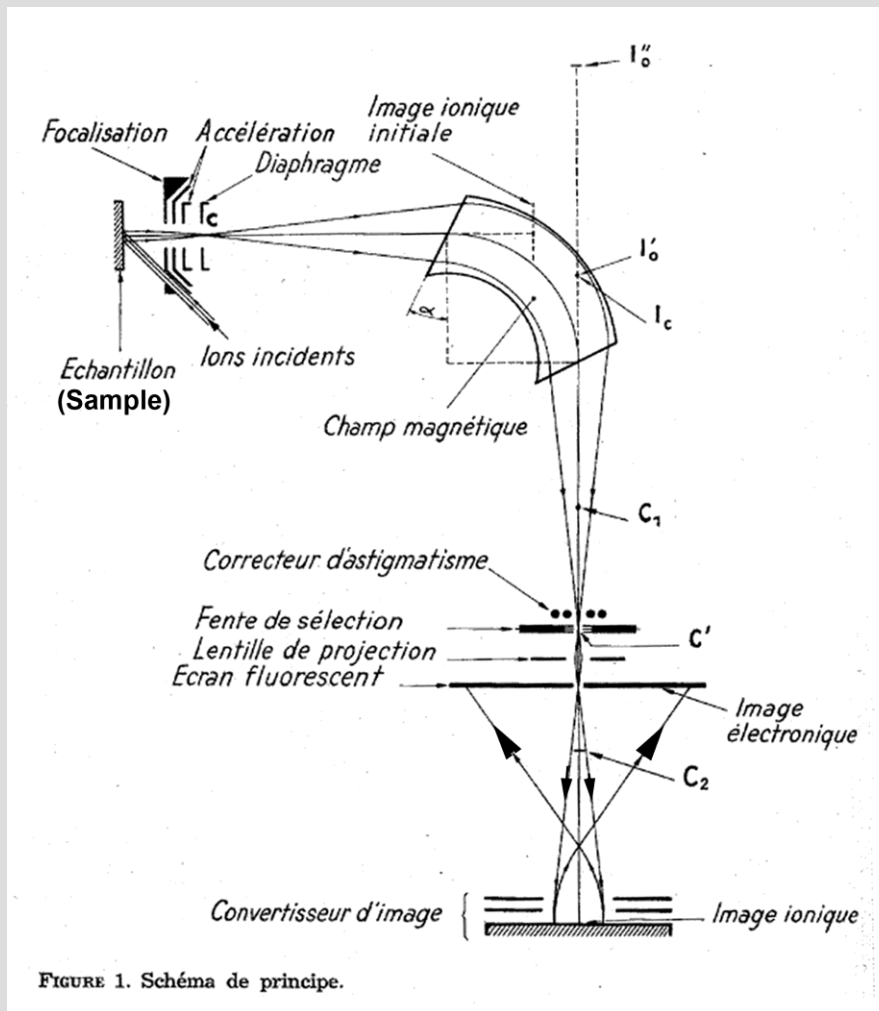
(C)

Figure 8. (A) Ray Fitzgerald, ca. 1970; (B) Klaus Keil, ca. 1964; (C) Kurt F.J. Heinrich, ca. 1962.

1960-1970

Early development of microanalysis

Castaing's secondary-ion mass spectrometry (SIMS), 1962



1960-1970

First commercial SEM

Cambridge Stereoscan, 1965



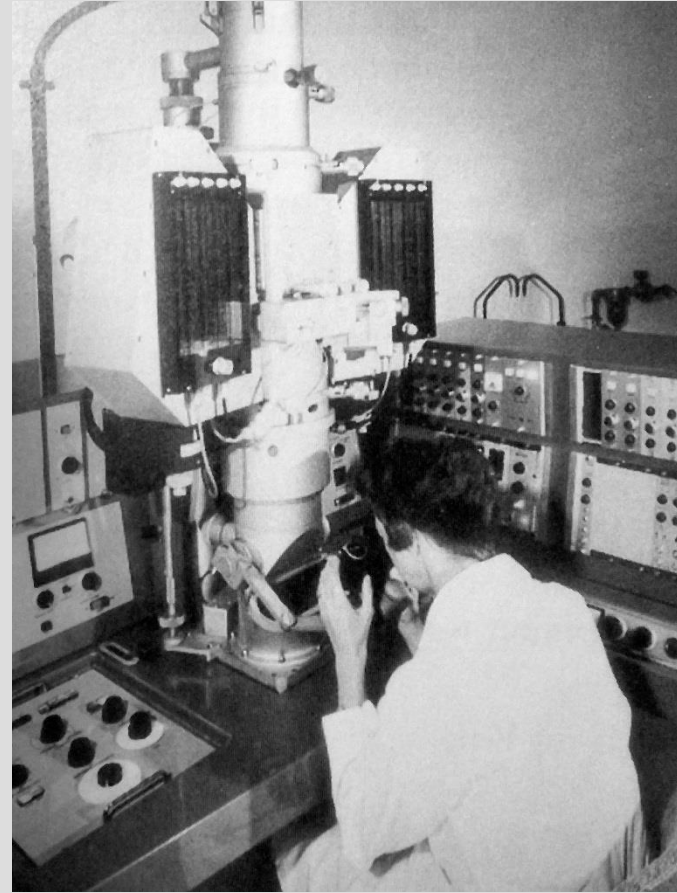
1960-1970

Early development of microanalysis

AEI EMMA-4 analytical TEM with WDS x-ray microanalysis, 1969-70



Following development work by Peter Duncumb



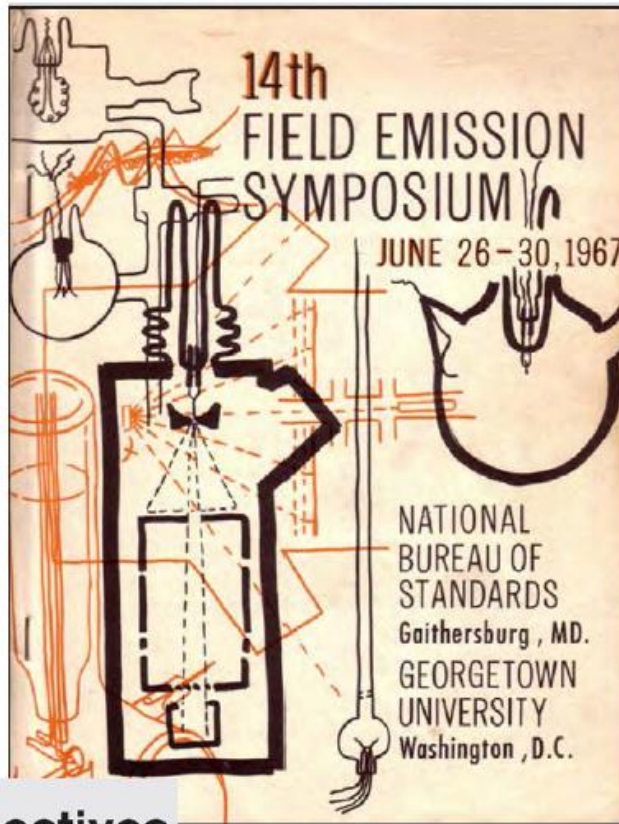
1960-1970

Development of the atom probe

Müller and Panitz, 1967

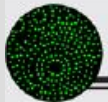


First Publication on Atom Probe



The Atom-Probe Field Ion Microscope
Erwin W. Müller and John Panitz
Physics Department, The Pennsylvania State University
University Park, Pa.

A serious limitation of the field ion microscope has been its inability to identify individually imaged atoms. A newly conceived Atom-Probe FIM, consisting of a combination probe hole FIM and mass spectrometer having single particle sensitivity, will be described. During operation, the observer selects an atomic site of interest and places it over the probe hole. Pulsed field evaporation sends the chosen particle through the hole and into the spectrometer section which may be of the magnetic sector or time-of-flight type. Each has its own special advantages depending upon the particular application. These might include: identification of bright atom spots in the controversial adsorption experiments, investigation of the atomic nature of impurity and interstitial atom spots, analysis of segregations and precipitations, or the investigation of short range order in alloys. In some cases an adjustable probe hole covering an area of several atomic sites is advantageous. Experiences with a prototype time-of-flight instrument will be reported.



Perspectives

1960-1970

First visualization of atoms by electron microscopy

Albert Crewe's STEM imaging atoms:

"If you've seen one, you've seen them all, lets turn it off and go home.:"

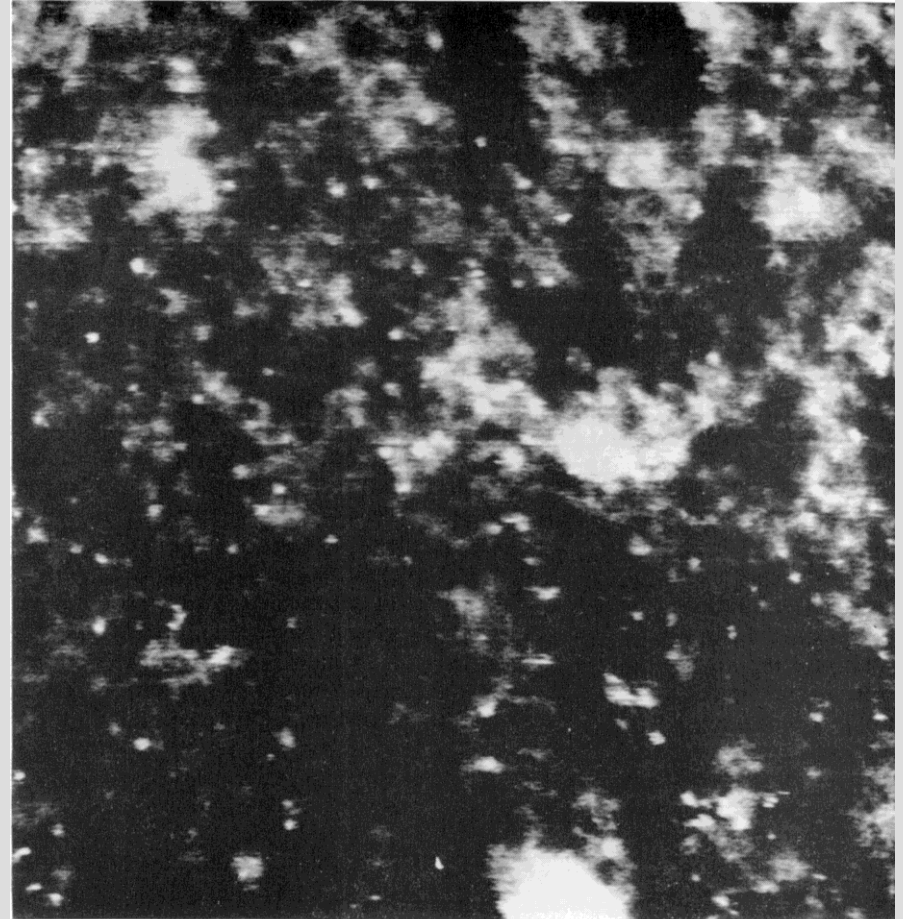
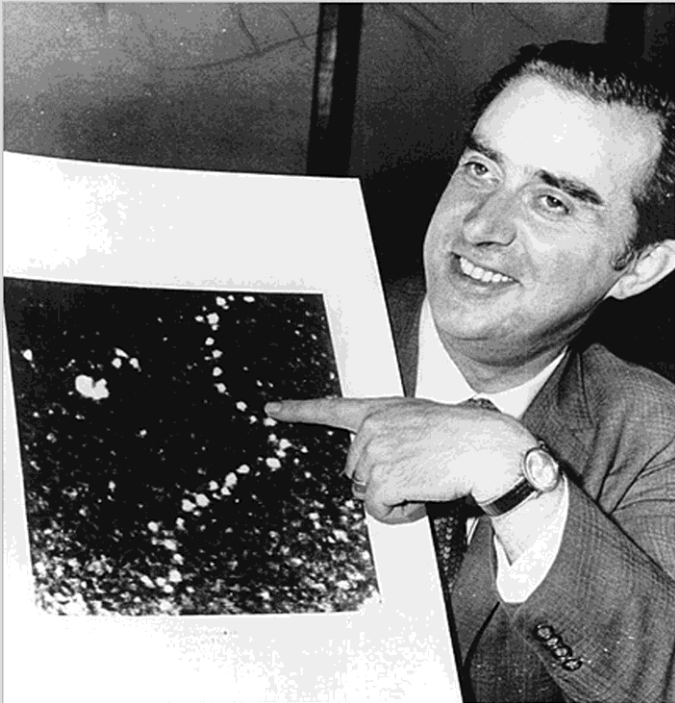
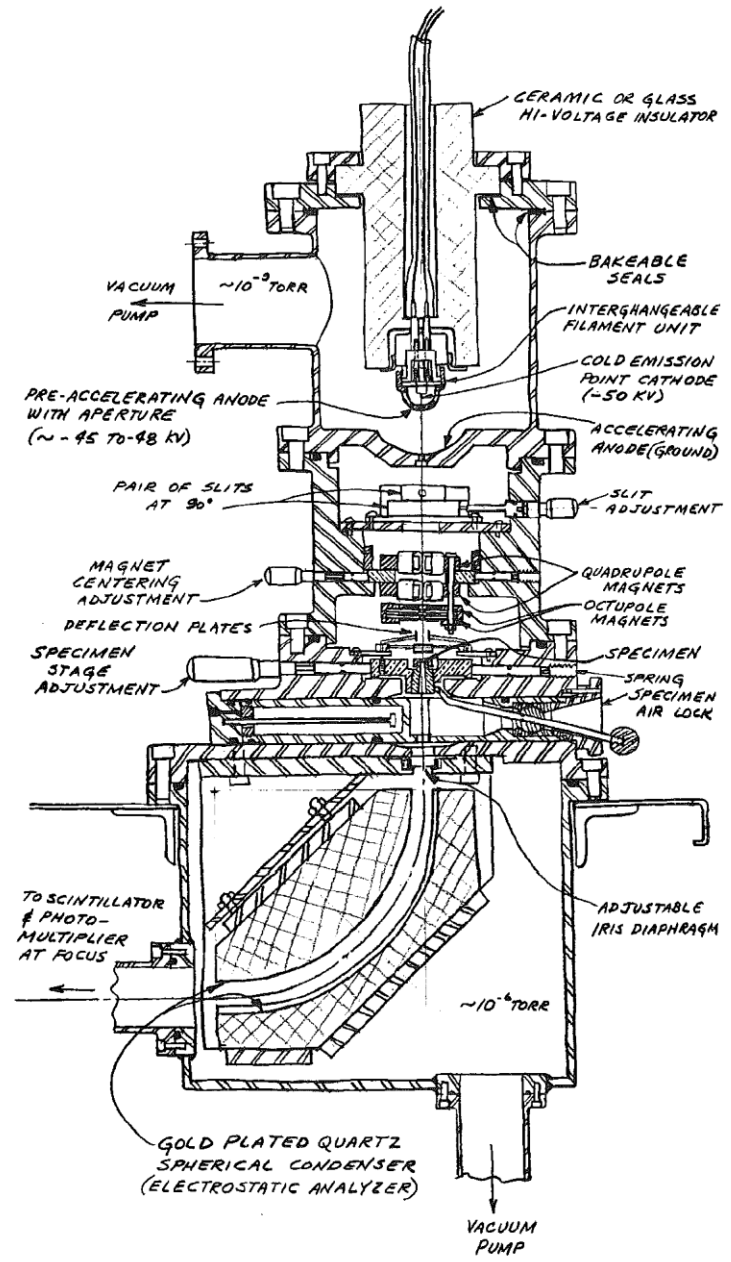
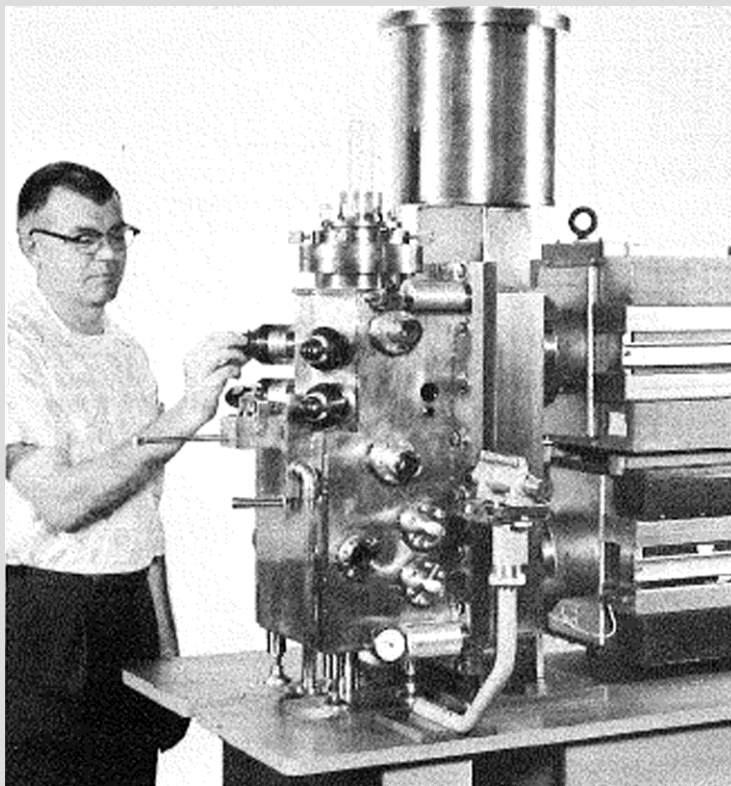


Fig. 4. Micrograph showing single silver atoms (the bright spots) on a thin carbon film. Full scale is 29 nm. This micrograph appears to be of poorer quality than the uranium atoms in Fig. 3. The reason for this is that the elastic scattering cross-section of silver is approximately three times less than for uranium. This is probably close to the threshold limit of detectability under these conditions. (Photo by M. Retsky.)

1960-1970 1964 Crewe STEM

Development of high-resolution (FEG) STEM

Crewe's 1964 instrument

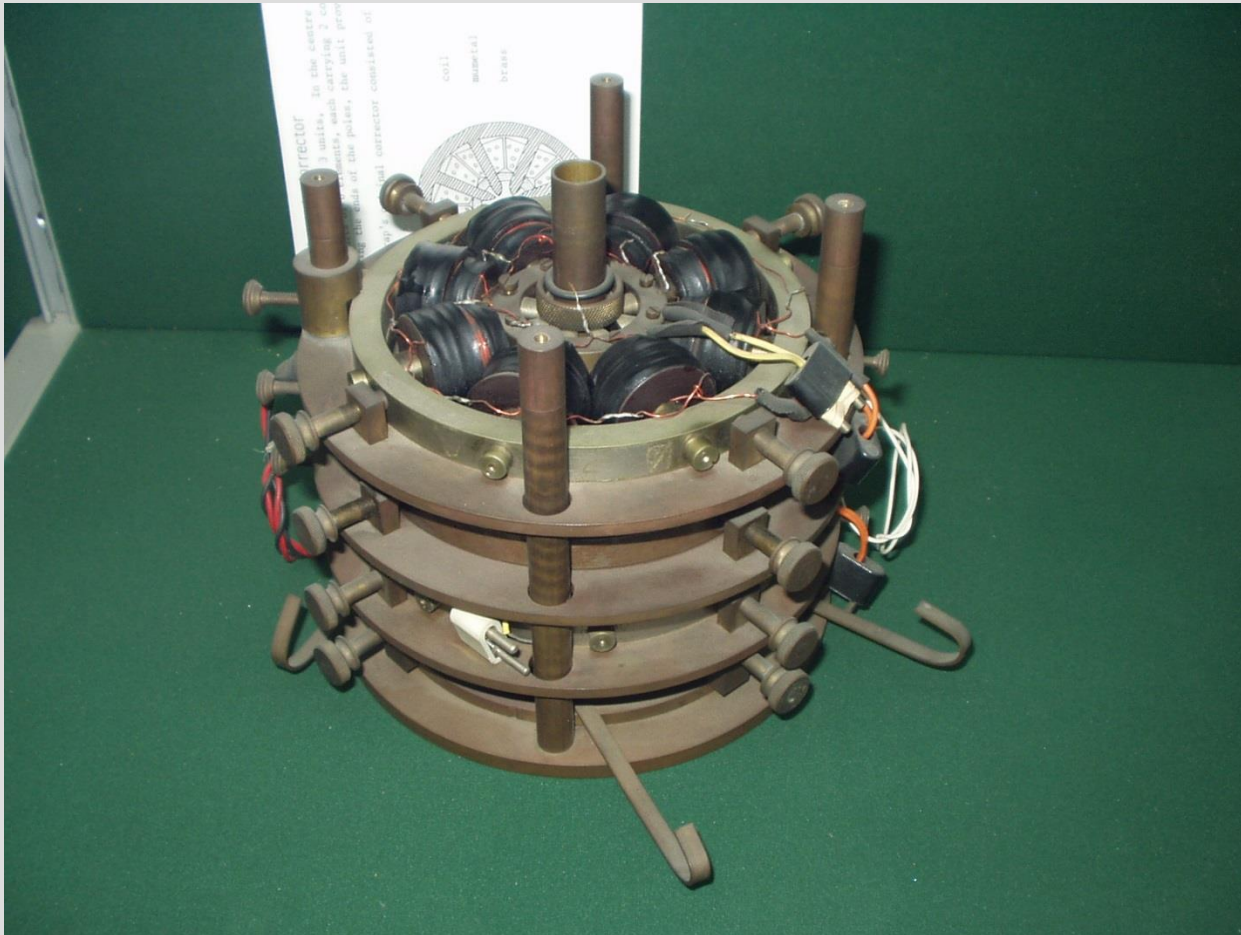


1960-1970

Continued development of TEM aberration correction

Deltrap's 1964 corrector (Cambridge, UK)

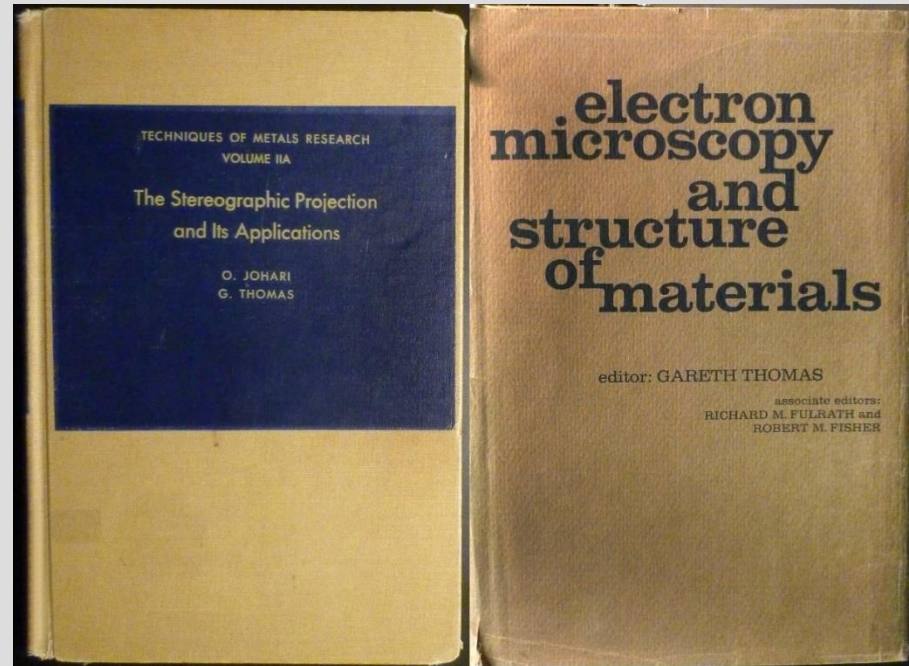
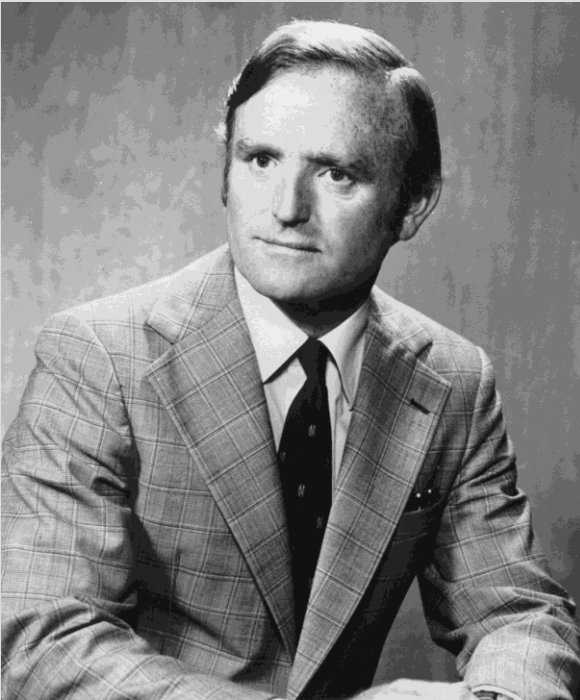
Worked on optical bench, but not tested in a TEM



1960-1970

Focus on physical science

Gareth Thomas



1960-1970

Focus on physical science

Gareth Thomas

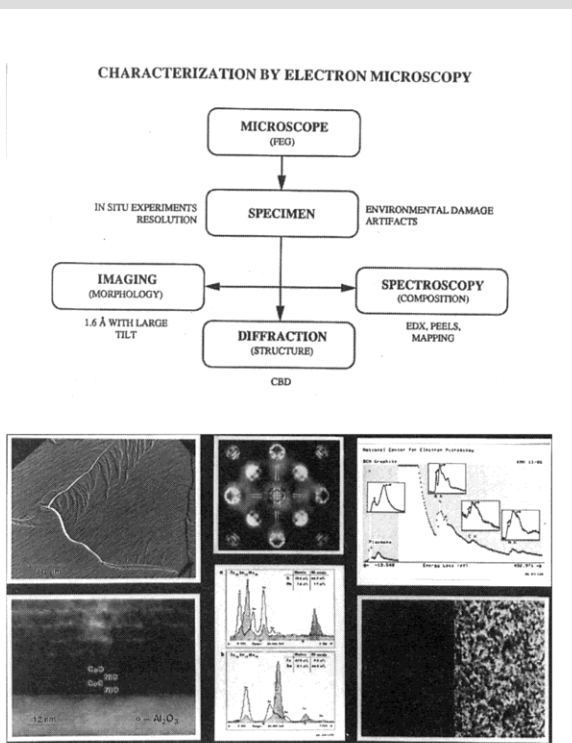
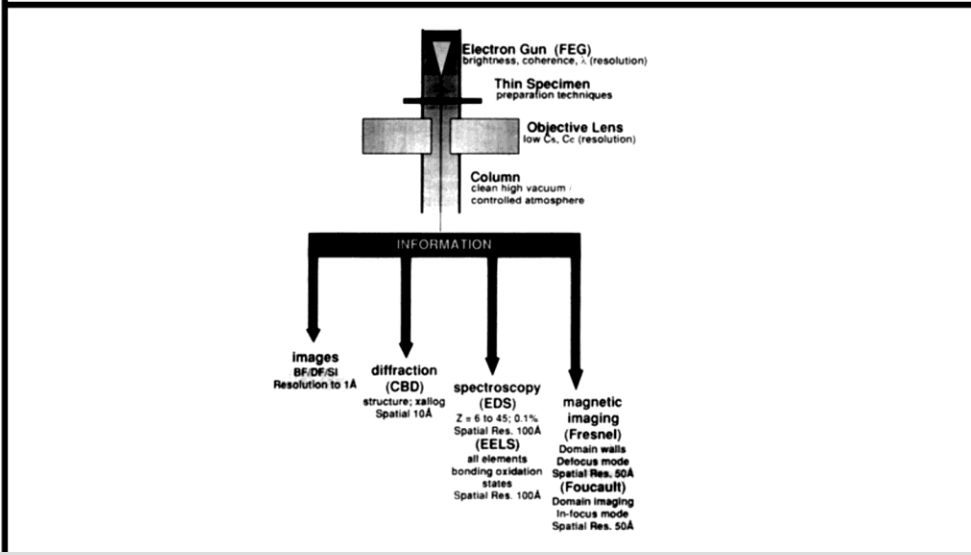
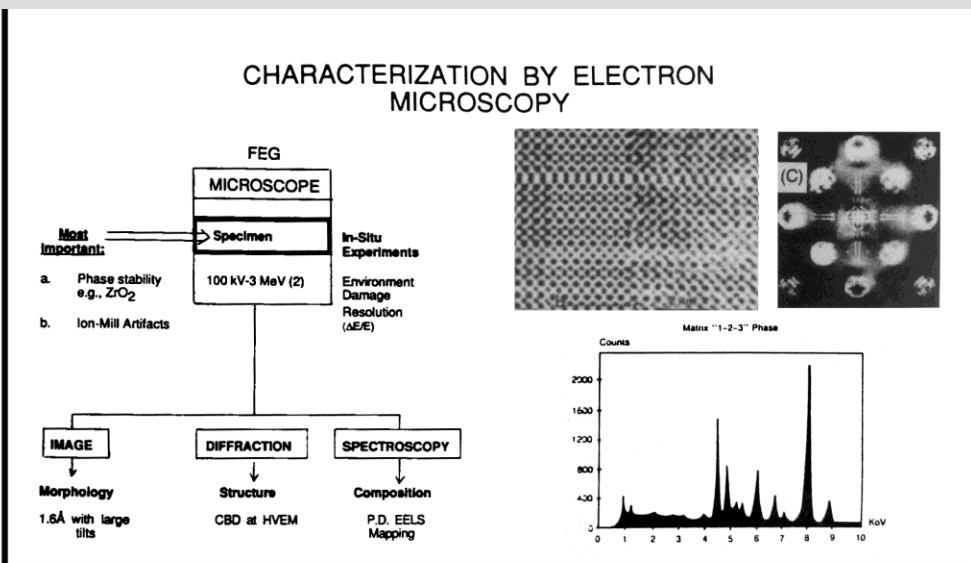


Fig. 1. Collage showing the principal advantages of modern electron microscopy in materials research. From left to right: Lorentz imaging of Co-Ni-Cr thin film for recording media (discs) showing domain wall perturbation at a crack (courtesy Li Tang). CBD pattern of spinel allowing space group to be determined from particles ~100 Å dia. Energy loss spectrum of boron- and nitrogen-doped graphite; the absorption edge shapes show no intercalation but substitution of C by B and N (courtesy K. Krishnan). High resolution images of the (111) stacking in multilayers of CoO-NiO for magnetic applications (courtesy Wei Cao). Energy dispersive X-ray microanalytical data from RE permanent magnets; X-ray mapping images corresponding to the EDS spectra (courtesy A. Hütten).

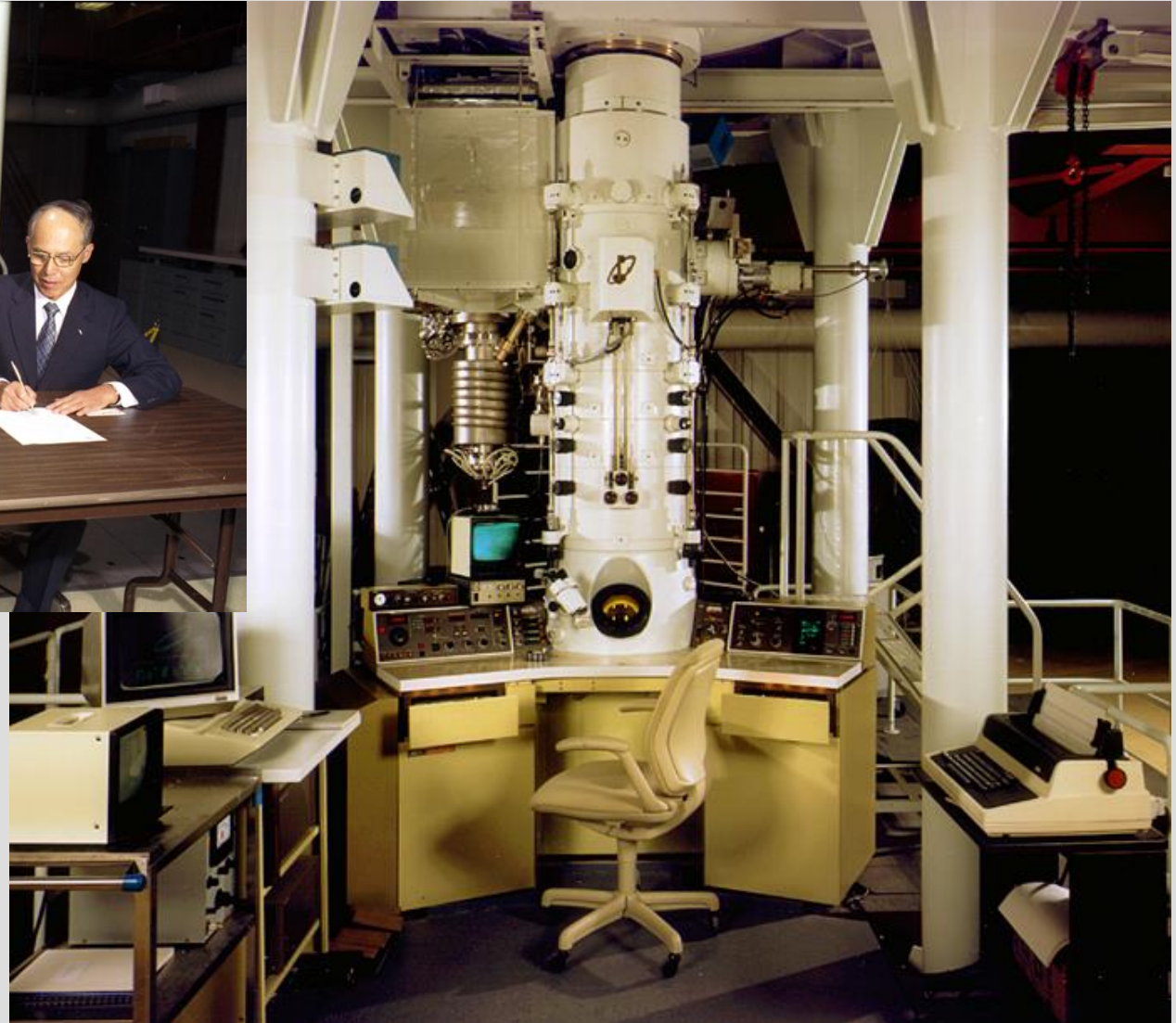


1960-1970

Focus on TEM in physical science



Gareth Thomas
1 MeV ARM, Berkeley

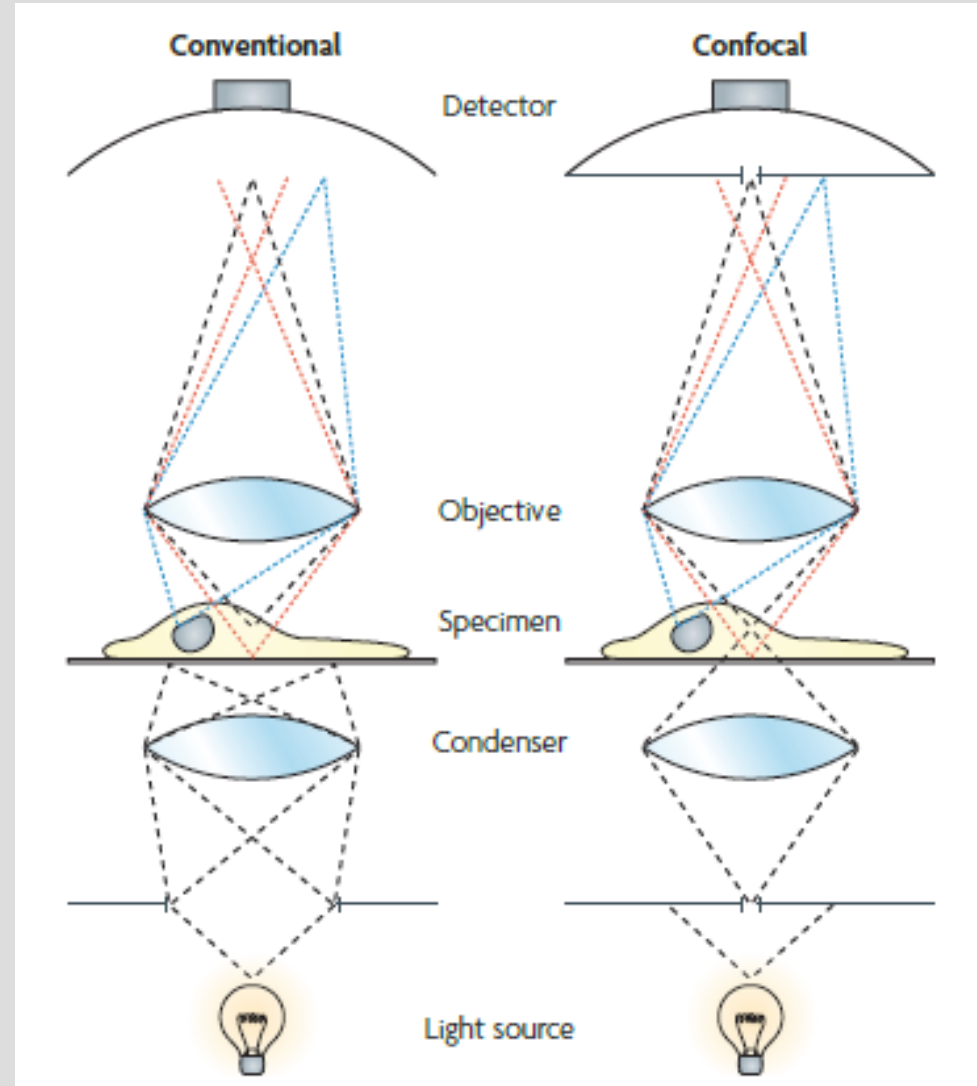


1960-1970

Development of confocal light microscopy

First patent: Marvin Minsky, 1961

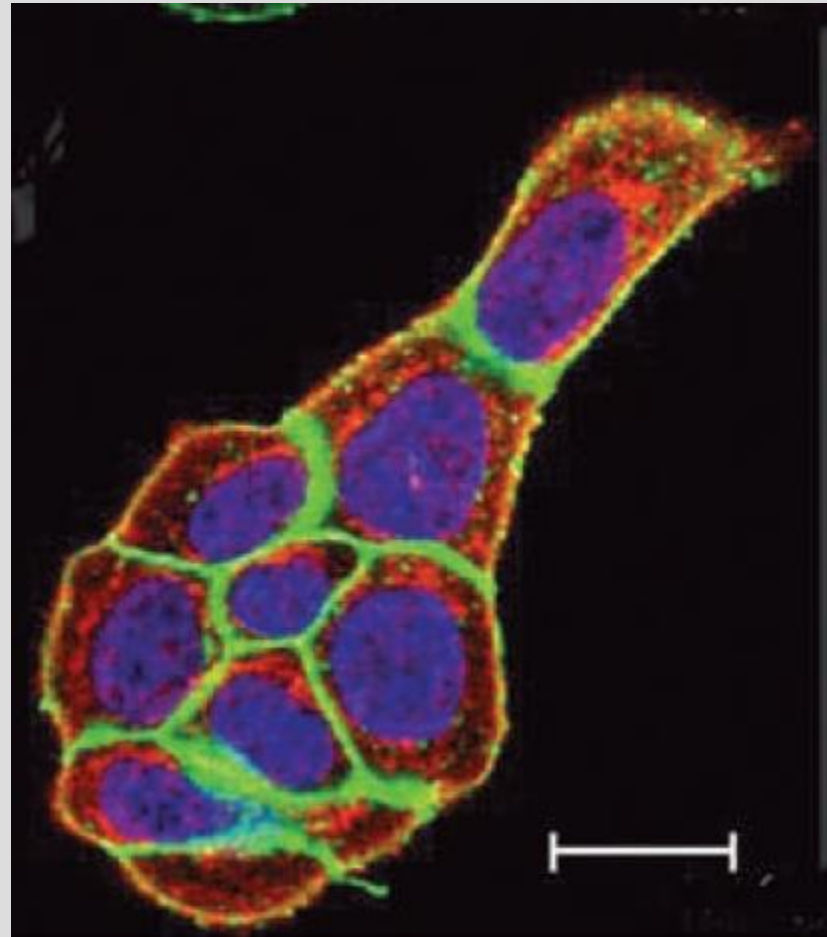
First instrument: Mojmir Petran, 1967



1960-1970

Development of fluorescent antibodies for light microscopy

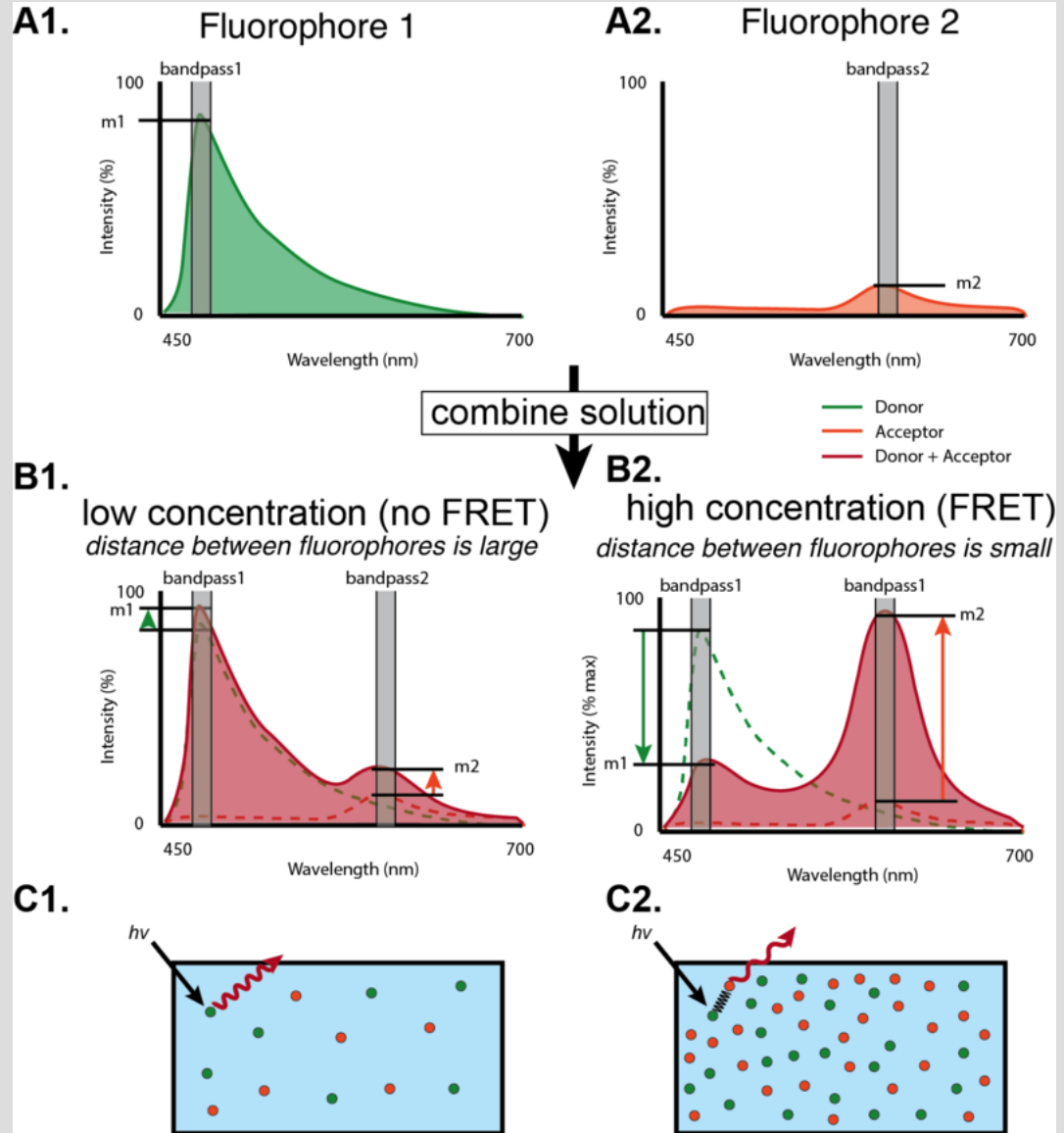
Albert Coons, 1961



1960-1970

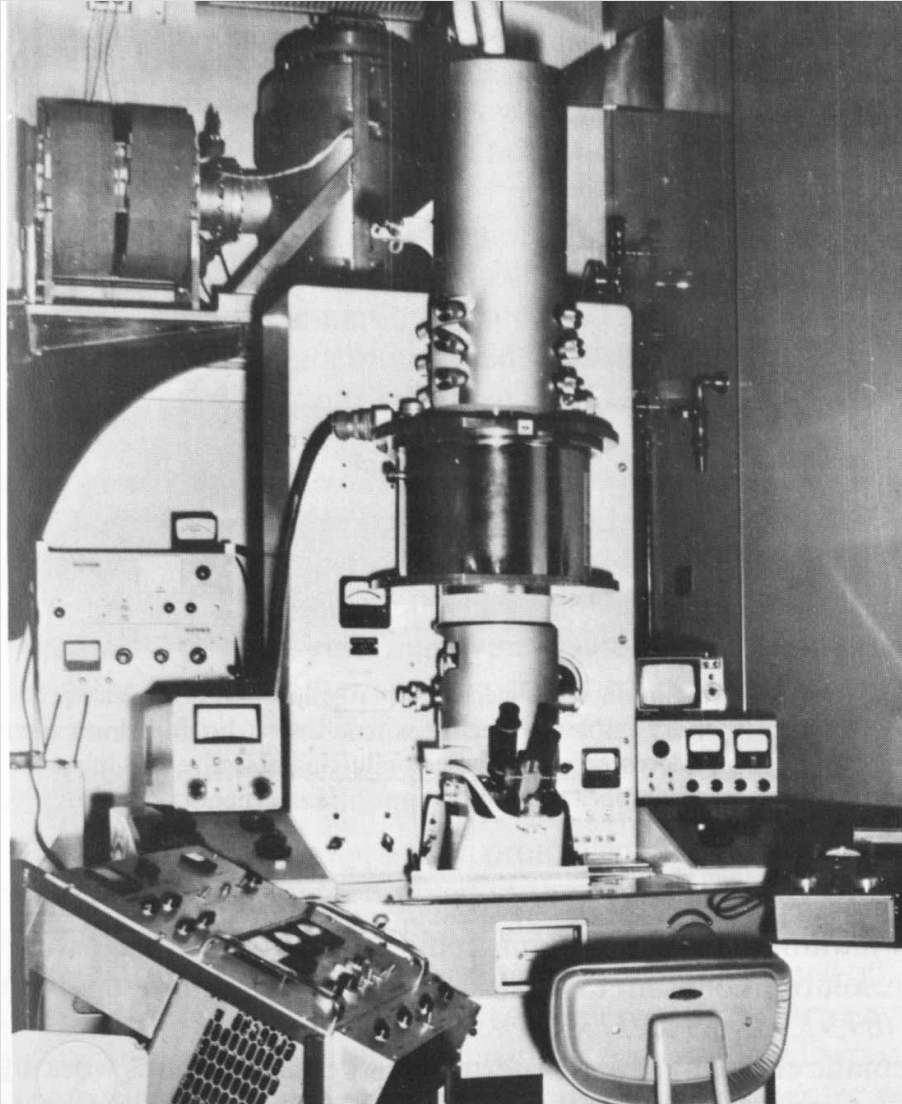
Development of Förster Resonance Energy Transfer (FRET) for light microscopy

Stryer and Haugland, 1967



1960-1970

Early development of cryo-TEM



Humberto Fernández-Morán



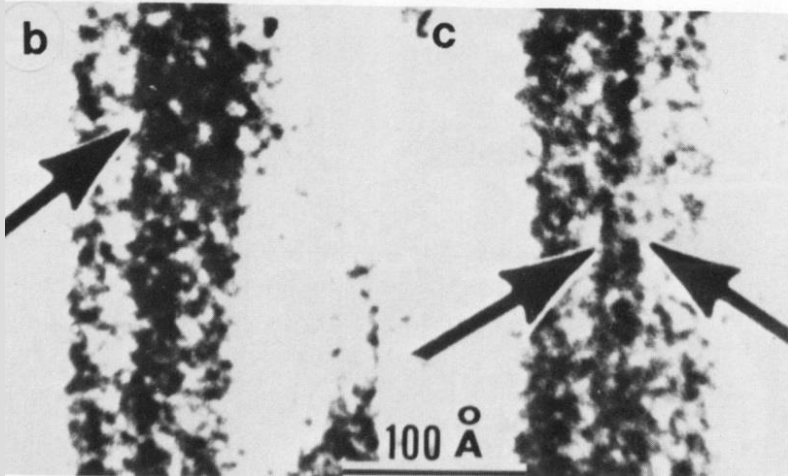
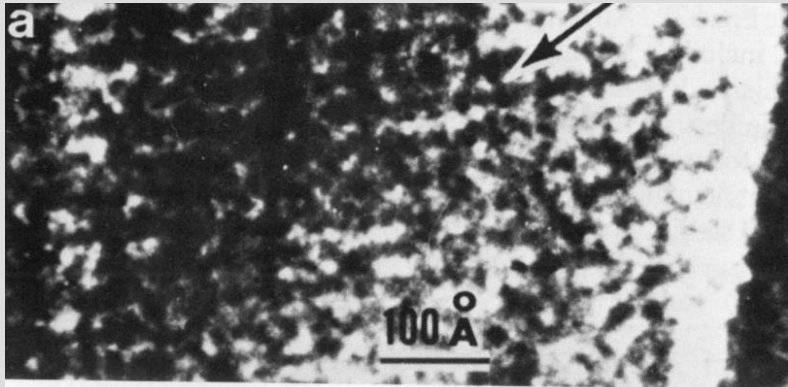
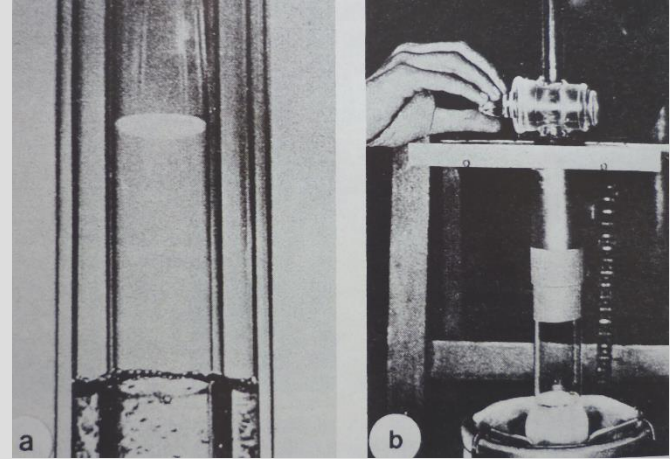
Fernández-Morán's cryo-EM with
superconducting lens for operation
at 4°K (1966)

1960-1970

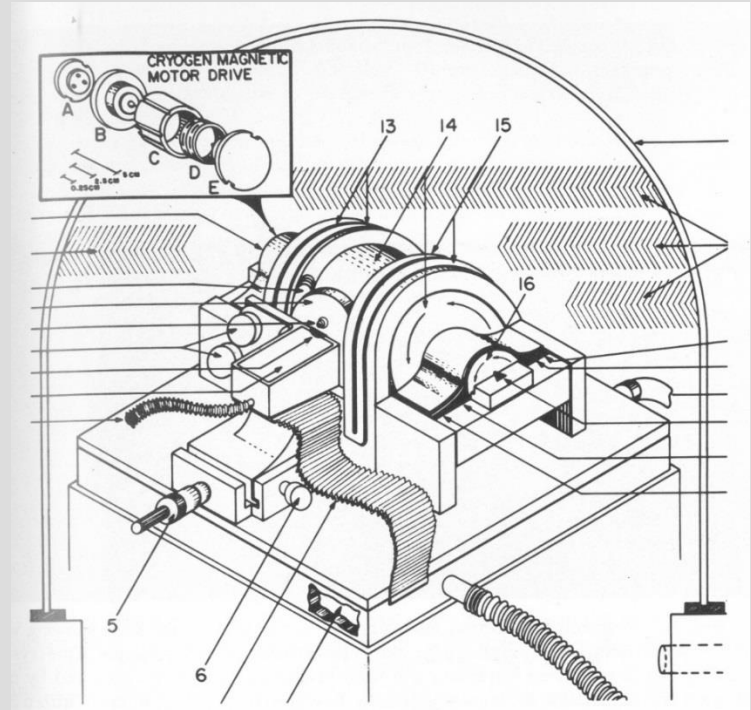
Early development of cryo-TEM

Humberto Fernández-Morán
Cryo-sections in 1966!

Sample
frozen
at 2 K



Catalase and asbestos at 4 K (1966)



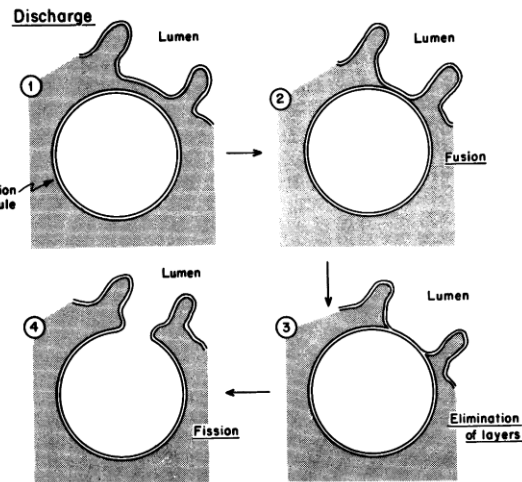
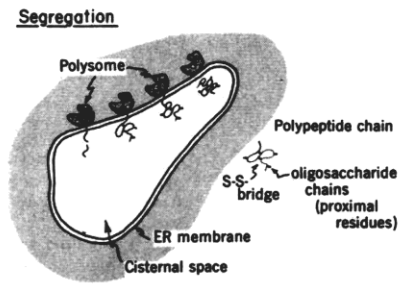
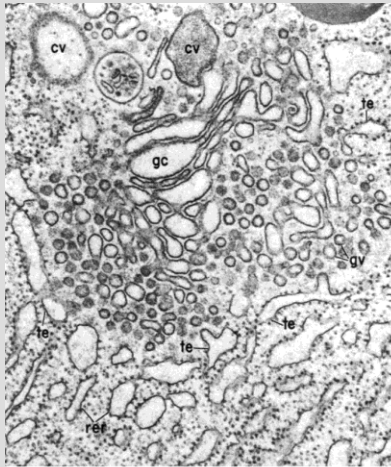
Helium cryo-ultramicrotome with diamond knife, 1968

1960-1970

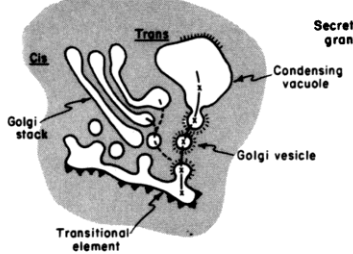
Final development of traditional TEM specimen preparation

Development of "Epon" by Luft (1961) led to ideal ultramicrotomy)

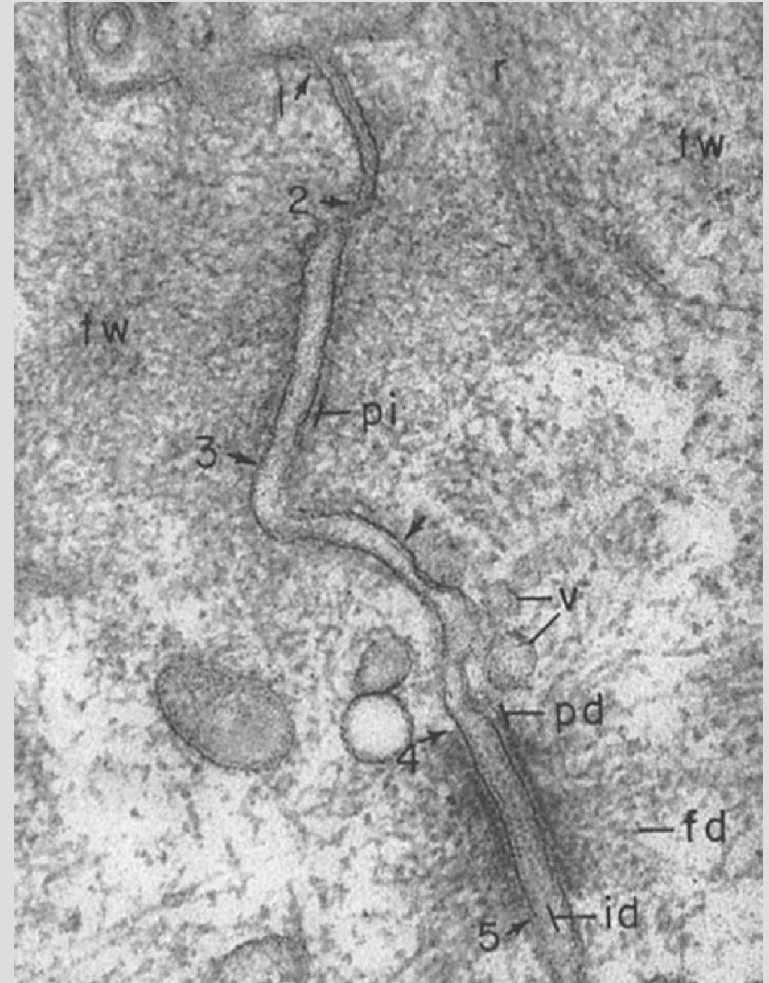
State of the Art, mid 1960s to 1970s



Intracellular Transport



Golgi vesicles



Desmosome structure

1960-1970

Traditional biological TEM

State of the Art, 1964

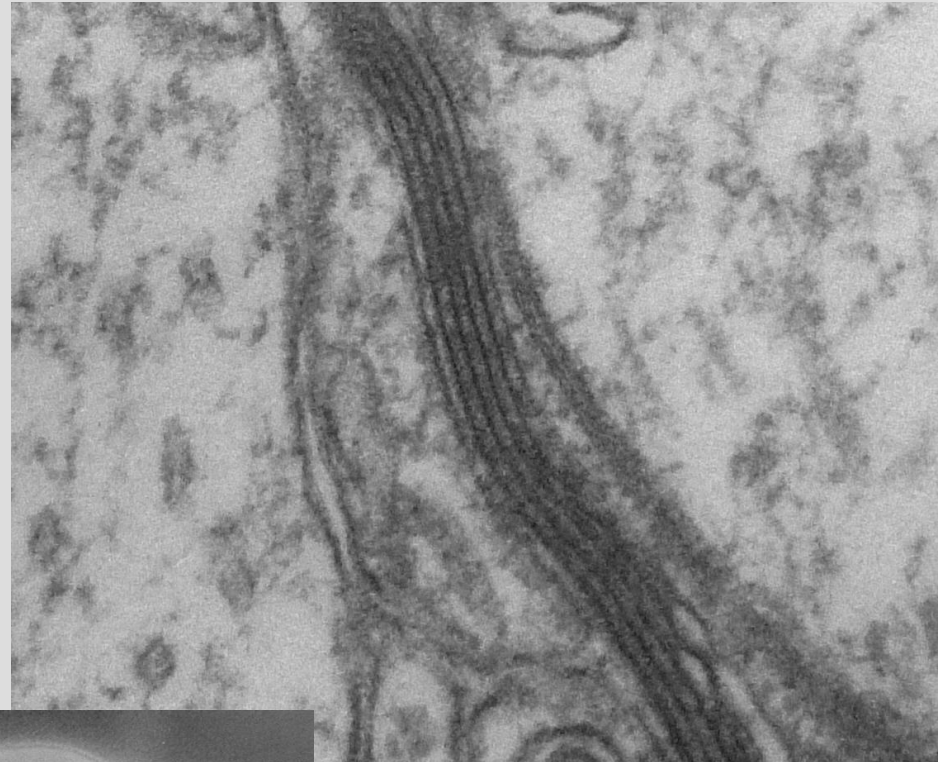


Siemens Elmiskop 10A -- still operating in 2017!

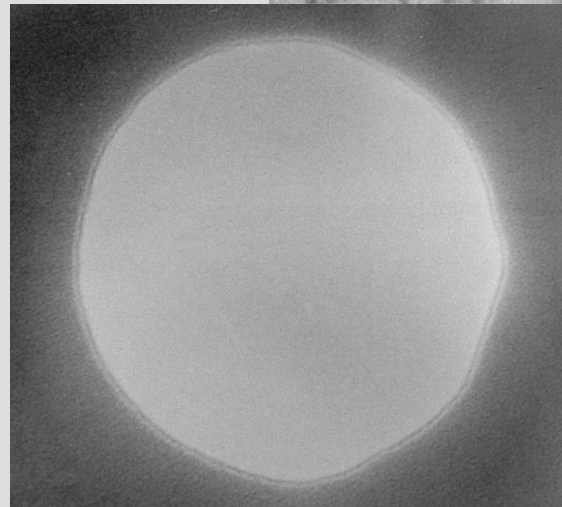
First commercial TEM with 5 Å guaranteed.



(1973)



Prepared and imaged in 2017 with 1964 facilities



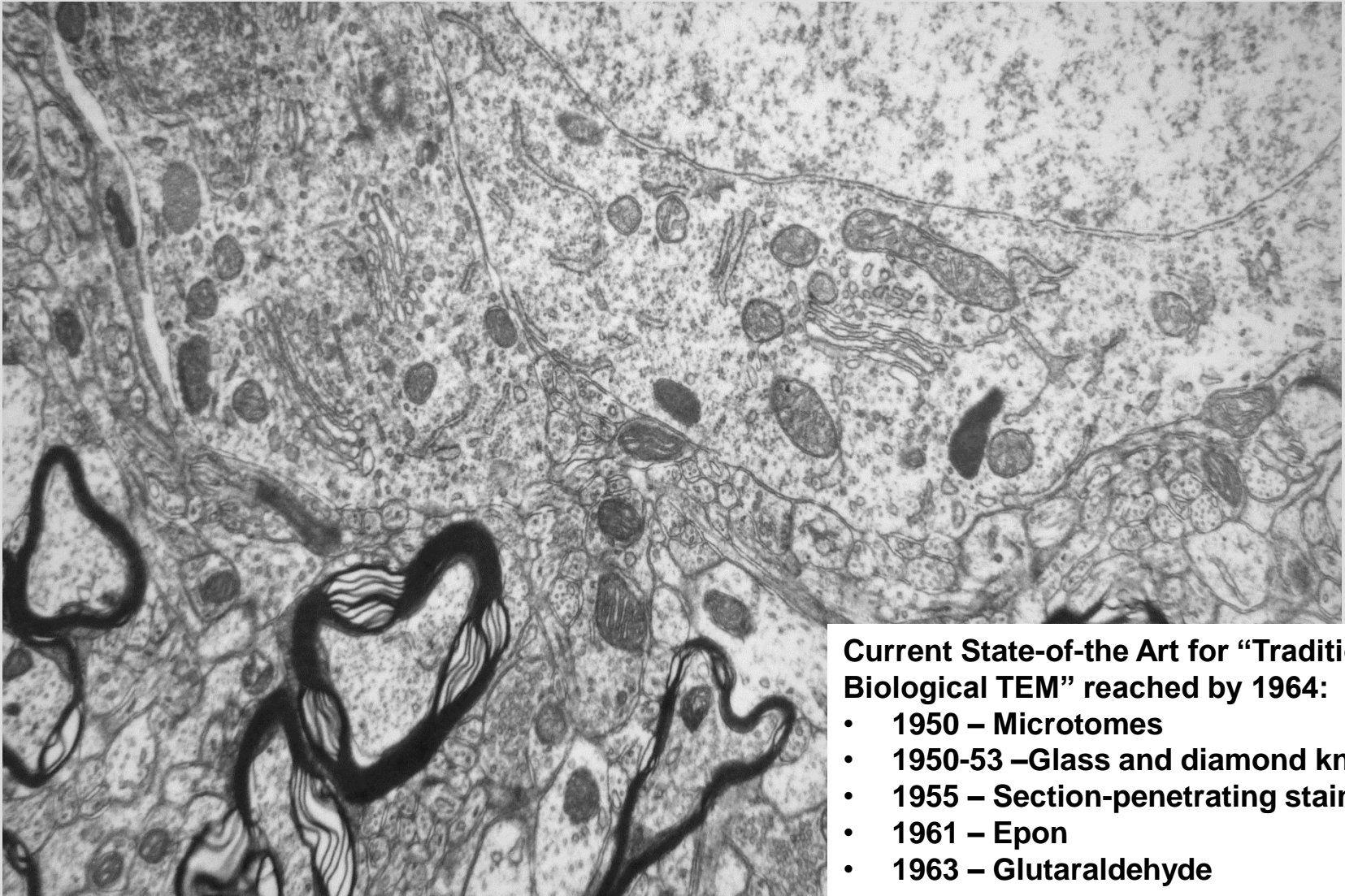
5 Å Fresnel fringe

1960-1970

Traditional biological TEM

State of the Art, 1964

Well-fixed rat-brain section prepared and imaged with 1964 equipment



Current State-of-the Art for “Traditional Biological TEM” reached by 1964:

- 1950 – Microtomes
- 1950-53 – Glass and diamond knives
- 1955 – Section-penetrating stains
- 1961 – Epon
- 1963 – Glutaraldehyde

1960-1970

Nobel Prize #2

Traditional biological TEM

State of the Art biological TEM in the 1960s-1970s – discoveries in Cell Biology



The Nobel Prize in Physiology or Medicine 1974

"for their discoveries concerning the structural and functional organization of the cell"



Albert Claude

🕒 1/3 of the prize

Belgium

Université Catholique de Louvain
Louvain, Belgium

b. 1899
d. 1983



Christian de Duve

🕒 1/3 of the prize

Belgium

Rockefeller University
New York, NY, USA

b. 1917



George E. Palade

🕒 1/3 of the prize

USA

Yale University, School of Medicine
New Haven, CT, USA

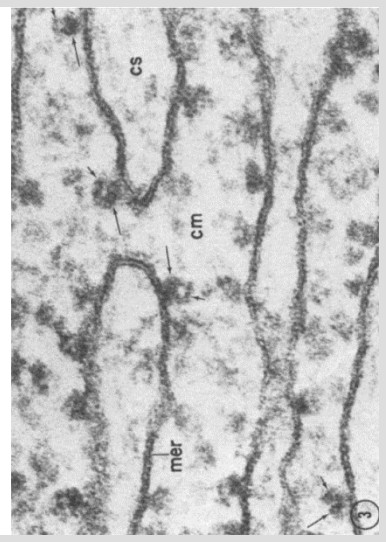
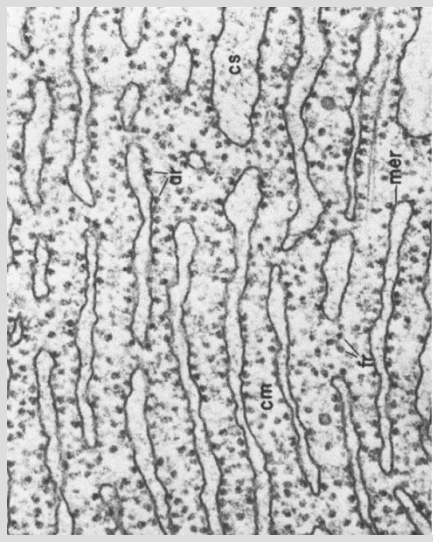
b. 1912
(in Iasi, Romania)
d. 2008

CYTOCHEMISTRY AND ELECTRON MICROSCOPY

The Preservation of Cellular Ultrastructure and Enzymatic Activity by Aldehyde Fixation

DAVID D. SABATINI, M.D., KLAUS BENSCH, M.D., and RUSSELL J. BARNETT, M.D.

THE JOURNAL OF CELL BIOLOGY · VOLUME 17, 1963



Improved fixation was critical, first Palade's buffered Oso4, then glutaraldehyde

1960-1970

Nobel Prize #3

Development of image-processing and 3-D reconstruction

Reconstruction of Three Dimensional Structures from Electron Micrographs

D. J. DE ROSIER
A. KLUG

MRC Laboratory of Molecular Biology,
Hills Road, Cambridge

NATURE, VOL. 217, JANUARY 13, 1968.

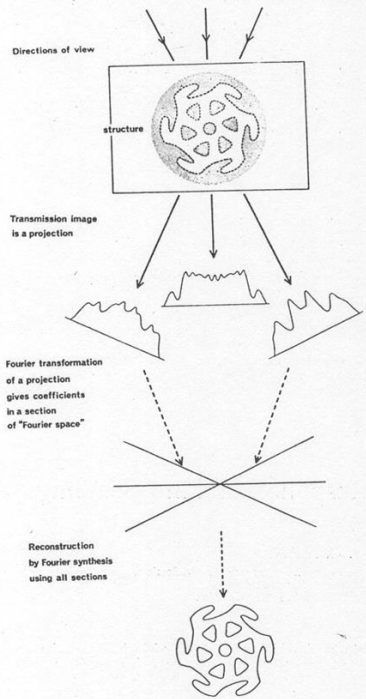


Fig. 6. Schema for the general process of reconstruction of a structure from its transmission images.

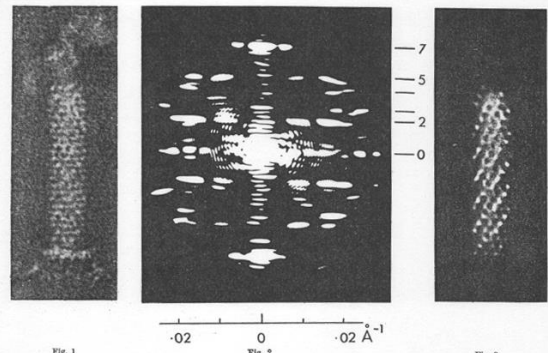
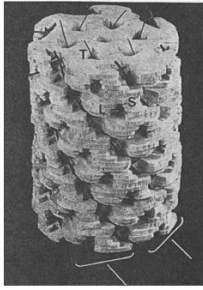


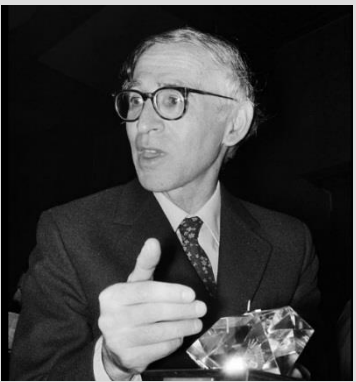
Fig. 1. Electron micrograph of a tail of bacteriophage T4, negatively stained with uranyl formate. ($\times 500,000$)

Fig. 2. Optical diffraction pattern of the phage tail image in Fig. 1. Stronger exposures show that the order in the micrograph extends to spacings of about 25 Å. The strong meridional peak on the seventh layer line arises from the spacing of 88 Å between annuli. The layer lines are approximately equally spaced at the orders of an approximate repeat of $7 \times 28 = 200$ Å. The helical selection rule for the diffraction pattern is $l = 2n + 7m$, the only permitted values of l being those which are multiples of six.

Fig. 3. Optically filtered image of phage tail in Fig. 1, admitting only the diffracted rays corresponding to the far side of the particle. The dominant features are two distinct sets of oblique striations, which correspond to two distinct sets of helical lines existing along two cylindrical surfaces of different diameter, and thus correspond to features at different depths in the particle.



David DeRosier



Sir Aaron Klug
at 1982 Nobel
ceremony

The general method of reconstruction which we developed (Fig. 9) is based on the projection theorem, which states that the two-dimensional Fourier transform of a plane projection of a three-dimensional density distribution is identical to the corresponding central section of the three-dimensional transform normal to the direction of view. The three-dimensional transform can therefore be built up section by section using transforms of different views of the object, and the three-dimensional reconstruction then produced by Fourier inversion. The important feature of the method is that it tells one how many

1960-1970

Development of image-processing and reconstruction

Principles – The “Crowther criterion”

Proc. Roy. Soc. Lond. A. **317**, 319–340 (1970)

Printed in Great Britain

The reconstruction of a three-dimensional structure from projections and its application to electron microscopy

BY R. A. CROWTHER, D. J. DEROSIER† AND A. KLUG, F.R.S.

*Medical Research Council Laboratory of Molecular Biology,
Hills Road, Cambridge*

(Received 5 December 1969)

A transmission electron micrograph is essentially a projection of the specimen in the direction of view. In order to reconstruct a three-dimensional image of the specimen, it is necessary to be able to combine data from a number of different views. A formal solution of this problem is given in terms of Fourier transforms. Its realization requires data reduction and interpolation. The final solution is given by a least squares approach, which also indicates how many views must be included to give a valid reconstruction of a given particle to a given degree of resolution. Interpolation procedures of varying power are given, to be employed according to the economy with which the available data must be used.

An alternative procedure is described for direct reconstruction without the use of Fourier transforms, but it is shown to be in general less practicable than the Fourier approach.

In other words, the minimum number of views, m , to reconstruct a particle of diameter D to a resolution of d ($= 1/R_{\max}$) is given by

$$m \simeq \pi D/d.$$

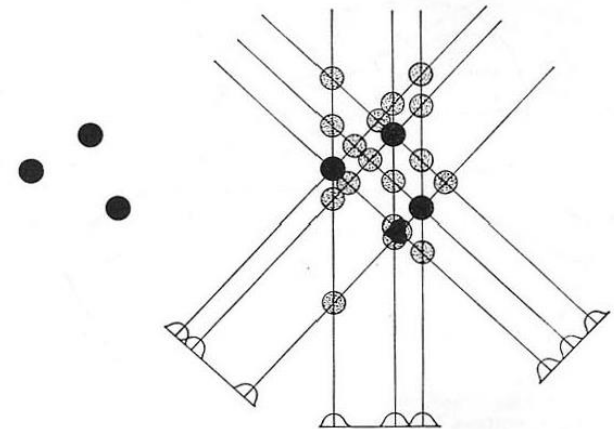
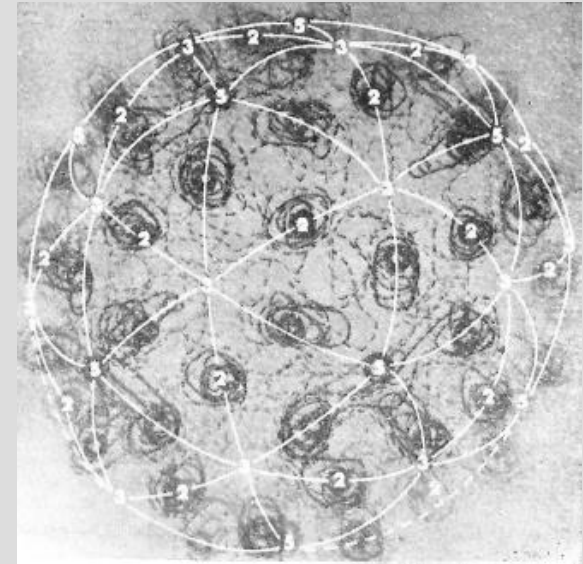


FIGURE 6. Two-dimensional illustration of density space reconstruction by back-projection. The ‘object’ is shown on the left. On the right, its structure is reconstructed by back-projection from three projected views of the object. Note that, even in so simple an example, there is a chance overlap producing a spurious feature of weight equal to those in the true structure. There are also subsidiary features which, in the case of equal resolved atoms, it is possible to discriminate against by some form of threshold.



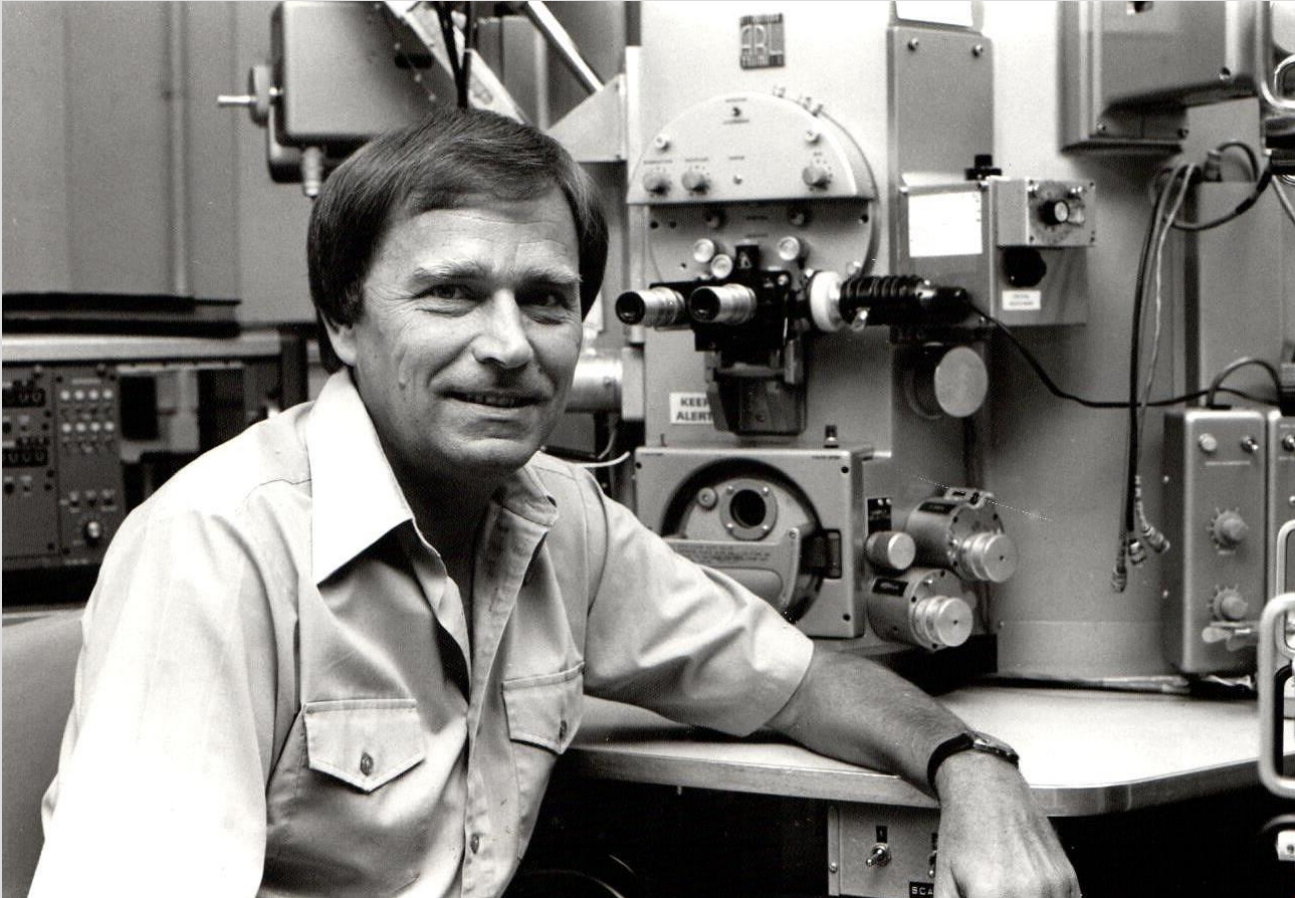
1970-1980



1970-1980

MAS 50th congratulations!

Much success with the 50th Anniversary Meeting of MAS!
Klaus Keil: former MAS President



Klaus Keil using a somewhat advanced ARL electron microprobe in the University of New Mexico, Albuquerque, probably ~ 1975

1970-1980

EM pioneers at Toronto ICEM, 1978



Keith Porter / James Hillier / Ernst Ruska / Albert Prebus / Cecil Hall

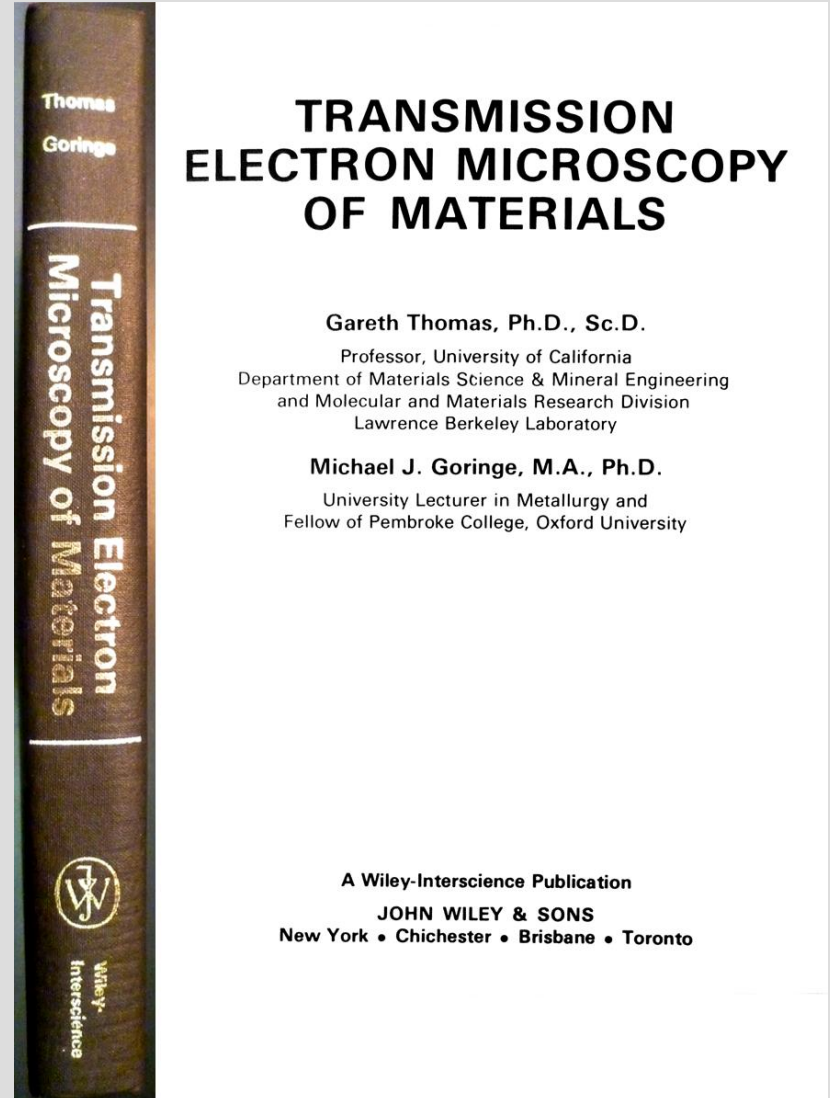
1970-1980

Continued focus on TEM in materials science



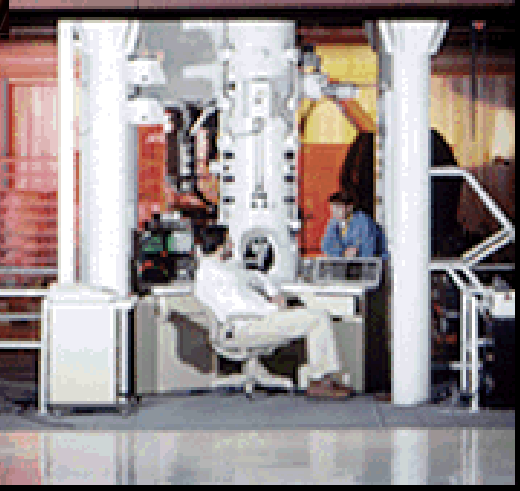
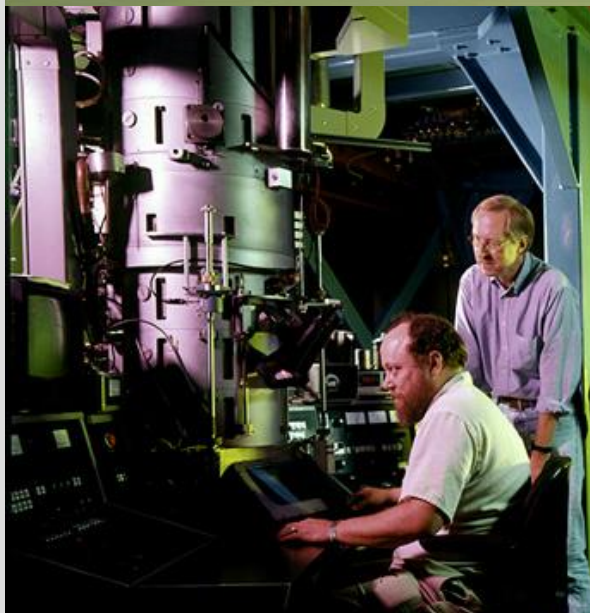
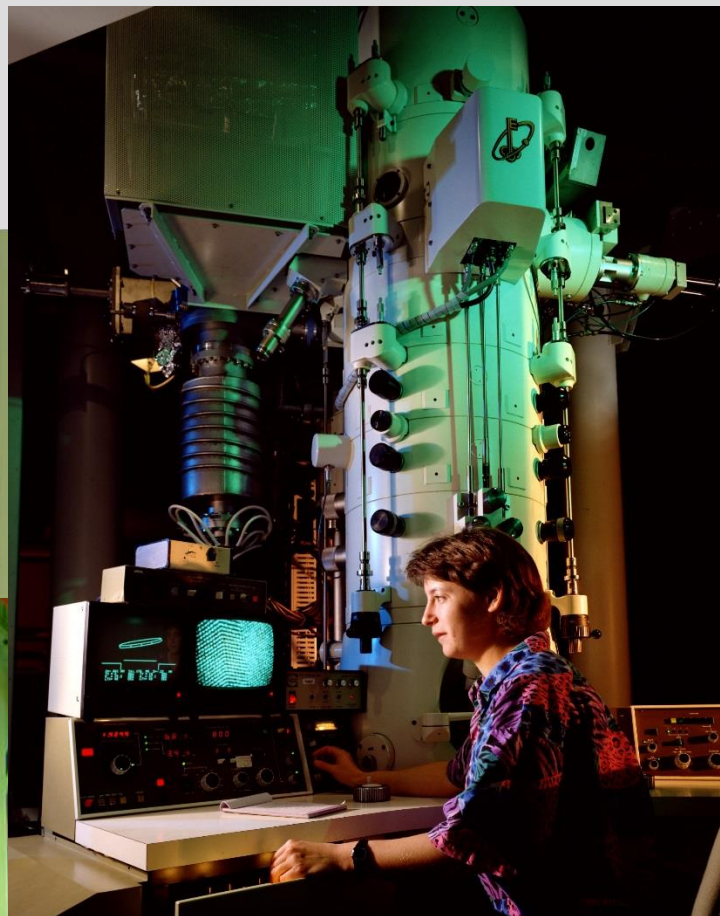
**Hastuji
Hashimoto:
Single
atoms by
HREM,
1971**

**Gareth
Thomas:
Strong
promotion
of TEM for
materials**



1970-1980

HVEM applications



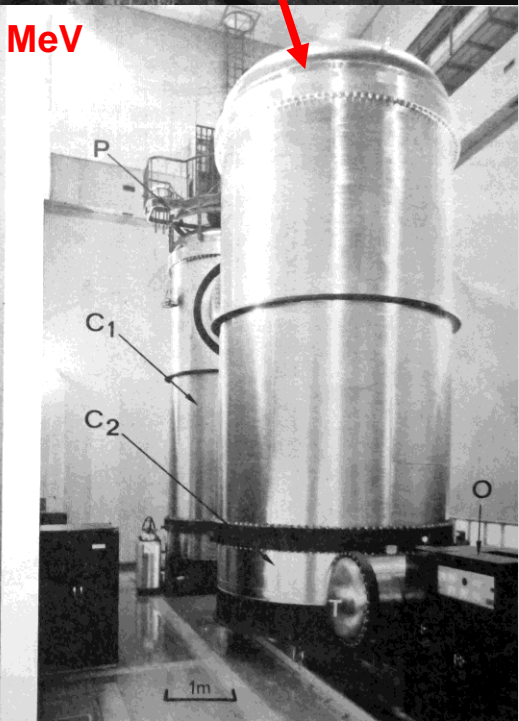
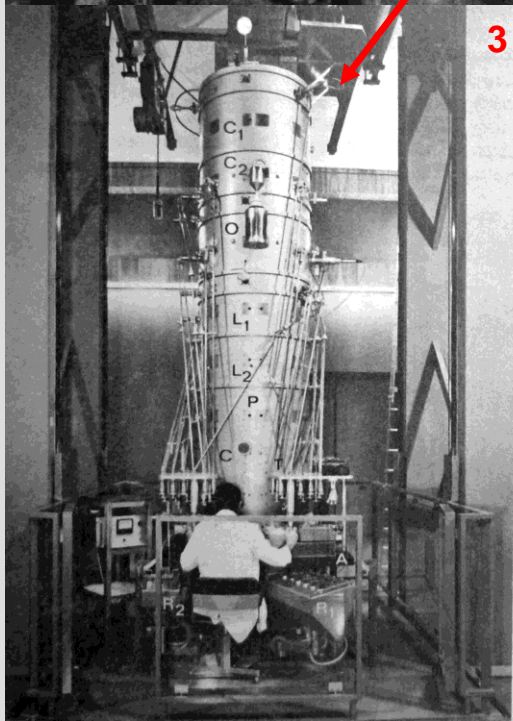
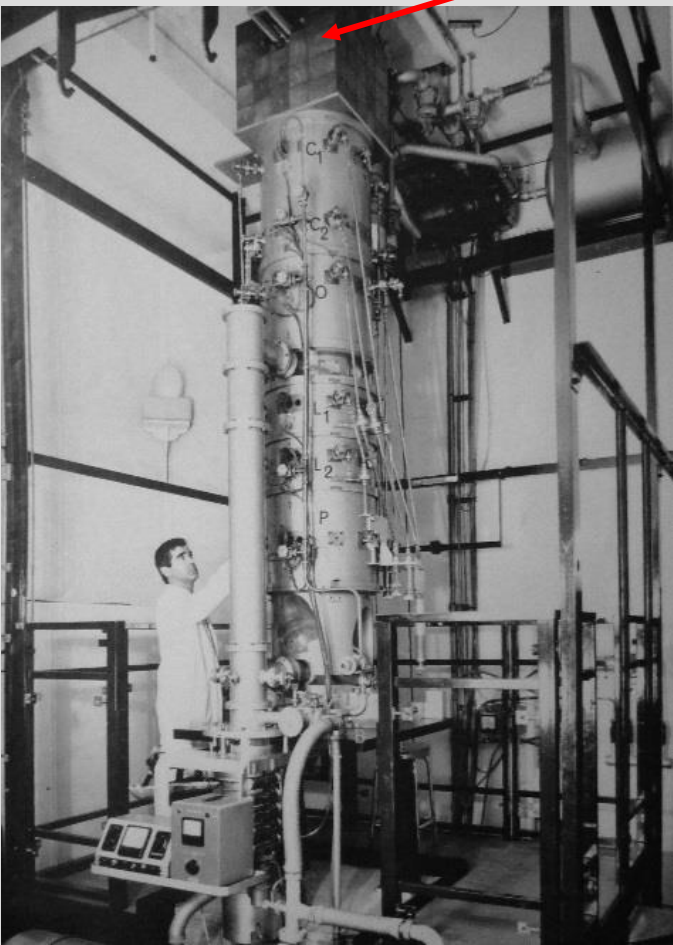
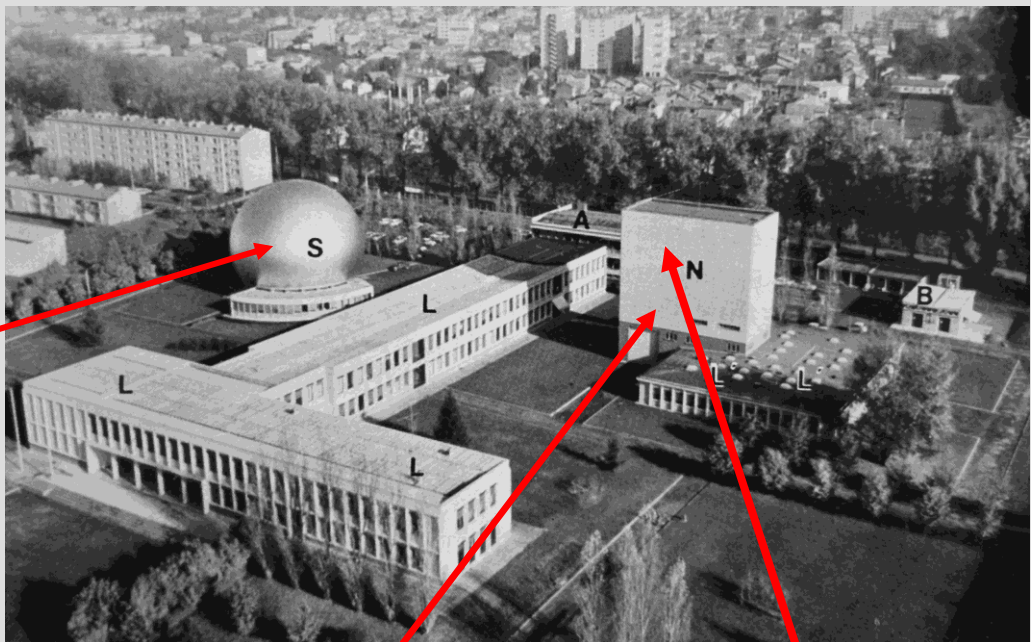
N C E M

NATIONAL CENTER FOR
ELECTRON MICROSCOPY

1970-1980

HVEM applications

Toulouse 1 MeV
and 3 MeV HVEMs,
1970s



1970-1980

HVEM applications

Hitachi 3 MeV TEM, Osaka, 1970



1970-1980

Continued focus on TEM in materials science

Imaging atomic columns: Cowley and Iijima, 1972



1970-1980

Continued focus on TEM in materials science

Special-purpose specimen holders: Peter Swann

Ned Sue Graham Howard Bill John Paul
Edwards Burrows Briers Cheetham Bishop Woodhall Butler



Harvey Flower Tony Lloyd Leo Christadoulou Peter Swann

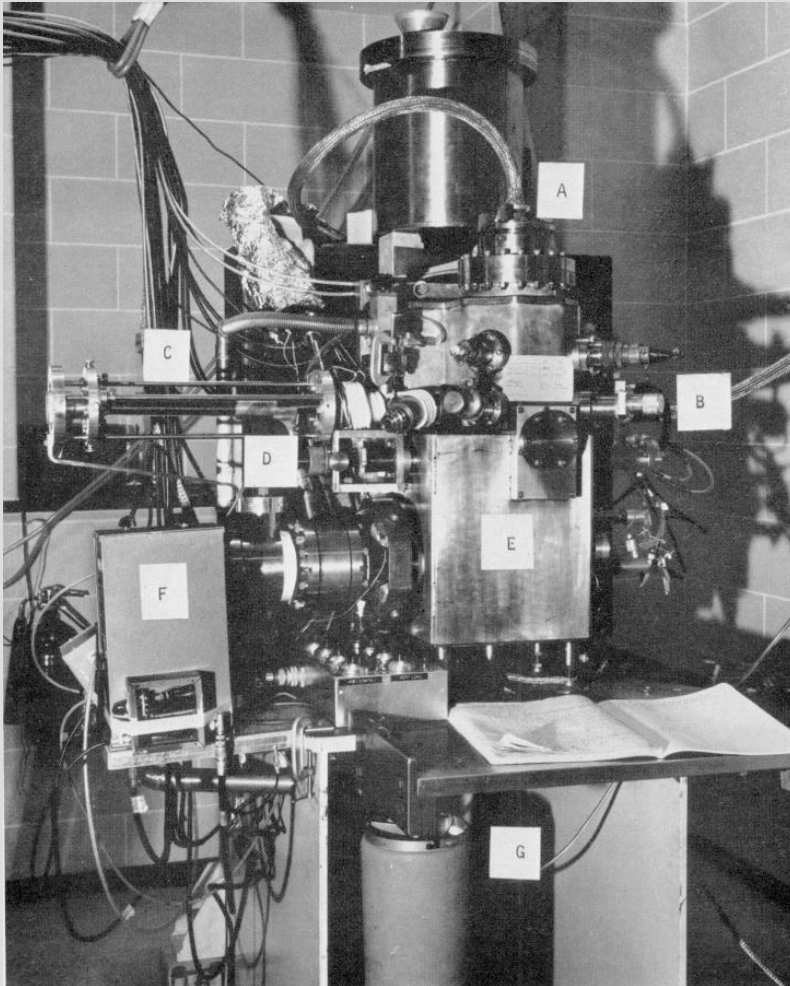
P Swann Research group 1976



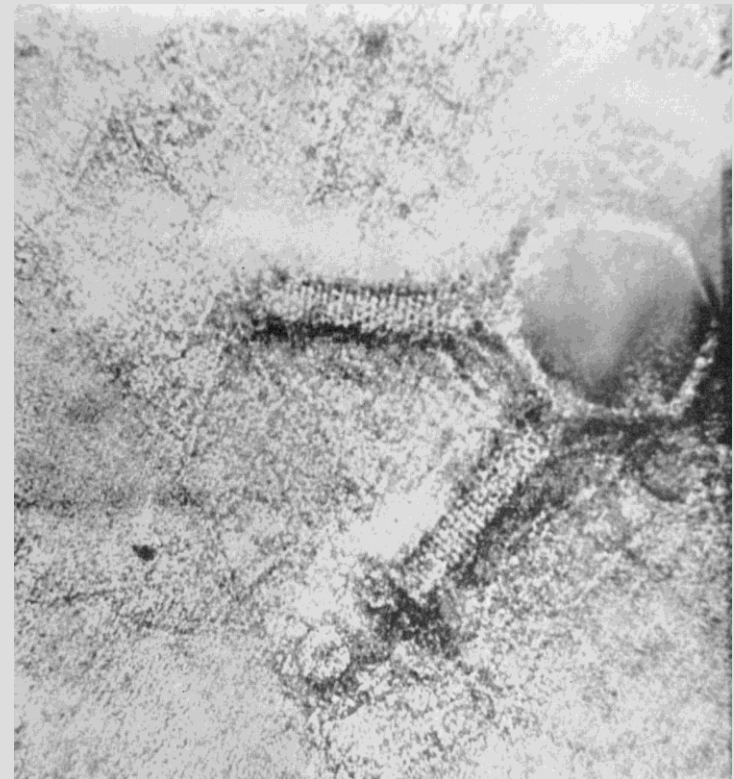
1970-1980

Continued development of HR-STEM

Crewe, Wall, Issacson



1970 0.5-nm STEM



T4 phage

1970-1980

Continued development of HR-STEM

Towards 1 MeV STEM: Crewe et al.

E. Zeitler / Ultramicroscopy 123 (2012) 13-21

19

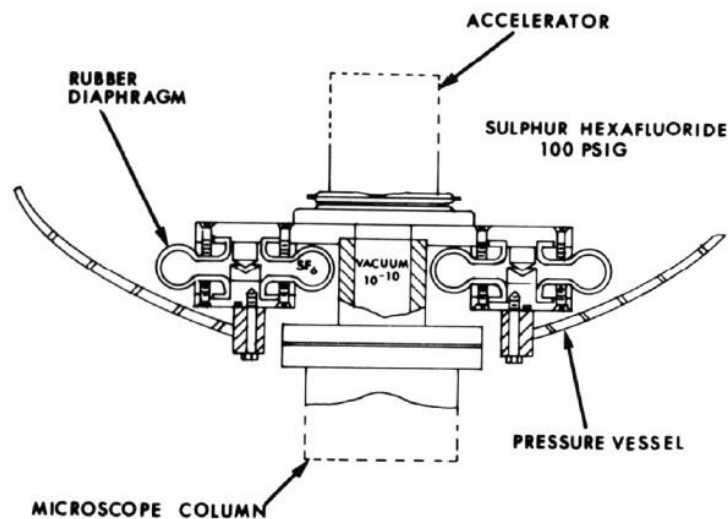


Fig. 10. Air-mount feed-through of microscope column—the "Doughnut".

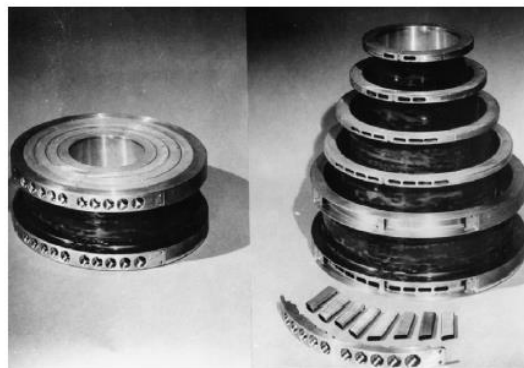


Fig. 11. Objective lens: Divided windings and water-cooling system.

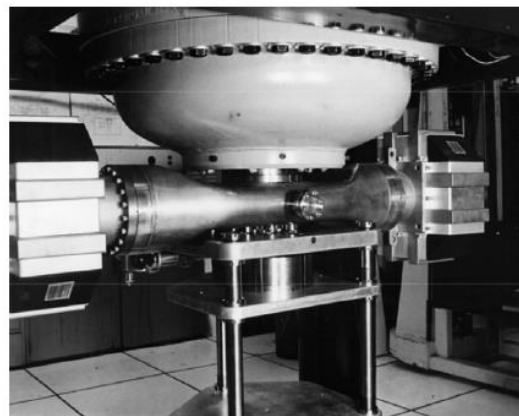
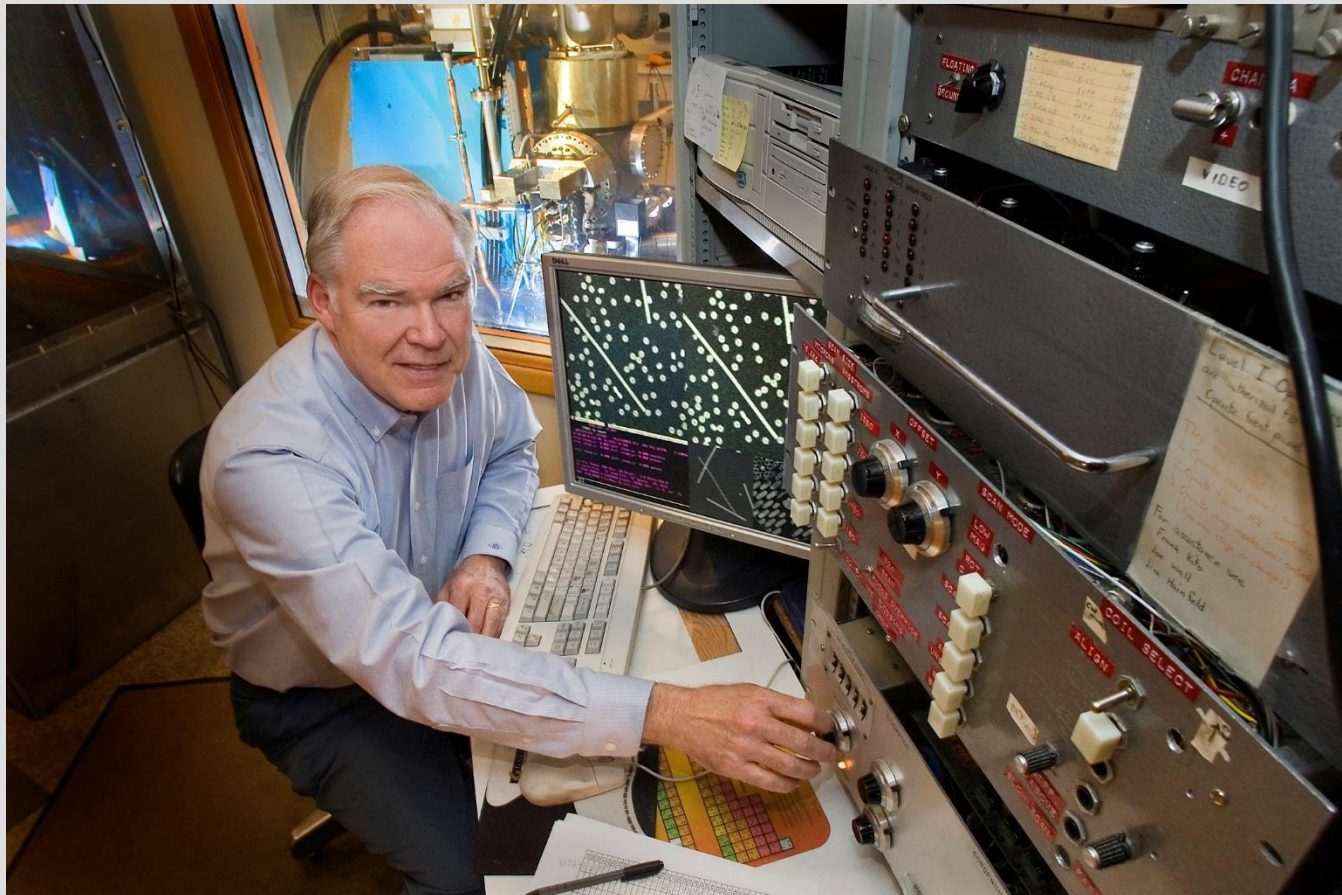


Fig. 12. Down to earth. The microscope from the accelerator to the objective lens, resting on its shelf.

1970-1980

Continued development of HR-STEM

Joe Wall and his Brookhaven STEM

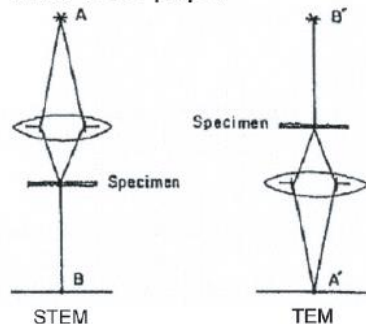


1970-1980

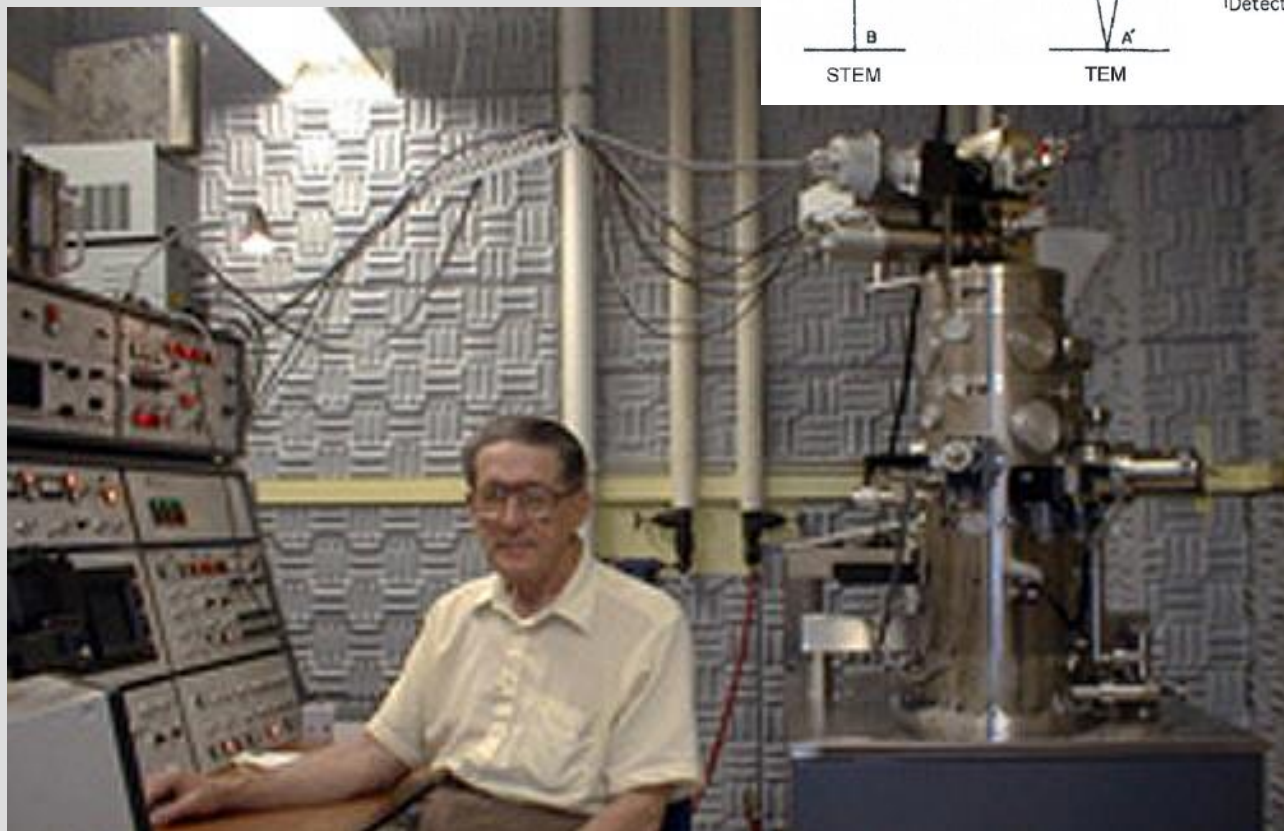
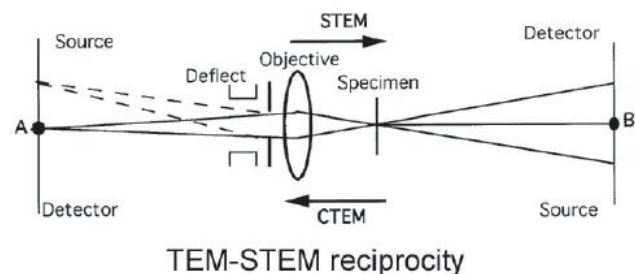
Continued development of HR-STEM

John Cowley and his analytical STEM "MIDAS"

from 1969 paper



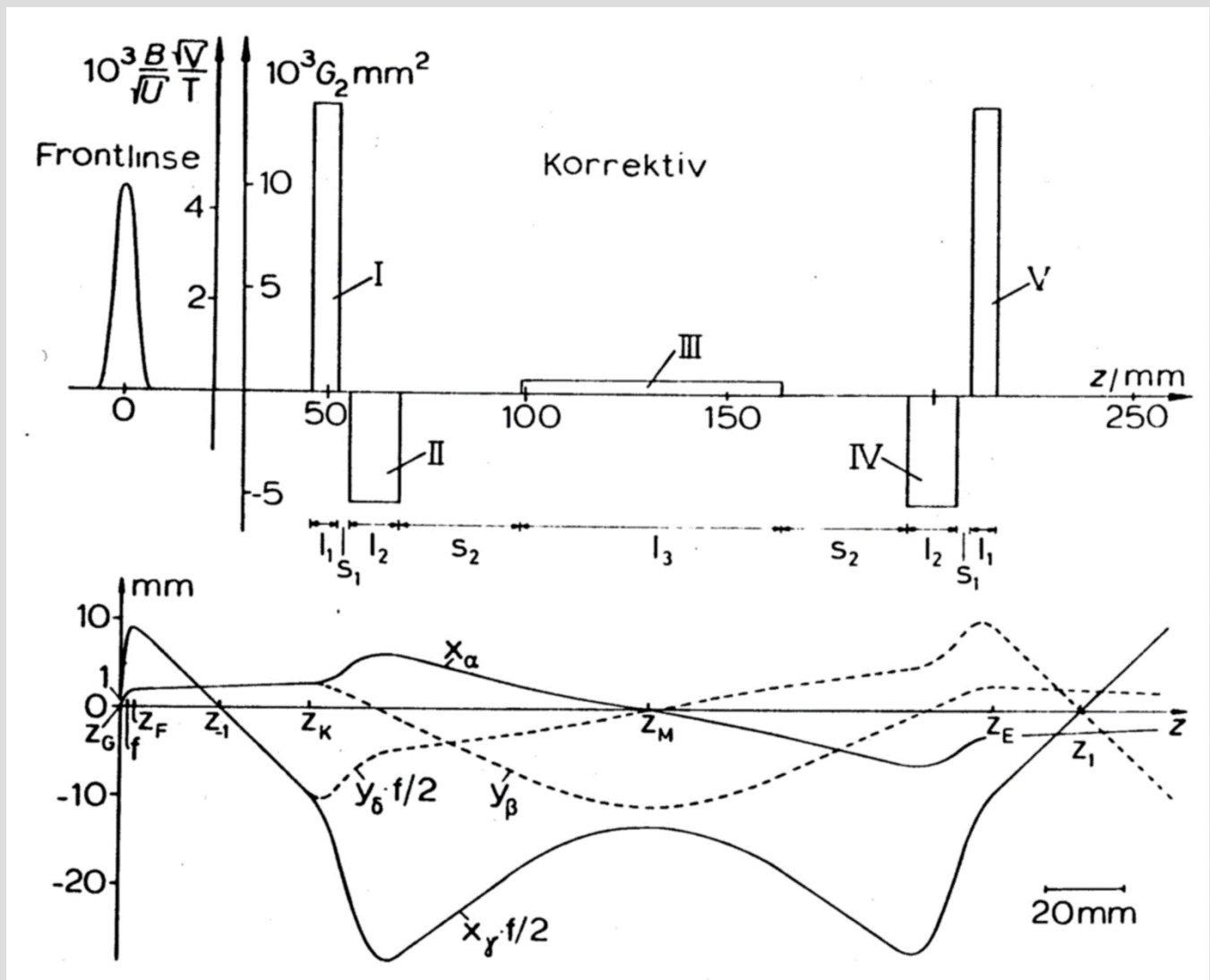
from 1999 paper



1970-1980

Realization of aberration correction

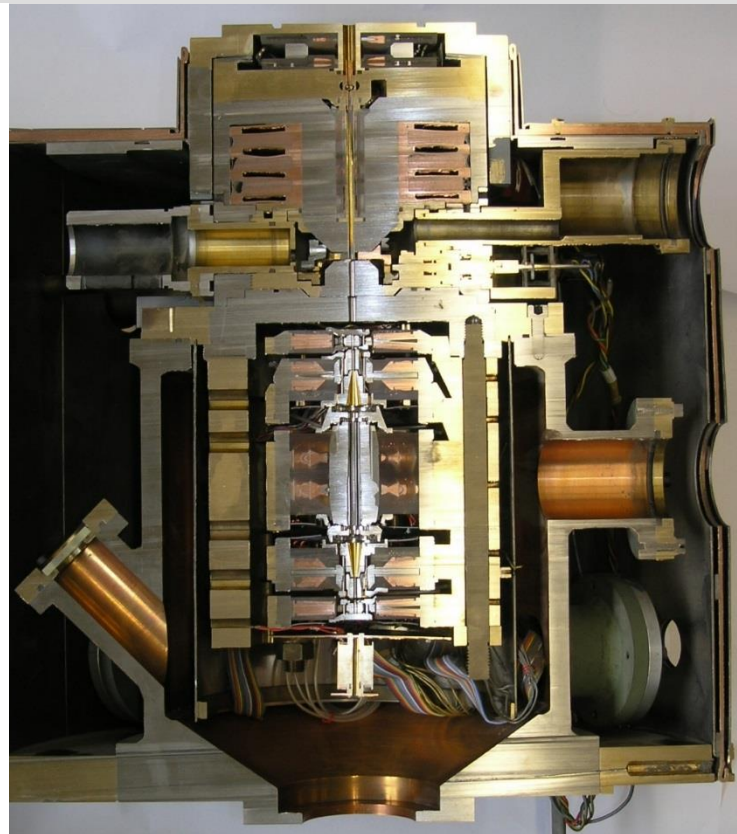
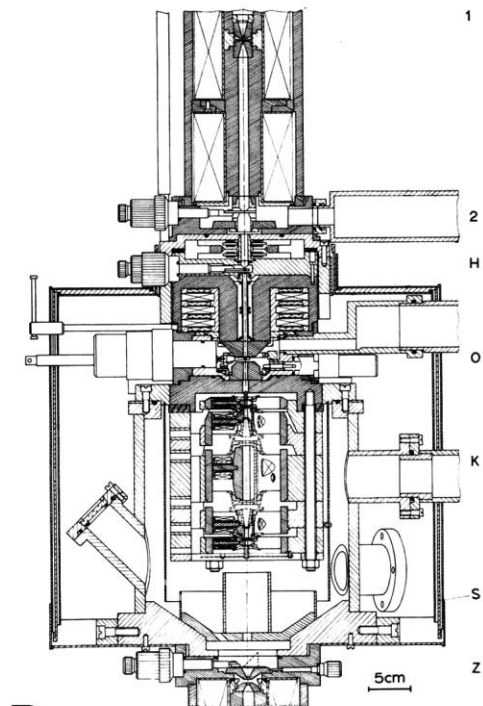
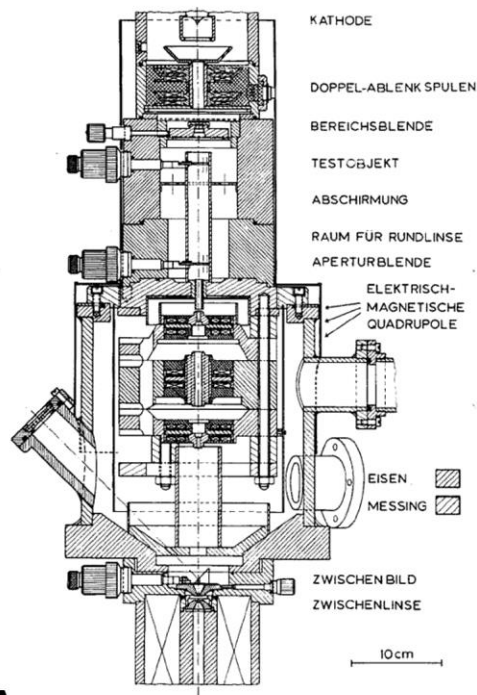
The Darmstadt corrector: Principal rays



1970-1980

Realization of aberration correction

The Darmstadt corrector: Construction



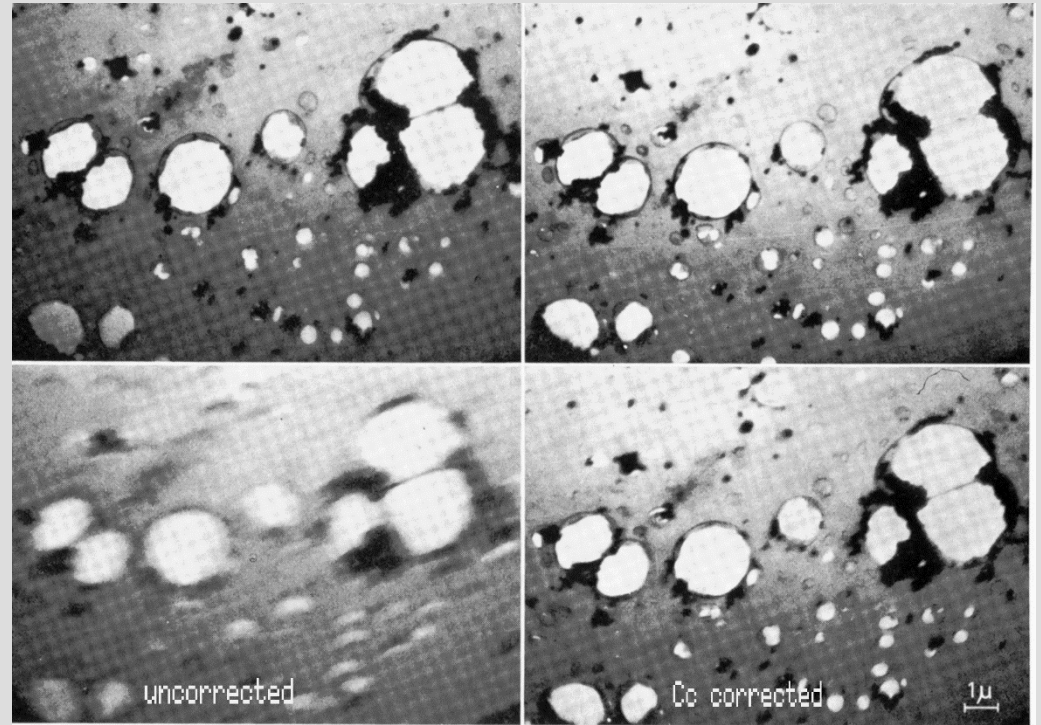
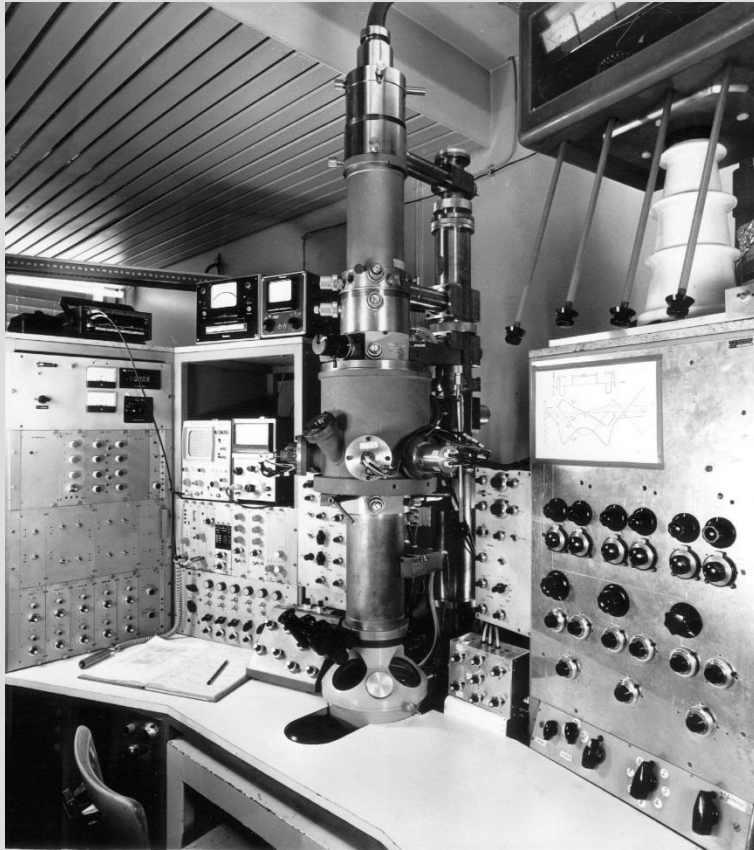
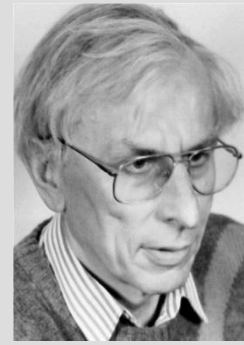
A

B

1970-1980

Realization of aberration correction

Harald Rose et al.: The Darmstadt corrector

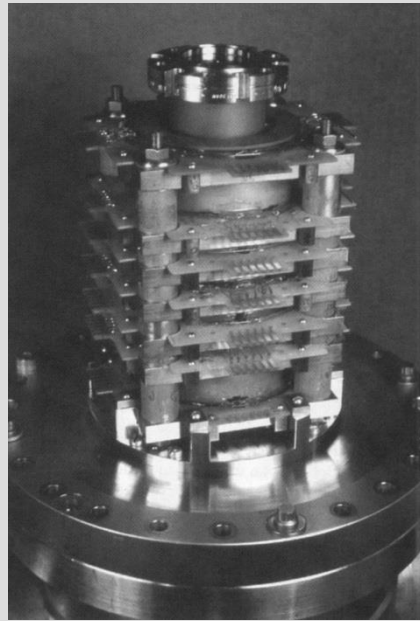
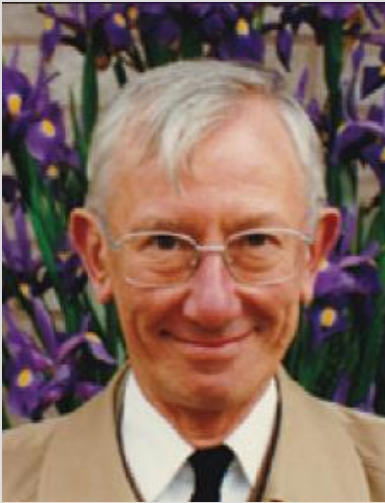


First experimental proof of chromatic correction, left: corrector on, right corrector; upper row: $dE = 2\text{eV}$, bottom: $dE = 130\text{eV}$ (1977)

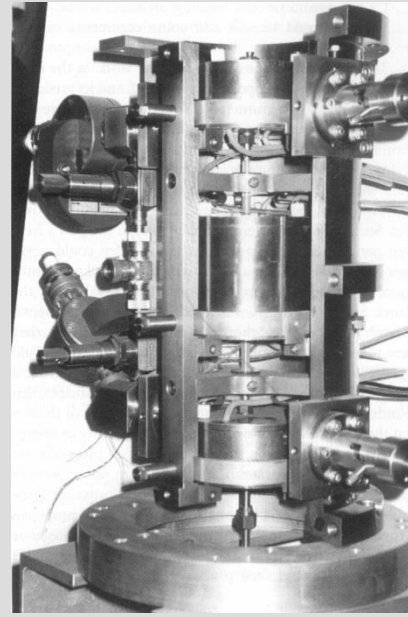
1970-1980

Realization of aberration correction

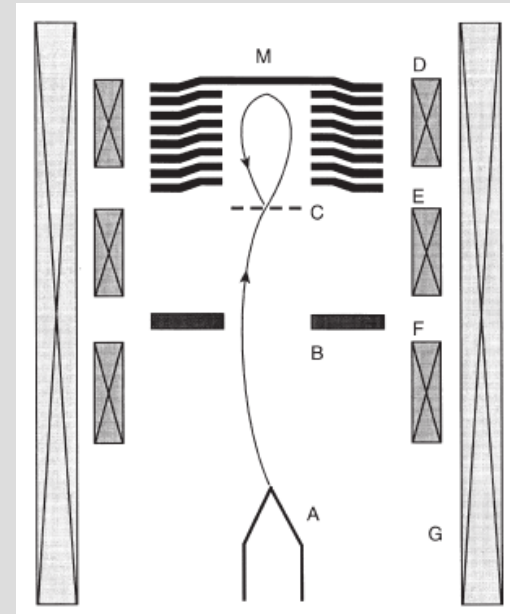
Peter Hawkes: Re-consideration of possible corrector designs



Octupole-quadrupole



Sextupole

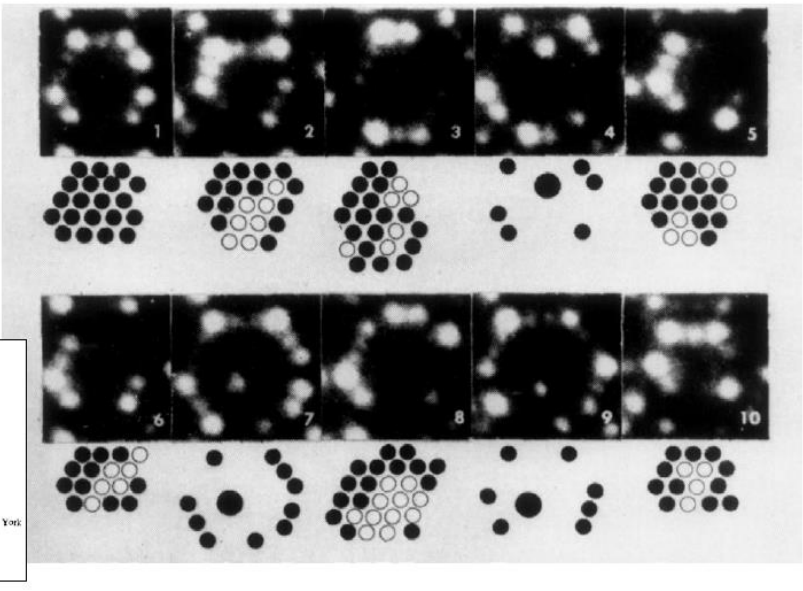


Mirror

1970-1980

Continued development of the atom probe

- Vacancies observed
- Knock-on damage cascades were mapped by cinematography of FIM



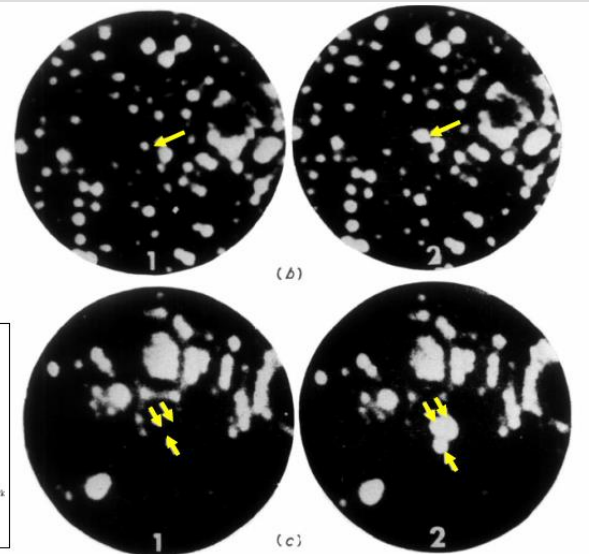
J. Phys. F: Metal Phys., Vol. 3, February 1973. Printed in Great Britain. © 1973.

The direct observation of point defects in irradiated or quenched metals by quantitative field ion microscopy†

DAVID N SEIDMAN‡
Department of Materials Science and Engineering, Cornell University, Ithaca, New York 14850, USA

MS received 21 September 1972

- Surface atoms and defects are visible in FIM
- E.g. Self-interstitial atoms produce large image in FIM



J. Phys. F: Metal Phys., Vol. 3, February 1973. Printed in Great Britain. © 1973.

The direct observation of point defects in irradiated or quenched metals by quantitative field ion microscopy†

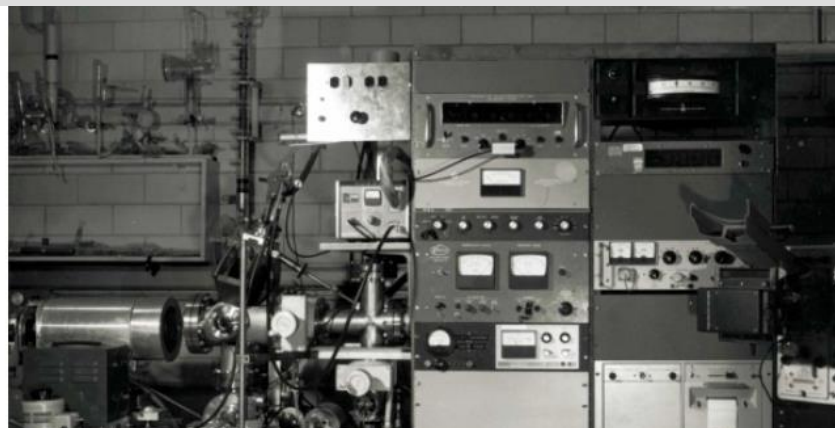
DAVID N SEIDMAN‡
Department of Materials Science and Engineering, Cornell University, Ithaca, New York 14850, USA

MS received 21 September 1972

1970-1980

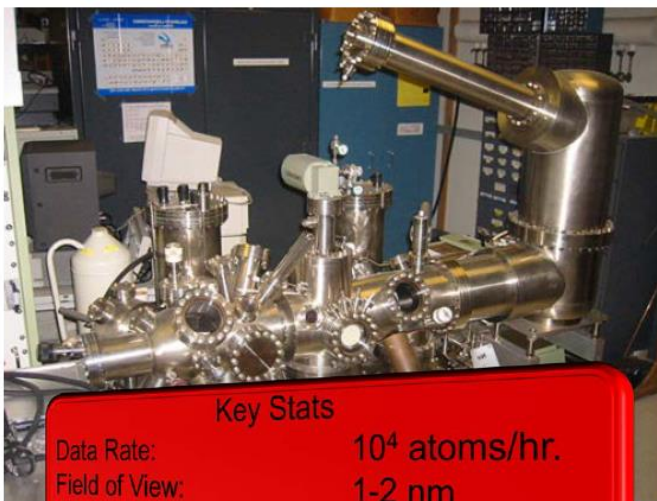
Continued development of the atom probe

Work of George Smith et al.,
Oxford



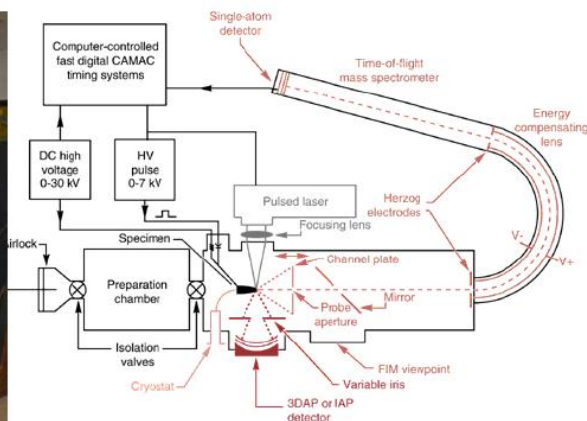
The Vacuum Generators APFIM 100

1975



Key Stats

Data Rate:	10^4 atoms/hr.
Field of View:	1-2 nm
Mass Resolving Power:	2000

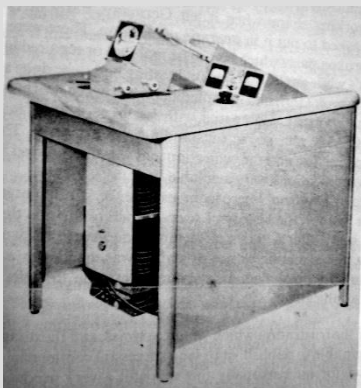


- Developed in conjunction with Smith et al. at Oxford
- First commercial atom probe

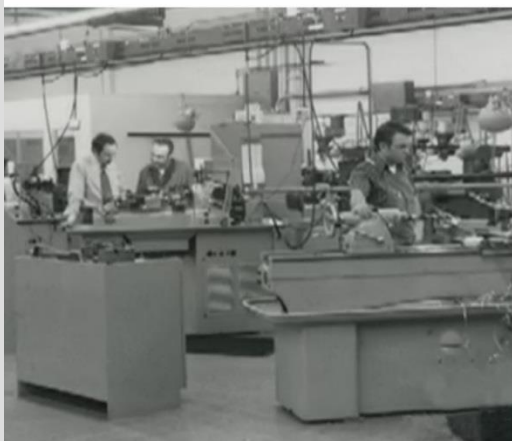
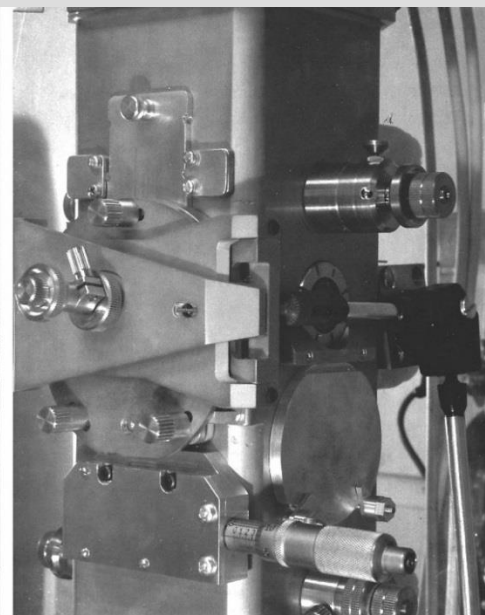
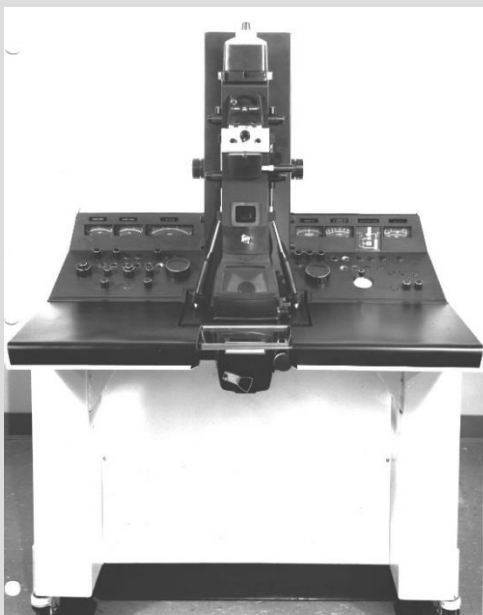
1970-1980

Non-mainstream TEMs

Gertrude Rempfer: Development of the Elektros electrostatic TEM



Rempfer's early Ferrand electrostatic TEM (never produced)

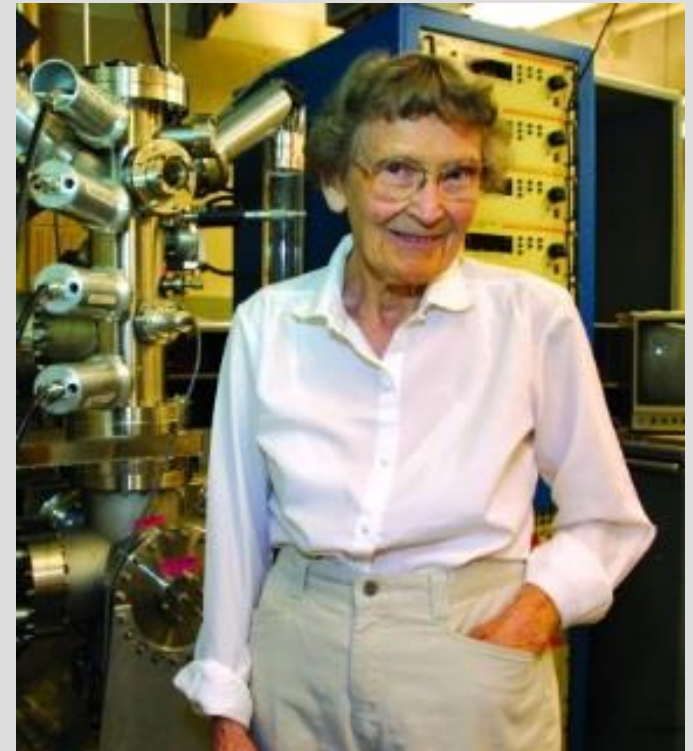


1970-1980

Non-mainstream TEMs

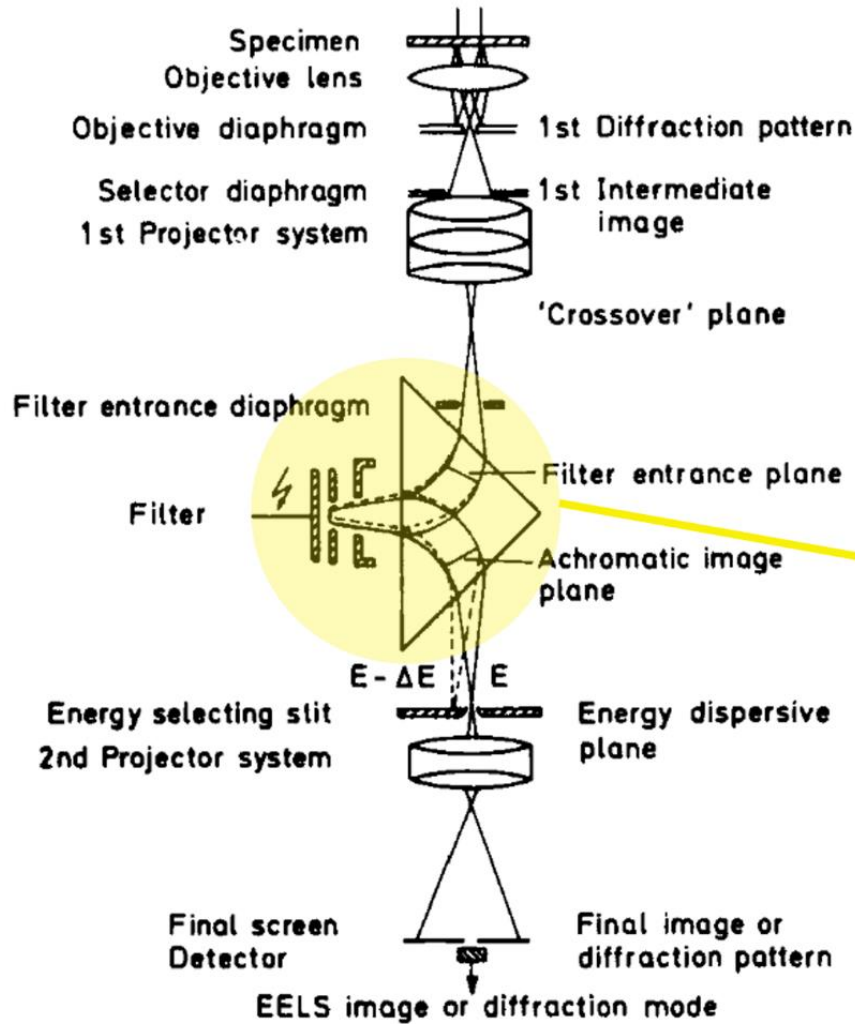


Gertrude Rempfer's Elektros
ETEM 101: About 40 produced;
about 5 still functional.
(Demonstrated at M&M2015!)



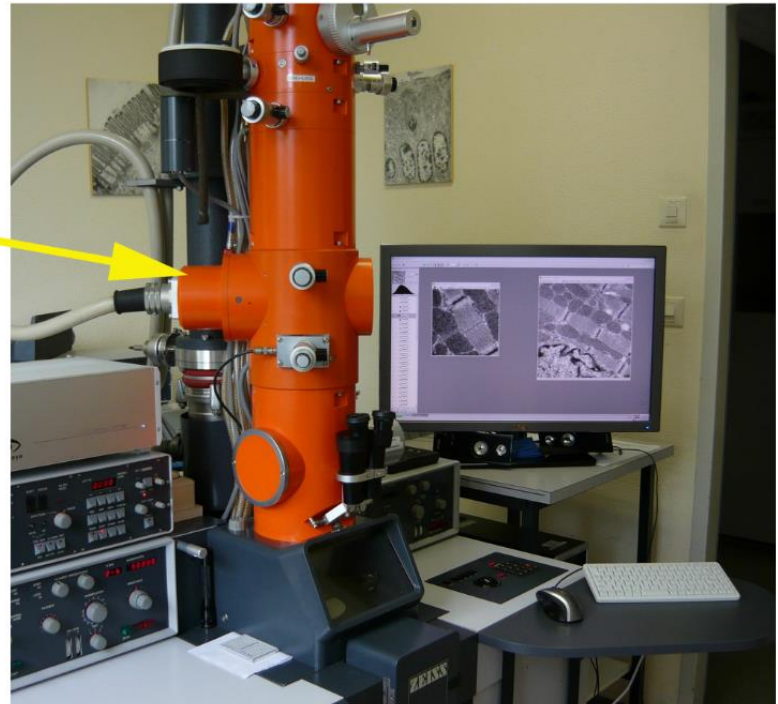
1970-1980

Non-mainsteam TEMs



Castaing-Henry imaging energy filter in Zeiss EM902 TEM

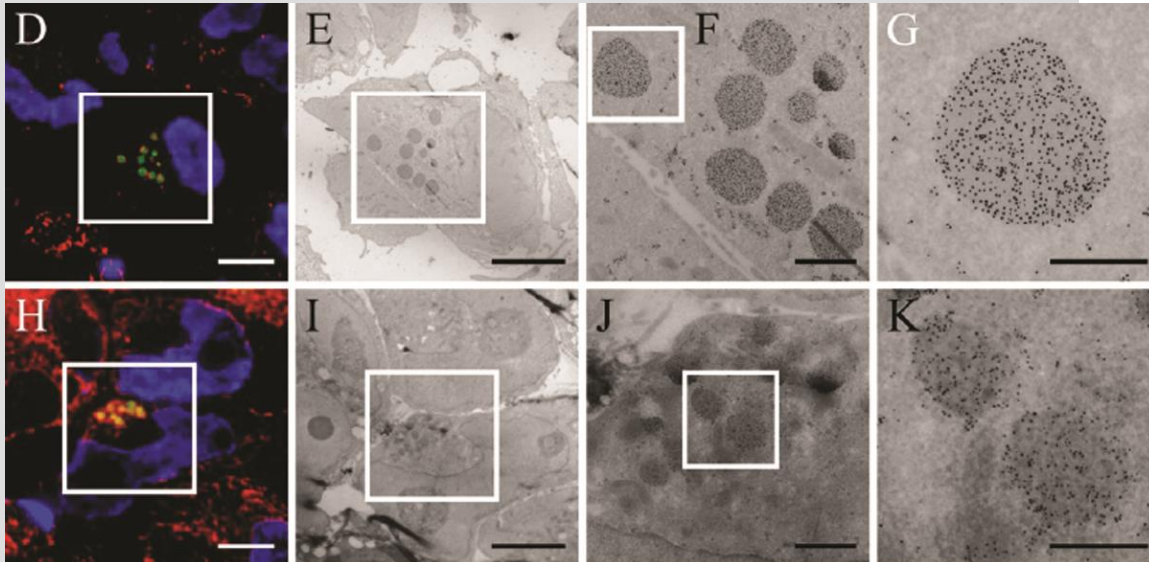
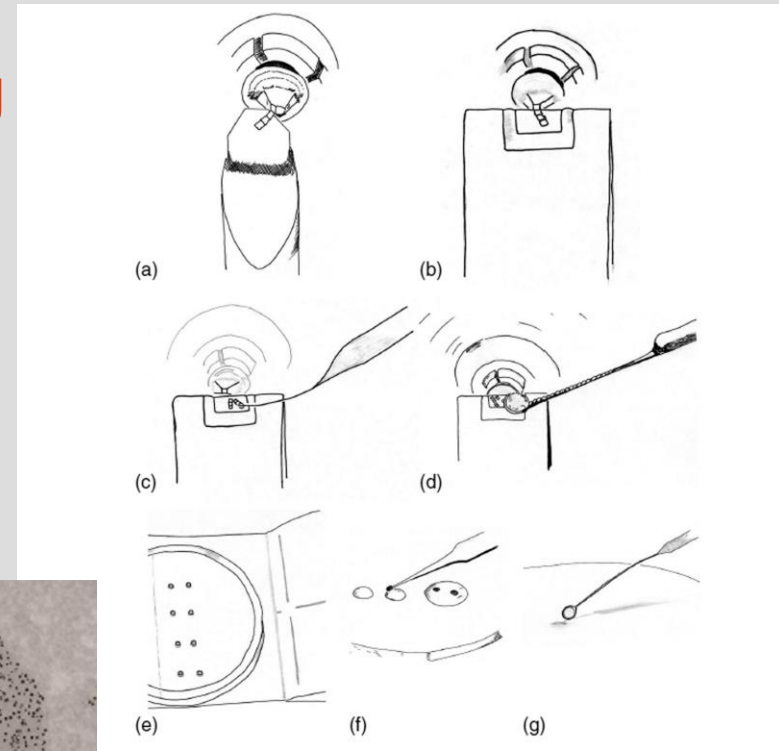
TEM shown at University of Giessen, Germany



1970-1980

“Cryosections” for immunolabeling

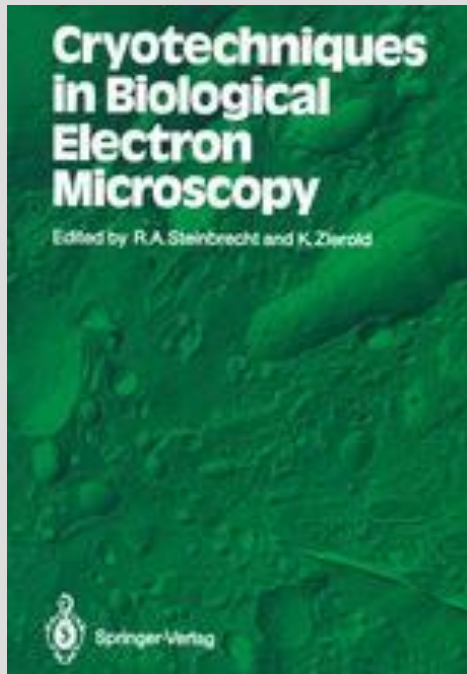
Kiyoteru Tokuyasu



Electron microscopy (TEM) image of a 200-nm-thick cryosection of an SRB showing the intricate tubular structure. (D-G) Double immunolabeling on 60-nm or 200-nm (H-K) cryosections of RRBs. (D,H) Immunofluorescence colocalization of calreticulin (Cy3, red) and μ - Δ CH1 (Cy2, green). Nuclei labeled with 4',6-diamidino-2-phenylindole (blue). Images were collected either by CLSM (D) or by wide-field microscopy (WFM) (H). (G-K) Immunogold labeling colocalization of calreticulin (10 nm) and μ - Δ CH1 (15 nm) of the same sections shown in D and H. (G,K) Higher magnification of the squared areas in E,F and I,J, respectively. Bars: A = 2 μ m; C,F,J = 1 μ m; D,E,H,I = 5 μ m; G,K = 0.5 μ m. With permission, Vicidomini et al. *Traffic* 9:1828-1838, 2008.

1970-1980

Freezing methods for TEM preparation – HPF and others



Cryotechniques in Biological Electron Microscopy
Edited by R. A. Steinbrecht and K. Zierold
© Springer-Verlag Berlin Heidelberg 1987

Abstract

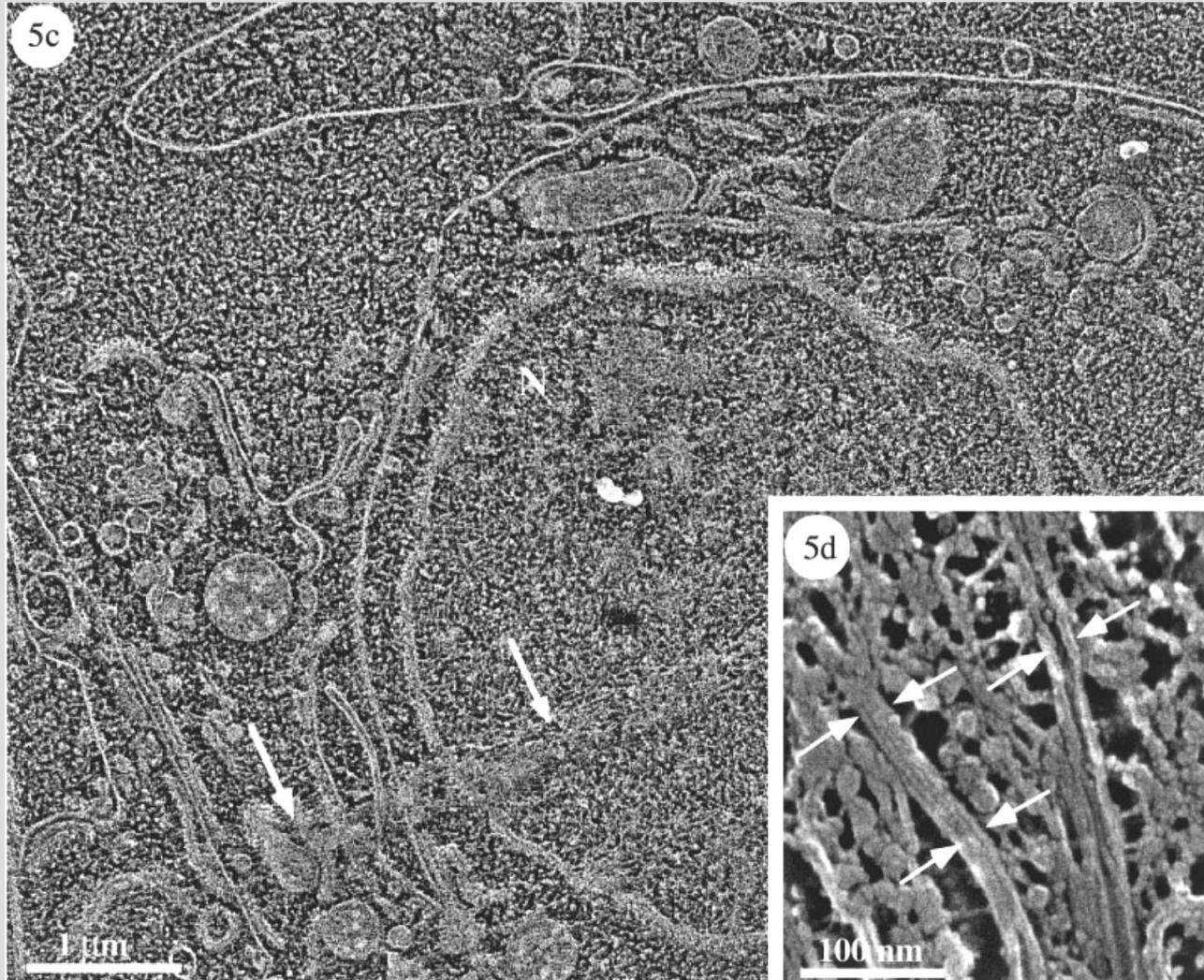
Pressure-freezing has often been regarded as a method for highly technical specialists. At the beginning of its development, this may have been true: it was introduced in 1968 by Moor and Riehle at the European conference on electron microscopy in Rome. The interest of the audience was not overwhelming, because everybody thought that this approach is oversophisticated and in principle unnecessary. In the following decade, many technically less pretentious freezing methods have been developed, which work in the absence of pressure. All of them became standardized and their methodology has been described in numerous reviews and textbooks (e.g. Rash 1983; Gilkey and Staehlin 1986; see also Sitte et al., Chap. 4, this Vol.). The compiled experience shows the manifold profits of applying impact-, plunge-, jet- and spray-freezing. In one aspect, however, all of these techniques are inadequate: namely they only enable satisfactory cryofixation of objects or superficial layers, which are not thicker than 10–20 μm . This limitation is caused by the physical properties of aqueous systems and it indicates that thicker specimens can be well cryofixed only if these properties are altered.

1970-1980

Cryo-EM: not only TEM

State-of-the-art cryo-SEM

Cryo-ultramicrotomy to produce cryo-planed surfaces.



Larva of *H. pallidus*
fixed by high-pressure
freezing

Sublimated at -110°C ,
rotary shadowed with Pt,
overcoated with C,
imaged by FEG cryo-
SEM.

1970-1980

Low-loss SEM imaging

Oliver Wells



APPLIED PHYSICS LETTERS

VOLUME 19, NUMBER 7

1 OCTOBER 1971

Low-Loss Image for Surface Scanning Electron Microscope

Oliver C. Wells

IBM Thomas J. Watson Research Center, Yorktown Heights, New York 10598
(Received 14 June 1971; in final form 27 July 1971)

Images have been obtained from the surface scanning electron microscope (SEM) by collecting backscattered electrons that have suffered a small energy loss in the specimen. This method can be applied to smooth specimens when viewed at oblique incidence. The modulation depth in the electron channelling pattern can be as great as 75%, as compared with 2-5% for the secondary electron signal or 40% for the backscattered electron signal. In surface microscopy, the image is obtained from a surface layer of thickness about 100 Å, so that the effects of electron penetration are greatly reduced. A point-to-point resolution of 170 Å has been obtained.

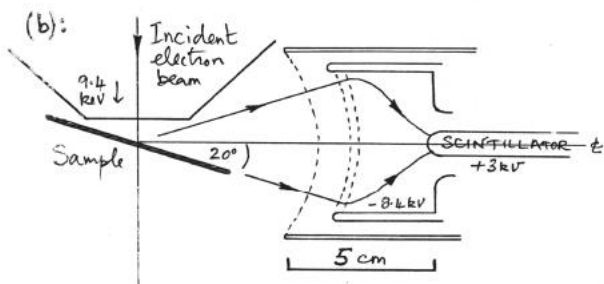
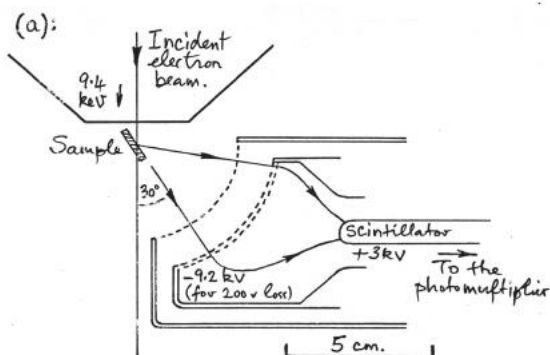


Fig. 1. LLE detector systems: (a) With sample tilt = 60°. (b) With sample tilt = 20°.

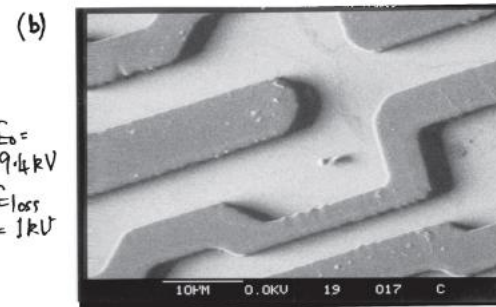
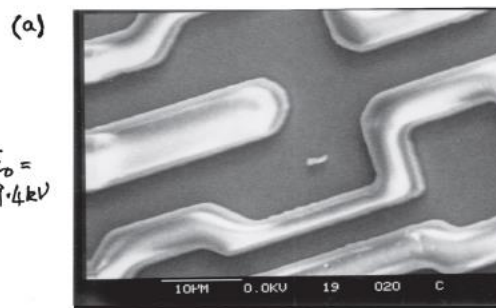


Fig. 13. Uncoated photoresist sample tilted by 20°: (a) SE image, showing charge effects. (b) LLE image, showing the surface details more clearly.

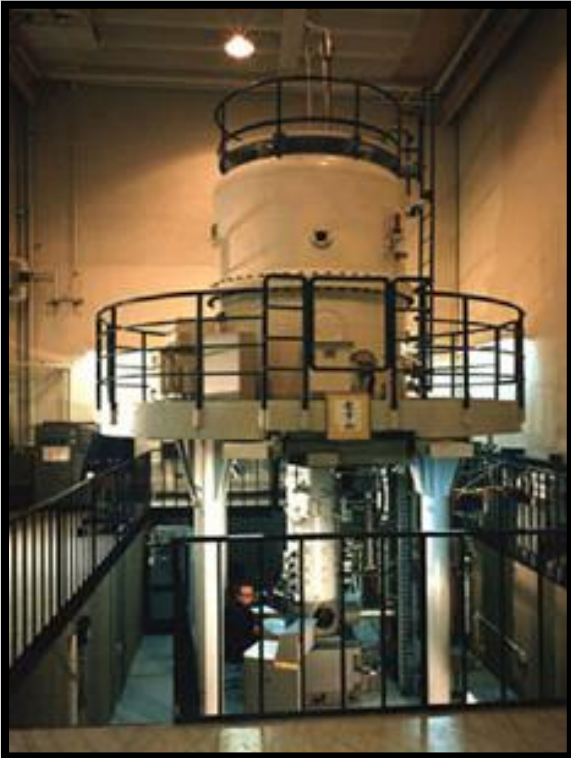
1970-1980

Applications of HVEM to biology

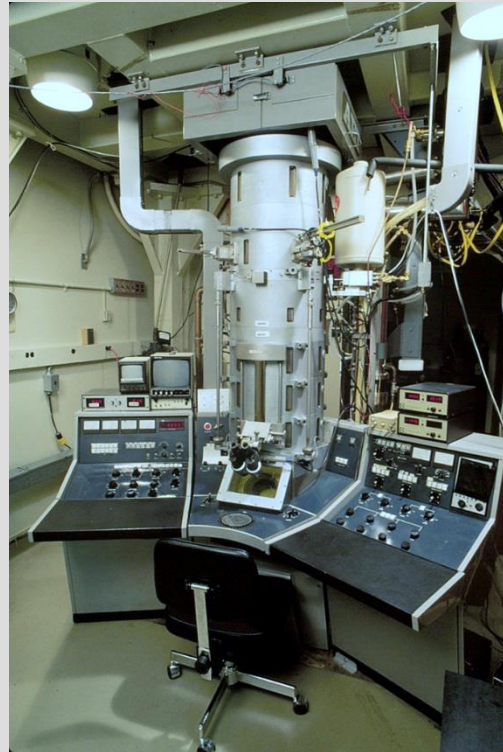
Four TEMs dedicated to biology

Intended for whole-cell ultrastructure

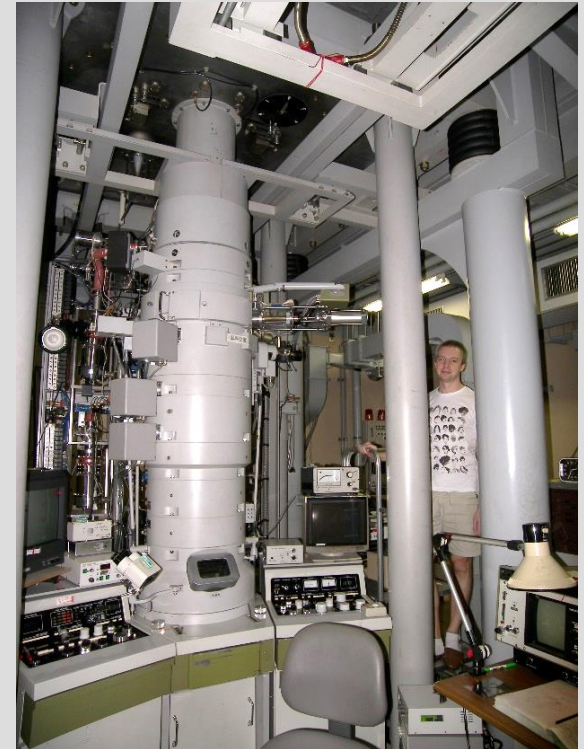
Boulder, CO
JEOL JEM-1000



Albany NY, Madison, WI
AEI EM-7 Mk II



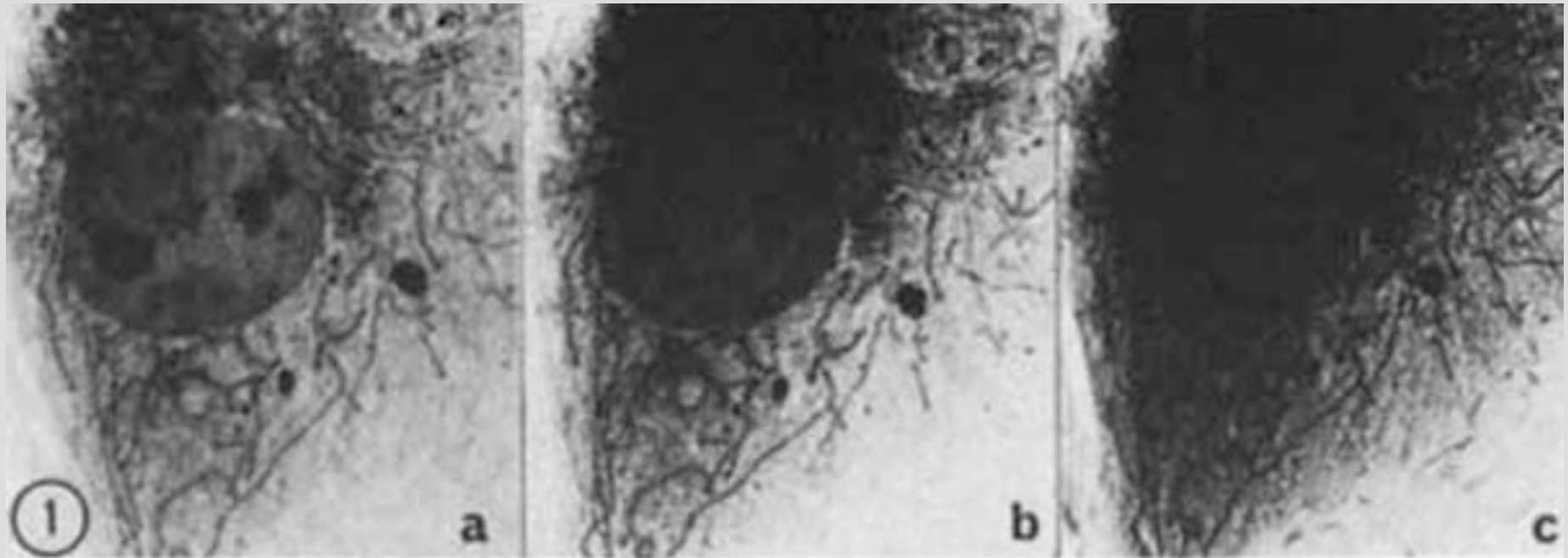
Okazaki, Japan
Hitachi HU-1250



1970-1980

Applications of HVEM to biology

Effect of accelerating voltage on a critical-point-dried whole cell



1000 keV

500 keV

100 keV

1970-1980

Applications of HVEM to biology

Early “Wet cell” results

Structure of Wet Specimens in Electron Microscopy

Improved environmental chambers make it possible
to examine wet specimens easily.

SCIENCE, VOL. 186

1 NOVEMBER 1974

D. F. Parsons



Donald Parsons

Reprinted from

Biochimica et Biophysica Acta

Elsevier Publishing Company, Amsterdam - Printed in The Netherlands

BBA 76079

HIGH-VOLTAGE ELECTRON MICROSCOPY OF WET WHOLE CANCER
AND NORMAL CELLS

VISUALIZATION OF CYTOPLASMIC STRUCTURES AND
SURFACE PROJECTIONS

D. F. PARSONS, V. R. MATRICARDI, J. SUBJECK, I. UYDESS AND G. WRAY

Electron Optics Laboratory, Biophysics Department, Roswell Park Memorial Institute, Buffalo, N.Y. 14203, and U.S. Steel Corporation, Applied Physics Laboratory, Research and Development Center, Monroeville, Pa. 15146 (U.S.A.)

(Received June 12th, 1972)

SUMMARY

A preliminary report is given of the observation of several types of cells (melanoma, 3T3, Ehrlich ascites tumor, bovine spermatozoa) in the wet state inside a differentially pumped (aperture limited) hydration chamber constructed for a high-voltage microscope. The hydration chamber functions efficiently and allows rapid insertion and examination of wet specimens on a routine basis. Initial work has shown that the scattering of water layers or drops is strong and has a pronounced effect on the resolution and contrast of the specimen. Methods have been developed for controlling the water layer thickness.

Cytoplasmic details (nuclei, mitochondria, melanin granules, axial filaments of spermatozoa) have been visualized in wet whole cells.

Attempts to observe cell movements in the hydration chamber have not yet been successful, but are continuing with special attention to minimizing radiation damage and optimizing medium nutrient composition.

INTRODUCTION

The successful development of differentially pumped, aperture limited hydration chambers for both conventional (100 kV and 200 kV)¹⁻⁵ and high-voltage (650-1200 kV) microscopes (refs 6-8; P. R. Swann and N. J. Tighe, personal communication) has made rapid examination of wet specimens a practical technique. Previous attempts to use environmental chambers closed by thin windows⁹⁻¹⁶ led to problems of frequent breakage of the windows, and their contamination. The scattering by windows also decreases contrast and resolution.

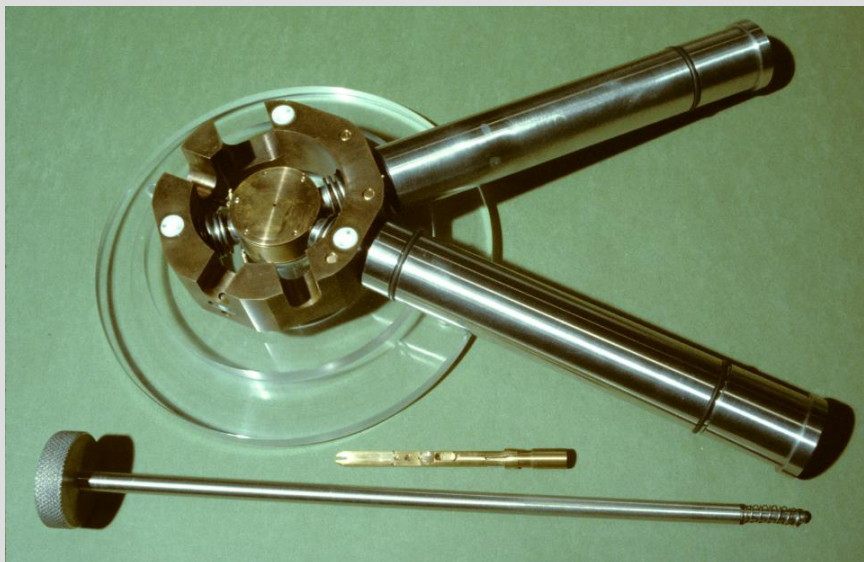
In preliminary reports we have demonstrated the practical use of the differentially pumped hydration chamber in making possible high resolution electron diffraction of wet unfixed protein crystals^{17,18} and cell membranes¹⁹.

The biological significance of electron microscopy of whole wet cells has only

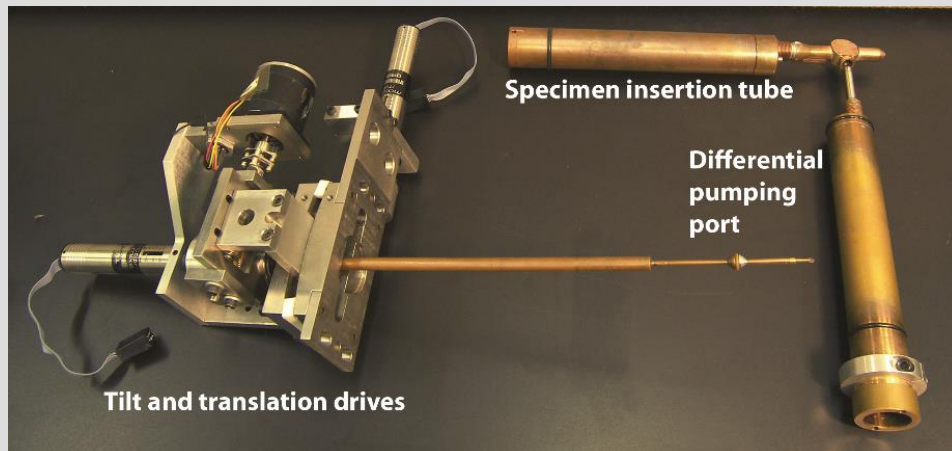
1970-1980

Applications of HVEM to biology

Early "Wet cell" work at Albany



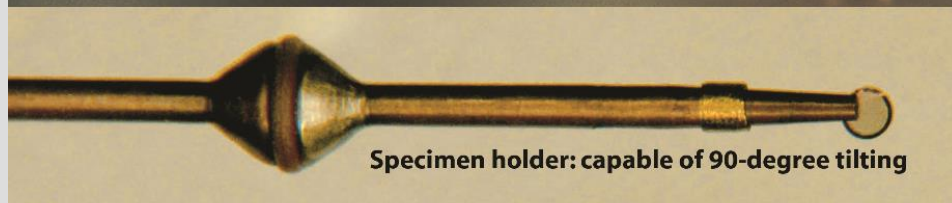
First version – uses existing TEM stage



Tilt and translation drives

Specimen insertion tube

Differential pumping port



Specimen holder: capable of 90-degree tilting



Electron diffraction of wet hemoglobin



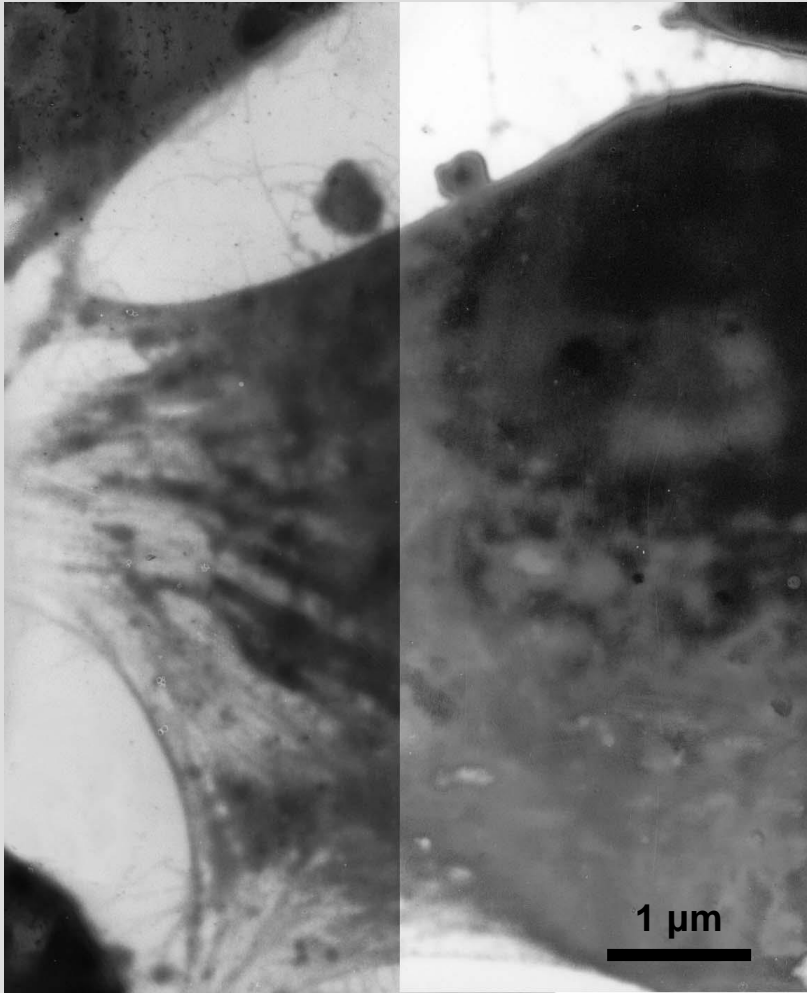
Specimen chamber:
four coaxial apertures

Second version – integrated tilt stage

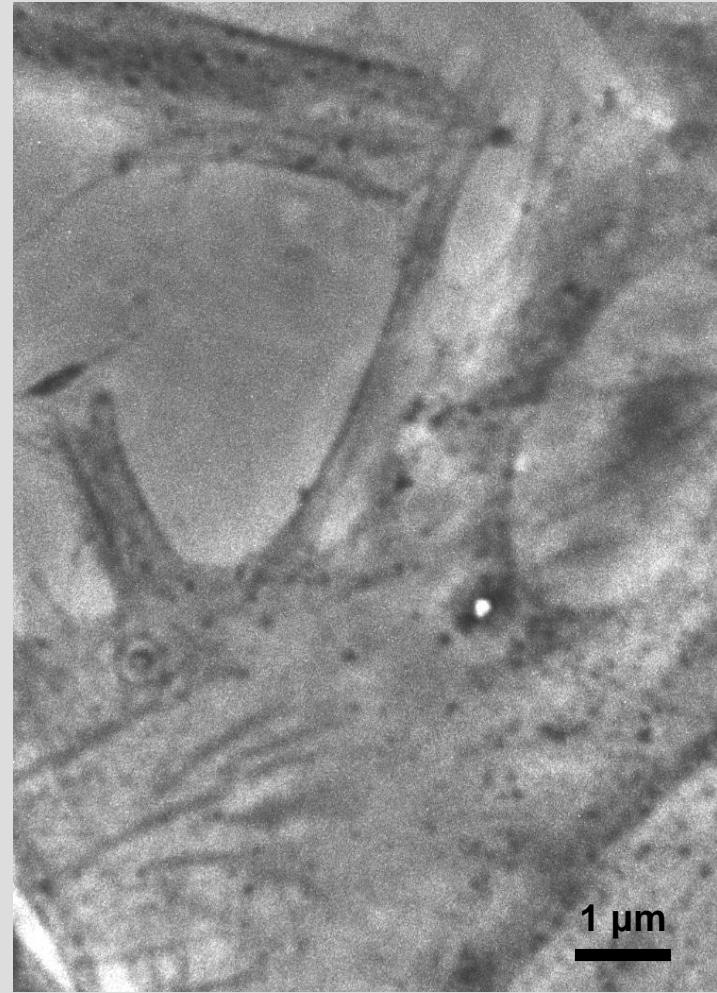
1970-1980

Applications of HVEM to biology

Early “Wet cell” results



HVEM of 3T3 cell cultured on EM grid, 1975

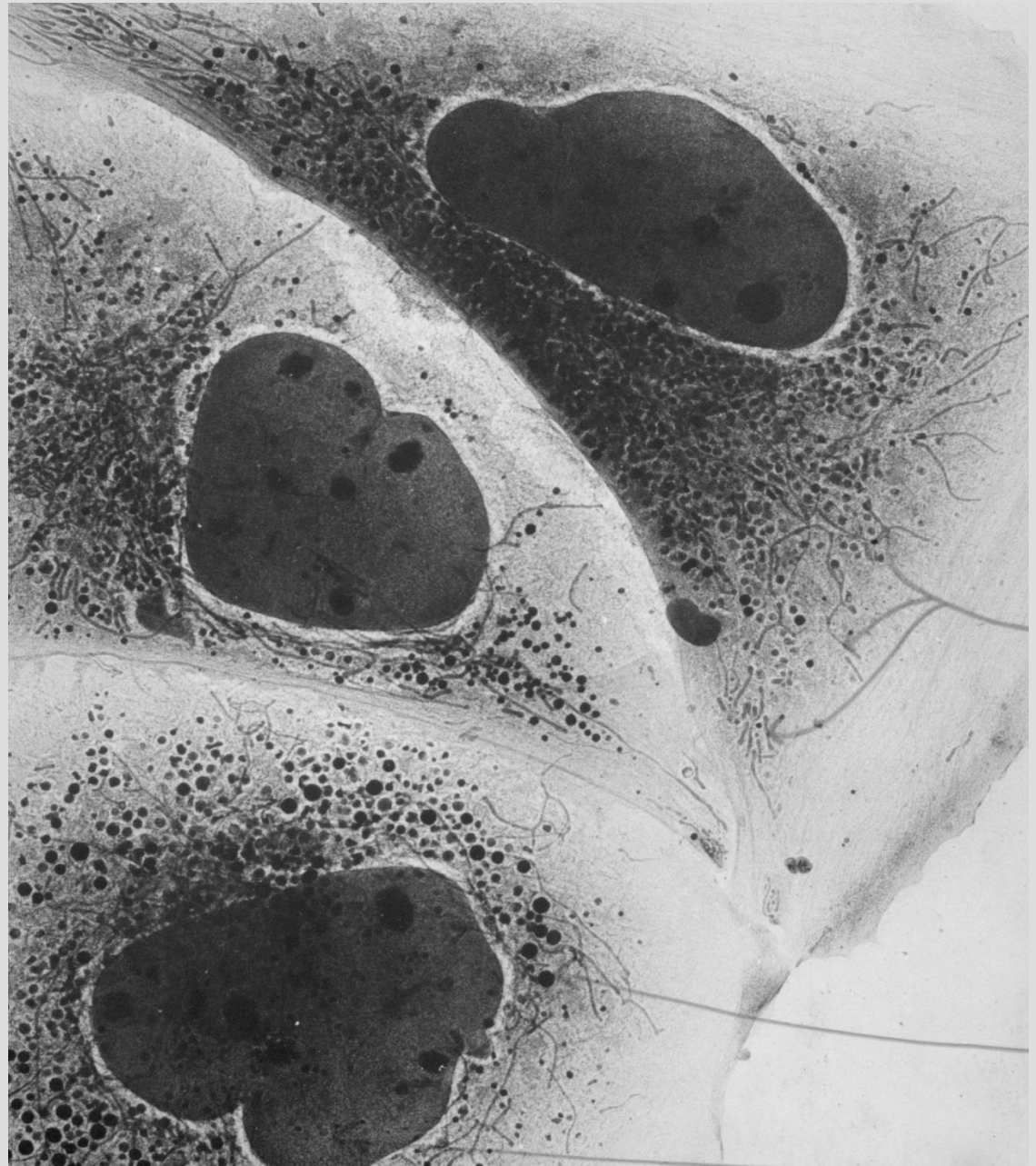


Light microscopy for comparison

1970-1980

Applications of HVEM to biology

HVEM of critical-point
dried whole cells

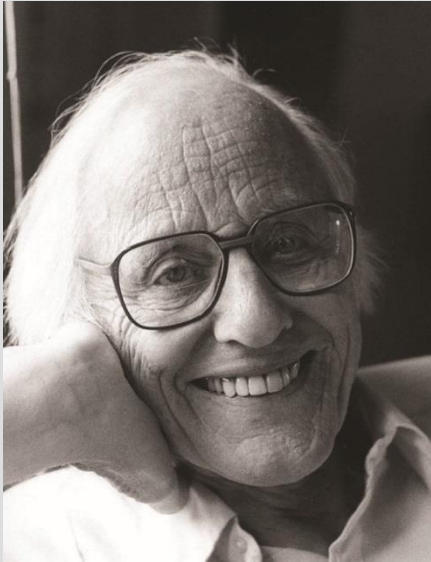


BHK cells

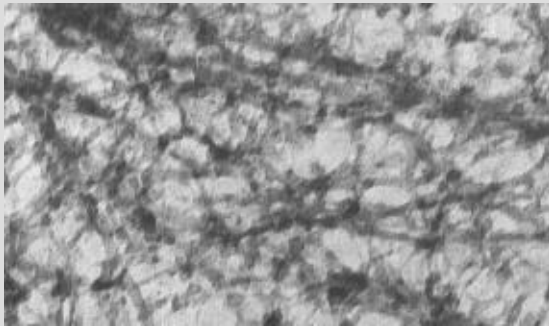
1970-1980

Applications of HVEM

Improved HVEM of critical-point dried cells

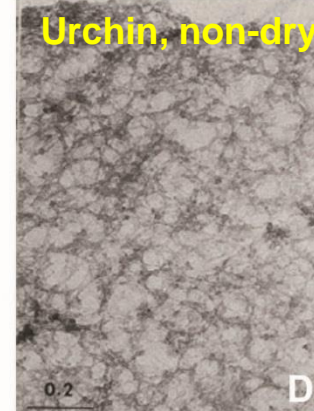
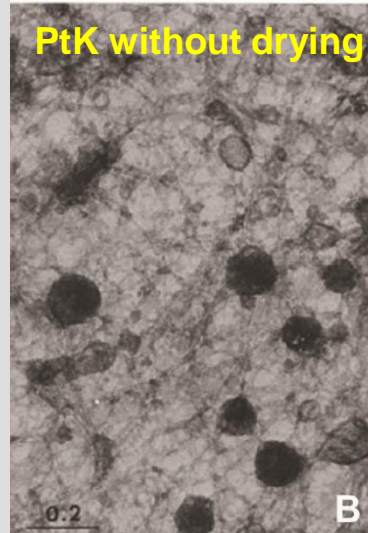
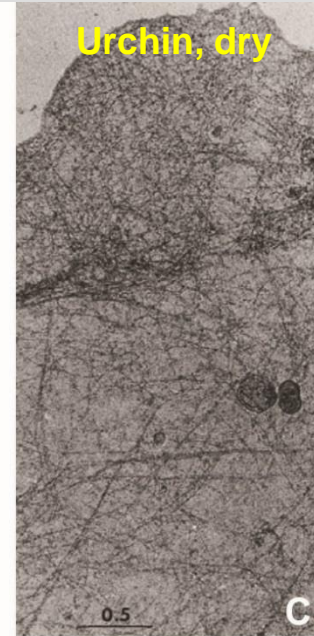
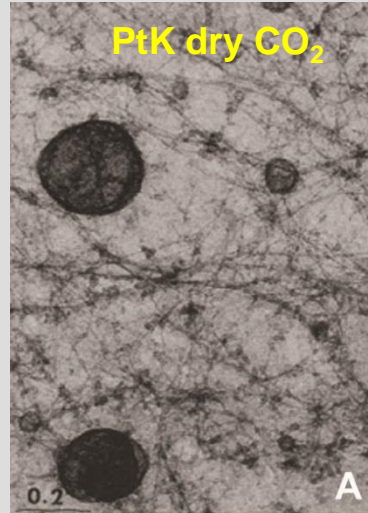


Hans Ris, Madison HVEM



“Microtrabecular lattice”

Ris (1985) JCB 100: 1474-1487

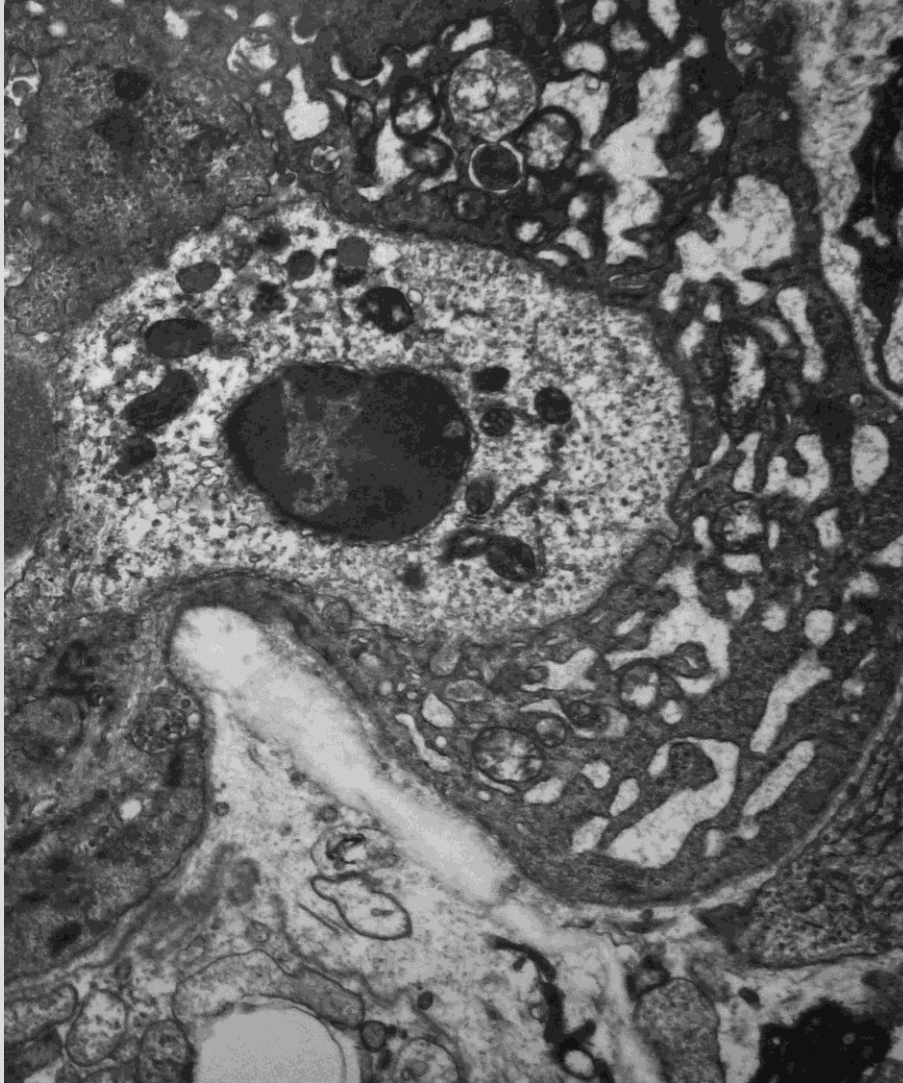


Ris' improved CPD method, with carefully dried CO₂

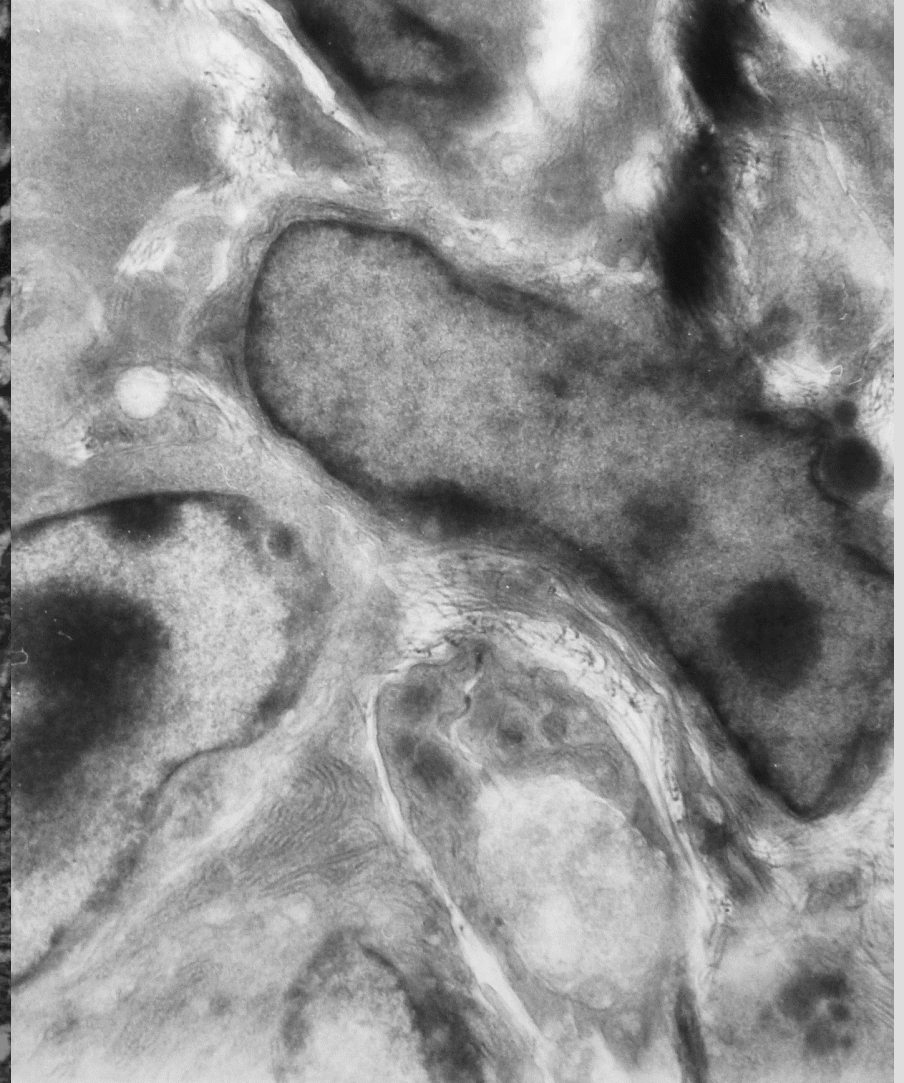
1970-1980

Applications of HVEM to biology

100-nm-thick section at 100 keV



1000-nm-thick section at 1 MeV



1970-1980

Applications of HVEM to biology

Stereo pairs of retinal rods at 3 MeV

© *Journal of Microscopy*, Vol. 97, Pts 1,2, January/March 1973, pp. 59-81.
Received 16 September 1972

The preparation and observation of thick biological sections in the high voltage electron microscope

by PIERRE FAVARD and NINA CARASSO, *Centre de Recherches d'Ivry C.N.R.S.*
67 rue Maurice Günsbourg, 94 Ivry, and *Laboratoire d'Optique Electronique du*
C.N.R.S. 29 rue Jeanne Marvig, 31 Toulouse

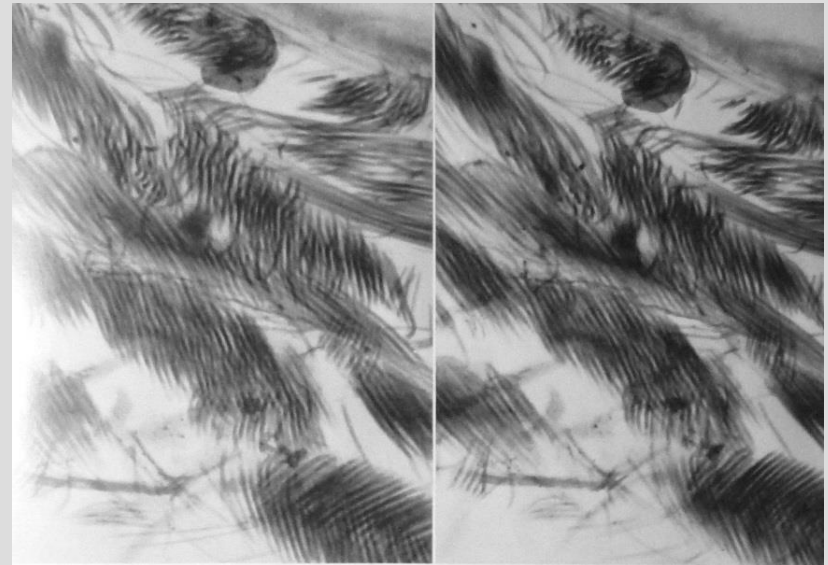
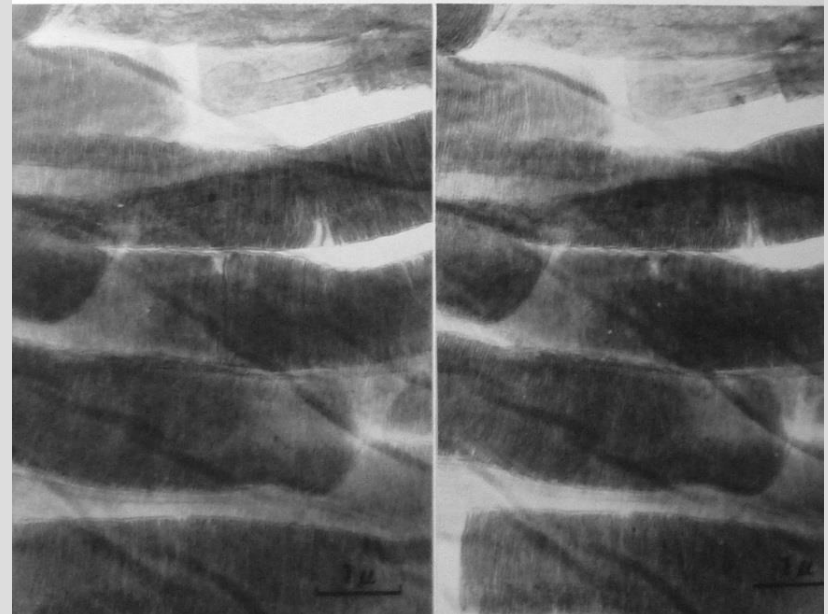


Fig. 1

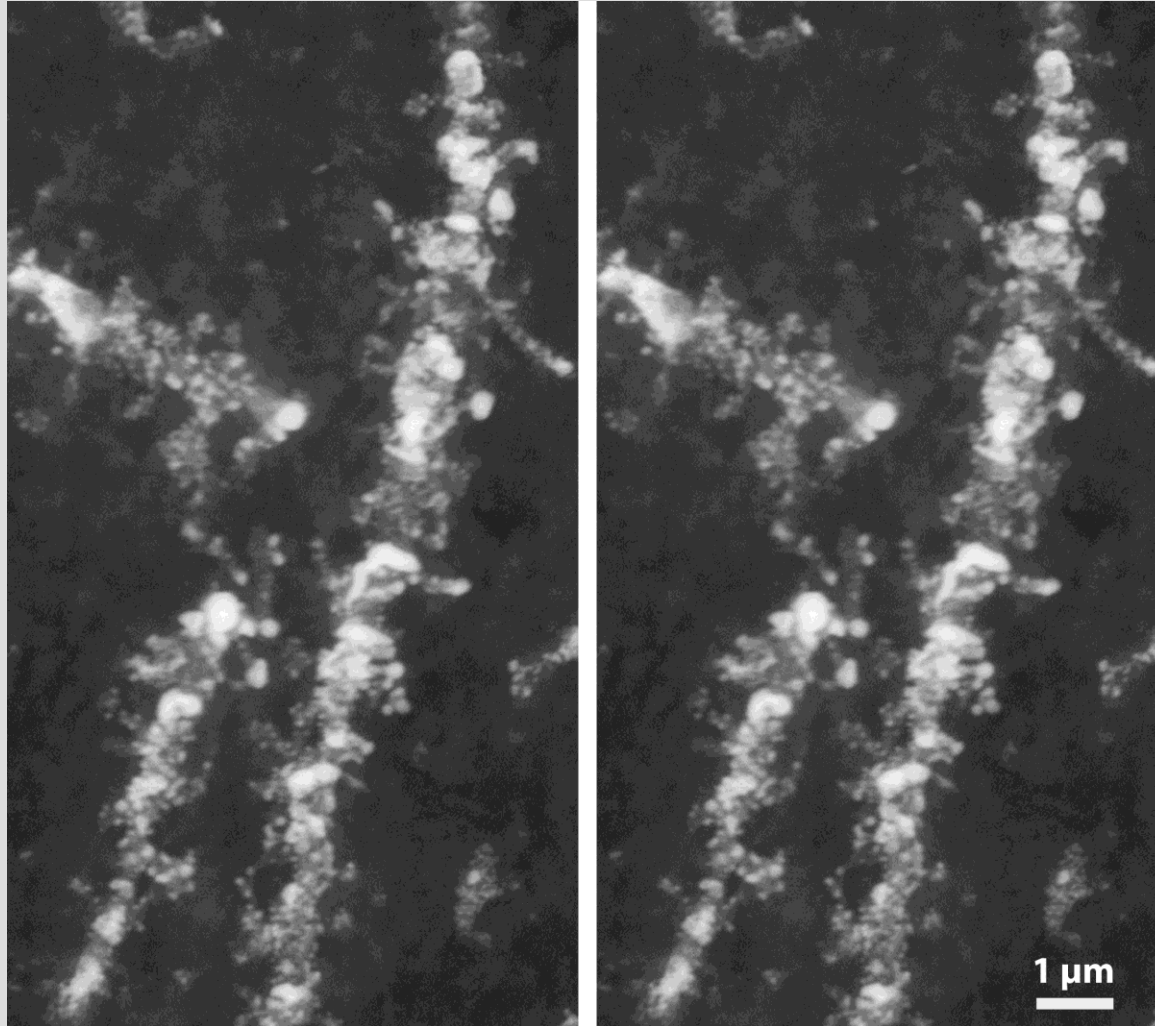
Fig. 2



1970-1980

Applications of HVEM to biology

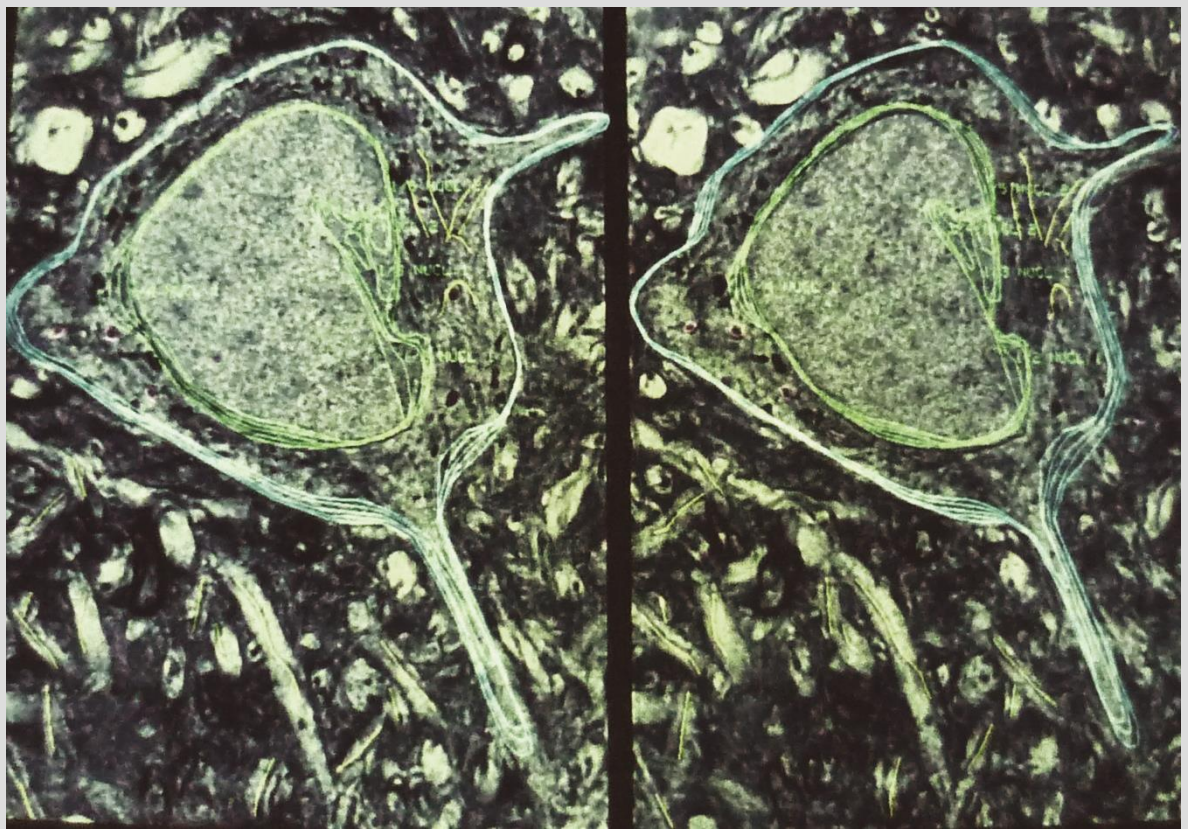
5- μm thick plastic section of silver-impregnated nerve dendrites (stereopair)



1970-1980

Applications of HVEM to biology

3-D models from stereo-tilt micrographs, early 1980s



1970-1980

Applications of HVEM to biology

3-D models from stereo-tilt micrographs, early 1980s

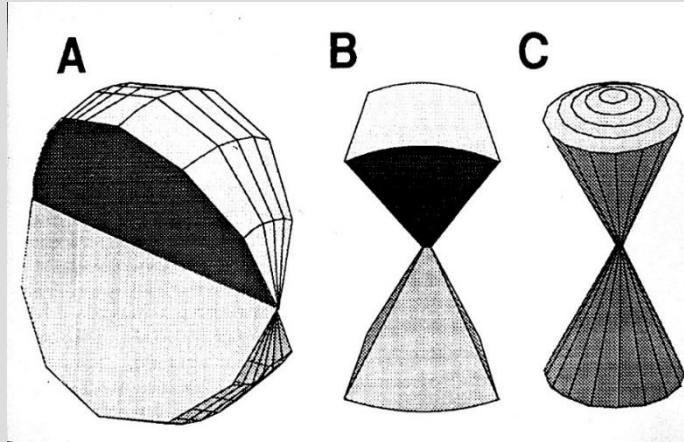
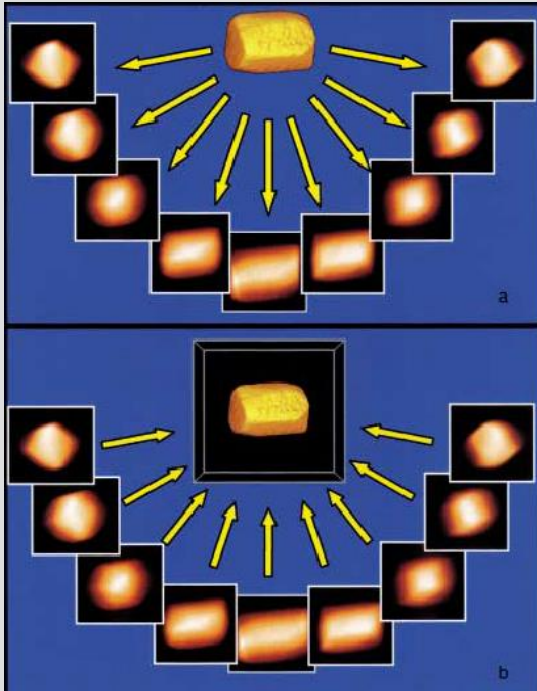


1970-1980

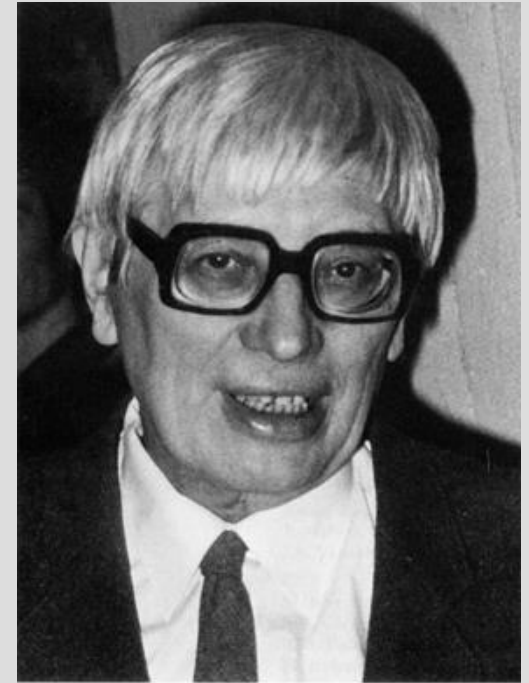
Development of electron tomography

Principles

Many views of an object are recorded, obtained by tilting the specimen in the TEM. They are combined to make a 3-D volume using image-processing methods.



Missing information due to limited tilt range in TEM



Walter Hoppe

Hoppe was head of the lab at Martinsried before Baumeister. He was mentor to Joachim Frank and Michael Radermacher.

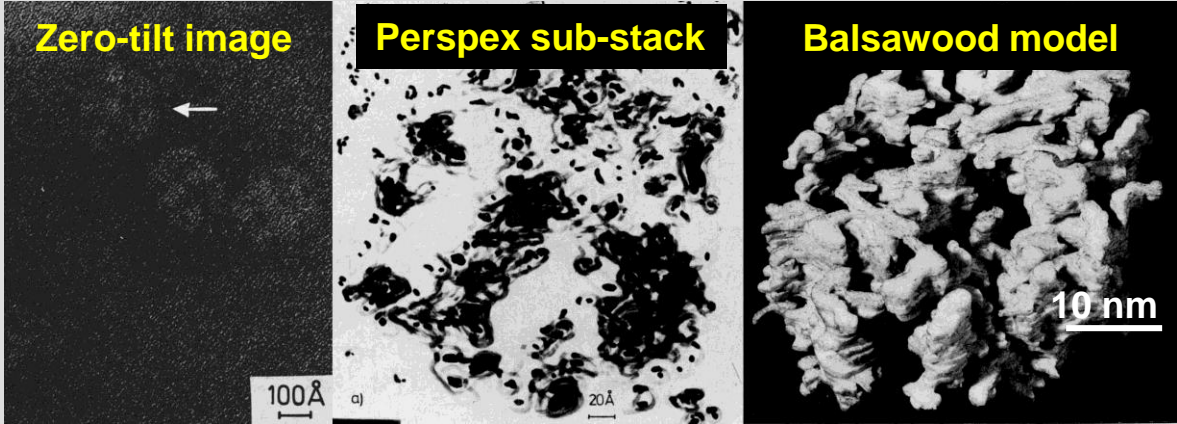
Walter Hoppe,
1917-1986

1970-1980

Development of electron tomography

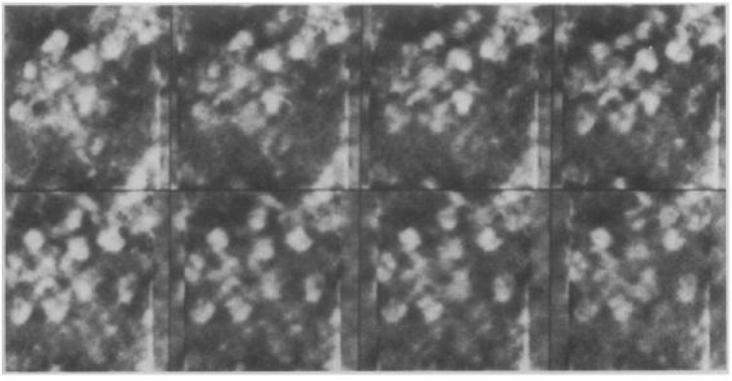
Fatty acid synthetase molecule (negatively stained)

The first published electron tomogram!



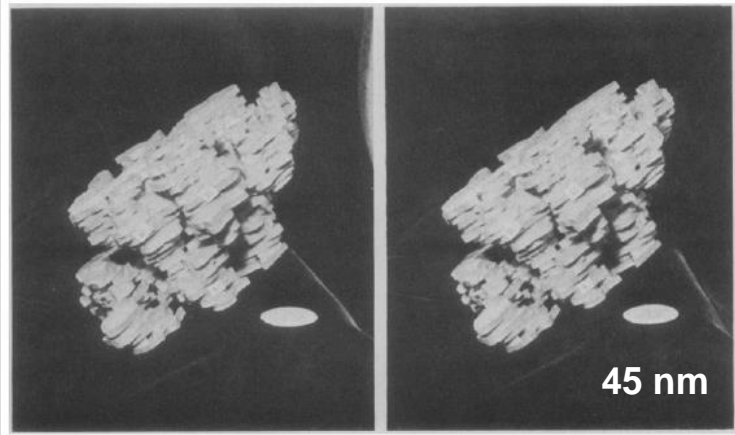
Hoppe et al. (1974) Hoppe-Seyler's Z. Physiol. Chem. 355:1483-1487.

Helical arrangement of chromatin Balbiani ring granules (plastic section)



Slices through reconstruction

Olins et al. (1983) Science 220:498-500.



Stereo view of Styrofoam model

1970-1980

Development of electron tomography

First implementation of automation,
 MPI Martinsried (originally Hoppe lab)

W. Hoppe, W. Kerzendorf, R. Guckenberger, R. Hegerl, V. Knauer,
 G. Nützel, M. Radermacher und D. Typke
 Max-Planck-Institut für Biochemie, Abteilung für Strukturforschung I,
 D-8033 Martinsried bei München, W. Germany

SCHRITTE ZUR AUTOMATISIERUNG DER DATENERFASSUNG FÜR
 DIE DREIDIMENSIONALE REKONSTRUKTION AUS ELEKTRONEN-
 MIKROSKOPISCHEN BILDERN

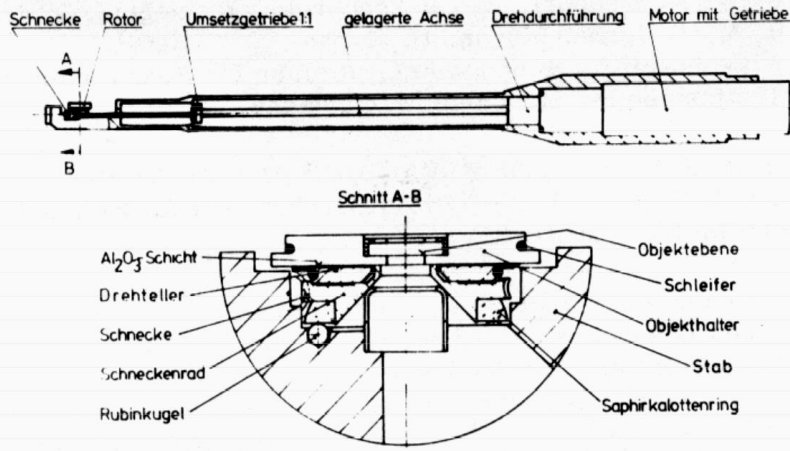
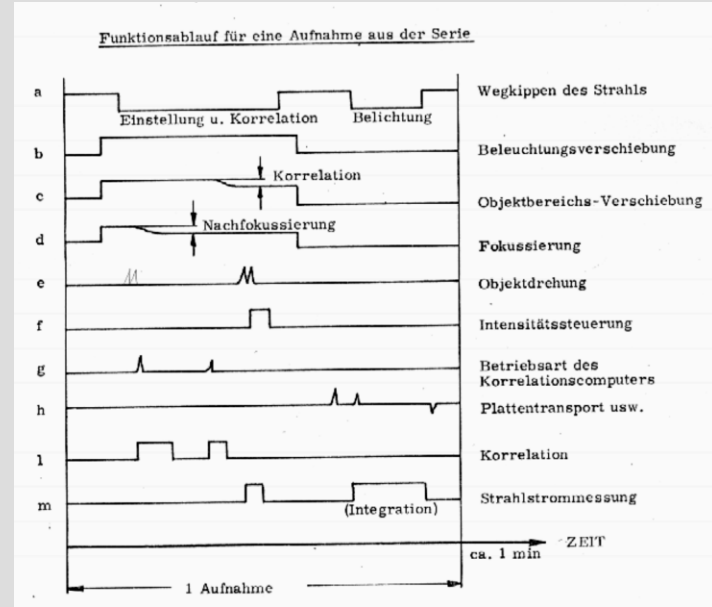


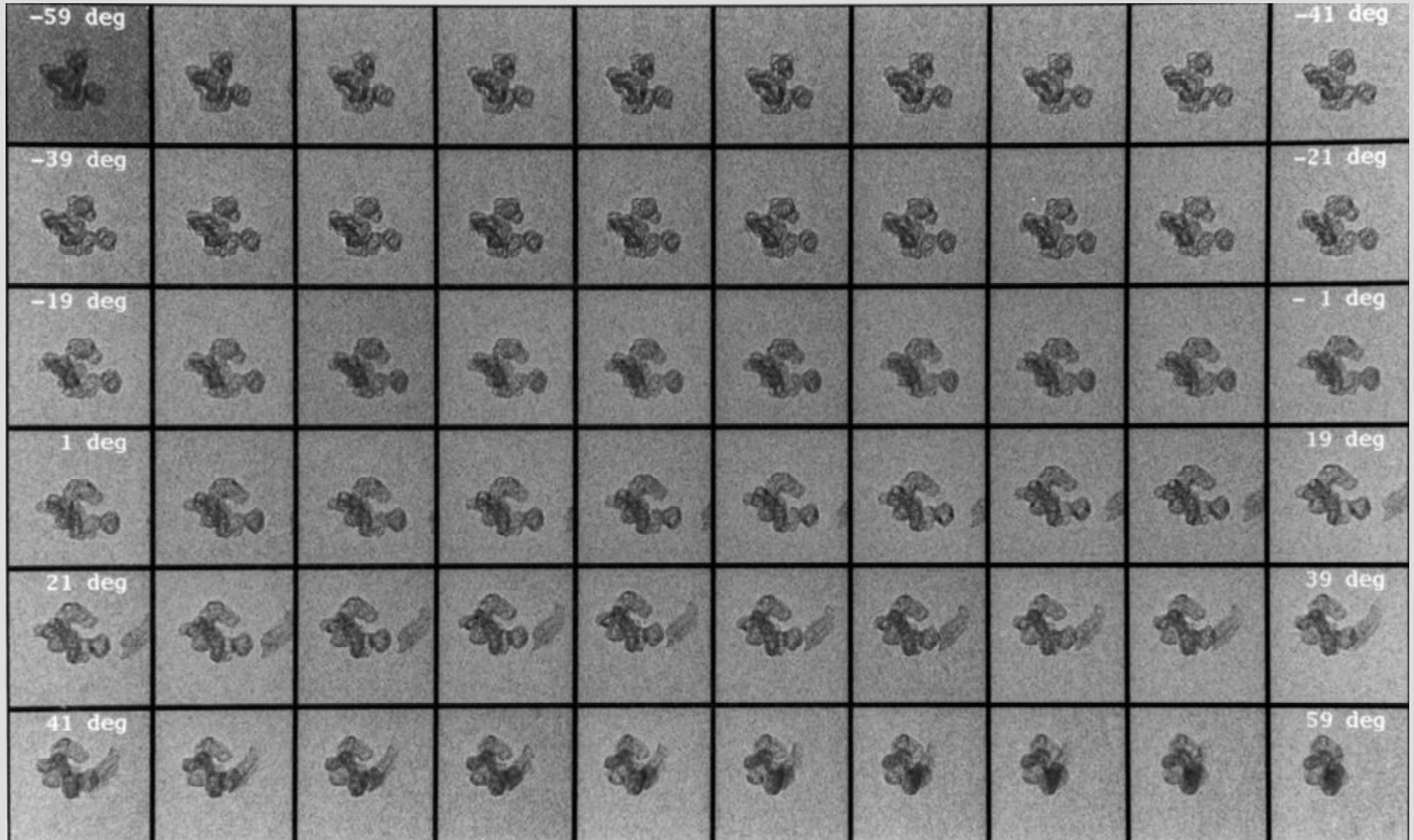
Fig. 1: Drehstab und Drehkörper des Goniometers für konische Kippung.



1970-1980

Development of electron tomography

First automated tilt series, MPI Martinsried



1970-1980

Development of electron tomography

First
tomograms
at Albany
(1986)

Images
from HVEM

Proc. Natl. Acad. Sci. USA
Vol. 83, pp. 9040-9044, December 1986
Cell Biology

Tomographic three-dimensional reconstruction of cilia ultrastructure from thick sections

(high-voltage electron microscopy/image processing/microtubule)

B. F. MCEWEN*, M. RADERMACHER*, C. L. RIEDER*[†], AND J. FRANK*[†]

*Wadsworth Center for Laboratories and Research, New York State Department of Health, Albany, NY 12201; and [†]School of Public Health Sciences, State University of New York at Albany, Albany, NY 12201

Communicated by Hans Ris, August 18, 1986

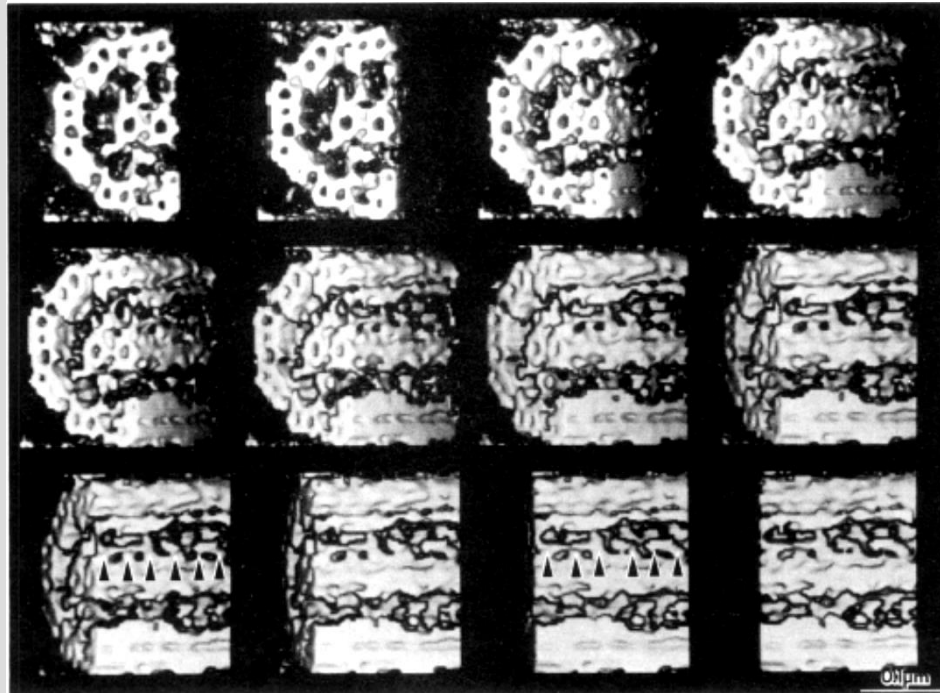


FIG. 3. Array of overlapping stereo pairs showing a portion of the reconstructed cilium in different orientations. Material was cut away so that internal features of the cilium would be visible in the rotated views and artifacts would be eliminated from the boundaries of the reconstruction. The depth of the cilium segment shown in this gallery is 170 nm. The windowed reconstruction was rotated about the y axis (vertical axis), from -5.13° to 95.13° in 11.25° increments, to obtain the views shown (the views at the end of the first and second rows are repeated at the beginning of the second and third rows, respectively). Neighboring images of this gallery form stereo pairs and, once one pair is fused, the whole gallery becomes visible as a stereo array. Nine distinct stereo views represent the structure in the range from 0° to 90° in 11.25° increments. Arrows indicate the longitudinal repeat of radial spokes attached to outer double microtubule 1.

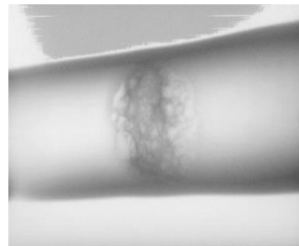
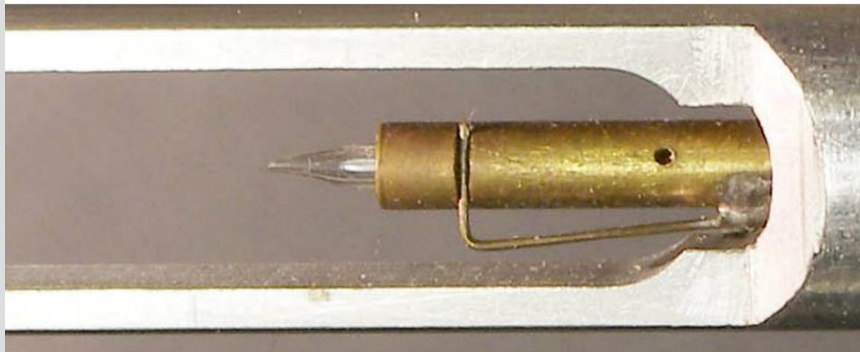
1970-1980

Development of electron tomography

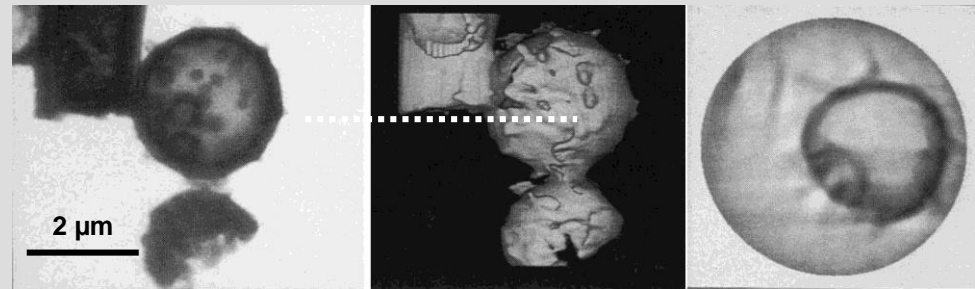
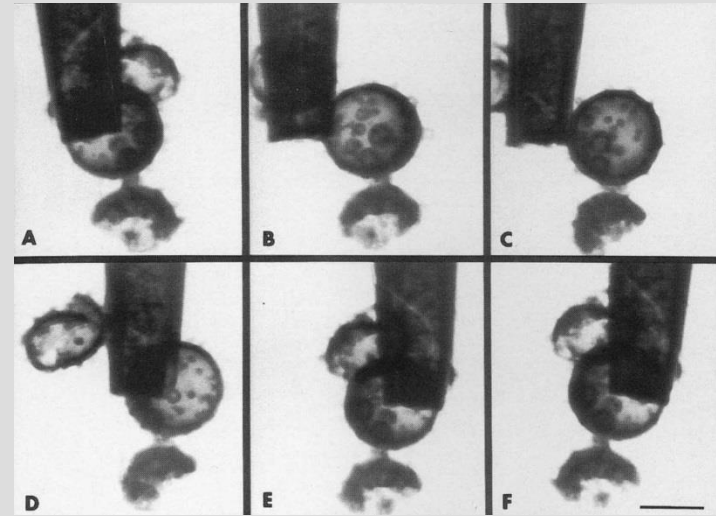
HVEM – 360° tilting

The first published 360°-tilt electron tomogram

Puff ball mounted on glass pipette



Patch-clamp membrane inside 1 μm diameter pipette tip



Slice as indicated

1970-1980

Early development of cryo-TEM

First cryo-TEM structure determination, Taylor & Glaeser, 1974

Electron Diffraction of Frozen, Hydrated Protein Crystals

Abstract. High-resolution electron diffraction patterns have been obtained from frozen, hydrated catalase crystals to demonstrate the feasibility of using a frozen-specimen hydration technique. The use of frozen specimens to maintain the hydration of complex biological structures has certain advantages over previously developed liquid hydration techniques.

KENNETH A. TAYLOR
ROBERT M. GLAESER

*Division of Medical Physics,
Donner Laboratory, and Lawrence
Berkeley Laboratory, University of
California, Berkeley 94720*

SCIENCE, VOL. 186

13 DECEMBER 1974

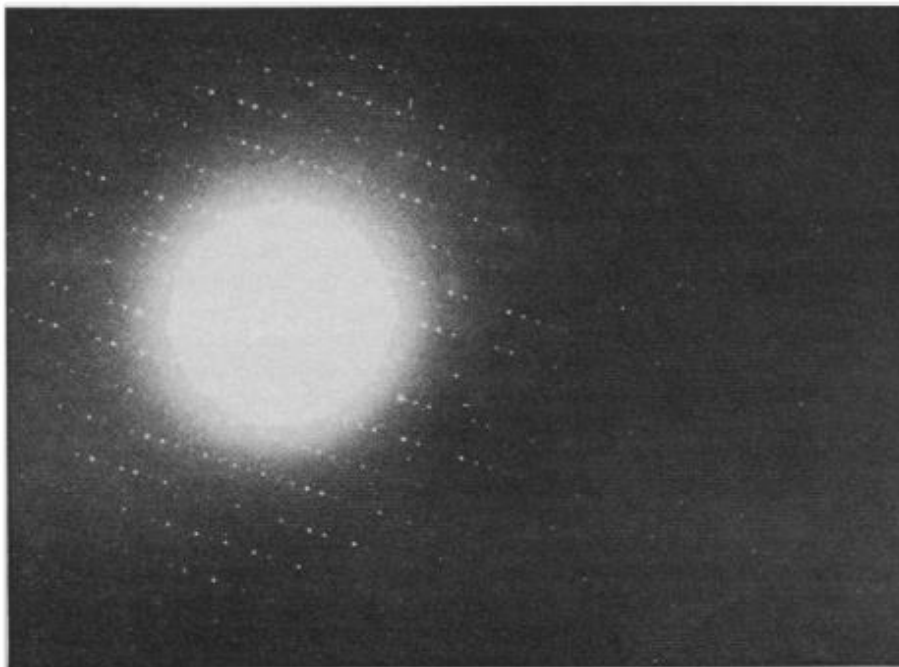
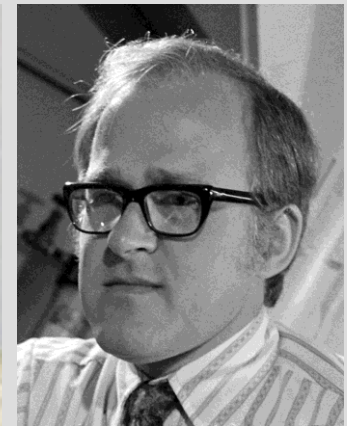


Fig. 1. Electron diffraction pattern of a catalase crystal which was frozen in liquid nitrogen and observed on a specimen stage cooled with liquid nitrogen. The resolution of the photographic reproduction is 4.5 Å, although that of the diffraction pattern on the original plate was 3.4 Å.



1970-1980

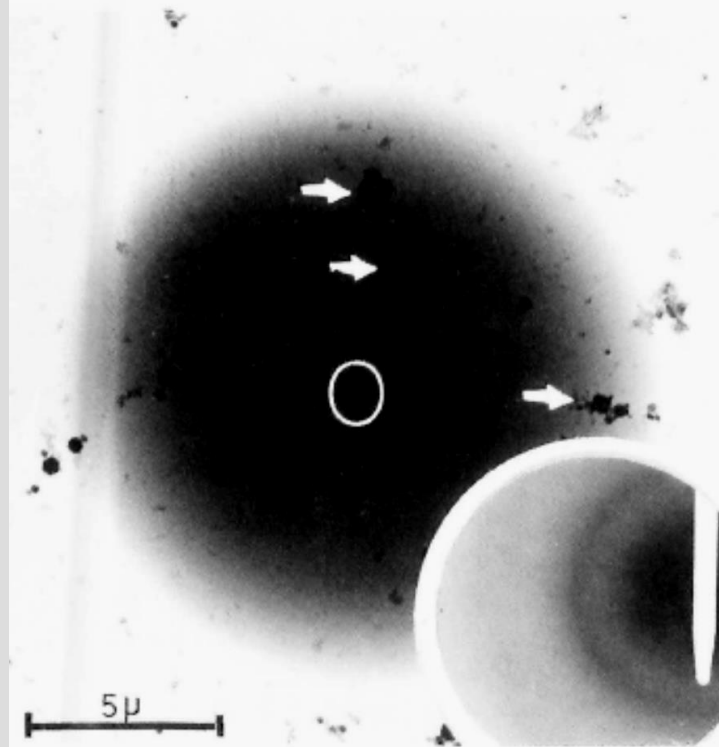
Early development of cryo-TEM

Jacques Dubochet:
First observation of
vitreous ice in the
TEM, 1981



Journal of Microscopy, Vol. 124, Pt 3, December 1981, pp. RP3–RP4.
Rapid Publication accepted 9 November 1981

VITRIFICATION OF PURE WATER FOR ELECTRON MICROSCOPY
J. Dubochet and A.W. McDowell
European Molecular Biology Laboratory (EMBL)
Postfach 10.2209, D-6900 Heidelberg, F.R.G.



Vitreous droplet of pure water spread on a carbon film. Some crystals produced by condensation of atmospheric water vapour are marked (arrow). Magnification: 3900 x. Insert: electron diffractogram from the circled area. $1 \text{ cm} = 0.2 \text{ \AA}^{-1}$.

1970-1980

Early development of cryo-TEM

Dubochet's phase diagram
from the 1988 paper.

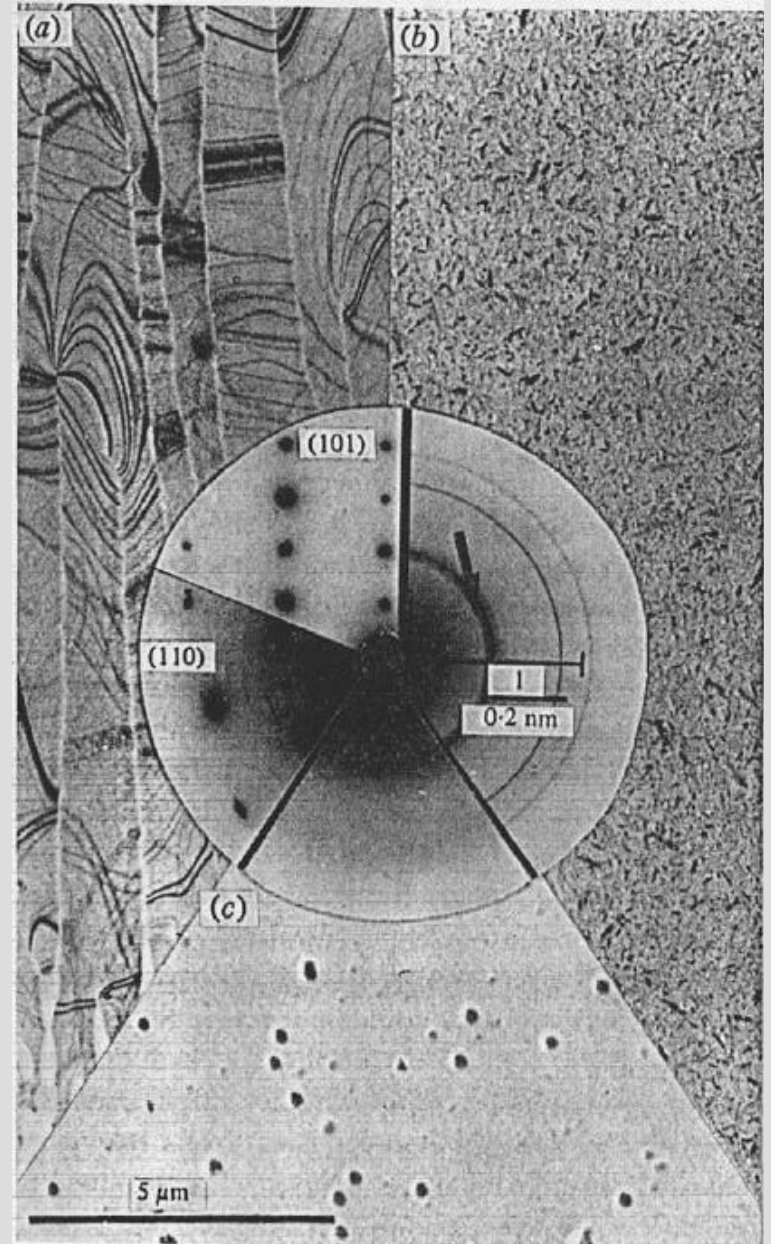
Quarterly Review of Biophysics 21, 2 (1988), pp. 129-228
Printed in Great Britain

129

Cryo-electron microscopy of vitrified specimens

JACQUES DUBOCHET¹, MARC ADRIAN², JIIN-JU CHANG³,
JEAN-CLAUDE HOMO⁴, JEAN LEPAULT⁵,
ALASDAIR W. McDOWALL⁶ AND PATRICK SCHULTZ⁴

European Molecular Biology Laboratory (EMBL), Postfach 10. 2209, D-6900 Heidelberg, FRG



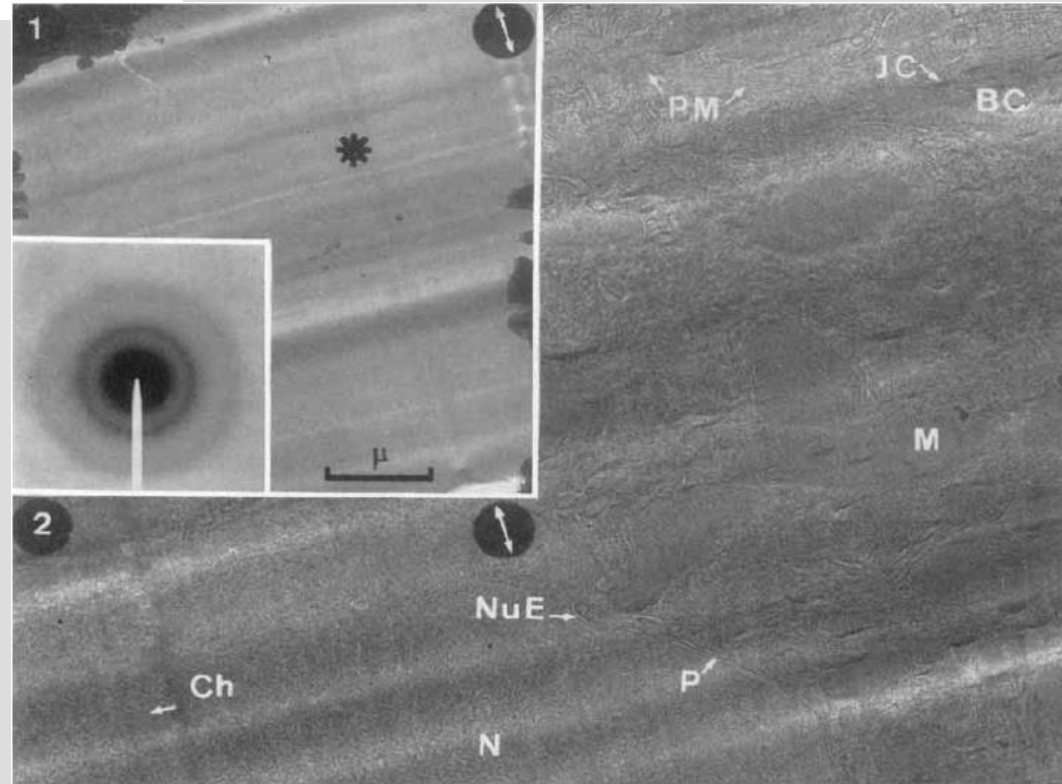
1970-1980

Early development of vitreous cryo-sectioning

Journal of Microscopy, Vol. 131, Pt 1, July 1983, pp. 1-9.
Received 15 June 1982; accepted 13 November 1982

Electron microscopy of frozen hydrated sections of vitreous ice and vitrified biological samples

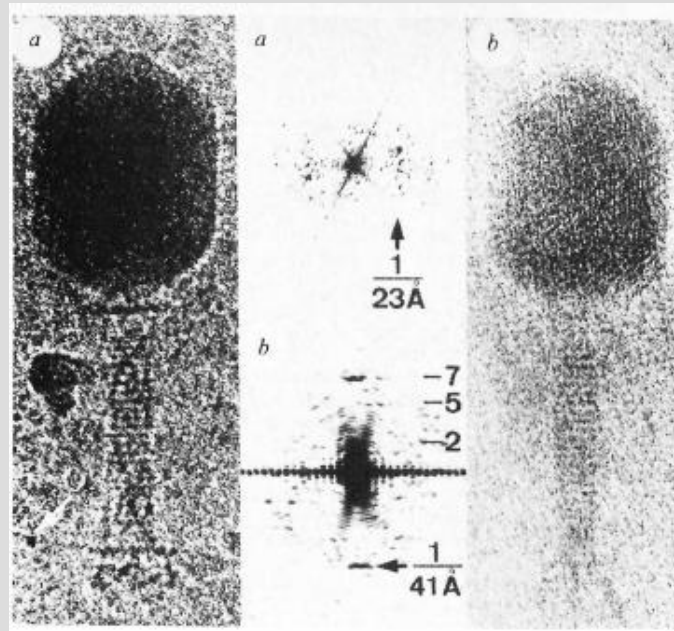
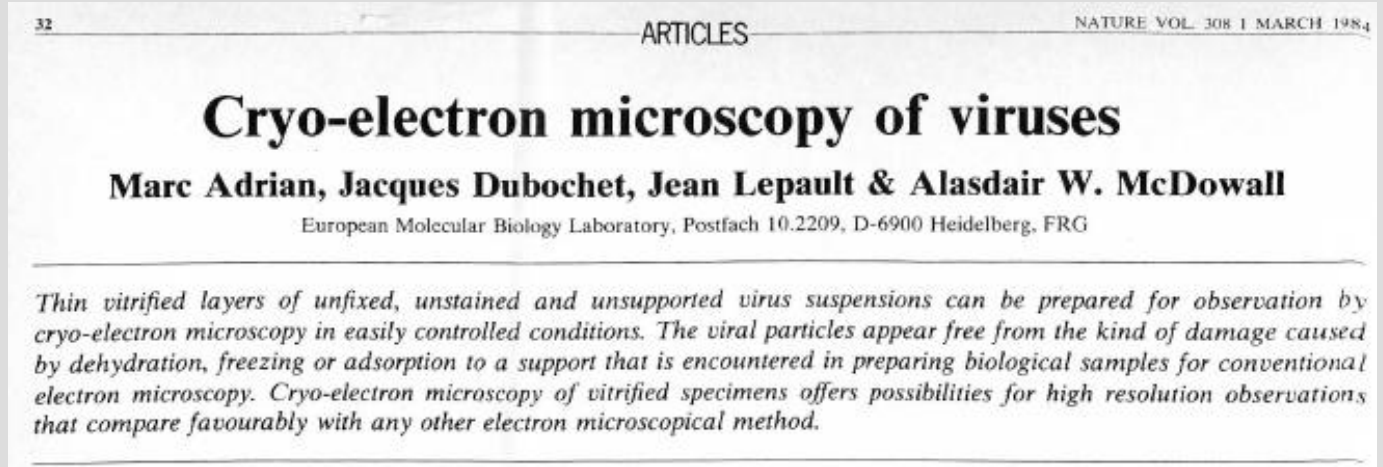
by A. W. MCDOWALL, J.-J. CHANG*, R. FREEMAN, J. LEPAULT, C. A. WALTER and J. DUBOCHET, *European Molecular Biology Laboratory (EMBL), Postfach 10.2209, Meyerhofstrasse 1, 6900 Heidelberg, Federal Republic of Germany*



1980-1990

Early development of cryo-TEM

First application
of cryo-TEM in
vitreous ice



Plunge-frozen
bacteriophage T4

1970-1980

Early development of cryo-TEM

Isolde Dietrich: superconducting-lens cryo-TEM, 1975

SHORT NOTE

A SUPERCONDUCTING LENS SYSTEM OPERATED IN THE FIXED-BEAM AND THE SCANNING MODE

G. LEFRANC, K.-H. MÜLLER and I. DIETRICH

Forschungslaboratorien der Siemens AG, D-8000 München 83, Fed. Rep. Germany

Received 8 July 1980

1. Introduction

A superconducting lens system for the fixed-beam transmission mode installed in a 400 kV microscope [1] has been in operation for several years. The system combines high resolving power and very small vibration and drift of the specimen, which is cooled to 4 K. A drastic reduction of radiation damage as a consequence of the specimen cooling could be proven [2].

In the meantime a further superconducting lens system constructed for application in commercial microscopes instead of the normal objective lens [3] has been tested. In comparison to the first system, handling is much easier and the liquid helium consumption is lower [4]. A point-to-point resolution of the order of 0.3 nm has been obtained. One can operate the new system in the conventional mode and, in addition, in the scanning mode without changing the z position of the specimen. The application of the system in the fixed-beam mode is described in more detail in [4].

2. Arrangement and performance

The superconducting lens system (fig. 1) consists of an objective lens OL of the shielding type [5] and an iron circuit intermediate lens IL₁. A stigmator St installed in the gap of the shielding lens allows correction of the image astigmatism in the fixed-beam mode as well as the probe astigmatism in the scanning mode. The specimen is positioned in the lower half of the gap. In the fixed-beam application the lens field

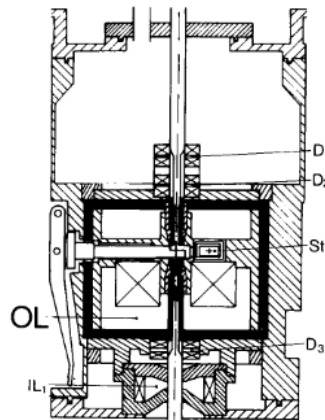
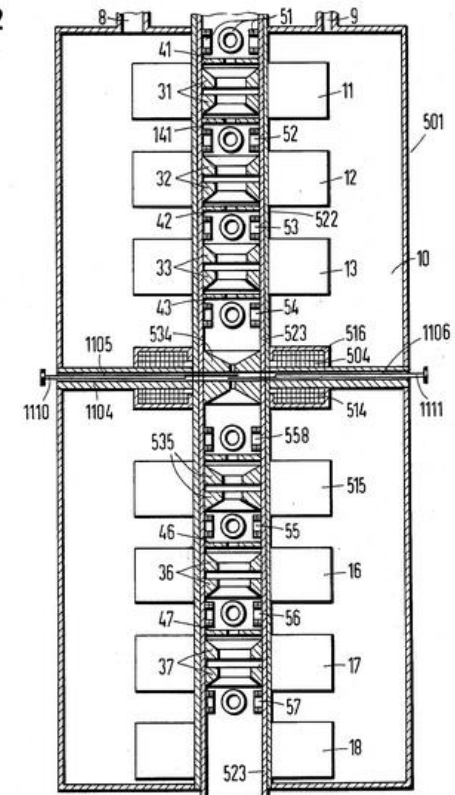


Fig. 1. Cross-section of superconducting lens system: OL, objective lens, IL₁, first intermediate lens, D₁, D₂, two-stage deflection system, St, stigmator, D₃, deflector.

is excited so that in case of a parallel entering beam its second parallel zone after the cross-over in the gap coincides with the position of the specimen (lens strength $k^2 \approx 5$). In the case of scanning one works with about half the field excitation which brings the beam cross-over into the specimen plane (fig. 2a and 2b). This cross-over is used as an electron probe. It can be shifted by the two-stage superconducting deflection system D₁, D₂ above the objective lens

U.S. Patent Oct. 28, 1975 Sheet 2 of 4 3,916,201

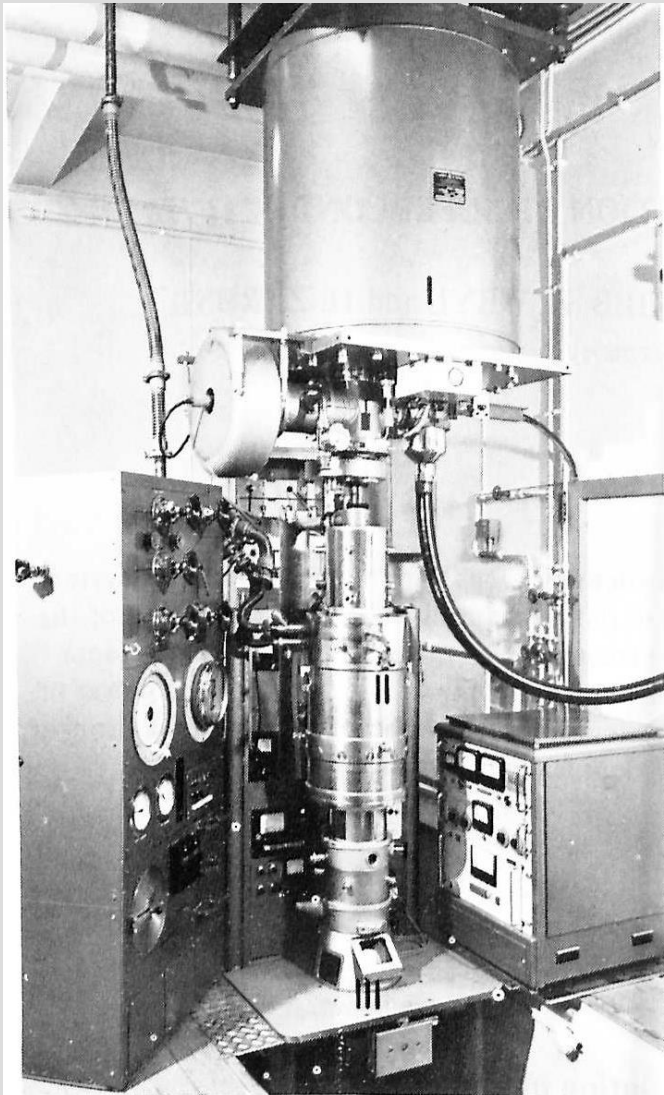
Fig. 2



1970-1980

Early development of cryo-TEM

Dietrich cryo-TEM, 1977



Ultramicroscopy 2 (1977) 241–249
© North-Holland Publishing Company

Resolution: 1.7 Å

IMPROVEMENTS IN ELECTRON MICROSCOPY BY APPLICATION OF SUPERCONDUCTIVITY

I. DIETRICH, F. FOX, E. KNAPEK, G. LEFRANC, K. NACHTRIEB, R. WEYL and H. ZERBST
Forschungslaboratorien der Siemens AG München, München, Fed. Rep. Germany

Received 4 January 1977

Resolution tests on amorphous carbon foils were carried out in an electron microscope with a superconducting system containing 4 lenses including a shielding lens at 200 kV beam voltage. Due to the mechanical and electrical stability of the system and the absence of contamination of the specimen the highest space frequencies transferred at vertically incident beam were 6 nm^{-1} corresponding to a resolution of 0.17 nm, a value which approaches the theoretical resolving power of the electron optical system. It should also be feasible to apply such a lens system for microprobe analysis without strongly reducing the theoretical resolution limit, if the construction of the shielding lens is slightly changed.

I. Dietrich et al. / Improvements in electron microscopy

243

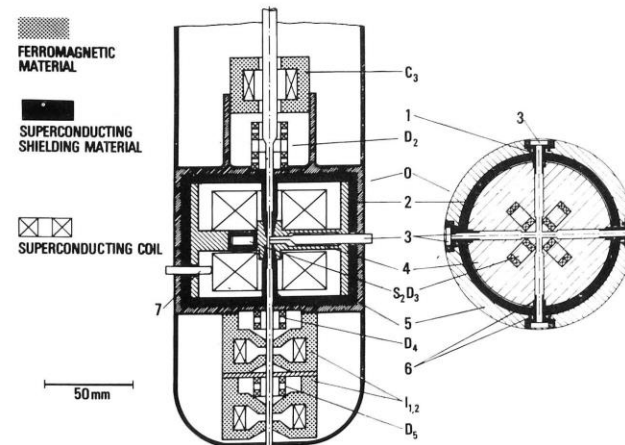
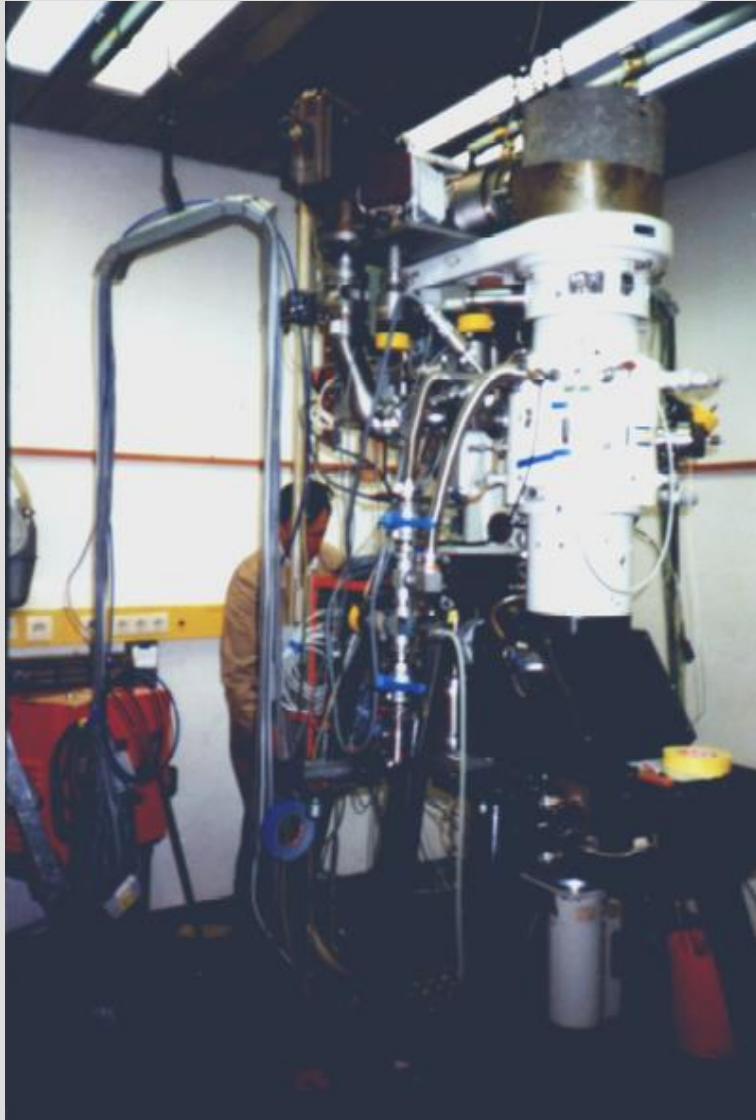


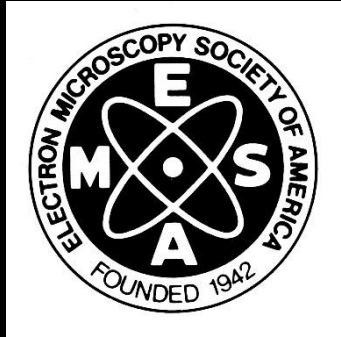
Fig. 2. Superconducting lens system with helium cooled specimen stage and transverse section of objective lens. 1 double flange sealing; 2 shielding casing; 3 channel for specimen and aperture (A_2 fig. 1) holders; 4 support disc; 5 wall of inner He chamber; 6 indium seals; 7 adjustment screw; (for A, C, D, O, I see fig. 1).

1970-1980

Early development of cryo-TEM

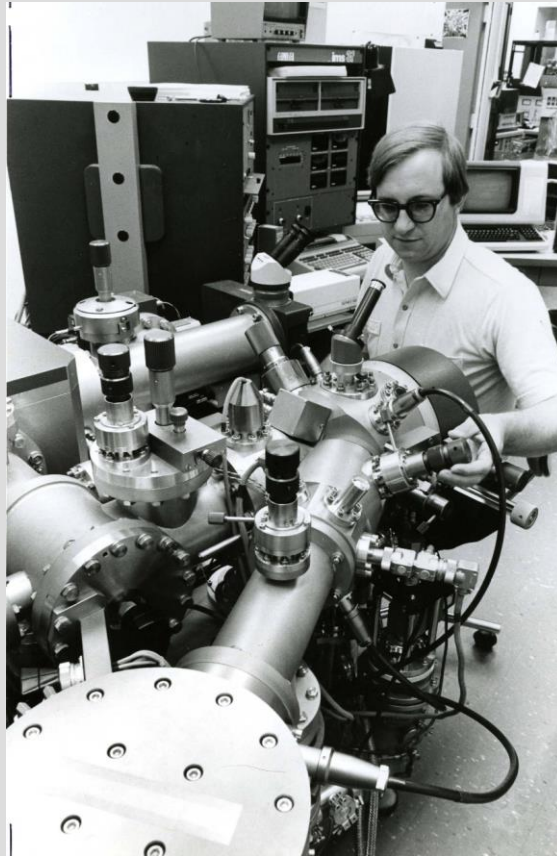
Superconducting cryo-TEM: Final version, 400 keV, FEG





1980-1990



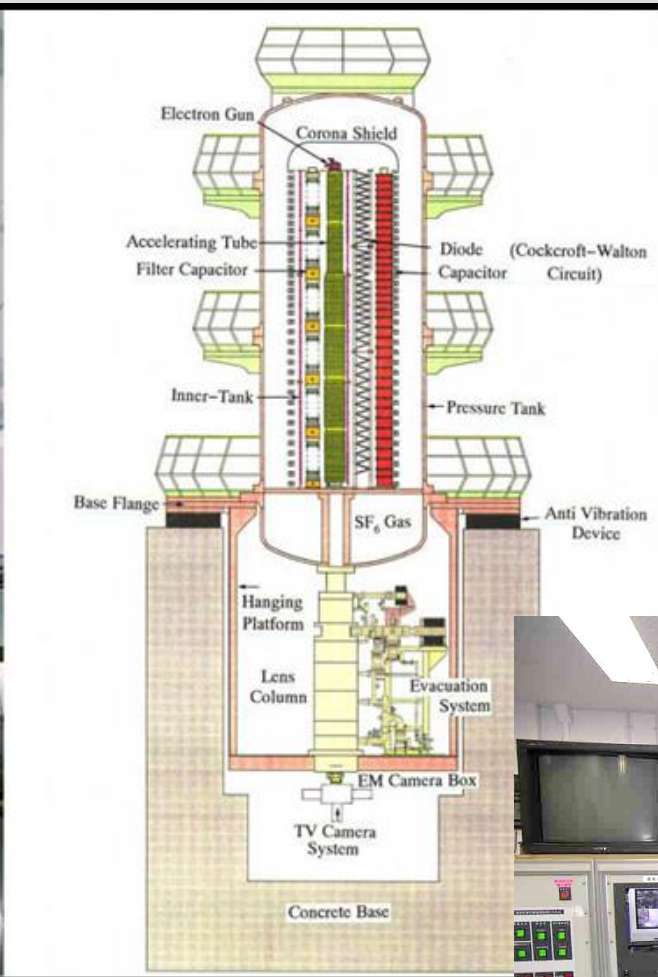
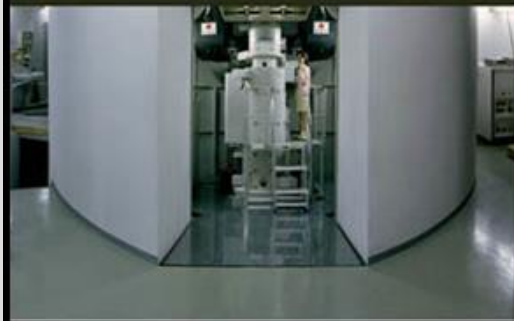


Dale Newbury uses a secondary ion mass spectrometry instrument

1984-08

Using a secondary ion mass spectrometry instrument, metallurgist Dale Newbury is able to map the distribution of elements both on and below a sample's surface.

1980-1990



HVEM still lives!

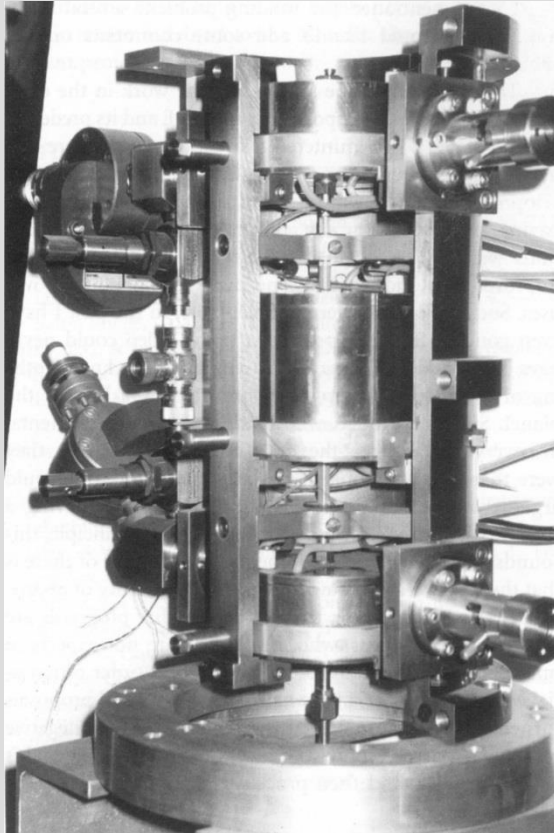
Hitachi 3 MeV TEM, Osaka, 1981



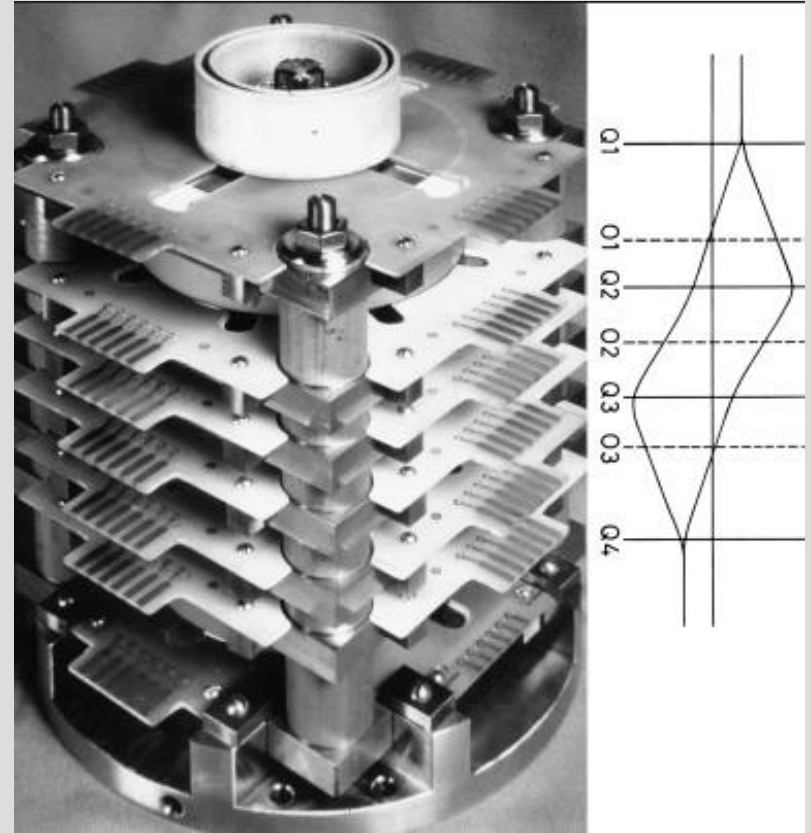
1980-1990

Attempts at aberration correction for STEM

Albert Crewe and colleagues



Sextupole type



Octupole-quadrupole type

1980-1990

Continued development of the atom probe

The Position-Sensitive Atom Probe

1988

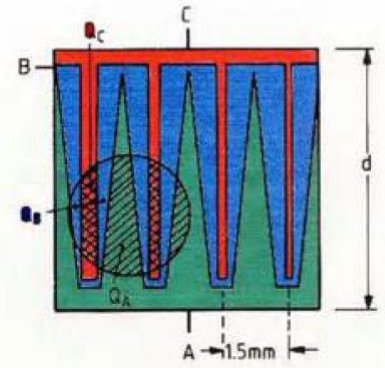
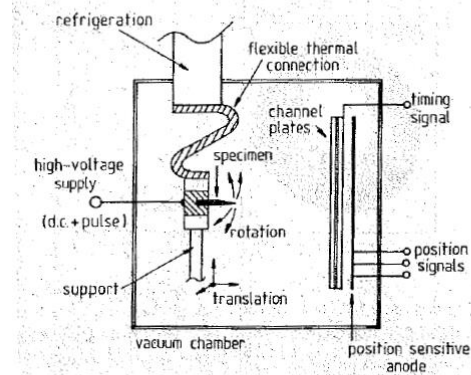
- Adapted a Wedge-and-Strip detector from astronomy to a VG APFIM 100
- 1988 Fall MRS presented by George Smith
- First operational 3DAP



Key Stats

Data Rate:	10^3 atoms/hr.
Field of View:	15 nm
Mass Resolving Power:	100

The Position-Sensitive Atom Probe (PoSAP)



Application of a position-sensitive detector to atom probe microanalysis
 A. Cerazo, T. J. Godfrey, and G. D. W. Smith
 Departments of Metallurgy and Science of Materials, Oxford University, Parks Road, Oxford OX1 3PH,
 United Kingdom
 (Received 21 December 1987; accepted for publication 2 March 1988)

$$x/d = \frac{z_c}{z_A + z_B + z_C}$$

$$y/d = \frac{z_A}{z_A + z_B + z_C}$$

1980-1990

Continued development of the atom probe

Position-Sensitive or 3-Dimensional Atom Probe

G.W. Smith, A. Cerezo - Oxford

M.K. Miller – ORNL

(circa **1986-89**)

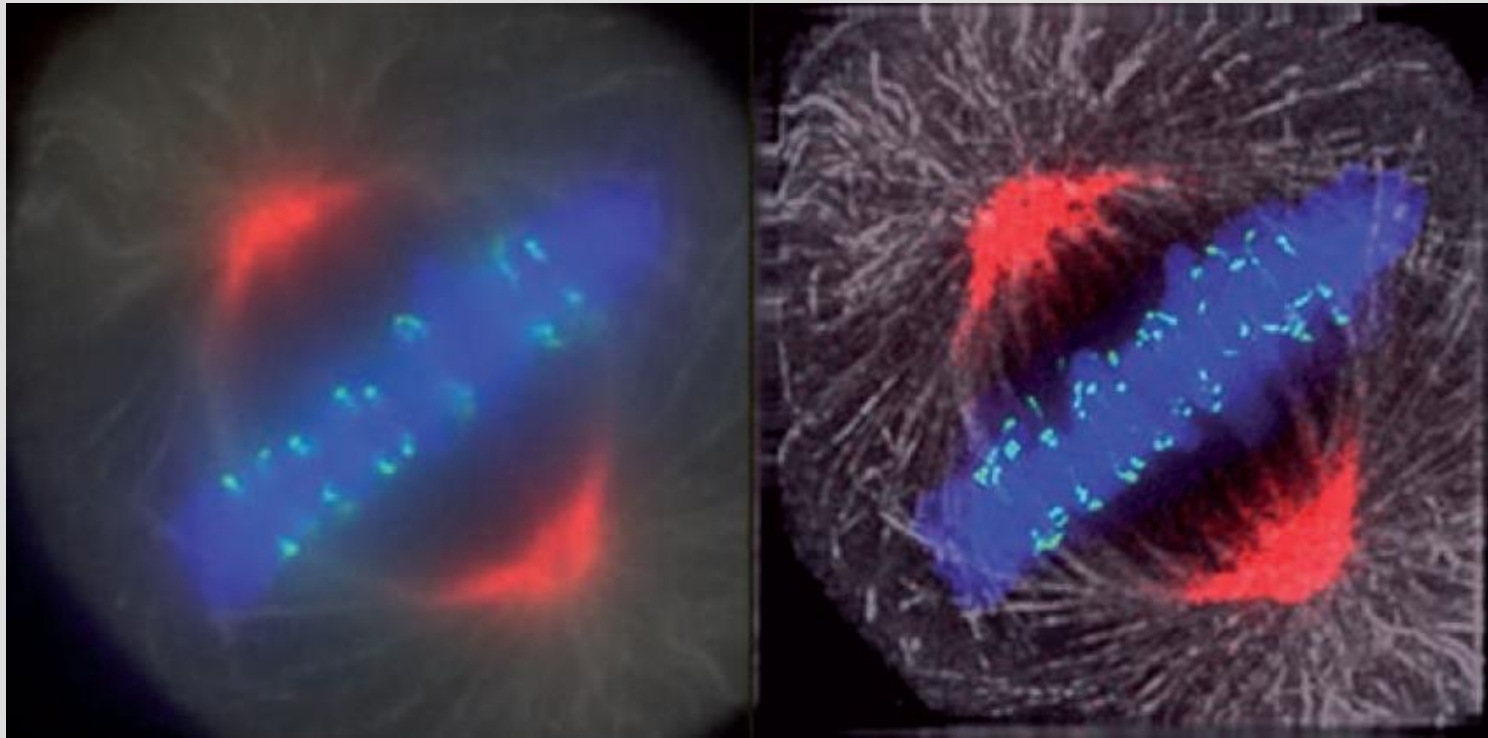


1980-1990

New developments in light microscopy

1983: Point-spread-function deconvolution

Agard and Sedat, others

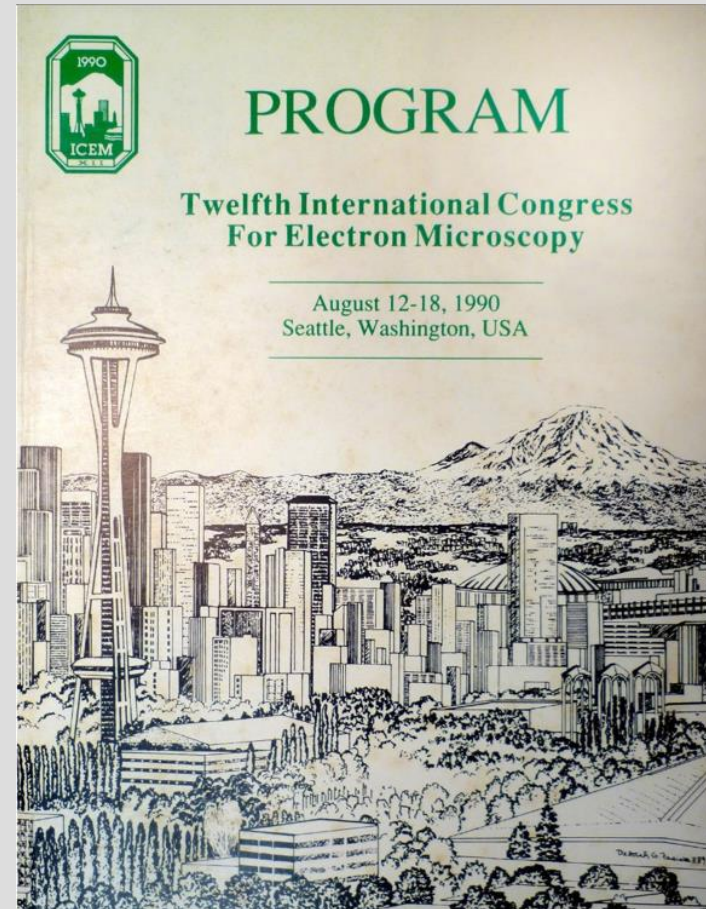


1980-1990

XII ICEM in Seattle (the last in the US)



Organizers: Can you recognize them all?



ELECTRON MICROSCOPY 1990



VOLUME 4: MATERIAL SCIENCES

1980-1990

Development of TEM microanalysis



Andrew Somlyo

- Uses cryo-sections of tissue, frozen in homemade device.
- Sections are freeze-dried in the TEM

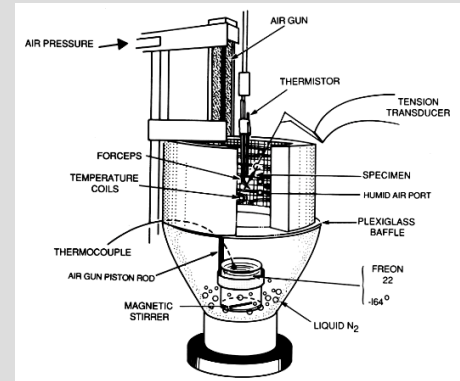


FIG. 2. Schematic view of the environmental chamber and freezing apparatus. The environmental chamber is isolated from the coolant by a plexiglass baffle that is removed the instant prior to triggering the air gun, which raises the beaker of supercooled Freon 22 at a speed of 80 cm/sec into the environmental chamber, freezing the preparation at the desired time during the physiological response. For mammalian tissues, the chamber is maintained at 37° with high humidity to prevent drying and cooling of evaporation.

JOURNAL OF ULTRASTRUCTURE RESEARCH 88, 135-142 (1984)

Compositional Mapping in Biology: X Rays and Electrons

ANDREW P. SOMLYO

*Pennsylvania Muscle Institute, Departments of Physiology and Pathology,
University of Pennsylvania School of Medicine, B42 Anatomy-Chemistry Building/G3,
Philadelphia, Pennsylvania 19104*

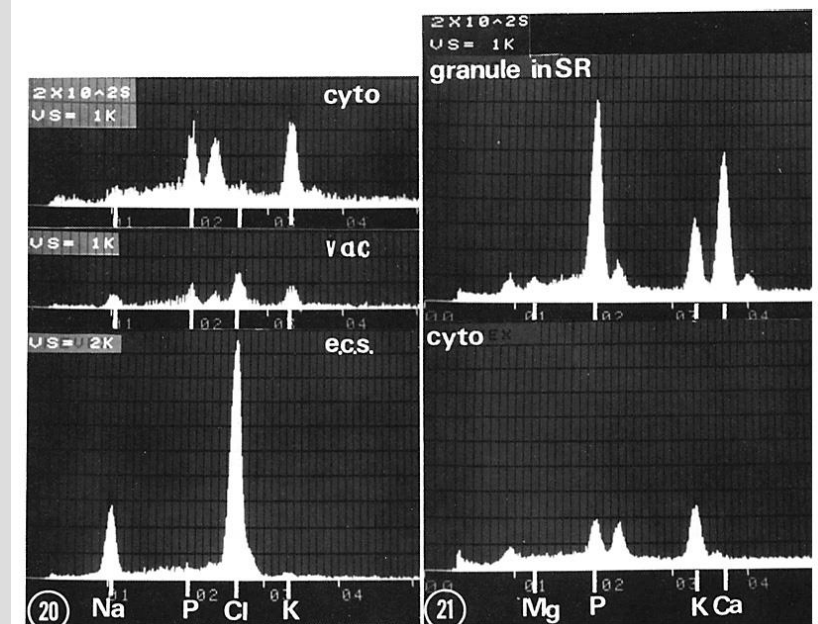
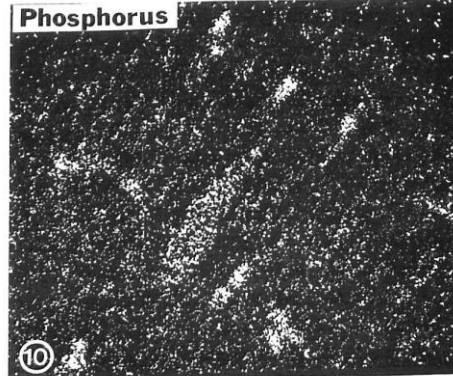
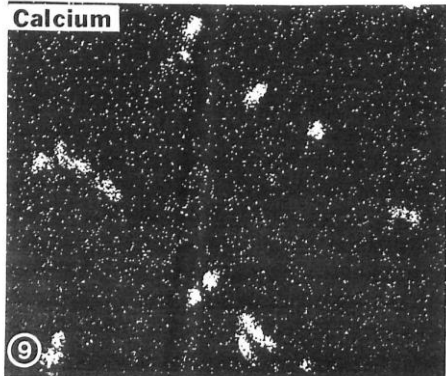


FIGURE 20 X-ray spectra of the cytoplasm (*cyto*) vacuole (*vac*), and extracellular space (*e.c.s.*) from a frozen-dried thin section of a frog toe muscle incubated in $2.2 \times$ hypertonic NaCl. The ordinate gives the number of counts for the energies shown on the abscissa. The positions of the characteristic energies of Na, P, Cl, and K are indicated. Note the NaCl peaks over the *vac* and the *e.c.s.* Instrument and osmium peaks, and the extraneous continuum were subtracted by the computer program.

FIGURE 21 X-ray spectra of the cytoplasm (*cyto*) and a granule in the longitudinal SR from a muscle exposed to $2.5 \times$ hypertonic sucrose. Note the Ca, P, and Mg peaks from the granule.

1980-1990

Development of TEM microanalysis

Richard Leapman, Brian Andrews



Ultramicroscopy 24 (1988) 237-250
North-Holland, Amsterdam

237

QUANTITATIVE X-RAY MAPPING OF BIOLOGICAL CRYOSECTIONS

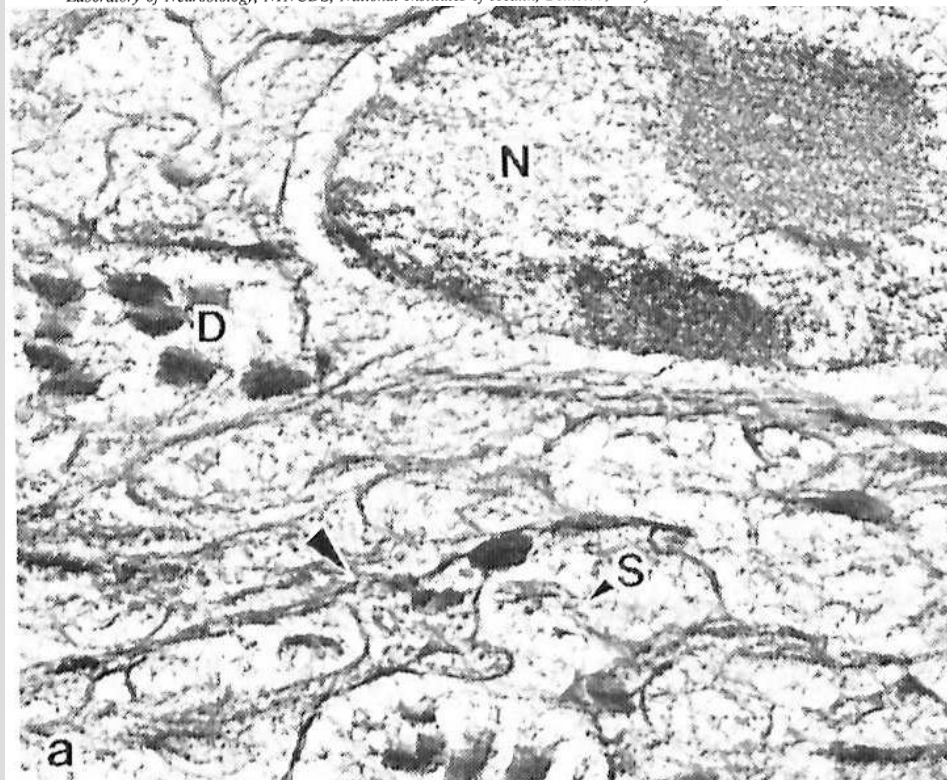
C.E. FIORI, R.D. LEAPMAN and C.R. SWYT

Biomedical Engineering and Instrumentation Branch, DRS, National Institutes of Health, Bethesda, Maryland 20892, USA

and

S.B. ANDREWS

Laboratory of Neurobiology, NINCDS, National Institutes of Health, Bethesda, Maryland 20892, USA

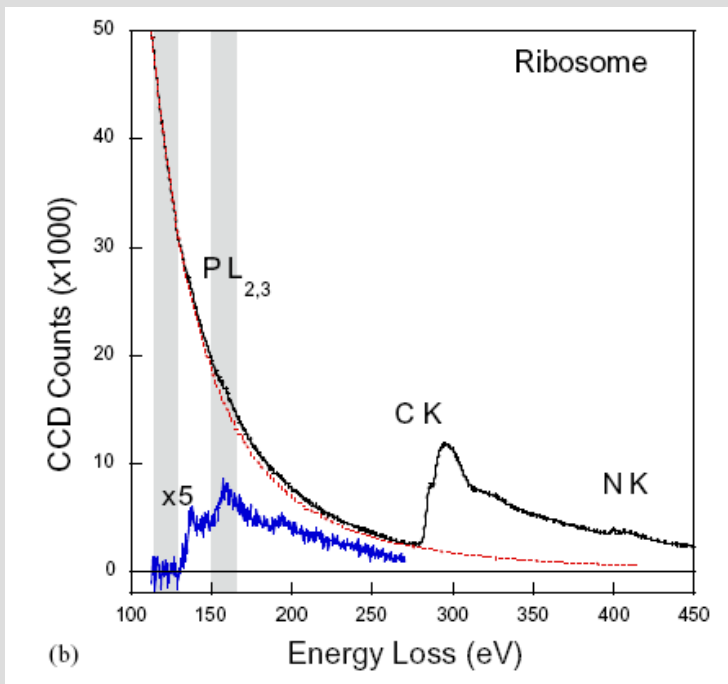


Compartment	Number of pixels	Concentration (mmol/kg wet wt)		
		P	K	Ca
Nucleus	600	70 ± 3	83 ± 2	-1.0 ± 0.5
Dendrite	250	92 ± 5	72 ± 3	1.2 ± 1.0
Spine	18	48 ± 14	83 ± 8	-2.2 ± 2.5

1980-1990

Modern biological microanalysis

Single-atom detection, EFTEM tomography



Spectrum showing regions used for background subtraction

Leapman, RD, et al. (2004) *Ultramicroscopy* 100, 115-125

Journal of Microscopy, Vol. 210, Pt 1 April 2003, pp. 5-15
Received 5 May 2002; accepted 10 January 2003

Detecting single atoms of calcium and iron in biological structures by electron energy-loss spectrum-imaging

R. D. LEAPMAN
Division of Bioengineering & Physical Science, ORS, National Institutes of Health, Bethesda, MD 20892, U.S.A.

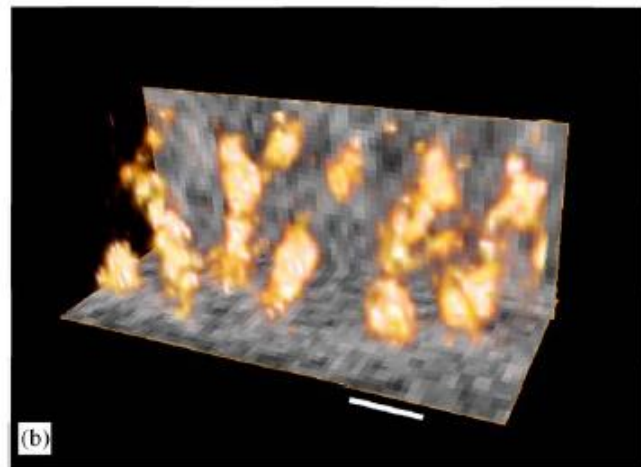
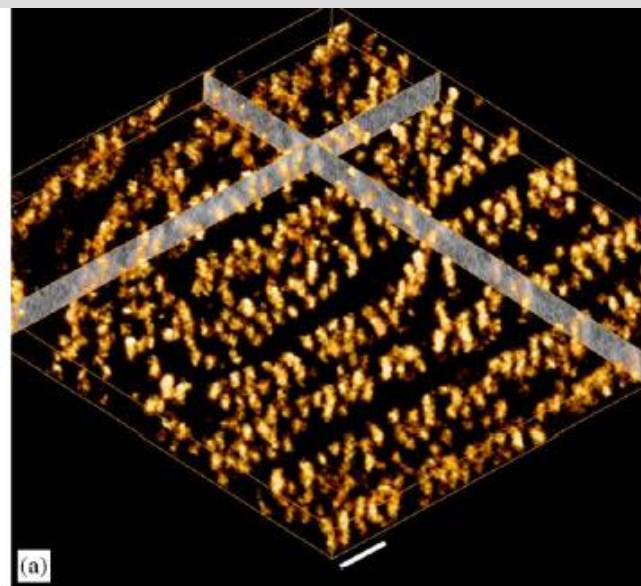
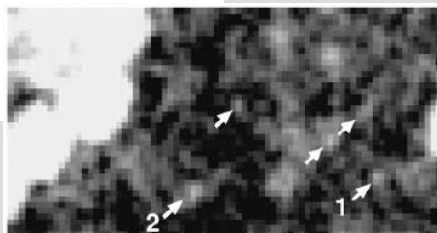
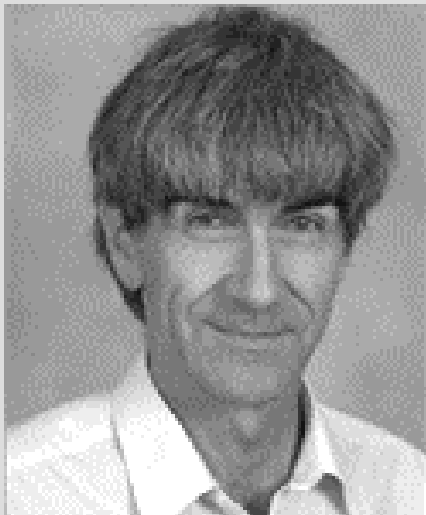
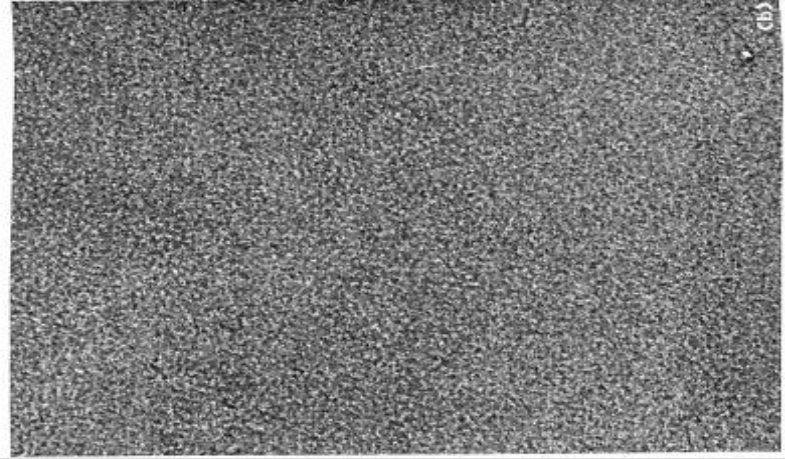
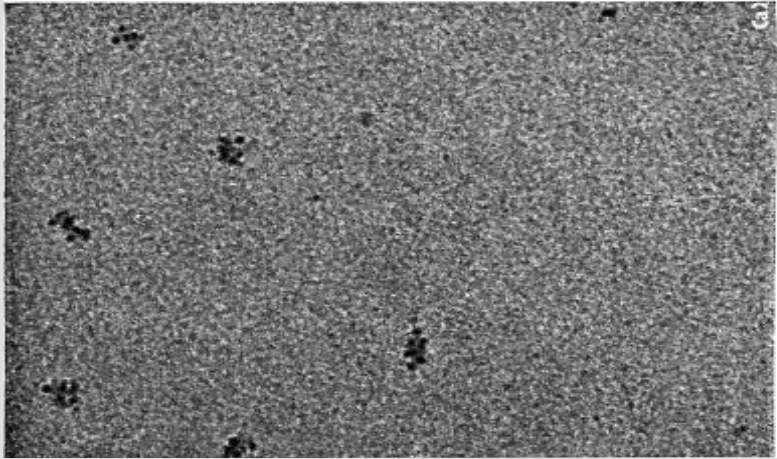


Fig. 6. Volume-rendered, tomographic reconstruction of phosphorus in a section of *C. elegans* cell: (a) Rows of ribosomes are evident along stacks of endoplasmic reticulum membranes. Slices through the reconstruction in the *x-z* and *y-z* planes are also shown. Bar = 100 nm. (b) Higher magnification of volume-rendered phosphorus distribution showing individual ribosomes located at different heights within the section. Bar = 20 nm.

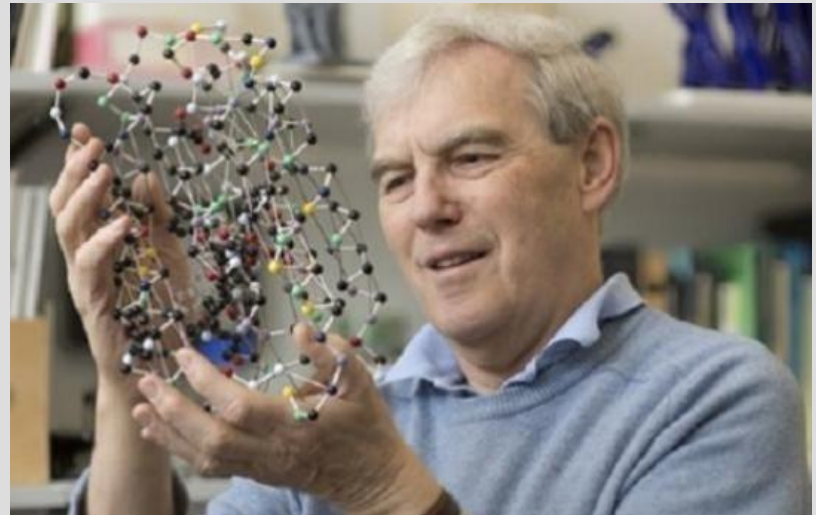
1980-1990

Development of image-processing and 3-D reconstruction

Averaging many examples in low-dose micrographs



Nigel Unwin



Richard Henderson

1980-1990

Development of image-processing and reconstruction

Sub-nm 3-D resolution of unstained biological molecules

J. Mol. Biol. (1975) **94**, 425–440

Molecular Structure Determination by Electron Microscopy of Unstained Crystalline Specimens

P. N. T. UNWIN AND R. HENDERSON

*Medical Research Council
Laboratory of Molecular Biology
Hills Road, Cambridge, England*

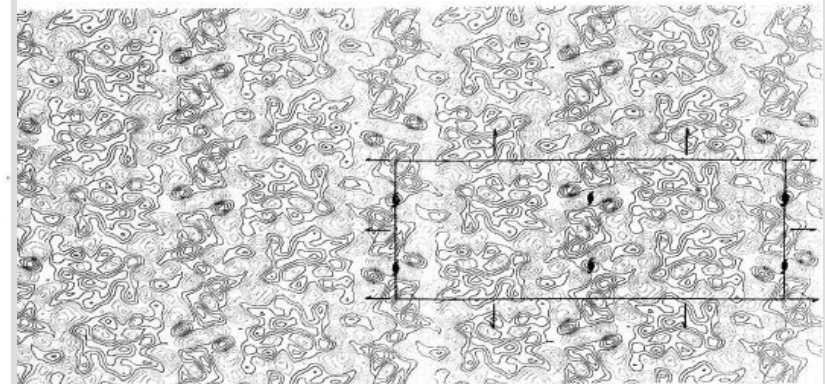
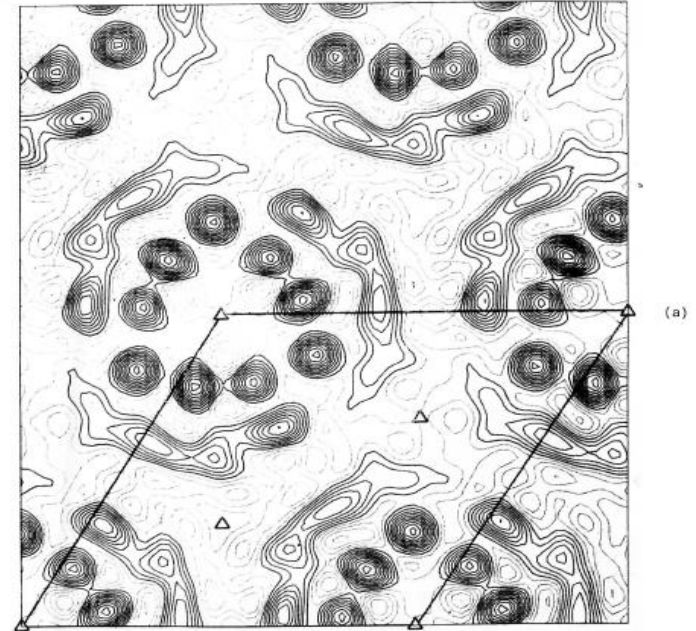
(Received 15 November 1974)

The projected structures of two unstained periodic biological specimens, the purple membrane and catalase, have been determined by electron microscopy to resolutions of 7 Å and 9 Å, respectively. Glucose was used to facilitate their *in vacuo* preservation and extremely low electron doses were applied to avoid their destruction.

The information on which the projections are based was extracted from defocussed bright-field micrographs and electron diffraction patterns. Fourier analysis of the micrograph data provided the phases of the Fourier components of the structures; measurement of the electron diffraction patterns provided the amplitudes.

Large regions of the micrographs (3000 to 10,000 unit cells) were required for each analysis because of the inherently low image contrast (<1%) and the statistical noise due to the low electron dose.

Our methods appear to be limited in resolution only by the performance of the microscope at the unusually low magnifications which were necessary. Resolutions close to 3 Å should ultimately be possible.



1980-1990

Development of image-processing and reconstruction

First reconstruction of asymmetric, non-crystalline samples

Contributions of Frank group at Albany, incl. Radermacher and Penczek

Ultramicroscopy 46 (1992) 241–262
North-Holland

ultramicroscopy

Three-dimensional reconstruction of single particles negatively stained or in vitreous ice

Joachim Frank and Michael Radermacher

Wadsworth Center for Laboratories and Research, New York State Department of Health, P.O. Box 509, Albany, NY 12201-0509, USA

and

Department of Biomedical Sciences, State University of New York at Albany, Albany, NY 12222, USA

Received at Editorial Office 9 April 1992

The random-conical reconstruction method has been highly successful in three-dimensional imaging of macromolecules under low-dose conditions. This article summarizes the different steps of this technique as applied to molecules prepared with negative staining or vitreous ice, and sketches out the current directions of development. We anticipate that by using new instrumental developments, transfer function correction and computational refinement techniques, a resolution in the range of 7–10 Å could ultimately be achieved.

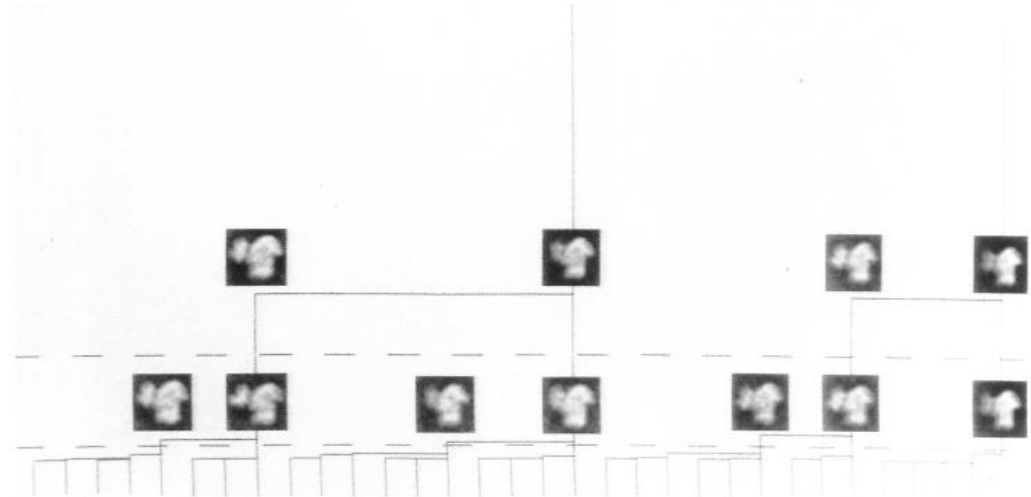
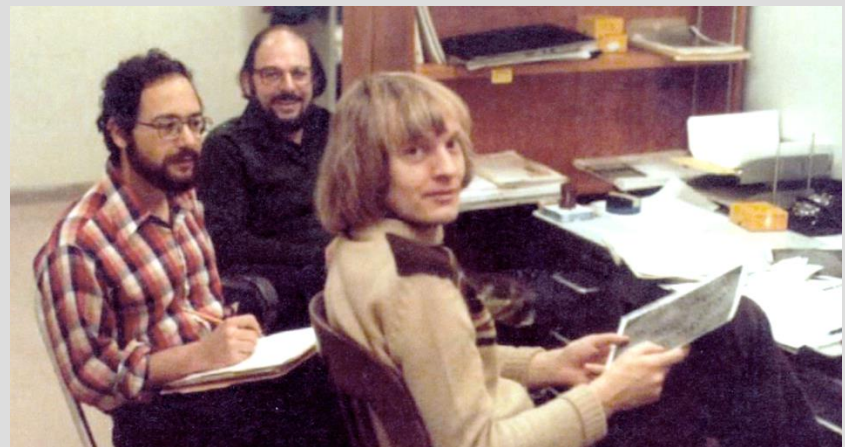
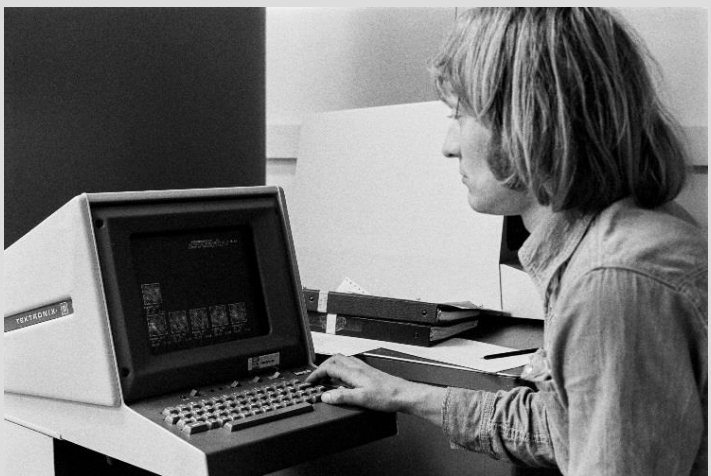


Fig. 8. Classification dendrogram obtained by applying hierarchical ascendant classification (using complete linkage) to images of the eukaryotic 40S ribosome complexed with initiation factor 3. The branching pattern of the inverted tree reflects the hierarchical similarity relationships among groups of images. The groups of particles associated with the top levels of the hierarchy are characterized by their group averages and are shown inserted in the diagram. The higher we are in the hierarchy, the more particles fall into the group, and the better is the average defined statistically, but the worse is the resolution. (From Srivastava, Verschoor, and Frank, unpublished data; see also ref. [42].)

1980-1990

Development of image-processing and reconstruction

First reconstruction of asymmetric, non-crystalline samples



Joachim Frank, 1980

Joachim Frank today



Michael Radermacher



Pawel Penczek



1980s computer lab

1980-1990

Development of image-processing and reconstruction

Ultramicroscopy 46 (1992) 241–262
North-Holland

ultramicroscopy

Three-dimensional reconstruction of single particles negatively stained or in vitreous ice

Joachim Frank and Michael Radermacher

Wadsworth Center for Laboratories and Research, New York State Department of Health, P.O. Box 509, Albany, NY 12201-0509, USA
and
Department of Biomedical Sciences, State University of New York at Albany, Albany, NY 12222, USA

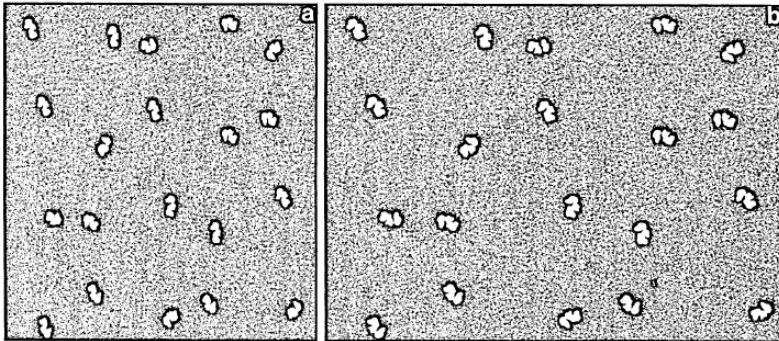
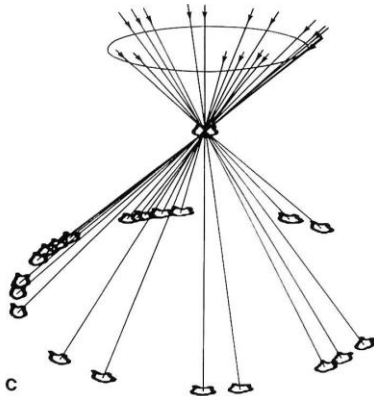


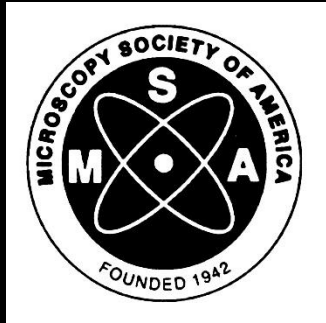
FIGURE 1. Data collection used in the three-dimensional reconstruction method illustrated with the aid of model images generated by placing an averaged lateral view of the 40S ribosomal subunit from HeLa¹⁶ into random orientations. (a) Image field with untilted specimen. (b) The same field with the specimen tilted 50°.

Penczek, P., Radermacher, M., & Frank, J. (1992). Three-dimensional reconstruction of single particles embedded in ice. *Ultramicroscopy*, 40(1), 33-53.

Data collection and reconstruction follow the protocol of the random-conical technique of Radermacher et al. [*J. Microscopy* 146 (1987)]. A reference-free alignment algorithm has been developed to overcome the propensity of reference-based algorithms to reinforce the reference motif in very noisy situations. In addition, an iterative 3D reconstruction method based on a chi-square minimization constraint has been developed and tested. This algorithm tends to reduce the effects of the missing angular range on the reconstruction, thereby facilitating the merging of random-conical data sets obtained from differently oriented particles.



Contributions of Frank group at Albany, incl. Radermacher and Penczek

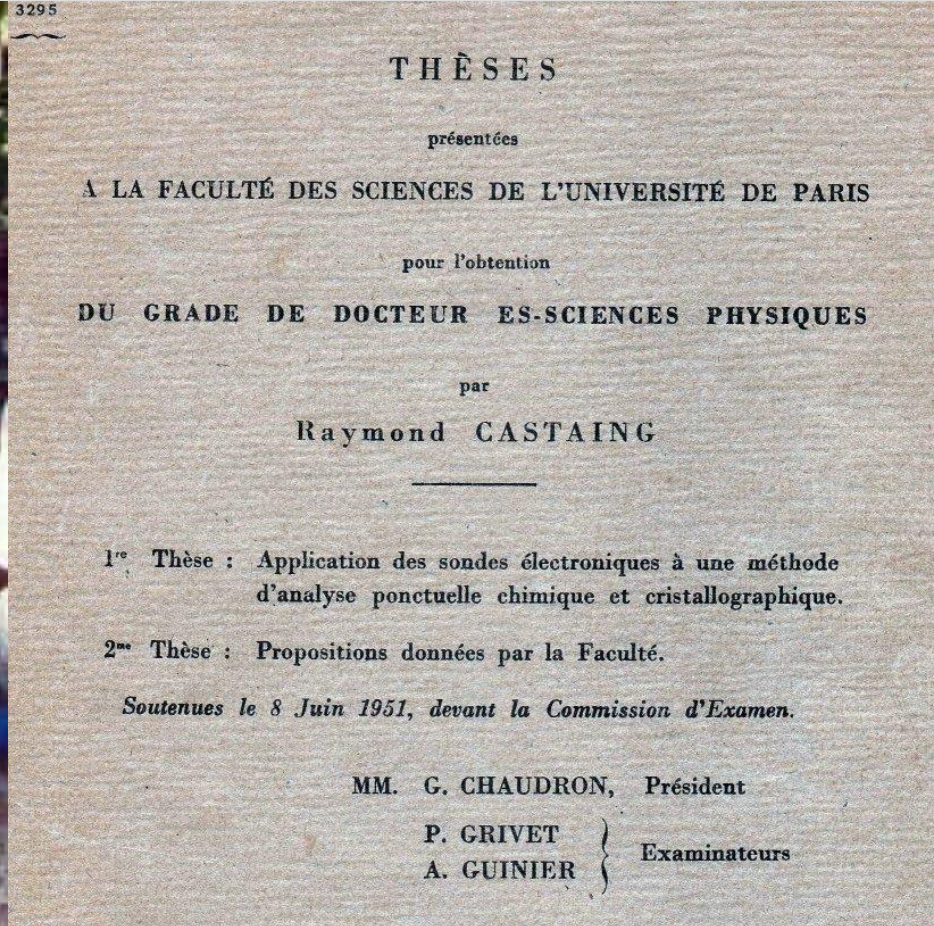


1990-2000



1990-2000

1999 MAS meeting in Portland

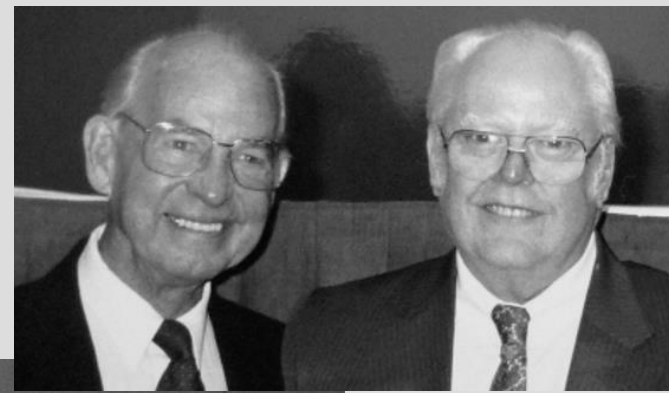


Raymond Castaing and his wife with Jean Philibert
(at the 1999 meeting in Portland) Courtesy of Peter Duncomb

1990-2000

50th Anniversary of MSA

Publication of Sterling Newberry's book:
EMSA and its People: the First 50 years



Distinguished
Scientist
awards, 1992:
Fritiof
Sjöstrand (l)
and James
Hillier (r)



Left to right: O. F. Schuette, G. I. Simard, E. F. Fullam, J. Hillier, J. S. Bryner, A. G. Richards,
J. S. Bryner, Mary S. Jaffe, unidentified, T. Rochow, E. P. Olivieto, G. B. Levy, C. S. Barrett,
E. A. Boettner, S. P. Newberry, S. M. Zollers, A. Prebus, J. L. Watson, F. O. Schmitt

Charter members living in 1992

1990-2000

Development of automated electron tomography

Basic low-dose principles for automation, 1991

Ultramicroscopy 40 (1992) 71–87
North-Holland

ultramicroscopy

Towards automatic electron tomography

K. Dierksen, D. Typke *, R. Hegerl, A.J. Koster ¹ and W. Baumeister
Max-Planck-Institut für Biochemie, W-8033 Martinsried, Germany

Received 10 October 1991

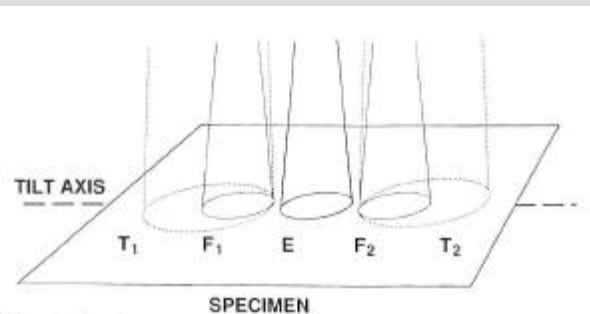


Fig. 6. Specimen areas used in low-dose procedures for automatic recording of tilt series: tilt areas T_i , focus areas F_i and exposure area E , $i = 1, 2$. The tilt areas T_i are shown with a larger size to indicate that tilt displacements are normally measured and corrected at lower magnification.

1990-2000

Principles of TEM automation

Basic low-dose principles for automation, 1992

Ultramicroscopy 46 (1992) 207-227
North-Holland

ultramicroscopy

Automated microscopy for electron tomography

A.J. Koster, H. Chen, J.W. Sedat and D.A. Agard

Department of Biochemistry and Biophysics and the Howard Hughes Medical Institute,
University of California at San Francisco, San Francisco, CA 94143-0448, USA

Received at Editorial Office 20 May 1992



Bram Koster

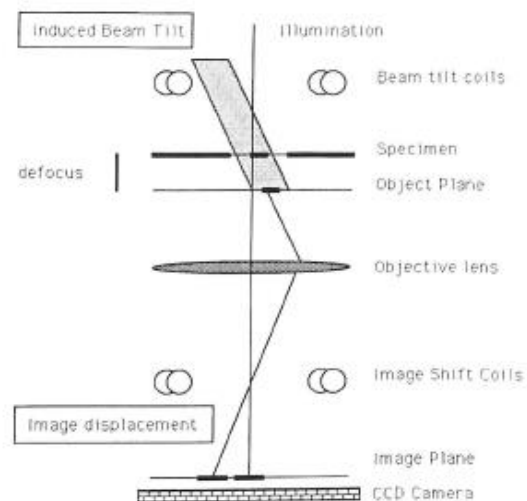


Fig. 1. The principle of the automatic focusing method: image displacement, resulting from an induced beam tilt, is linearly related to the amount of defocus.

Auto-focus

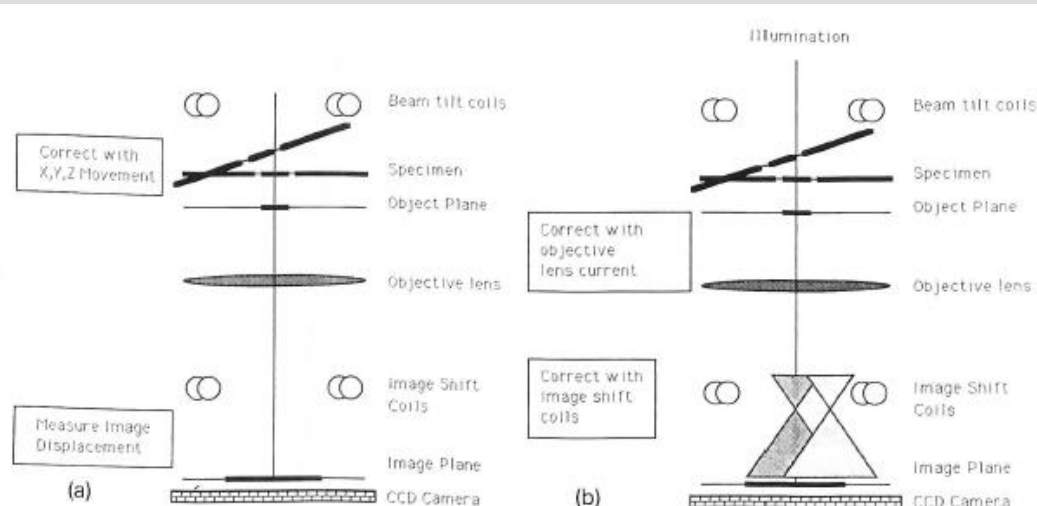
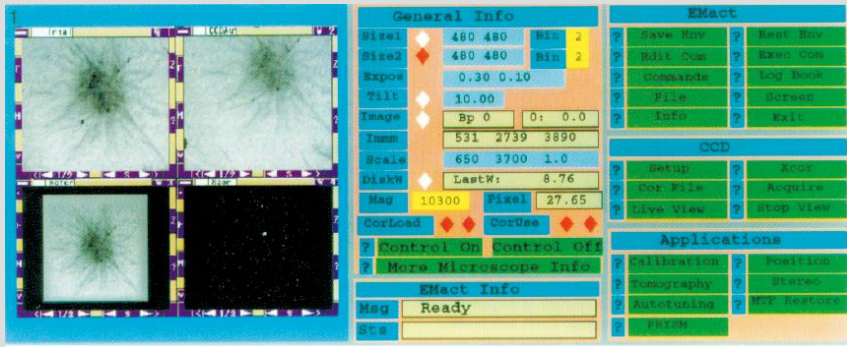


Fig. 2. Correction for the image shift and defocus change when the specimen is tilted at a non-eucentric height. The correction can be done (left) by movement of the specimen stage, or (right) by adjusting the electron optics.

Correction of image shift

1990-2000

Development of automated electron tomography

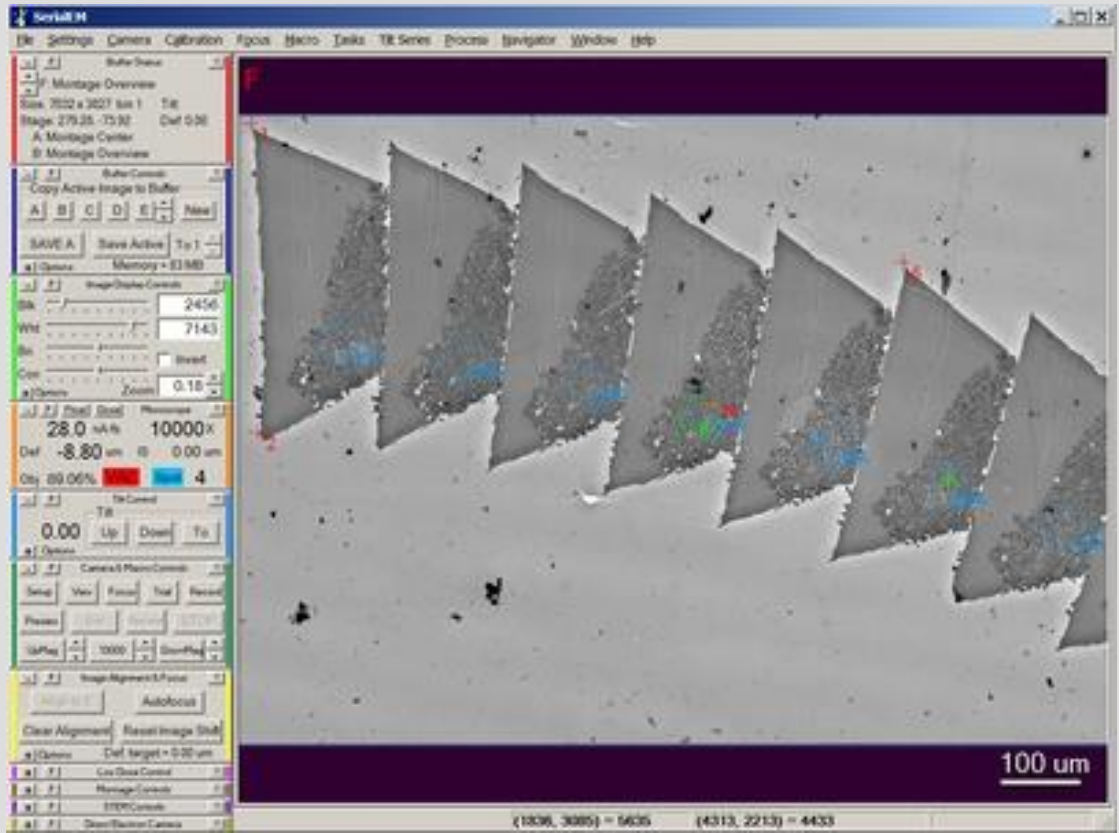


← Agard lab – Koster et al.

Serial EM →



David Mastrorarde



1990-2000

Nobel Prize #4

Development GFP for light microscopy

 The Nobel Prize in Chemistry 2008
Osamu Shimomura, Martin Chalfie, Roger Y. Tsien

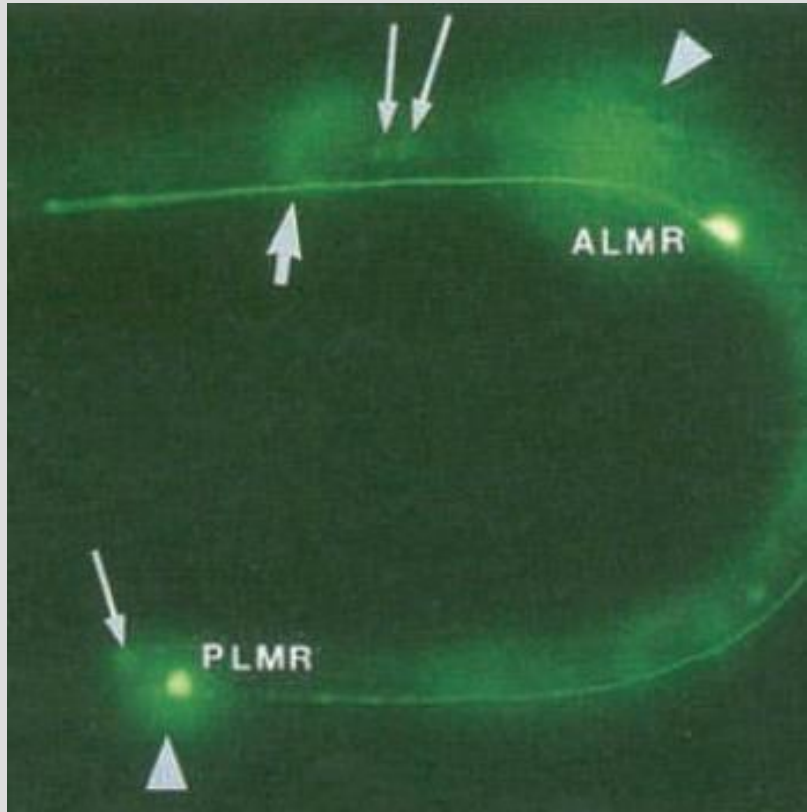
Share this:

The Nobel Prize in Chemistry 2008

 <p>Photo: U. Montan Osamu Shimomura Prize share: 1/3</p>	 <p>Photo: U. Montan Martin Chalfie Prize share: 1/3</p>	 <p>Photo: U. Montan Roger Y. Tsien Prize share: 1/3</p>
---	---	--

The Nobel Prize in Chemistry 2008 was awarded jointly to Osamu Shimomura, Martin Chalfie and Roger Y. Tsien *"for the discovery and development of the green fluorescent protein, GFP"*.

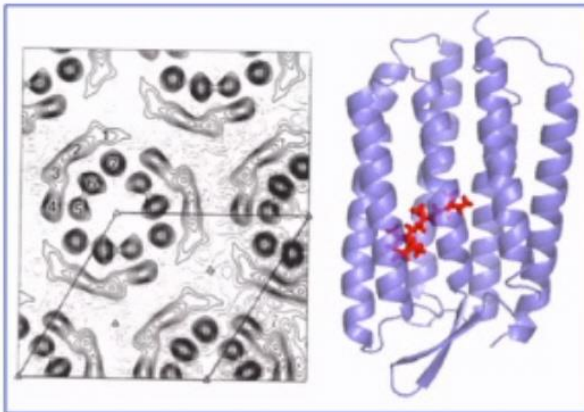
Green Fluorescent Protein: Chalfie et al., 1994



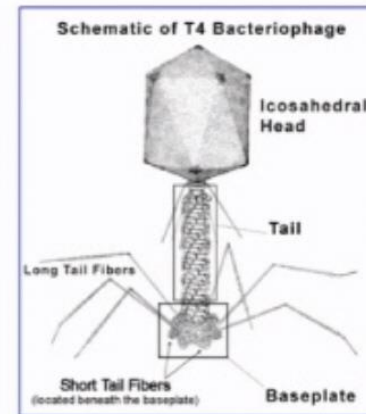
1990-2000

Development of image-processing and reconstruction

Tilting and implicit averaging: two-dimensional crystals or molecules with high symmetry



Purple membrane protein
Henderson and Unwin, Nature 1975



Bacteriophage tail
DeRosier and Klug, Nature 1968

→ *... but most molecules are NOT symmetric or ordered in crystals* ←

1990-2000

Continued development of the atom probe



Tomographic Atom Probe

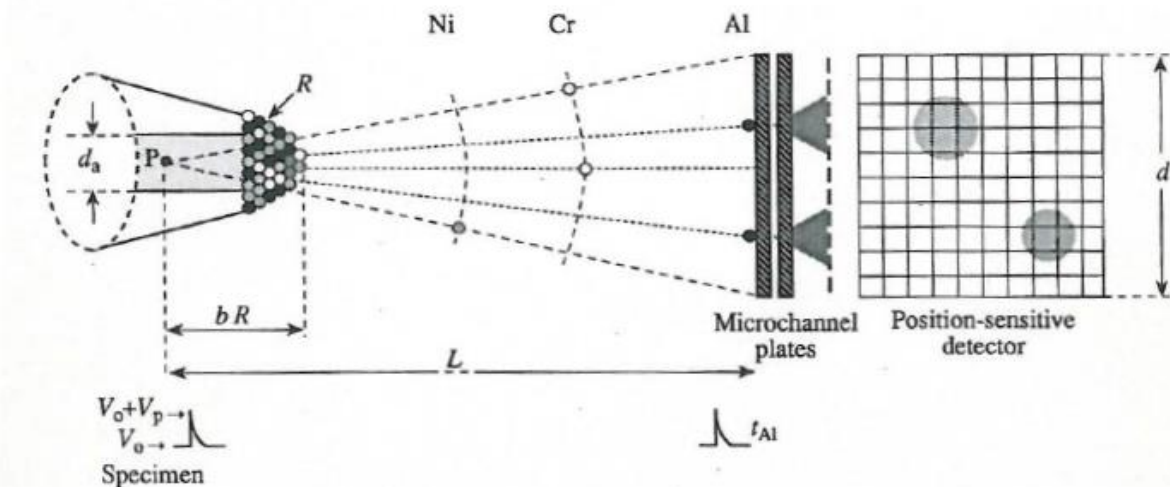
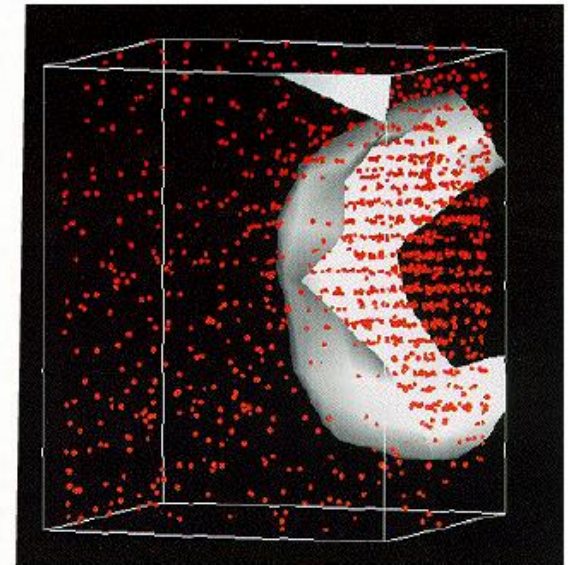


FIG. 1 Schematic view of the tomographic atom probe. The coordinates of atoms on the surface of a sample (a sharply pointed tip) are deduced from the position of ion impacts on the detector by means of a simple proportional operation. The magnification is $G = L / bR$. For a pure stereographic projection, the ion trajectories intercept at a single point (P) which is located at $2R$ from the tip surface ($b = 2$).

Field-evaporated ions originating from the specimen surface are identified by time-of-flight mass spectrometry. Their positions are deduced from the coordinates of ion impacts on the detector. For each impact, an electron shower is produced by the microchannel plates, and the measurement of this charge received on a 10×10 anode array allows the position of the spot centre to be determined.

D. Blavette, A. Bostel, J. M. Sarrau, B. Deconihout, and A. Menand: An atom-probe for three dimensional tomography. *Nature* 363:432–435 (1993).

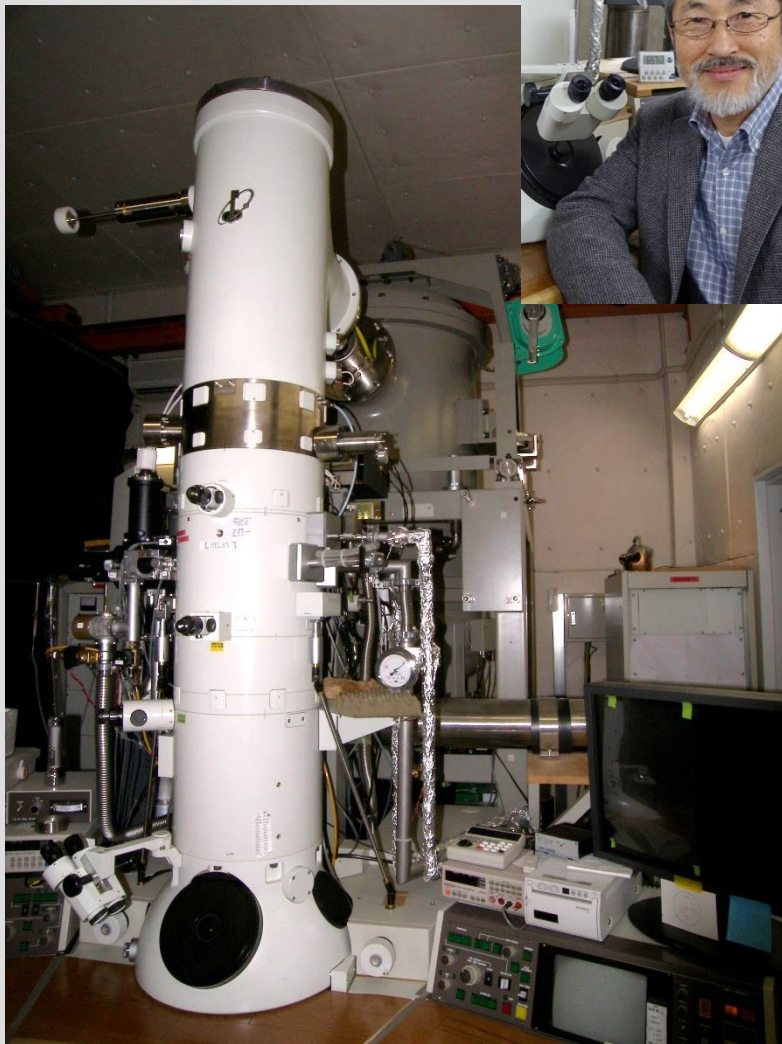
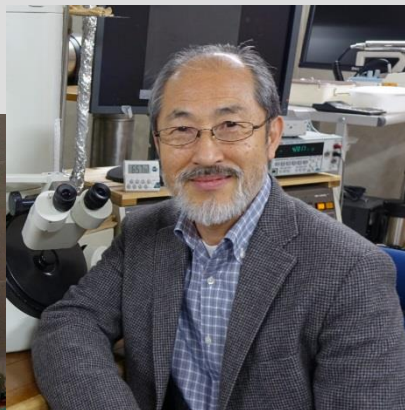


1990-2000

Modern liquid-helium cryo-TEM

Yoshinori Fujiyoshi

Six generations of 300 keV FEG Helium TEMs

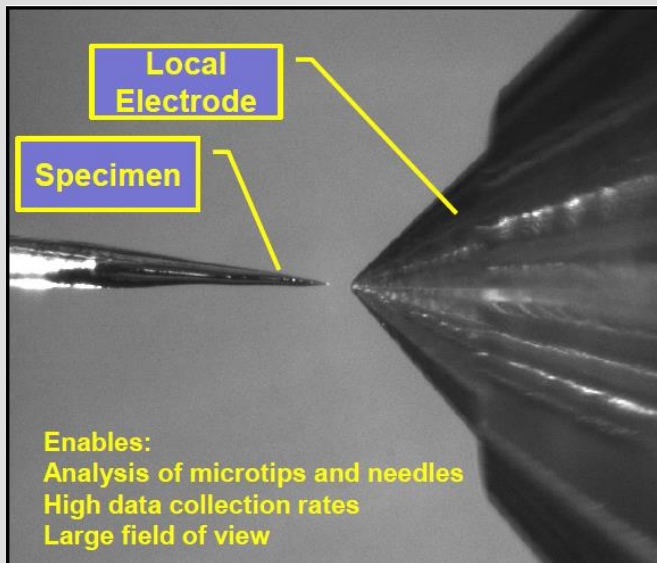


Liquid He
generating
plant (in lab
basement)



1990-2000

Continued development of the atom probe



1990-2000

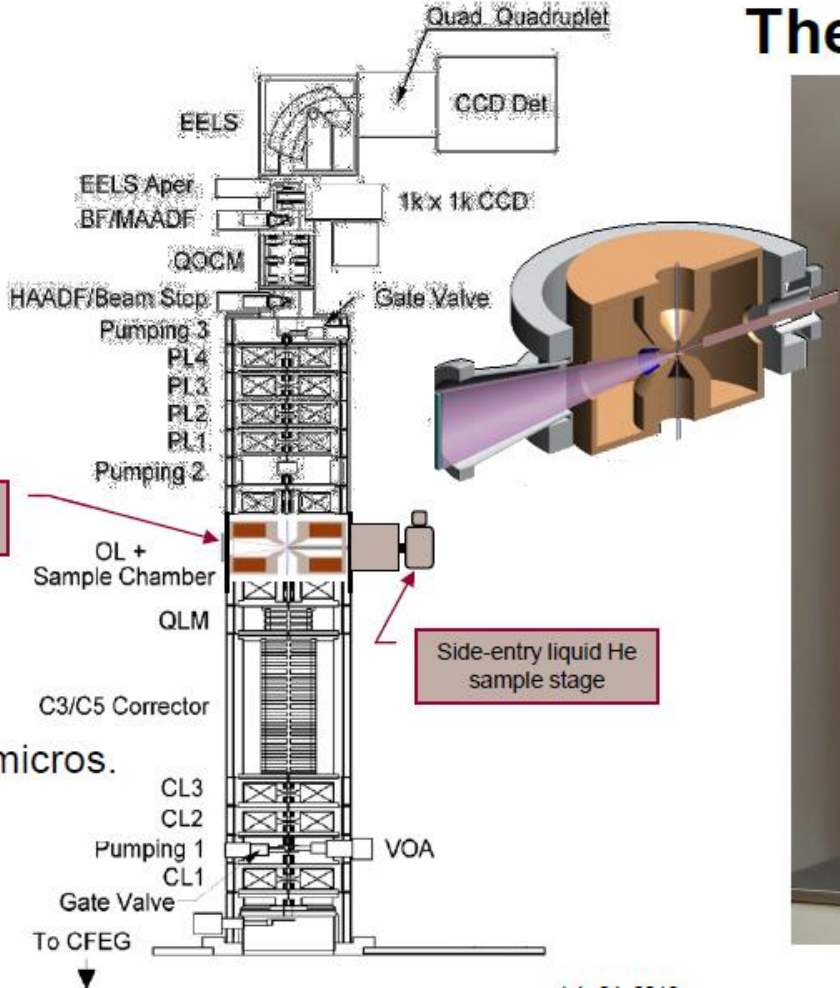
Continued development of the atom probe



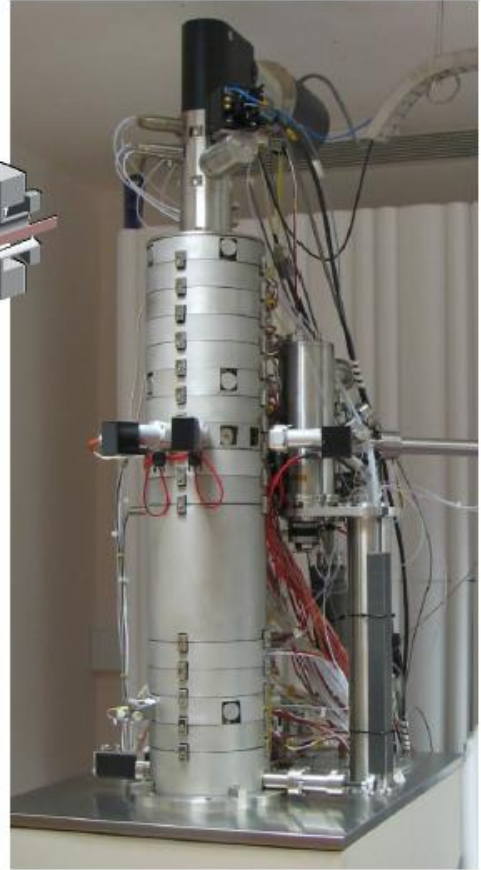
STEM+LEAP

Build objective lens assembly with atom probe inside

Position-Sensitive Detector



The ATOM Project



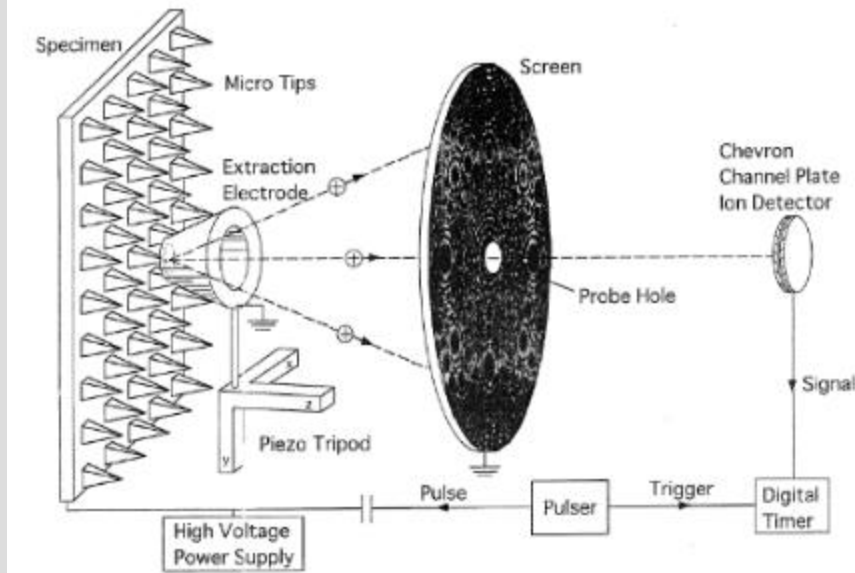
O. Krivanek et al., Ultramicros.
108 (2008) 179.



1990-2000

Continued development of the atom probe

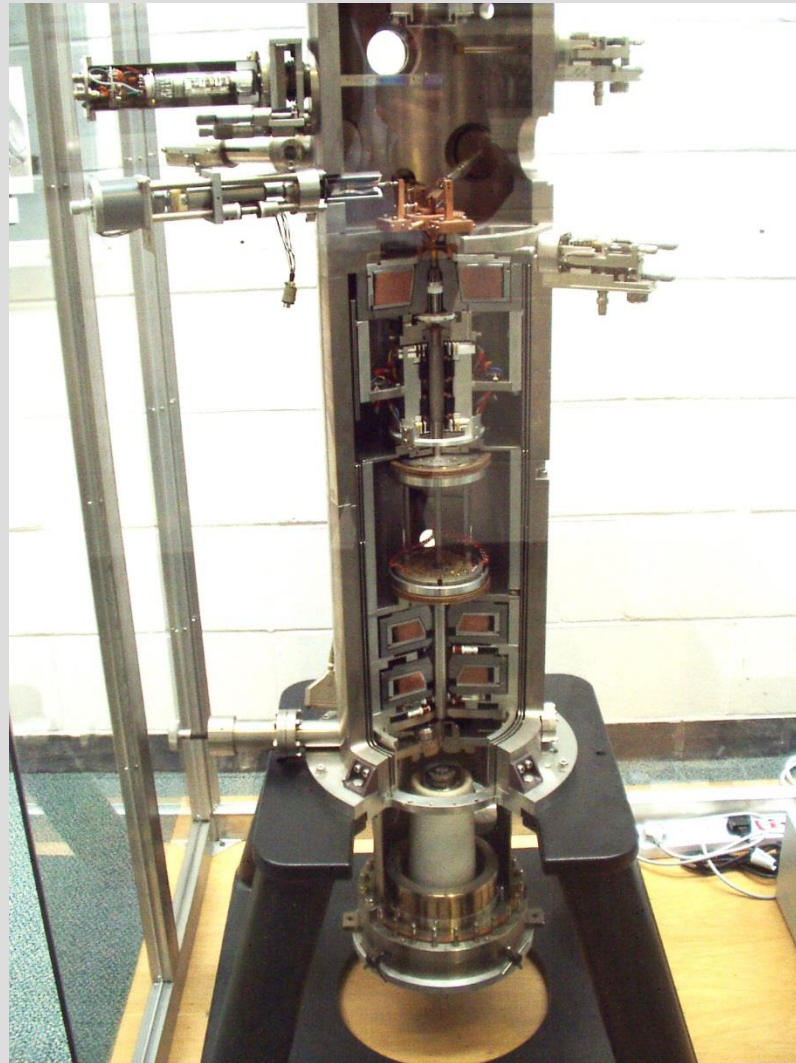
Scanning Atom Probe Nishikawa, Kimoto Appl. Surf. Sci. (**1994**)



1990-2000

Realization of aberration correction

Ondrej Krivanek: Early design of STEM corrector at Cambridge – 1995-7



1990-2000

First corrected HREM - 1997

Cs correction improved resolution of an existing HRTEM

CEOS: Haider et al. 1998 J. Elect. Microc. 47:395-405

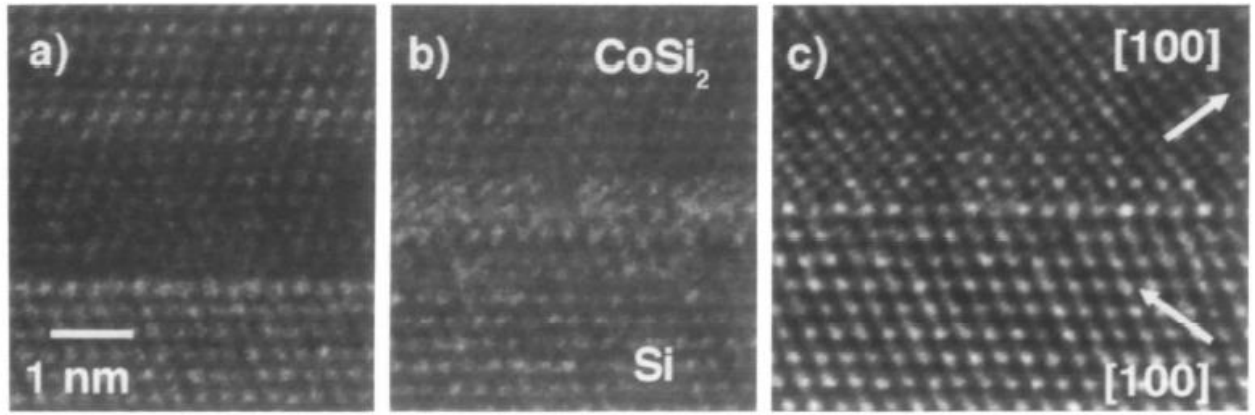
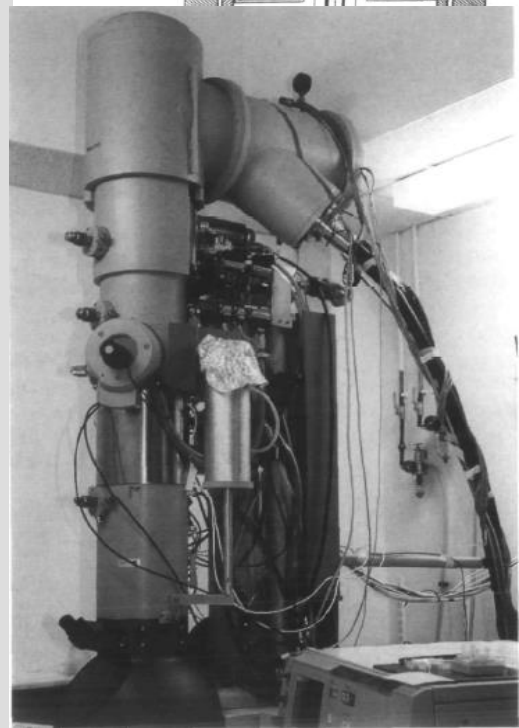
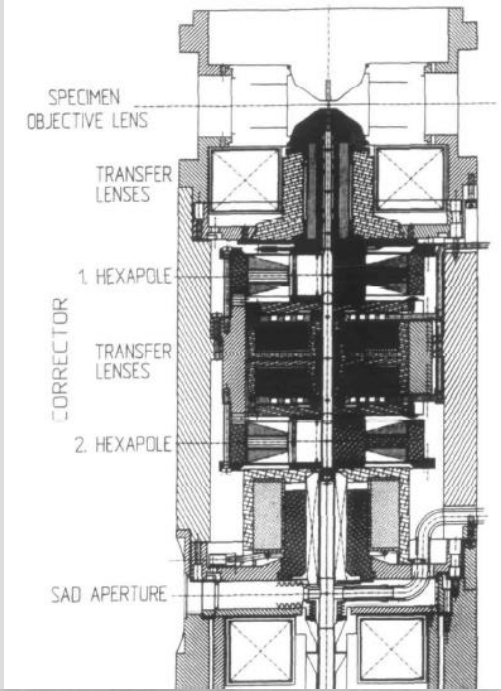


Fig. 9 Structure images of an epitaxial Si(111) / CoSi₂ interface. The images (a) and (b) were taken in the uncorrected microscope at (a) Scherzer defocus and (b) defocus of least confusion. Image (c) has been taken with the corrected microscope (C₃ = 0.05 mm) at Scherzer defocus. This image does not show any artefacts or delocalization.



1990-2000

First corrected HREM - 1997

Cs correction improved resolution of an existing STEM

O.L. Krivanek et al.

In: J.M. Rodenburg (Ed.), IoP Conference Series, vol. 153, 1997, p. 35.

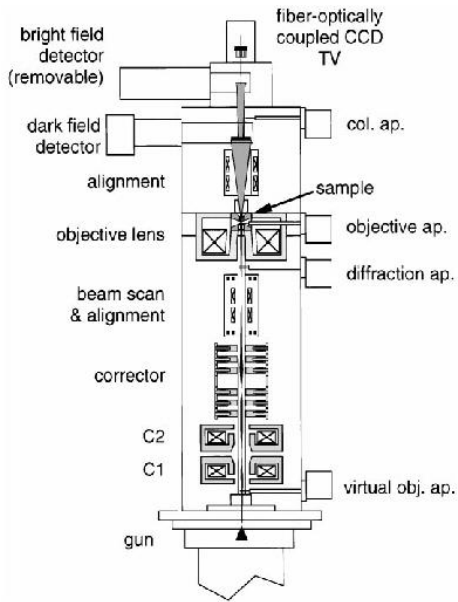


Fig. 2. Schematic diagram of the electron column of the C_s -corrected STEM.

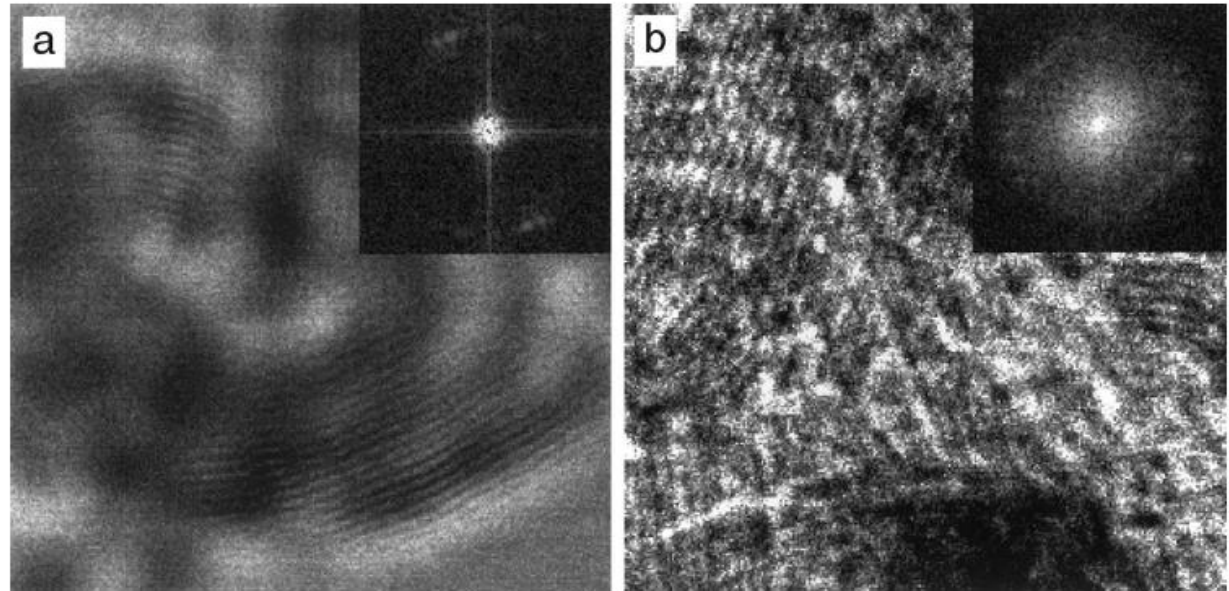


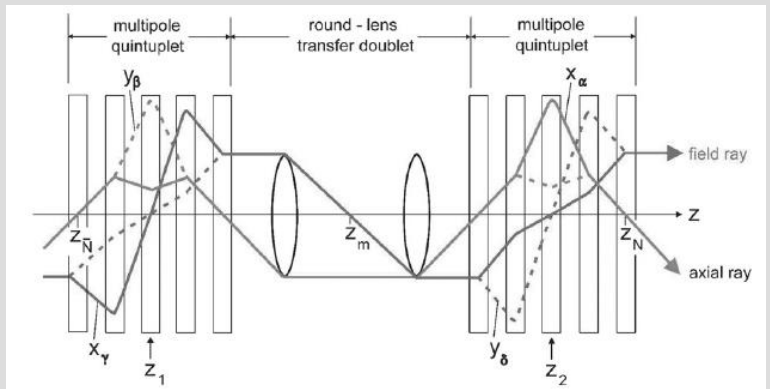
Fig. 4. Axial bright field STEM images of graphitized carbon (002) lattice planes ($d = 3.44 \text{ \AA}$) recorded at 100 keV: (a) HB5 without corrector, (b) HB5 with the corrector. Inset show diffractograms of the images.

2000-2010

TEAM project started - 2004

0.5 Å resolution, Cs correction – funded by DoE

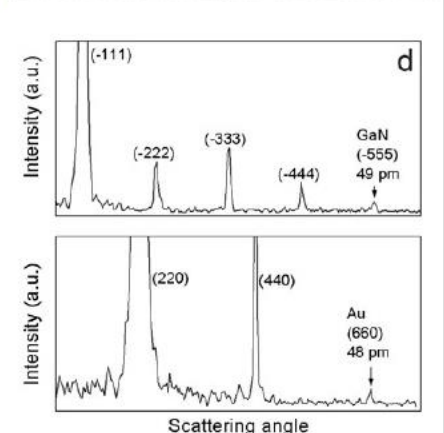
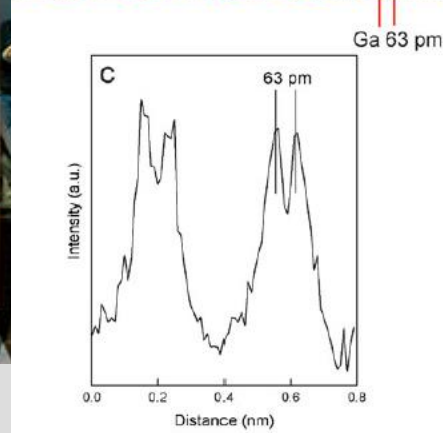
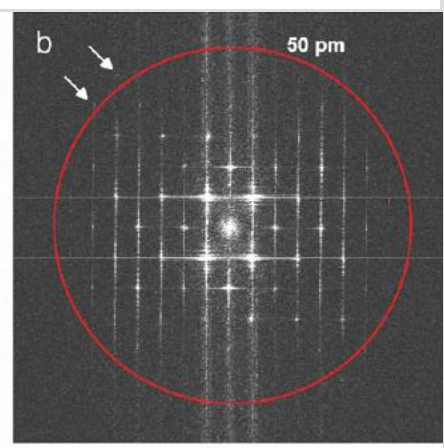
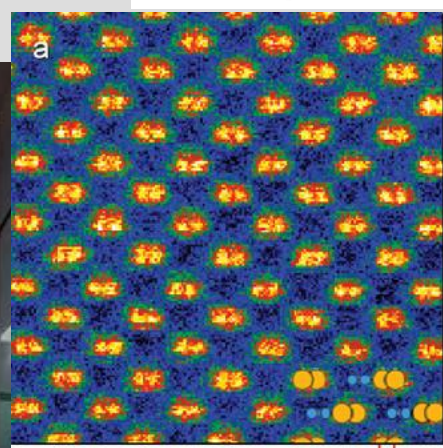
Operational microscope 2008



Berkeley TEAM I



Berkeley TEAM II

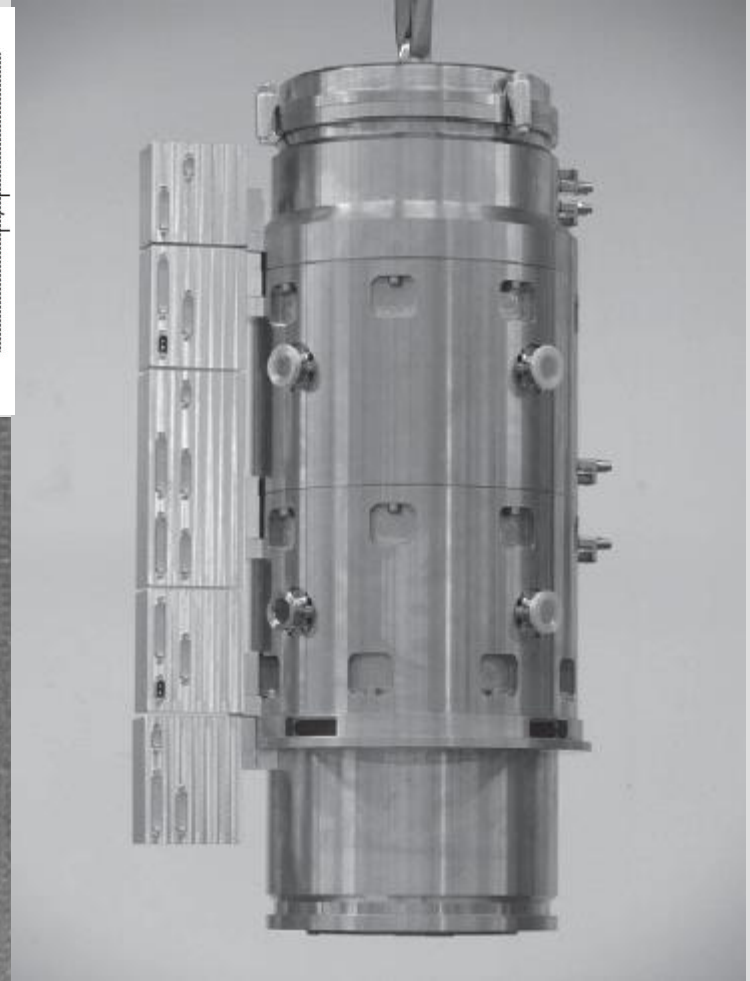
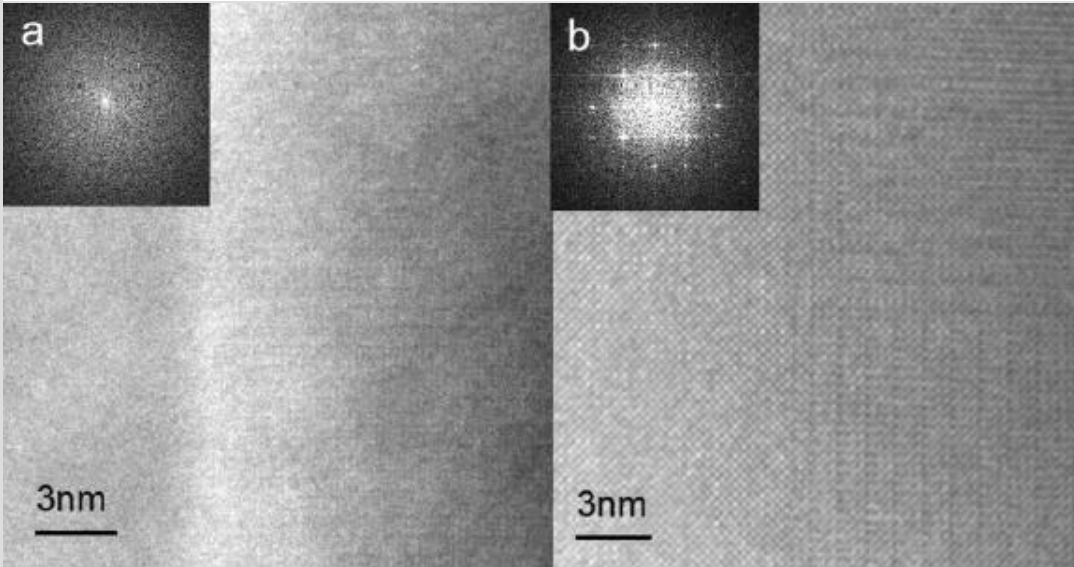
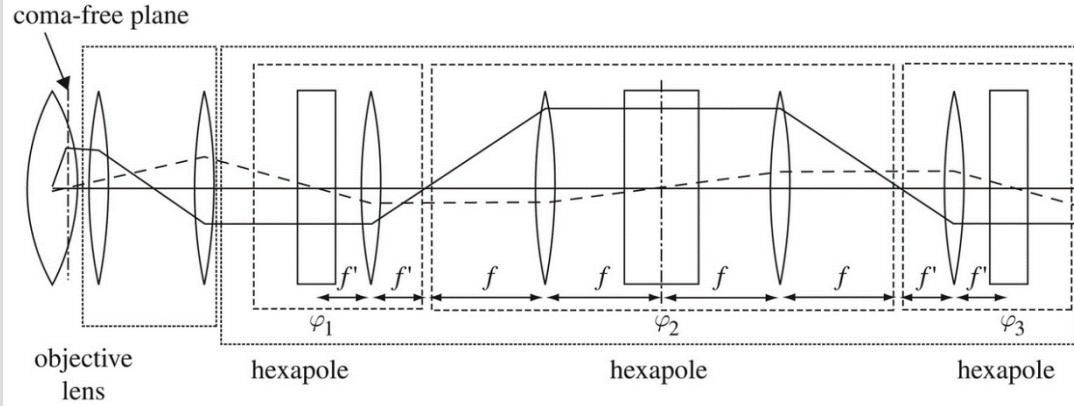


2000-2010

TEAM project started - 2004

0.5 Å resolution, CEOS Cc and Cs correction – funded by DoE

Operational microscope 2008



Kabius et al., 2009 J. Microsc 58(3): 147–155

Cc-Cs corrector for Argonne TEAM TEM

1990-2000

CEOS – culmination of the Scherzer academic line



O. Scherzer



H. Rose

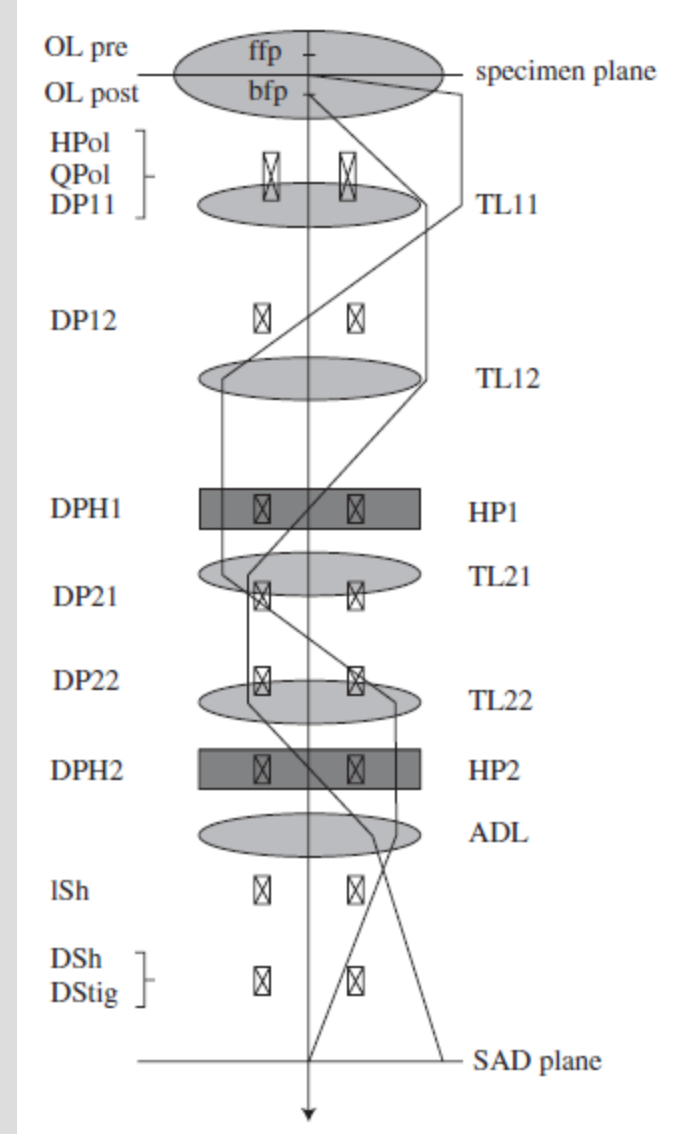
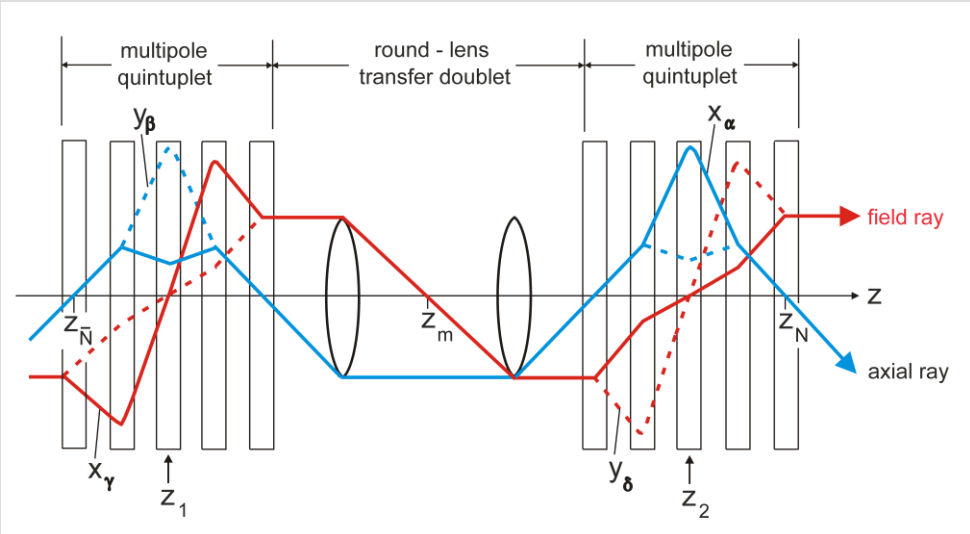


M. Haider



CEOS

Corrected Electron Optical Systems GmbH



1990-2000

NION – First US HREM production in 40+ years!

Aberration-corrected
analytical HRSTEM



The Nion Company was established in 1997 by Ondrej Krivanek and Niklas Dellby in the state of Washington, USA



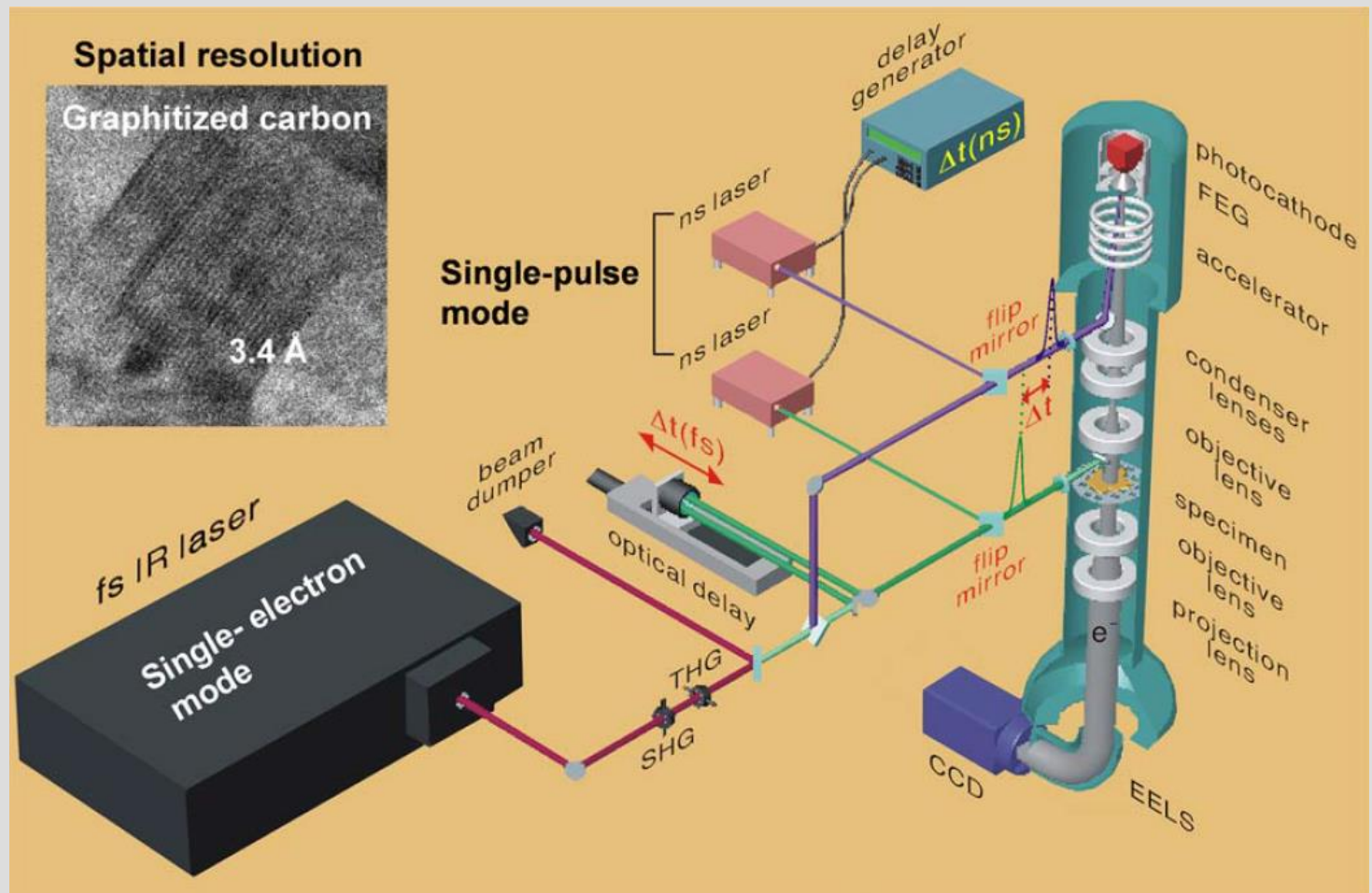


2000-2010



2000-2010

Realization of ultrafast HRTEM – 2005-6



King et al. (2005) J. Appl. Phys. 97: 111101

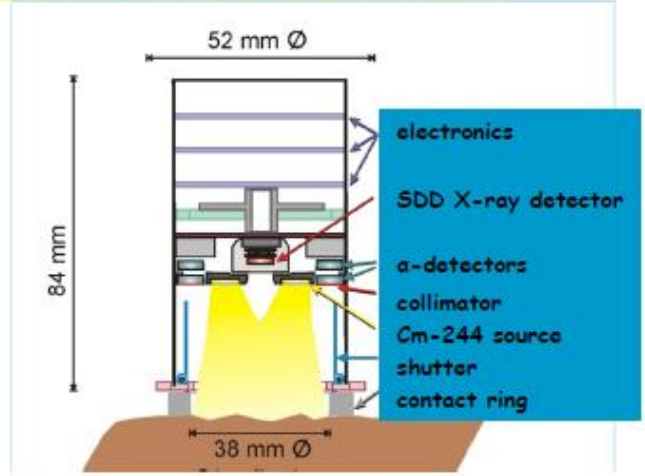
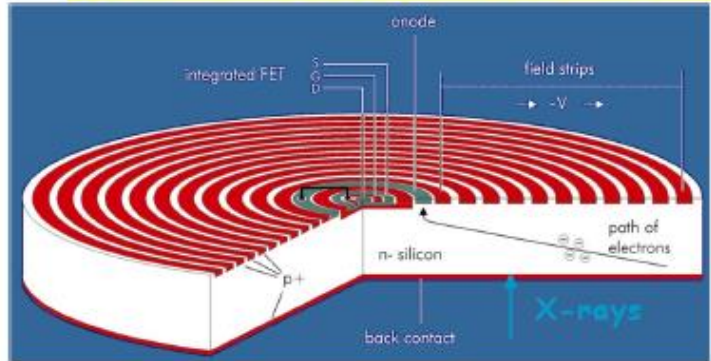
Zewail (2006) Ann. Rev. Phys. Chem. 57: 65-103

Park et al. (2009) Ultramicroscopy 110: 7-19

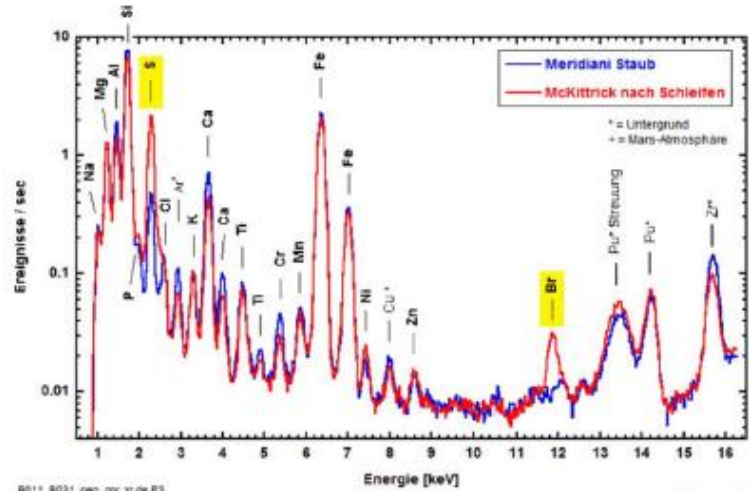
2000-2010

SSD detector for x-ray microanalysis -- 2004

SDD with integrated JFET → Low Noise X-ray Detector



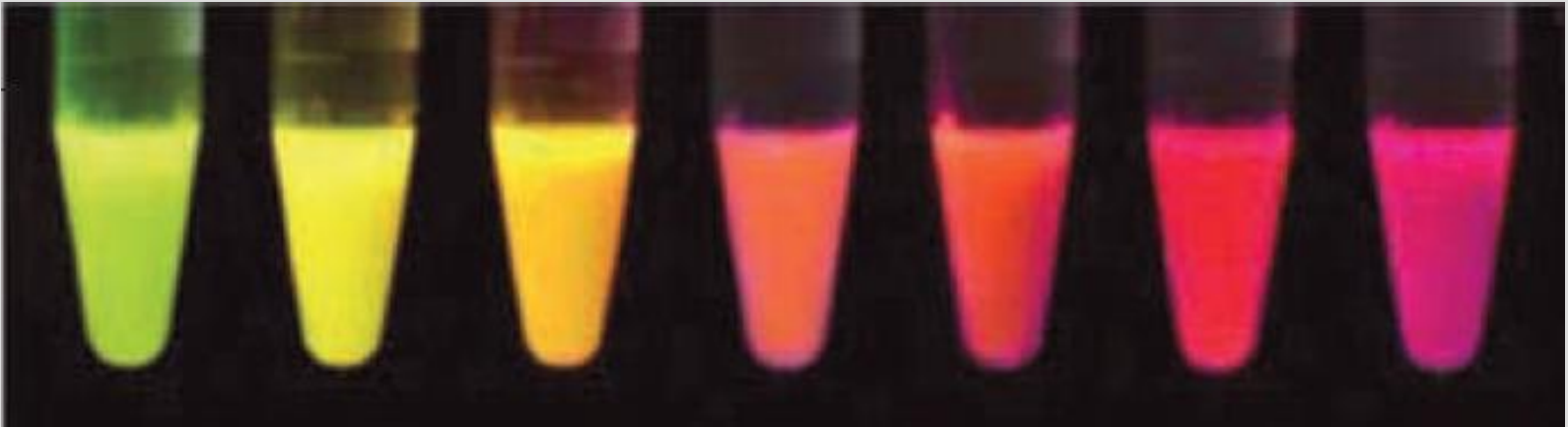
L.Strüder, IEEE-NSS Rome 2004,
R.Rieder, MPI für Chemie, Mainz



2000-2010

Advances in immuno-fluorescence light microscopy

Purified fluorescent proteins: Patterson, Shaner, Kaede, etc.



2000-2010

Nobel Prize #5

Advances in fluorescence light microscopy

Super-resolution (STEM, PALM, STORM, etc.): Hell, Betzig, Moerner, et al.

The Nobel Prize in Chemistry 2014



Photo: A. Mahmoud
Eric Betzig
Prize share: 1/3

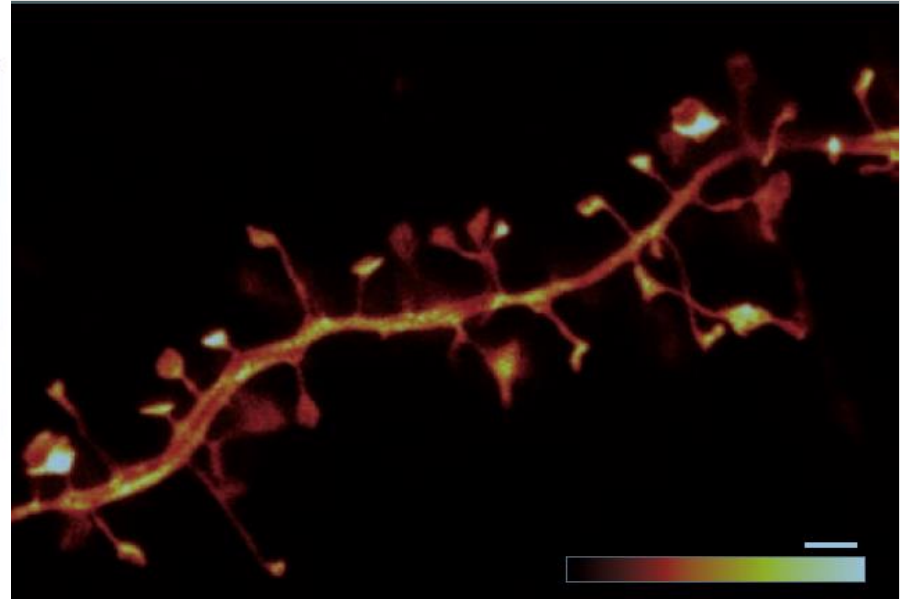


Photo: A. Mahmoud
Stefan W. Hell
Prize share: 1/3



Photo: A. Mahmoud
William E. Moerner
Prize share: 1/3

The Nobel Prize in Chemistry 2014 was awarded jointly to Eric Betzig, Stefan W. Hell and William E. Moerner *"for the development of super-resolved fluorescence microscopy"*.



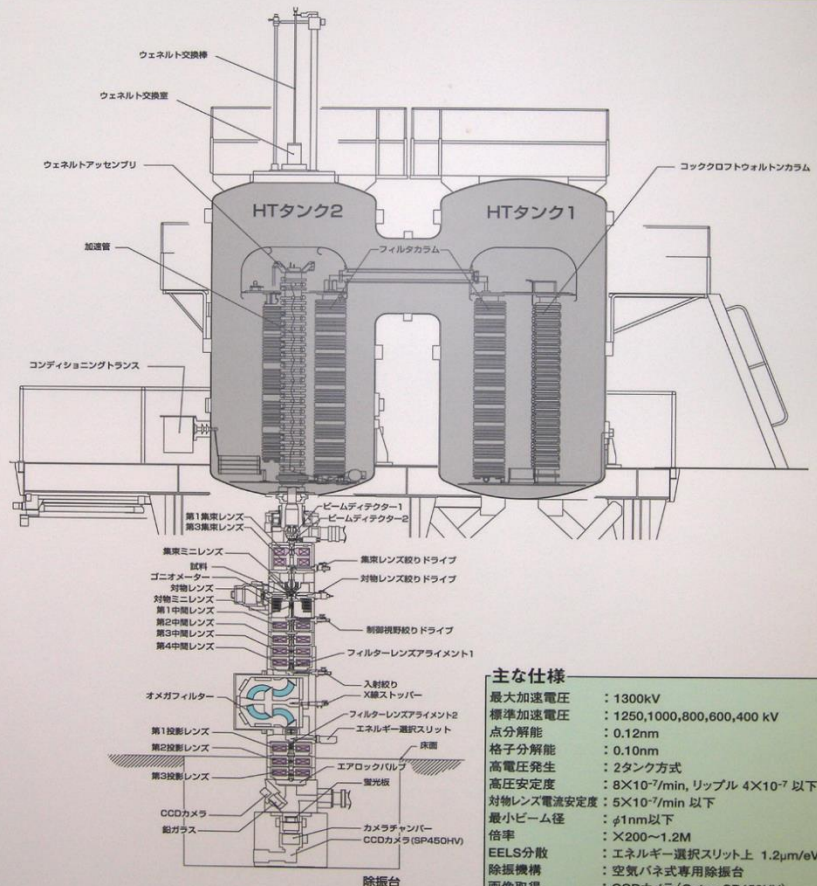
2000-2010

HVEM is still alive!



1 MeV TEM with in-column omega filter, 2015

超高圧電子顕微鏡 断面図 JEM-1300NEF



主な仕様

最大加速電圧	: 1300kV
標準加速電圧	: 1250,1000,800,600,400 kV
点分解能	: 0.12nm
格子分解能	: 0.10nm
高電圧発生	: 2タンク方式
高電圧安定度	: 8×10^{-7} /min, リップル 4×10^{-7} 以下
対物レンズ電流安定度	: 5×10^{-7} /min 以下
最小ビーム径	: $\phi 1$ nm以下
倍率	: $\times 200 \sim 1.2$ M
EELS分散	: エネルギ選択スリット上 1.2 μ m/eV
除振機構	: 空気バネ式専用除振台
画像取得	: CCDカメラ (Gatan SP450HV)
	取得領域 : 24.0 \times 24.0 mm ²
	ピクセル数 : 1330 \times 1330
	ピクセルサイズ : 18 \times 18 μ m ²



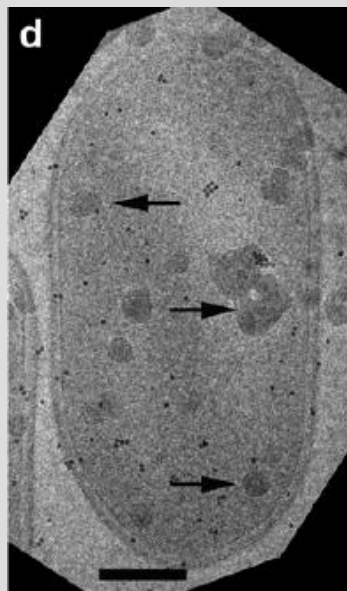
2000-2010

Developments in cryo-EM

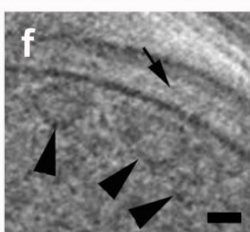
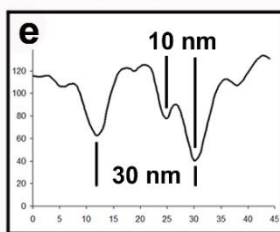
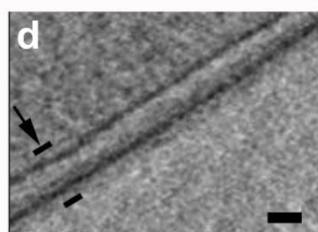
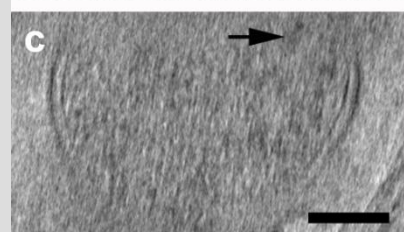
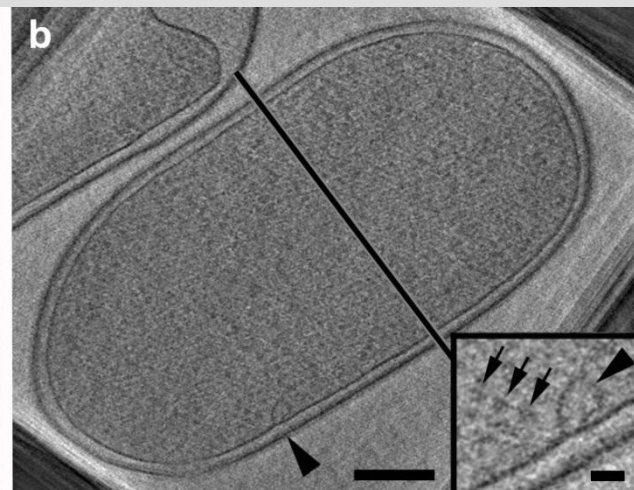
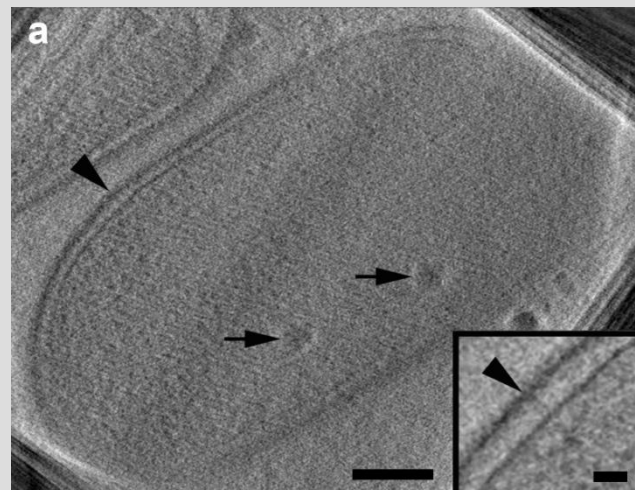
FIB as alternative to vitreous cryo-sectioning

TEM tomography of FIB-milled *E. coli* cells

Transverse and cross-sections (1.8 nm thick) of a cut-in-half cell

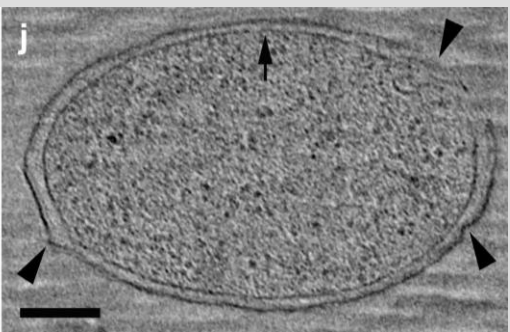
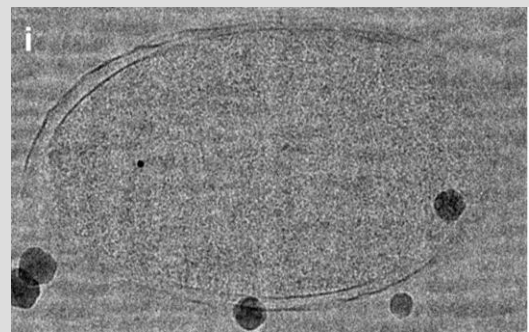


Projection image



Cryo-ultramicrotome oblique section for comparison

Projection



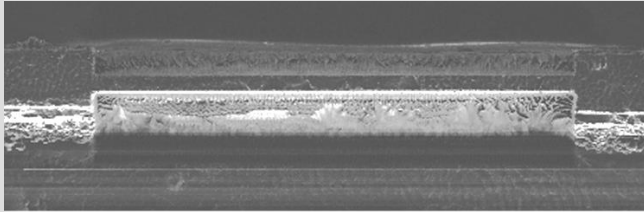
Tomographic slice

2000-2010

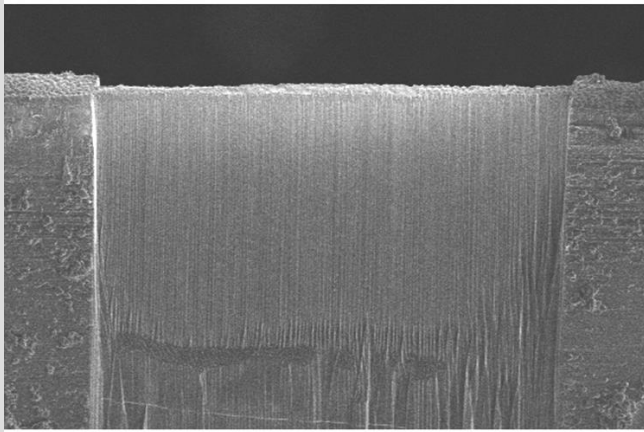
Developments in cryo-EM

Preparing FIB-milled “H-bar” specimens

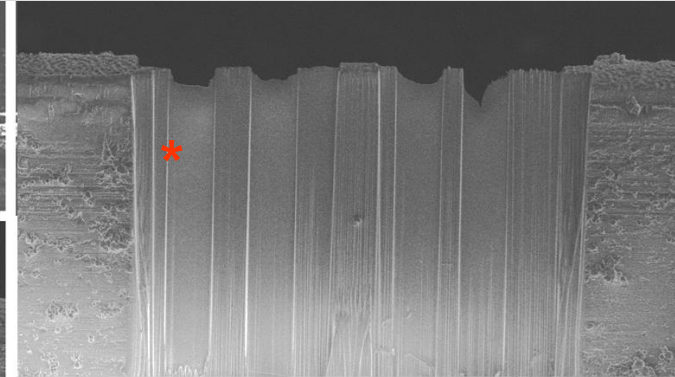
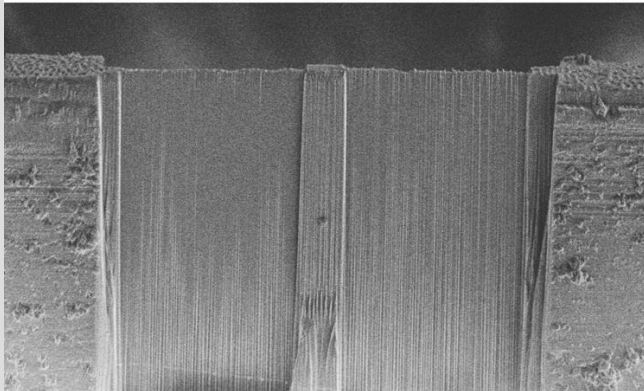
Edge view of first step



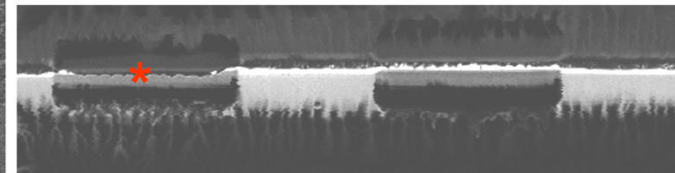
First step



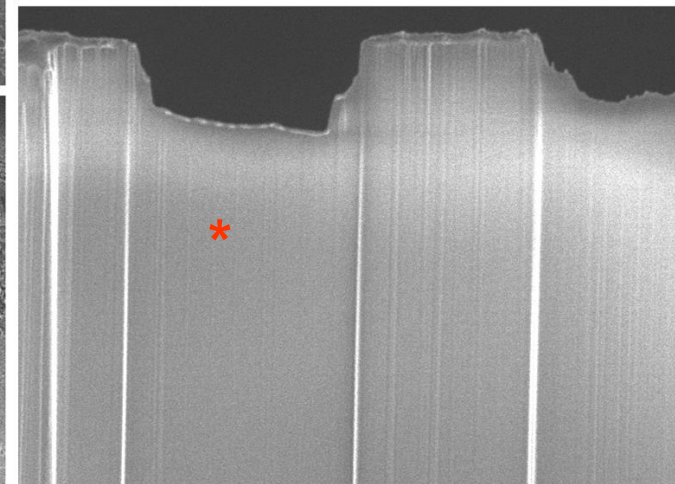
Second step



Third step



Edge view of third step



Final TEM lamella

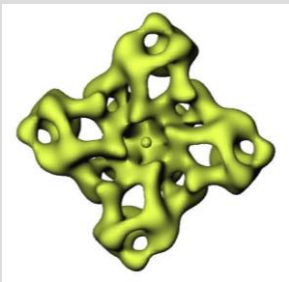
2000-2010

Developments in cryo-EM

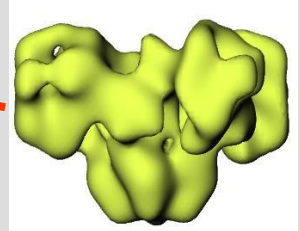
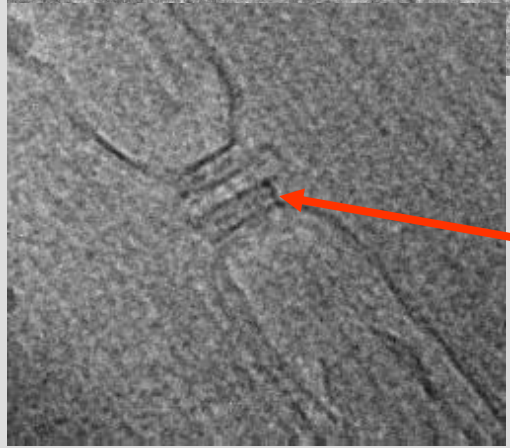
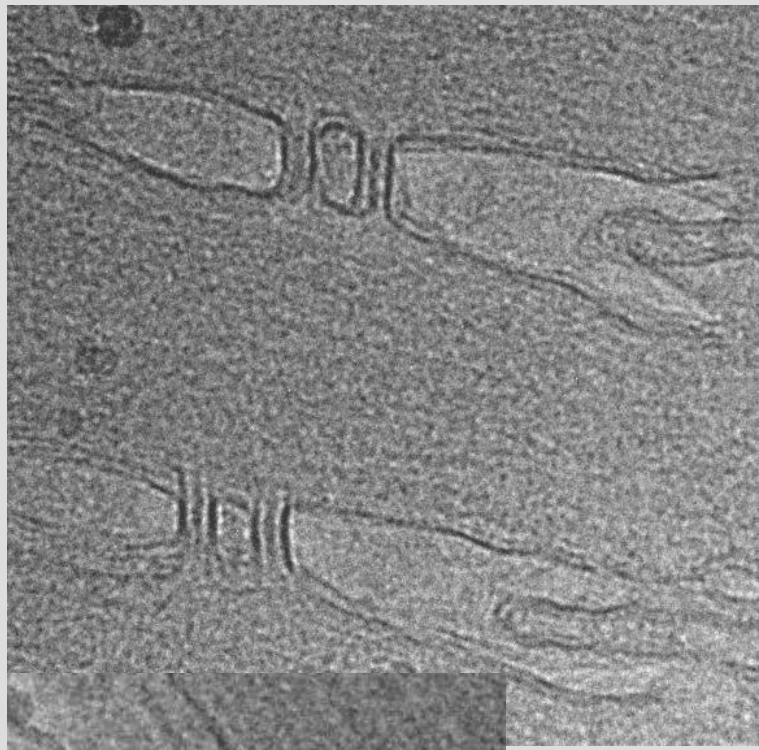
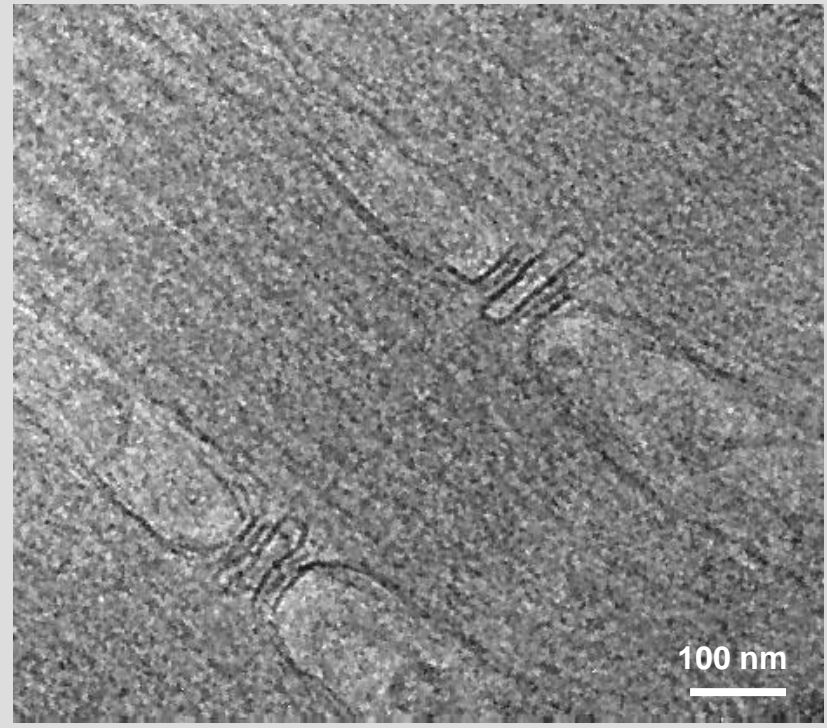
FIB milling of Muscle tissue

“Triad junctions” of sarcoplasmic reticulum and T-tubules, with ryanodine receptors (RyR)

Object is to extract and average in-situ RyR to study interactions with proteins removed by extraction from the cell



Top view

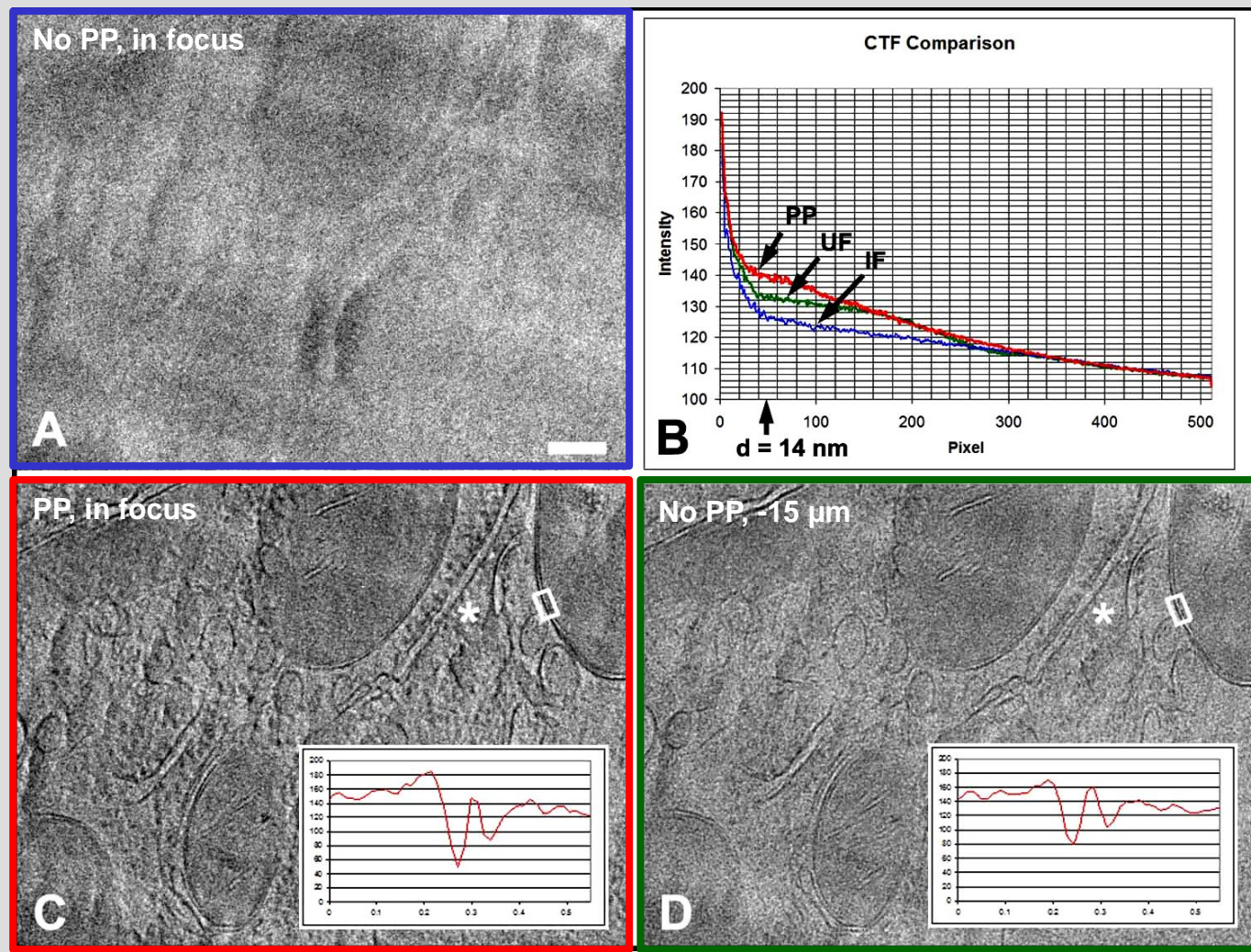


Side view

2000-2010

Advances in cryo-TEM Vitreous cryo-sections imaged with phase plate

Liver tissue: 400 kV, imaged with Zernike phase plate (cut-on 14 nm), section 200 nm thick



2000-2010

MSA Council, 2001-2006



2000-2010

MSA Council, 2007-2010



2007



2008



2009



2010



2010- Present



2010- present

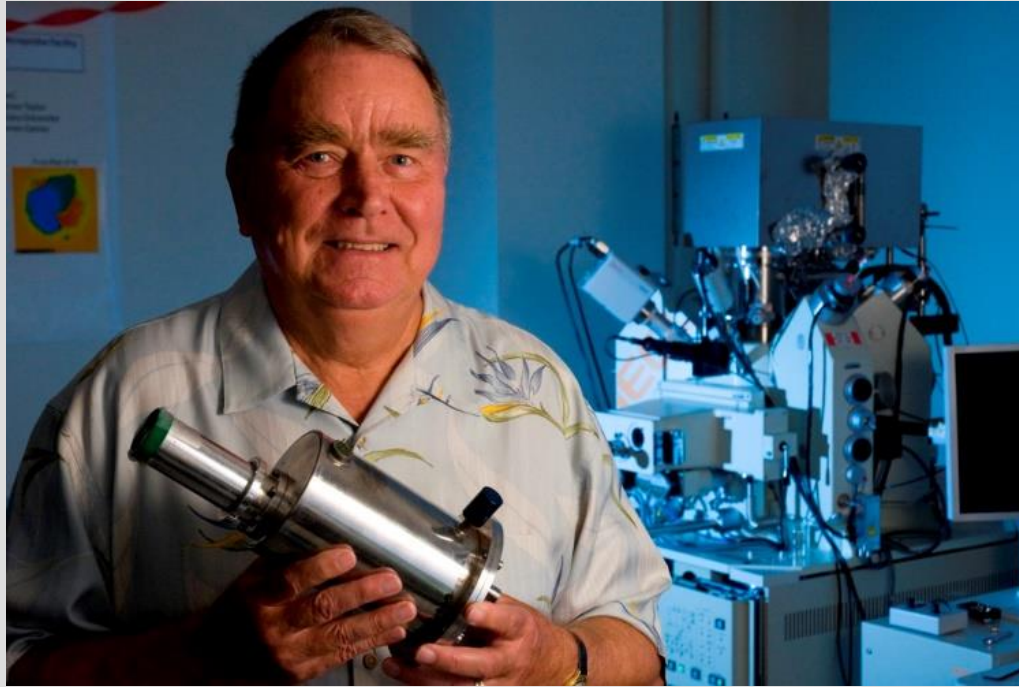
MAS 2014 meeting



Dale Newbury and John Small at a meeting in 2014, as well as Gordon Cleaver in front of the old ARL microprobe built in 1968

2010- present

Solid-state EDS detector



Kraus Keil: in 2012 with the original EDS spectrometer that was developed by R. Fitzgerald, K. Keil and K.F.J Heinrich: Application of solid-state energy-dispersion spectrometer in electron microprobe x-ray analysis. Science 159, 528-530, 1968. As you know, this seminal paper started a revolution in the field of microanalysis. A second paper celebrating 40 years of EDS analysis was published in 2008 (K. Keil, R. Fitzgerald and K.F.G. Heinrich: Celebrating 40 years of energy dispersive X-ray spectrometry in electron probemicroanalysis. Microscopy & Microanalysis 14, Suppl. 2, CD 1152, 2008).

2010- present

MAS 2016 EPMA topical conference



2010- present

EMAS 2017 EPMA meeting in Konstanz



2010- present

meV EELS

Krivanek et al.,
2014 EMAG 2013
(IOP) 522:012023

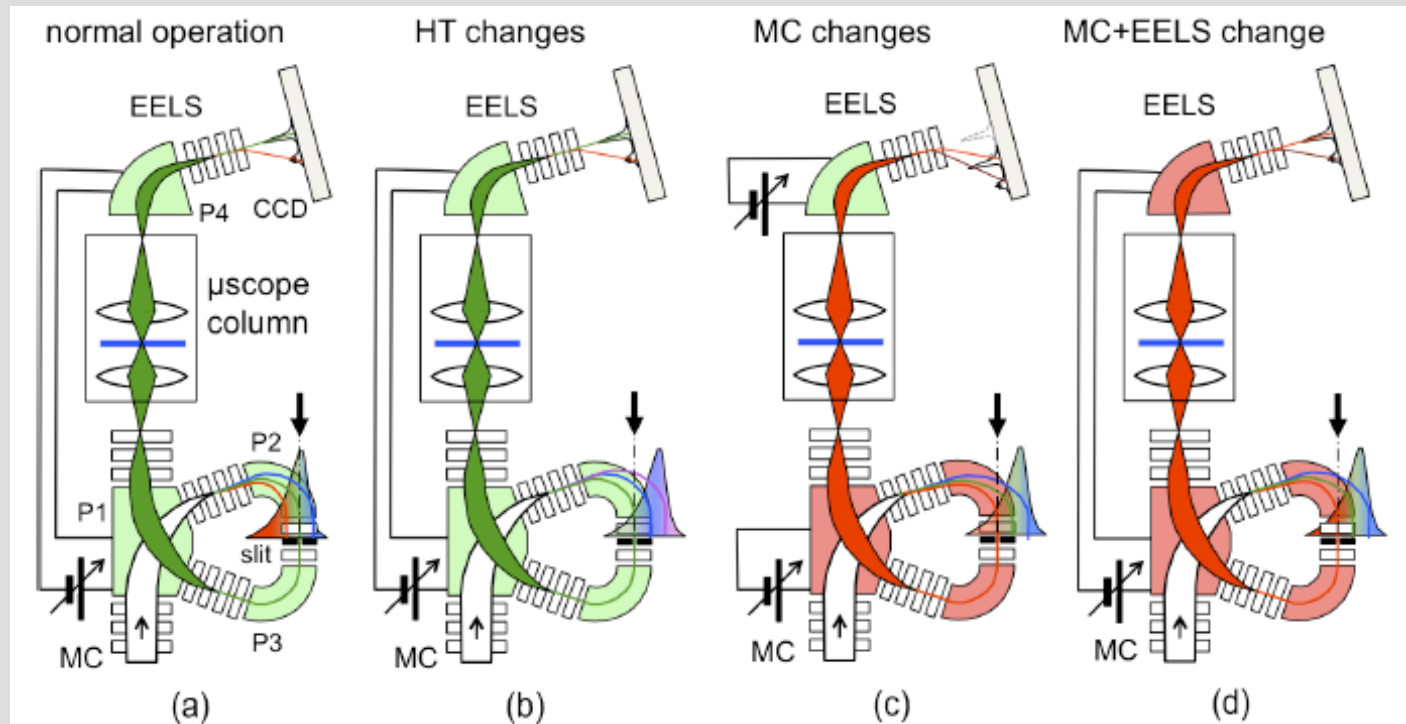


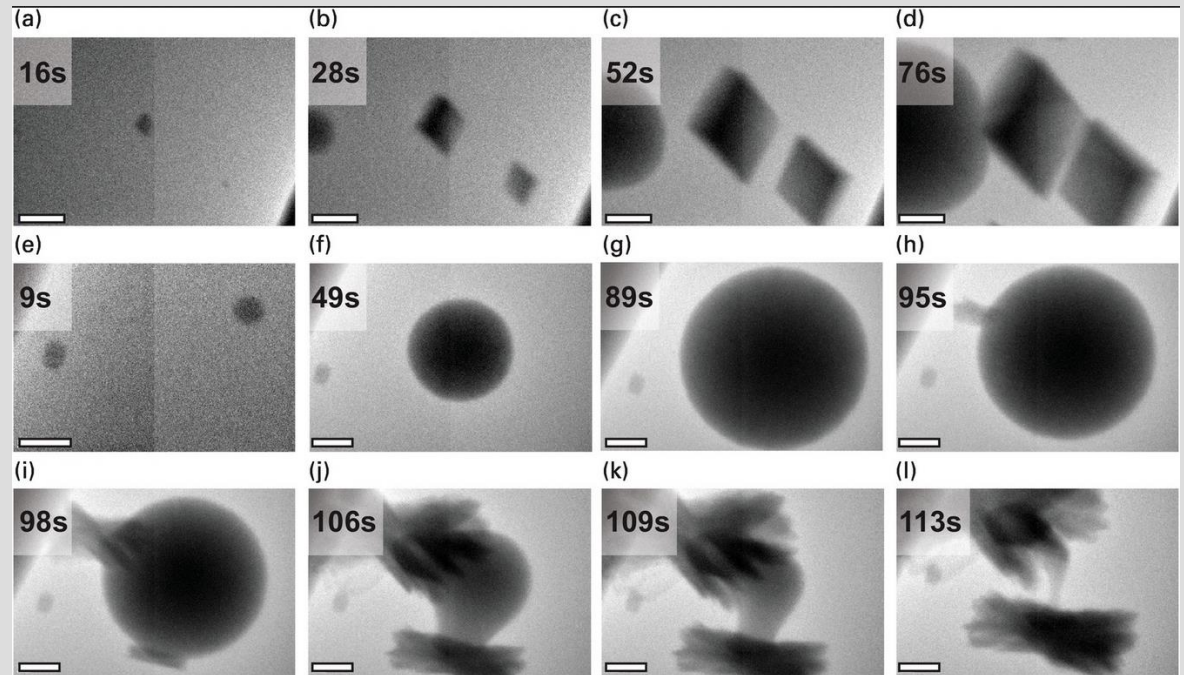
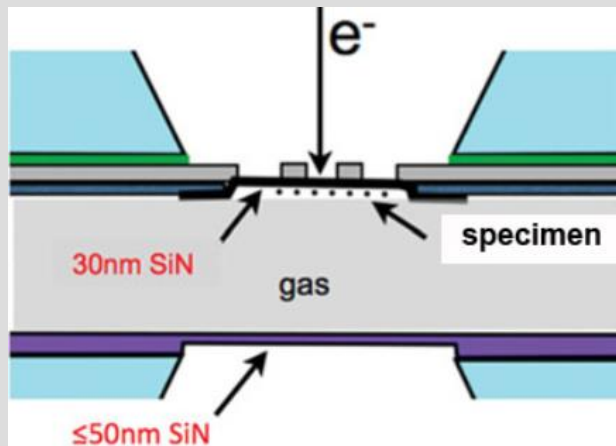
Fig. 2. Schematic diagram illustrating how various instabilities affect the HERMES™ energy resolution. MC = monochromator, P1 to P4 = prisms of the system. The microscope column is represented only by the condenser-objective lens, with a thin sample in its middle. Downward-pointing arrows mark the energy admitted by the energy-selecting slit.

A STEM-EELS system operating at this advanced level is likely to be able to attain <10 meV energy resolution with an atom-sized (<2 Å) electron probe, and thereby to open up a new field for experimental study: phonon spectroscopy with atomic spatial resolution. It is not every day that a new type of physical interaction becomes available in the electron microscope. It promises to make our efforts to improve the energy resolution further very worthwhile, every step of the way.

2010- present

New implementation of “operando” ETEM

After 40 years, environmental, *in-situ*, experiments are being done again!



Nielsen, M., & De Yoreo, J. (2016). In F. Ross (Ed.), *Liquid Cell Electron Microscopy* (Advances in Microscopy and Microanalysis, pp. 291-315). Cambridge: Cambridge University Press.

2010- present

Commercially available aberration-corrected HTEMs



FEI Titan



Hitachi HS-3300V



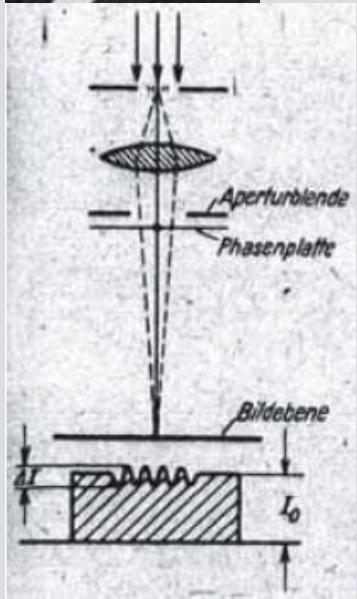
JEOL ARM

2010- present

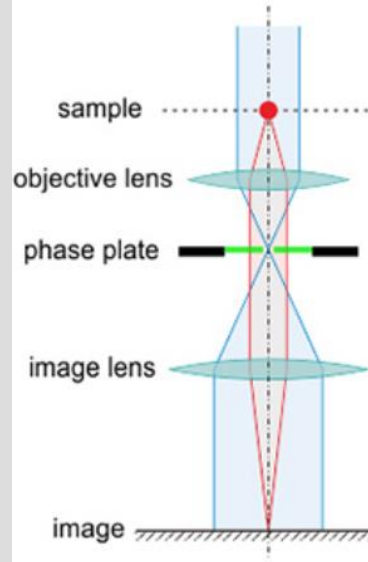
Practical implementation of TEM phase-plate imaging



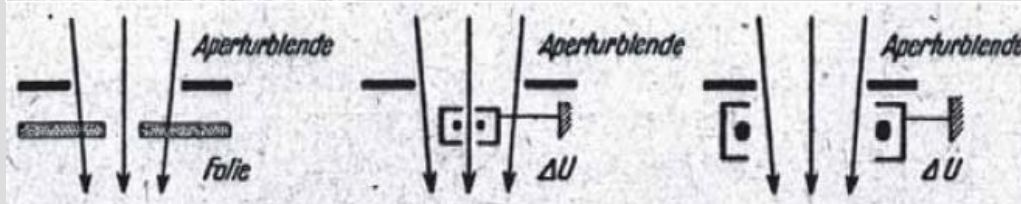
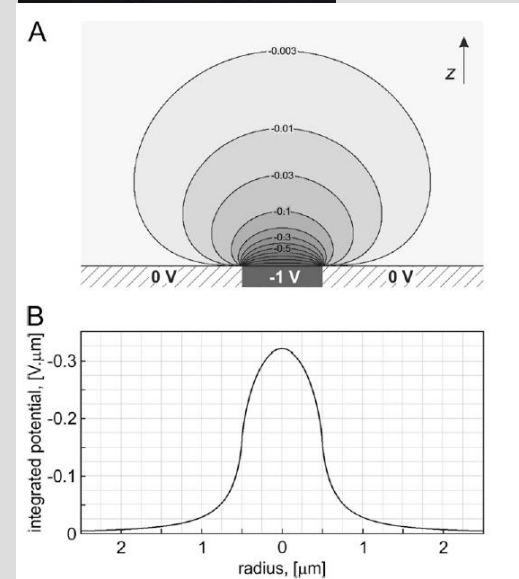
Hans Boersch
Original theory



Kuniaki Nagayama
Modern revival



Radostin Danev
Practical implementation



2010- present

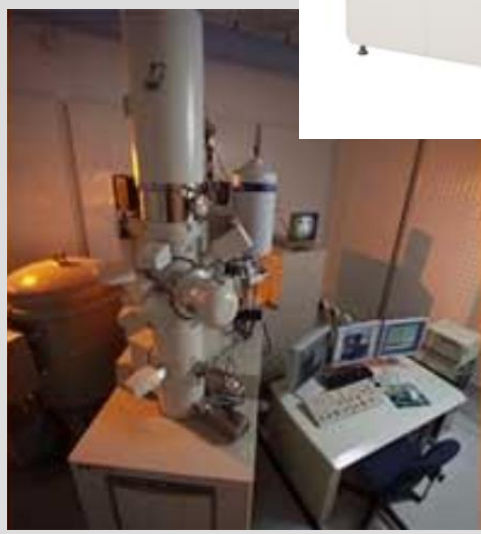
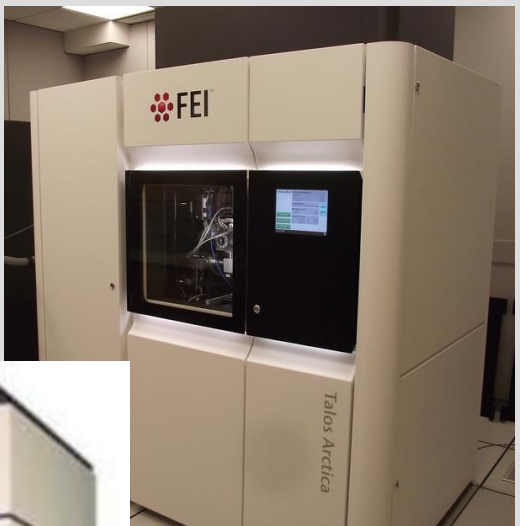
New implementation of TEM phase-plate imaging

Commercial availability of phase-plate equipped TEMs

JEOL



“FEI”



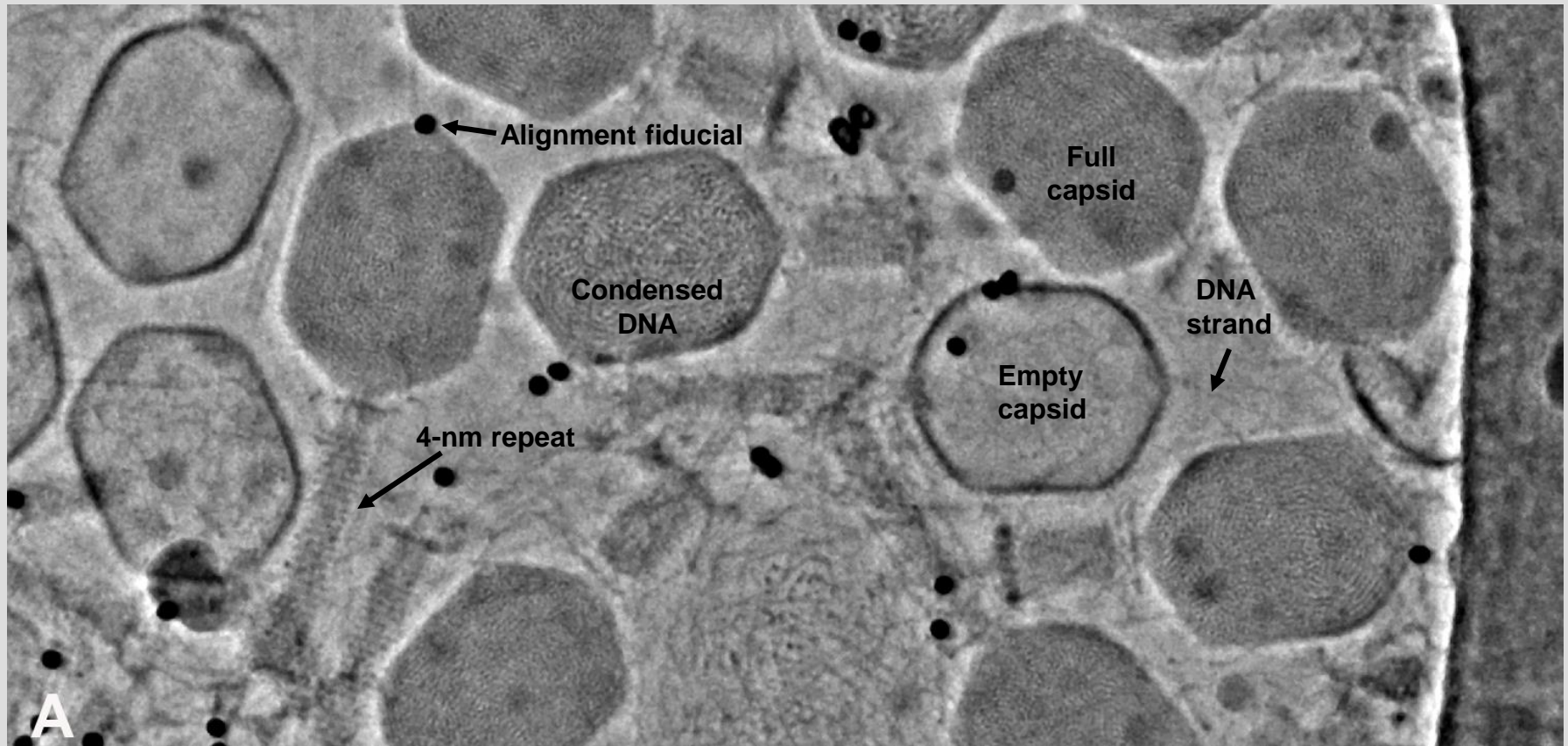
2010-Present

Advances in cryo-TEM

Phase-plate imaging for cryo-EM

Modern image of bacteriophage T4

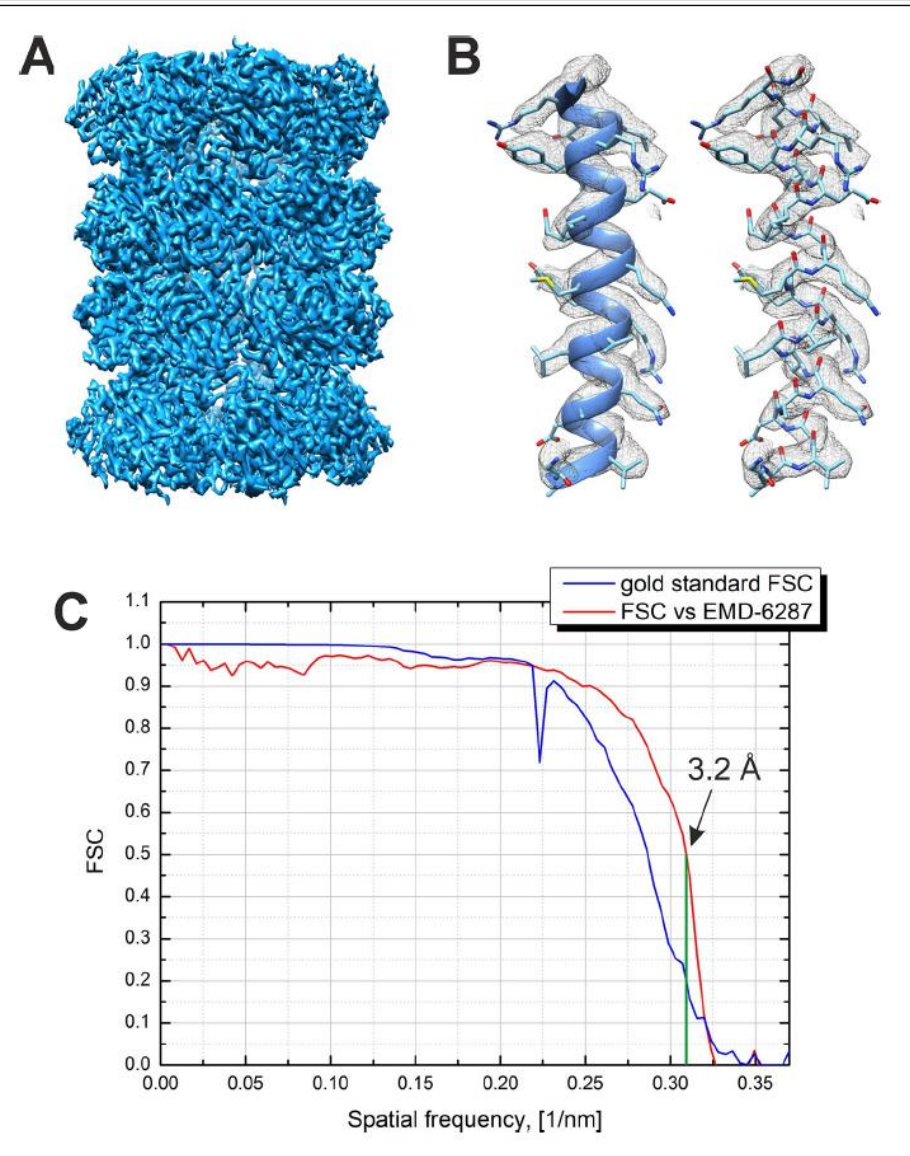
30 $e^-/\text{\AA}^2$, 300 keV, zero-loss filtered, JEM-3200FSC/PP, TVIPS F-416 camera



2010- present

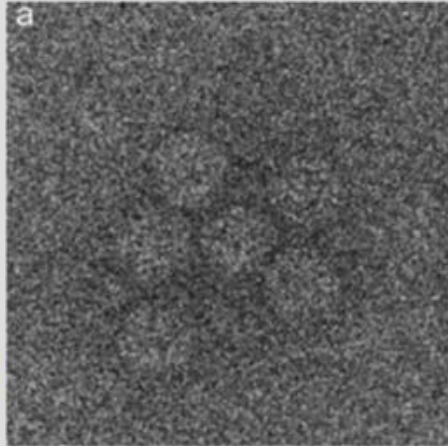
New implementation of TEM phase-plate imaging

Applications in high-resolution
Cryo-TEM

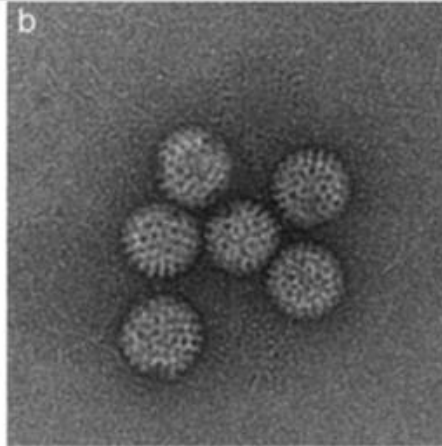


2010- present

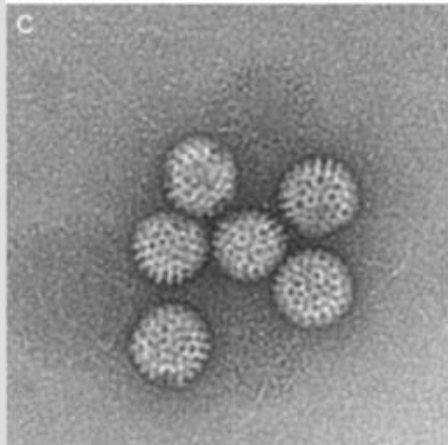
“Cryo-EM Revolution” – direct-electron detectors



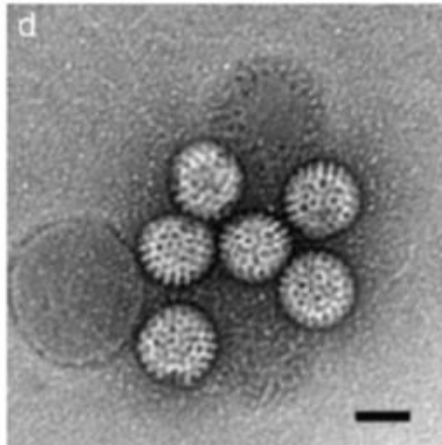
1.6 e-/pixel
0.04 e-/Å²



160 e-/pixel
0.4 e-/Å²



1400 e-/pixel
35 e-/Å²



64000 e-/pixel
160 e-/Å²

Mc Mullan et al. (2008) Nucl. Instr. and Meth. A.



Gatan K2



“FEI” Falcon series



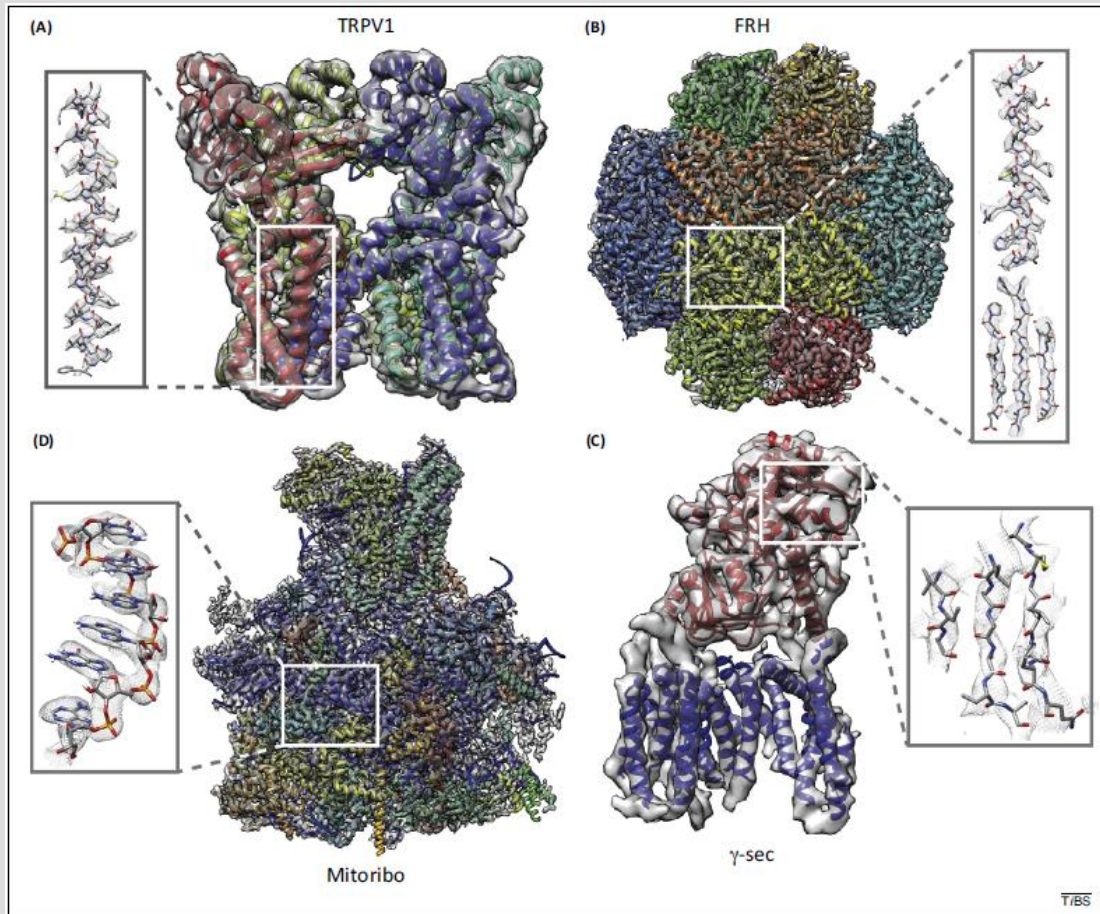
Direct Electron DE series

2010- present

“Cryo-EM Revolution” correction of beam-induced motion

Li, X. *et al.* (2013) Electron counting and beam-induced motion correction enable near-atomic-resolution single-particle cryo-EM. *Nat. Methods* 10, 584–590

Li, X. *et al.* (2013) Influence of electron dose rate on electron counting images recorded with the K2 camera. *J. Struct. Biol.* 184, 251–260



Near-atomic resolution of near-native-state macromolecules now feasible. Amino-acid side chains now can be located and identified.

“Movie mode” capability of direct electron detectors allow correction of beam-induced motion.

2010-Present

MSA Council, 2011-2014



2011



2012



2013



2014

2010-Present

MSA Council, 2015-2017





Acknowledgements:

MSA Archives

Tom Kelly (M&M2016)

John Fournelle (MAS)

Nature milestones

